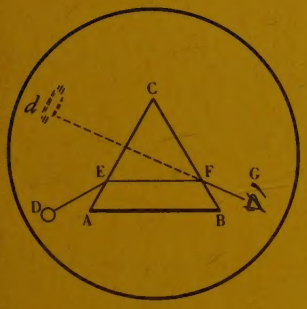

UNIVERSITY OF ILLINOIS
MAR 19 1962
CHICAGO

optics and spectroscopy

volume xi
numbers 5-6
november-december 1961

OPTICAL SOCIETY OF AMERICA

USSR ACADEMY OF SCIENCES

RUSSIAN EDITORIAL STAFF FOR
OPTIKA I SPEKTROSKOPIYA sponsored by
USSR ACADEMY OF SCIENCES

Editor: S. E. FRISH

Assistant Editor: P. P. FEOFILOV
Corresponding Secretary: L. S. SAZONOV

Associate Editors:

M. V. VOLKENSTEIN	V. P. LINNIK	N. N. SOBOLEV
M. M. GUREVICH	S. L. MANDEL'SHTAM	A. N. TERENIN
M. A. EL'IASHEVICH	I. V. OBREIMOV	A. I. TUDOROVSKII
A. A. LEBEDEV	V. K. PROKOF'EV	V. M. CHULANOVSKII

Translated from *OPTIKA I SPEKTROSKOPIYA* on the initiative of THE OPTICAL SOCIETY OF AMERICA, INC. with a grant-in-aid from THE NATIONAL SCIENCE FOUNDATION. *Optics and Spectroscopy* is a cover-to-cover translation of *Optika i Spektroskopiya* and no attempt is made to edit the material other than to correct obvious misprints. The views are those of the original authors and do not represent the Optical Society of America.

TRANSLATION EDITORIAL STAFF

Scientific Editors

CYRUS FELDMAN, *Oak Ridge National Laboratory*

CARL W. GARLAND, *Massachusetts Institute of Technology*

MATHEW G. GIBBONS, *Oakland, California*

Administrative Editor: PATRICIA R. WAKELING, *OSA*

Published monthly by the Optical Society of America, Inc. Executive office: 1155 Sixteenth Street, N.W., Washington, D.C. Subscriptions for one year to members of the Society: Associates $13.00; Regular members and Fellows $17.00. Subscriptions for non-members of the Society: One year U. S. and Possessions, $25.00; Foreign $28.00. Back numbers: $3.00 per copy. Subscriptions, changes of address and undeliverable copies should be referred to the Executive offices in Washington, D.C. The office of publication is 2500 South State Street, Ann Arbor, Michigan. Second class postage paid at Ann Arbor, Michigan.

Printed in the U.S.A. by Edwards Brothers, Inc., Ann Arbor, Michigan.

MEASUREMENT OF THE ABSOLUTE VALUES OF OSCILLATOR STRENGTHS IN ATOMIC SPECTRA

II. Resonance Lines of Atoms of Group II

Yu. I. Ostrovskii and N. P. Penkin (pp. 565-570)

Received 28 December 1960

The absolute oscillator strengths of the resonance lines ($^1S_0-^1P_1^0$) of calcium ($f_{4227} = 1.49 \pm 0.04$), strontium ($f_{4607} = 1.54 \pm 0.05$), and barium ($f_{5535} = 1.40 \pm 0.05$) have been measured. The results of the measurements are compared with the theoretical and experimental data of other authors.

In order to measure the oscillator strengths of the nance lines of calcium, strontium, and barium, we the method and experimental equipment described tail in our previous papers.[1,2] We return once more e problem of determining the f-numbers of these by simultaneously measuring the absorption and ersion. In ref. 1, the oscillator strengths of the nance lines of Mg I, Ca I, Sr I, and Ba I were mea-d. The total absorption was measured by means of graphic photometry, which did not furnish highly rate results (15-25%). In the present investigation, electric equipment[2] was used. This permitted us to rmine the f-numbers much more accurately.

ium.

Metallic calcium was placed in an absorption tube ich the temperature could be kept constant between nd 600°C.

In order to reduce the amount of scattered light, ral glass filters (ZhS-4, FS-1, and SS-5)[3] were d in front of the slit of the monochromator. At low eratures (i.e., at low calcium vapor pressures) the ows at the ends of the tube remained clear for a time, despite the continuous pumping of the tube to ssure of $<10^{-3}$ mm Hg. At high vapor pressures, s necessary to add a small amount of argon in order event the gradual deposition of metal onto the win-. The pressure of the added gas did not exceed 0.2 oil ($\approx 10^{-2}$ mm Hg).

The introduction of an inert gas into the absorption must broaden the absorption line and consequently to incorrect f-numbers. We therefore studied the ndence of the measured f-numbers on the pressure e added gas.* Figure 1 shows the results of these

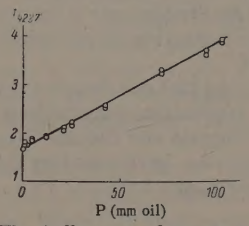

Fig. 1. The influence of argon pressure in the absorption tube on the measured value of the oscillator strength of the resonance line of calcium.

sponded to a certain region of the strip chart recording of the total absorption. The results of the measurements are given in Fig. 2. Since it is impossible to graph such a large number of points, we plotted only the mean values of f_{4227}, obtained in the interval log Nfl ± 0.05. In the circles, we indicate the number of independently processed exposures which contributed to the mean value given.

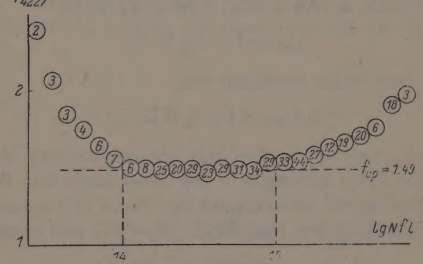

Fig. 2. Experimental values of the absolute f-number of the resonance line of calcium.

As seen from Fig. 2, the measured value of f-number is constant for Nfl values from 10^{14} to 10^{15}. This interval contains 218 points. The mean value of the f-number obtained from these is 1.49. The root mean square error of an individual measurement is 3%.

As indicated in our previous work,[2] besides the statistical errors arising from the inaccuracy of the measurement of the hooks and recordings, other systematic errors are possible. These errors are caused by the inaccuracy of the determination of the width of the monochromator's exit slit, by the error in the determination of the dispersion of the spectral equipment, and by other causes. In order to evaluate and reduce the influence of these errors, the exposures were made in four series, separated by intervals of 1 to 3 weeks. Each series of

f-number appears to be an atomic constant. The me of the upper level, from which the emission of ine occurs, depends on the experimental conditions. relationships depicted in Figs. 1-4 must be under-l in precisely this sense.

surements for the resonance line of calcium. They obtained at a constant optical thickness of the layer = 2.7×10^{15} cm^2), but at various pressures of argon. lows from the graph that the dependence of the mea-d f-numbers on the gas pressure is well approxi-d by a straight line. At the argon pressures which sed ($P < 10^{-2}$ mm Hg), the Lorentz broadening should istort the measured value of the oscillator strength ore than 0.2-0.3%. About 450 exposures of the hooks e resonance line 4226.73 A of calcium at optical nesses ranging from 2.5×10^{13} to 6×10^{15} cm^{-2} obtained and processed. Each exposure corre-

measurements was preceded by an alignment of the equipment and a measurement of all the parameters which were needed for the determination of f-numbers. Each series contained data obtained with different monochromator exit slits. The results of the measurements are given in Table 1.

Due to the large number of measurements, the statistical error is negligibly small (the root mean square error of the mean is less than 0.1%). Therefore, as a measure of the error of the results, we list the maximum deviation from the mean in each series.

Thus, the oscillator strength of the resonance line of calcium is $f_{4227} = 1.49 \pm 0.04$. In ref. 1, we obtained $f_{4227} = 1.3 \pm 0.2$. Our results differ substantially from those of Steinhäuser,[4] who obtained $f_{4227} = 2.3$. We are inclined to attribute this discrepancy to experimental errors introduced by Steinhäuser's inaccurate method of measuring the depolarization of resonance fluorescence in a magnetic field.[5]

It should be noted that our results agree very well with the quantum-mechanical calculations of Trefftz[6] ($f_{4227} = 1.46$) and Ushpalis and Chiplis[7] ($f_{4227} = 1.5$). The Vainshtein[8] calculations, performed by the one-electron approximation, give $f_{4227} = 2.32$.

Strontium

The hooks and absorption profiles of the strontium resonance line 4607 A were obtained under approximately the same conditions as for calcium. SZS-7, ZhS-11, and SZS-18 filters[3] were placed in front of the slit of the monochromator.

The dependence of the measured value of f on the argon pressure is similar to that obtained for calcium (Fig. 1).

About 500 exposures (Fig. 3) were processed; 343 of them correspond to Nfl values between 5×10^{13} and 10^{15}; the measured value of f_{4607} remains constant in this interval. The mean of the f-numbers obtained from these exposures is 1.54. The results of the measurements are given in Table 2. As a final result we have

$$f_{4607} = 1.54 \pm 0.05.$$

In ref. 1, the value obtained was

$$f_{4607} = 1.5 \pm 0.2.$$

Ours appear to be the only measurements of the absolute oscillator strength of the resonance line of strontium. Eberhagen[9] determined the value of f-number of the intercombination line 6893 ($^1S_0 - {}^3P_1$) and obtained

$$f_{6893} = 0.0013 \ (\pm 20\%).$$

Using the ratio[10] $f_{4607}/f_{6893} = 1660$, we obtain

$$f_{4607} = 2.2 \pm 0.7,$$

which is compatible with our results.

Barium

The hooks and absorption profiles of barium vapor were obtained under the same conditions as for calcium and strontium. OS-12, PS-7, and ZhZS-18 filters were

Table 1

Series No.	Number of exposures	f_{4227} (mean)
1	17	1.50
2	67	1.51
3	77	1.45
4	57	1.50

Table 2

Series No.	Number of exposures	f_{4607} (mean)
1	110	1.50
2	110	1.59
3	123	1.54

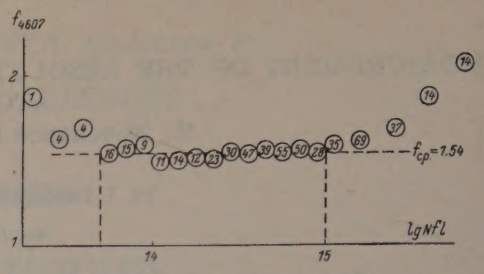

Fig. 3. Experimental values of the absolute f-number of the resonance line of strontium.

used for the preliminary monochromatization of the light.[3]

Figure 4 gives the results of the processing of about 800 exposures of the hooks and the correspondi recordings of the absorption obtained from four serie of measurements.

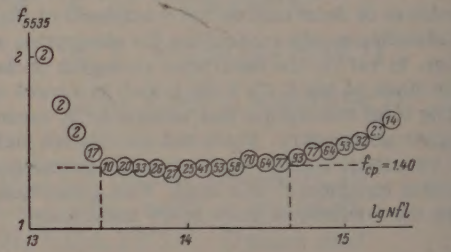

Fig. 4. Experimental values of the absolute f-number of the resonance line of barium.

The measured values of f_{5535} remain practically constant for Nfl values from 2.8×10^{13} to 4.5×10^{14}. This interval contains 463 independently obtained and processed exposures.

The distribution of the results according to serie is given in Table 3.

The mean value of the oscillator strength of the resonance line of barium is

$$f_{5535} = 1.40 \pm 0.05.$$

In ref. 1, we obtained

$$f_{5535} = 1.6 \pm 0.2$$

Wessel,[11] using an atomic beam absorption method, fo

$$f_{5535} = 1.8 \pm 0.25.$$

It should be pointed out that although $6p\,^1P_1^0$ is the initial level for the line 5535 A, other transitions also occur from this level to lower levels[12]: $5d\,^1D_2$ (λ 1500 $5d\,^3D_2$ (λ 8844.75 A), and $5d\,^3D_1$ (λ 9026.3 A).

Consequently, our measured value of f_{5535} appea be too high. The contribution of these transitions to measured value of the oscillator strength for the res ance lines of Ba I could be calculated if their relativ numbers were known. However, if it is assumed that oscillator strength of the first line contributes 0.2 to f_{5535}, and that of each of the two remaining intercomb tion lines contributes 0.005 (this order of magnitude obtained for f-numbers in our investigation of analog transitions[13]), it appears that the total contribution o abovementioned three lines to the measured value of does not exceed 2-4%. The real distortion is probabl considerably smaller. From direct measurement of mean lifetime $\tau_{p\,^1P_1^0}$ of this level, we obtained

$\tau_{6^1P_1^0} = (9.9 \pm 0.3) \cdot 10^{-9}$ sec.

By measuring the relative f-numbers of all lines
h originate from this level, it will be possible to cal-
e the value of f_{5535} much more accurately from the
e of τ obtained above.

We should note that in agreement with the theory of
nethod given in ref. 2 for the series Ca-Sr-Ba, we
rved a drop in the Nfl value at which the measured f
e for a given spectral line begins to be constant. This
xplained by the decrease in the Doppler width of the
with increasing atomic weight.

Thus the absolute values of the oscillator strengths
e resonance lines ($^1S_0$-$^1P_1^0$) of CaI, SrI, and BaI have
determined by the simultaneous measurement of the
s and the total absorption with an accuracy of better
5%. From the comparison of these results with our
ious data, obtained by the same method except for the
of photographic photometry,[1] it is easy to see the ad-
ages of the photoelectric recording of the equivalent
h of the absorption line. Within the limits of accuracy
e measurements, the results of the two investigations
e.

Using the new values of the oscillator strengths of the
nance lines of CaI, SrI, and BaI, we have revised the
lute values of the f-numbers of the resonance lines
aII, SrII, and BaII given by us in ref. 14. The results
is revision are given in Table 4.

Table 3

ies	Number of exposures	f_{5535} (mean)
	109	1.38
	108	1.35
	123	1.45
	123	1.41

Table 4

Ion	λ(A)	f
Ca II . . .	3933.67	0.84
	3968.47	0.43
Sr II . . .	4077.71	0.76
	4215.52	0.39
Ba II . . .	4554.04	0.66
	4934.09	0.33

The data obtained in this investigation also enabled us
alculate the absolute oscillator strengths of a large
ber of lines of BaI and CaI whose relative f-numbers
been measured in our earlier investigations.[13,15]

The measurement of the absolute oscillator strengths with our equipment requires a stable and intense source of continuous spectrum having a signal-to-noise ratio ≈500. Unfortunately, at the present time we do not have such a source for the ultraviolet region of the spectrum. For this reason, we have not yet succeeded in measuring the absolute f-number of the resonance line 2852 A of MgI. However, we are working toward that goal.

REFERENCES

1. Yu. I. Ostrovskii, N. P. Penkin, and L. N. Shabanova, Doklady Akad. Nauk SSSR, 120, 66 (1958), Soviet Phys.-Doklady 3, 538 (1958).
2. Yu. I. Ostrovskii and N. P. Penkin, Opt. i Spektr. 11, 1 (1961), Optics and Spectroscopy 11, 1 (1961).
3. "Catalogue of Color Glasses." State Press of the Defense Industry, Moscow, 1951.
4. A. Steinhäuser, Z. Physik 99, 300 (1936).
5. A. C. G. Mitchell and M. W. Zemansky, "Resonance Radiation and Excited Atoms." Macmillan, New York, 1934.
6. E. Trefftz, Z. Astrophys. 28, 67 (1950).
7. K. Ushpalis and I. Chiplis, Abstracts of reports given at the 13th All-Union Conference on Spectroscopy. Izd. Akad. Nauk SSSR, Moscow-Leningrad, 1960.
8. L. A. Vainshtein, Opt. i Spektr. 3, 313 (1957).
9. A. Eberhagen, Z. Physik 143, 392 (1955).
10. V. K. Prokof'ev, Zhur. Eksptl. i Teoret. Fiz. 1, 111 (1931).
11. G. Wessel, Z. Physik 26, 440 (1949); ibid. 30, 100 (1951).
12. H. N. Russell and C. E. Moore, J. Research Natl. Bur. Standards 55, 299 (1955).
13. Yu. I. Ostrovskii and N. P. Penkin, Opt. i Spektr. 9, 703 (1960), Optics and Spectroscopy 9, 371 (1960).
14. Yu. I. Ostrovskii and N. P. Penkin, Opt. i Spektr. 10, 8 (1961), Optics and Spectroscopy 10, 3 (1961).
15. Yu. I. Ostrovskii and N. P. Penkin, Opt. i Spektr. 10, 429 (1961), Optics and Spectroscopy 10, 219 (1961).

DETERMINATION OF THE EFFECTIVE CROSS SECTION FOR COLLISIONS OF EXCITI BARIUM IONS WITH ARGON ATOMS

F. S. Faizullov and N. N. Sobolev (pp. 571-576)

Received 26 December 1960

A method is proposed for determining effective cross sections for collisions of the second kind under gas-kinetic conditions. The method is based on temperature measurement by a generalized line reversal method. The effective cross section for a collision of the second kind of barium ions with argon atoms is found to be 4×10^{-17} cm^2.

A theoretical and experimental investigation of inelastic collisions among atomic systems presents great difficulties, especially at small relative velocities, i.e., in the nearly adiabatic region. Our present knowledge[1] does not permit a satisfactory prediction of even the order of magnitude of the effective cross section of an inelastic collision in the quasi-adiabatic region. For this reason, it can only be said that the effective cross section must be small in comparison to the gas-kinetic cross section. In order to establish an adequately based theory, it is necessary to conduct a systematic measurement of the effective cross sections of various collision processes among atoms and atomic ions over the widest possible range of relative velocities. However, it must be kept in mind that the measurement of small effective cross sections is an extremely complex matter. The use of beams of monoenergetic atoms or ions at such low energies is practically impossible. Until now, the only method available for measuring the effective cross sections of collisions of the second kind under gas-kinetic conditions has been the quenching of resonance fluorescence. However, the application of this method to the measurement of small effective cross sections is complicated considerably by the presence of Lorentz broadening. Therefore, the values for the effective cross sections of collisions of the second kind obtained by this method for weakly quenching gases, such as the inert gases, can only be considered as crude approximations.

In this paper, a new method is proposed for determining effective cross sections for collisions of the second kind under gas-kinetic conditions. The results of the measurements for collisions of barium ions with argon atoms are also given.

From pyrometric investigations of the state of argon behind a shock wave, we established[2] that the excitation temperature of a Ba ion, measured by the method of line reversal at "plug"* pressures of $p_2 \approx 0.4$ and 4 atm, is lower by 1000° and 400°, respectively, than the equilibrium temperature ($T_2 = 4500$°K) calculated on the basis of the conservation laws. With increasing pressure, the measured temperature approaches the equilibrium temperature, and at $p_2 \approx 12$ atm coincides with it. The divergence between the measured and equilibrium temperatures increases as the measured temperature increases.

*Russian term for region of hot gas between contact region and front of shock wave.

The observed drop of the experimental temperatures is apparently connected with the low efficiency of the collisions of the Ar atoms with the Ba ions, since an effect of this kind was not observed in air or nitrogen at these temperatures and pressures. The temperature of nitrogen and air behind a shock wave, measured by the line reversal method, coincided with the calculated tempe ature even at pressures of the order of tenths of an a mosphere. The equilibrium population of the excited level of an atom or an ion in the plasma can only be e tablished if the number of exciting collisions per sec (i.e., the number of collisions of the first kind) is pra tically equal to the number of collisions of the second kind, which transfers the atom or ion from an excited a lower level without radiation. The number of radiat transitions, i.e., the number of spontaneous transitio can be neglected. If the radiative transitions exceed nonradiative (for example, because of the minuteness the effective cross section for collisions of the secon kind), then the excited level will decrease in populati in comparison with the equilibrium population, and, c sequently, the temperature measured by the method o reversal of spectral lines will also decrease. This d crease in the line reversal temperature can be used determine effective cross sections for collisions of t second kind.

Let us examine this problem in more detail. Fol ing Biberman,[3] we will introduce the variable δ, whic characterizes the deviation of the observed populatio the excited level from the equilibrium population

$$\delta = \frac{\Phi_x}{\Phi_{x0}},$$

where Φ_x is the energy flux radiated by a given spect line through unit area at the "plug" boundary when t is a deviation from equilibrium and Φ_{x0} is the energy when the population of the level is at its equilibrium value. The value of δ appears to be a function of the ratio of the population of the excited level in the equi rium and nonequilibrium states, respectively. When absorption is absent, this function is simply equal to ratio of the populations; for high reabsorption (and w the form of the line is defined by the Doppler effect a collisions), the function is equal to the square root o this ratio.

When a deviation from equilibrium characterize the parameter δ occurs, a decrease in temperature will be observed. This decrease is defined by the ra

$$\frac{\Delta T_x}{T_x} = \frac{T_x - T_{x0}}{T_x} = \frac{\lambda T_{x0}}{C_2} \ln \delta.$$

Actually, for an equilibrium population at a temperat T_{x0}, the following flux should be observed

$$\Phi_{x0} \sim a \exp\left(-\frac{C_2}{\lambda T_{x0}}\right),$$

and for nonequilibrium population, the flux should be

$$\Phi_x \sim a \exp\left(-\frac{C_2}{\lambda T_x}\right),$$

re T_x is the corresponding temperature determined he spectrum-line reversal. Furthermore, it is as- ied that in both cases the coefficients of absorption .e., the populations of the lower level) are equal.

Having divided Φ_x by Φ_{x0}, we find the value of δ, and n go over to expression (2). It follows immediately m expression (2) that the temperature difference ΔT_x given δ (i.e., at the same deviation from equilibrium) reases with increasing temperature. At small T_x, this erence increases with the square of the temperature. s is qualitatively in satisfactory agreement with eriment. As was indicated above, ΔT_x actually does rease with increasing temperature.

From expression (2), it is possible to find δ, not n the flux ratio but from the equilibrium temperature the temperature determined by the reversal method nonequilibrium population. The values of δ corre- nding to our experimental conditions are given in the le.

T_x (°K)	δ	A_λ (A)	$N_i fl$ (cm^{-2})	N_i (cm^{-3})	$k_0 l$	β
3460	0.12	0.05	$5 \cdot 10^{11}$	$8 \cdot 10^{10}$	5.2	0.045
4160	0.57	0.55	$6 \cdot 10^{12}$	$9 \cdot 10^{11}$	6.2	0.4

The data given in the Table were obtained at the ilibrium temperature $T_{x0} = 4500°K$, calculated on the is of the conservation laws. Knowing δ, and with the of the relation[3]

$$\delta = \frac{\beta\sqrt{k_0 l}}{0.75 + \beta\sqrt{k_0 l}}. \qquad (3)$$

possible to find the value of $\beta = j/A$, which is the o of the probability for a transition caused by colli- ns of the second kind of an excited ion with surround- particles to the probability of spontaneous emission the 4554 A line[4] of Ba II, $A = 1.1 \times 10^8$ sec^{-1}). Here, s the index of absorption at the center of the spectral and l is the thickness of the radiating layer.

The quantity β, which characterizes the processes xcitation and quenching, serves as well as δ as a erion for proximity to the equilibrium concentration xcited ions. A small β value indicates that the popu- on of the excited level depends essentially on optical cesses, i.e., that the transition from the upper to the er level is mainly due to emission, and not to colli- ns of the second kind. At high β values, on the other d, collision processes predominate. As is seen from Table, β increases linearly with pressure. It follows m relation (3) that the deviation from equilibrium be- nes more significant as the value of $\beta\sqrt{k_0 l}$ decreases. both β and the optical density $k_0 l$ increase, the popu- ion of the excited level will approach the equilibrium ue.

Let us point out that the Biberman formula (3) was ived for a line of Lorentzian shape and a flat layer. s is the main reason for the approximateness of the sent calculations; in this real case, the shape of the line is determined by the Doppler effect and by colli- ns with electrons, atoms, and molecules. In order to ermine the value of β from relation (3), it is neces- y to know the value of k_0, i.e., to know the parameter $\Delta\lambda_L/\Delta\lambda_D$ and the concentration of optically active s $N_i f$. From experimental data obtained by measuring temperature by the generalized reversal method, it found that the total absorption A_λ of line Ba II 4554 A 'plug'' pressures of 0.4 and 4 atm amounts to 0.05 and 5 A respectively. According to the data in ref. 5, we will assume the parameter a to have a value between 1 and 10. (The parameter $a = \Delta\lambda_L/\Delta\lambda_D$ characterizes a line broadened by both Doppler effect and collisions.) Furthermore, knowing the Doppler half-width

$$\Delta\lambda_D = \frac{\lambda}{c}\sqrt{\frac{2kT}{\mu}} = 0.011 \text{ Å},$$

of Ba II 4554 at 4500°K, the value of $N_i fl$ can be found from total absorption curves[5] (this value will differ from the real value by not more than a factor of three because the value of a is not known accurately). Then from the formula

$$k_0 l = \frac{2e^2\lambda^2}{m_e c^2}\frac{N_i fl}{a\Delta\lambda_D}$$

the optical density for the center of the spectral line can also be calculated. Knowing $k_0 l$, one can find β using relation (3). The results of these calculations are also given in the Table.

It is seen from the Table that at a ''plug'' pressure ~ 0.4 atm, the number of transitions per second attributed to radiation is approximately 20 times greater than the number of transitions due to collisions of the second kind. At $p_2 \sim 4$ atm, the number of radiative transitions exceeds the number of nonradiative transitions by a factor of 2.5. As we have already stated, it is not until the pressure in the plug is ~ 12 atm, that the measured temperature differs from the equilibrium temperature by less than 100° (100° is the accuracy of our measurements). In this case, β is of the order of unity. Thus, to approach the equilibrium temperature within an accuracy of 100°, it is not necessary that $\beta \gg 1$. For this, it is sufficient that $\beta \geq 1$.

Let us now examine the problem of which kind of particles in collisions determine the population of the excited level under our experimental conditions. First of all, let us suppose that the excited ions of Ba collide with electrons. For this, we will calculate the value of $\beta_e = j_e/A$, where

$$j_e = N_e \int_0^\infty Q_e(\varepsilon) F(\varepsilon) v d\varepsilon \qquad (4)$$

is the probability of collisions of the second kind with electrons, N_e is the concentration of electrons,

$$F(\varepsilon) = \frac{2\pi\varepsilon^{1/2}}{(\pi kT)^{3/2}} \exp\left(-\frac{\varepsilon}{kT}\right)$$

is the Maxwell velocity distribution, $v = \sqrt{2\varepsilon/\mu}$ is the relative velocity, ε is the energy of colliding particles prior to collision, and μ is the reduced mass of the colliding particles.

Since there are no published data on the effective cross sections of the Ba ion, we will determine the effective cross section of a Ba ion for a collision of the second kind with an electron, using a quasi-classical approximation[4]:

$$Q_e(\varepsilon) = 578\pi a_0^2 \lambda^2 f_{\text{rad.}} \frac{\varepsilon_1}{\varepsilon_1 + \varepsilon},$$

where πa_0^2 is the area of the first Bohr orbit, λ is the emitted wavelength in microns, $f_{\text{rad.}}$ is the oscillator strength of radiation, and ε_1 is the excitation energy.

Substituting the last formula into expression (4) and integrating,[6] we obtain

$$j_e = 2.7 N_e f_{\text{rad.}} \lambda^2\theta\sqrt{kT}\,[\theta \exp\theta E_1(-\theta) + 1],$$

where $\theta = \varepsilon_1/kT$ and E_1 is the integral exponent. In our

case $\varepsilon_1 = 2.71$ ev, T = 4500°K, and $\theta = 7$. At such large values of θ, it is expedient to express the integral exponent in the form of an asymptotic series[6]

$$E_i(-\theta) = e^{-\theta} \sum_{k=1}^{n} (-1)^k (k-1)!\, \theta^{-k}.$$

Taking only the first three terms of the series, we obtain

$$i_e = 2.7 N_e f_{\text{rad.}} \lambda^2 (kT)^{1/2} \left[1 - \frac{2}{\theta}\right].$$

Substituting the corresponding numerical values[4] ($f_{\text{rad.}} = 0.333$), we find

$$i_e = 10^{-7} N_e \text{ сек.}^{-1} \text{ и } \beta_e = 10^{-15} N_e.$$

At the temperatures investigated, the electron concentration in the "plug" (N_e) is determined mainly by the quantity of barium introduced into the tube for the measurement, and can be assumed to be equal to the concentration of Ba ions, i.e., $N_e = N_1$. It follows from the Table that $N_1 \approx 10^{11}$-10^{12} particles* per cm^3 (for

*Hereinafter, when two values are given, they correspond to "plug" pressures of 0.4 atm and 4 atm, respectively.

l = 9.2 cm and[4] f = 0.666). The ionization of the N_2 (~ 0.01%) and O_2 (~ 0.01%) impurities and of the argon itself gives an electron concentration of ~ 10^{10}-10^{11} cm^{-3} at these temperatures, i.e., one order lower than ionization of Ba.

Thus, assuming the electron concentration N_e in the "plug" to be 10^{11}-10^{12} cm^{-3}, we obtain $\beta_e = 10^{-15}$, $N_e = 10^{-4}$-10^{-3}, since $x = 10^{11}$-10^{12}. We find that β_e is approximately two orders of magnitude lower than the experimental value (see Table). Consequently, collisions with electrons, because of their small concentration, cannot explain the observed concentration of excited Ba ions under the given conditions.

We will show that collisions with molecules of impurities (N_2 and O_2) are also insufficient to explain the observed drop of the temperatures.

In this case, we have

$$\beta_{N_2} = \frac{1}{A} 2 Q_{N_2} N_{N_2} \sqrt{\frac{2kT}{\pi}\left(\frac{1}{\mu_1} + \frac{1}{\mu_2}\right)},$$

Where Q_{N_2} is the effective cross section for quenching of the resonance radiation of the Ba ion by nitrogen (we neglect the quenching by the oxygen molecules because of their low concentration at these temperatures), and N_{N_2} is the concentration of N_2 molecules. Since the electron configuration of the Ba ion is similar to that of the alkali atoms, we can use the effective cross section for the quenching of the resonance radiation of sodium by nitrogen for the value of Q_{N_2}. This cross section is[1] 45.5×10^{-16} cm^2. Then, in accordance with the N_2 content of our argon ($N_{N_2} \approx 7 \times 10^{13}$-$7 \times 10^{14}$ cm^{-3}), we have $\beta_{N_2} \approx 6 \times 10^{-4}$-$6 \times 10^{-3}$.

Thus, if collisions with electrons and molecules played an important role, the deviations from equilibrium would be much greater than those actually observed.

Only one possibility remains for explaining the processes of excitation and quenching under the given conditions. This is the collision of Ba ions with Ar atoms. If this is the case, then using the values of β obtained from the experimental data (see Table), it is possible to find the effective cross-section for the quenching of the resonance radiation of Ba ion by argon. This cross section is

$$Q_{Ar} = \frac{A\beta}{2N_{Ar}\sqrt{\frac{2kT}{\pi}\left(\frac{1}{\mu_1} + \frac{1}{\mu_2}\right)}}.$$

Substituting the corresponding numerical values ($N_{Ar} = 7 \times 10^{17}$-$7 \times 10^{18}$ cm^{-3}) at T = 4500°K, we obtain $Q_{Ar} \approx 4 \times 10^{-17}$ cm^2, i.e., the effective cross section for collisions of the second kind is two orders of magnitude lower than the gas-kinetic cross section. This value agrees in order of magnitude with the effective cross section for the extinguishing of the resonance radiation of mercury by argon atoms.[7]

Thus, the inert gas argon has a very weak quenching effect, but its effectiveness is not zero, as some authors have supposed. The inert gases cannot participate in chemical reactions and they also cannot take up an electron or vibrational energy. However, when the distance between nuclei are small, the potential curves of the Bå-Ar and Bå*-Ar systems can come so close to each other that the transition from one to the other is possible. At this close an approach, the energy levels of the ions are so strongly excited by the interaction, even with the atoms of an inert gas, that the difference between the energy of the excited and the unexcited ion practically does not exist, and the transition from one to the other consists only in the rearrangement of the electron configuration. Since these transitions occur at very small internuclear distances, the effective cross section for this kind of quenching collision is very small.[8] As Bates observed,[10] the cross section can increase considerably on account of the increased time of interaction when an atom passes an ion and the axis of interaction is rotated.

It seems to us that the development of the described method for determining the effective cross sections of collisions of the second kind is very promising since, in a shock-tube, comparatively pure experimental conditions can be realized. In planning future work on the measurement of effective cross sections for collisions of the second kind by the proposed method, it is logical to turn first to systems which have already been measured by the method of quenching of resonance fluorescence. For example, a measurement of the effective cross section for the collision of a nitrogen molecule or an argon atom with the excited atom of sodium suggests itself. Of course, the measurements of the effective cross section of the collisions of nitrogen molecules with sodium must be conducted at pressures of less than 0.1 atm behind the shock wave. Under this condition, the radiation in the resonance line of sodium will play a predominant part when compared with that of collisions of the second kind.

REFERENCES

1. H. S. W. Massey and E. H. S. Burhop, "Electron and Ionic Impact Phenomena." Oxford Univ. Press, 19[illegible] Foreign Literature Press, Moscow, 1958.
2. F. S. Faizullov, N. N. Sobolev, and E. M. Kudryavtsev, Opt. i Spektr. 8, 761 (1960), Optics and Spectroscopy 8, 400 (1960).
3. L. M. Biberman, Doctoral dissertation, MEI, 1958.
4. C. W. Allen, "Astrophysical Quantities." Univ. of London, Athlone Press, London, 1955.
5. N. N. Sobolev, Trudy Fiz. Inst. SSSR 7, 159 (1956).
6. E. Jahnke and F. Emde, "Tafeln hoherer Funktionen (Tables and Functions), 5th ed., Tuebner, Leipzig, 1952. Physics and Mathematics Press, Moscow, 19[illegible]

L. O. Olsen, Phys. Rev. 60, 739 (1941).
P. Pringsheim, "Fluorescence and Phosphorescence." Interscience, New York, 1949. Foreign Literature Press, Moscow, 1951.
9. J. G. Clouston, A. G. Gaydon, and I. R. Hurle, Proc. Roy. Soc. A252, 143 (1959).
10. J. R. Bates, private communication.

VIBRATIONAL SPECTRA OF AROMATIC COMPOUNDS
XI. Calculation of Intensities in the Infrared Spectrum of Toluene

B. N. Snegirev (pp. 577-583)

Received 7 December 1960

Using the first approximation of the valence-optical scheme, we have carried out a calculation of the band intensities in the infrared spectrum of toluene and have predicted the values of the integrated intensities for the characteristic bands of the monoalkylbenzenes.

TERMINATION OF THE DERIVATIVES OF THE MOLECULAR DIPOLE MOMENT WITH RESPECT TO THE NORMAL COORDINATES

A calculation of the derivatives, p'_k, of the dipole moment of the toluene molecule with respect to the normal ordinates has been completed in the zeroth and the st approximations of valence-optical theory.[1] In the culation, we used formulas from ref. 1, formula (1) m ref. 2, the relation $A(L^{-1})' = L$, and the symmetry ordinates from ref. 3 with the same numbers (L and are the matrices of the normalized form coefficients the vibrations and of the kinematic coefficients in se coordinates).

In the zeroth approximation, the result of the computation has the form

$$A_1: \quad p'_k(0,\ a_k^{A_1},\ 0);$$
$$B_1: \quad p'_k(a_k^{B_1},\ 0,\ 0);$$
$$B_2: \quad p'_k(0,\ 0,\ a_k^{B_2}),$$

ere

$$a_k^{\varkappa} = (a_k^{\varkappa})_{\text{str.}} + (a_k^{\varkappa})_{\text{def.}} \quad (\varkappa = A_1,\ B_1,\ B_2),$$

$$(a_k^{A_1})_{\text{str.}} = \frac{\mu_q'^{CH_3}}{\sqrt{3}} L_k^{13} + \frac{\mu_q'}{\sqrt{2}}(L_k^4 - L_k^5 - \sqrt{2}\,L_k^6) + \mu'_{Q_0} L_k^7,$$

$$(a_k^{B_1})_{\text{str.}} = \frac{2}{\sqrt{3}} \mu_q'^{CH_3} L_k^{13} - \sqrt{\frac{3}{2}}\,\mu_q'(L_k^3 + L_k^4),$$

$$(a_k^{B_2})_{\text{str.}} = \frac{2}{\sqrt{3}} \mu_q'^{CH_3} L_k^9,$$

d k is the number of the normal vibration.

Vibrations of symmetry type A_2 are inactive in the frared spectrum. The quantities μ'_q and μ'_{Q_0} are the rivatives of the dipole moments of the CH and C—C nds with respect to their lengths, and $\mu'_q CH_3$ is the alogous derivative for the CH bonds of the methyl oup.

$$(a_k^{\varkappa})_{\text{def.}} = \frac{1}{r_0} \sum_{\lambda} f_\lambda \sum_{l} C_{\lambda l}^{\varkappa} (L^{-1})_l^k,$$

ere λ is the number of the electro-optical parameter l is the symmetry coordinate, and $r_0 = 1.09$ A (unit of ngth).

The values of $c_{\lambda l}^{\varkappa}$ are presented in Table 1.

$$(a_k^{A_1})_{\text{def.}} = \frac{4}{\sqrt{6}} \frac{\mu_q^{CH_3}}{r_0} L_k^{12} + \frac{\mu_q}{r_0}\left[\frac{3r_0}{\sqrt{2}\,s}(L_k^2 - L_k^3) + \right.$$
$$\left. + \frac{\sqrt{3}}{2}(L_k^8 - L_k^9) + \sqrt{\frac{3}{2}}\,(L_k^{10} - L_k^{11})\right],$$

$$(a_k^{B_1})_{\text{def.}} = \frac{\mu_q^{CH_3}}{r_0}\left(G_1 + \sqrt{\frac{2}{3}}\,L_k^{11} - \sqrt{\frac{2}{3}}\,L_k^{12}\right)$$
$$+ \frac{\mu_q}{r_0}\left[-\sqrt{2}\,(L_k^5 + L_k^6) - \frac{1}{\sqrt{2}}(L_k^7 + L_k^8)\right.$$
$$\left. + \frac{1}{\sqrt{2}}(L_k^9 + L_k^{10}) - G_1\right] + \frac{\mu_{Q_0}}{r_0} G_1,$$

$$(a_k^{B_2})_{\text{def.}} = \frac{\mu_q^{CH_3}}{r_0}\left(-\sqrt{\frac{2}{3}}\,L_k^7 - \sqrt{\frac{2}{3}}\,L_k^8 + G_2\right)$$
$$+ \frac{\mu_q}{r_0}(\sqrt{6}\,L_k^4 - G_2) + \frac{\mu_{Q_0}}{r_0} G_2,$$

$$G_1 = \sum_{l=1}^{13} {}^{B_1}X_{3l2}\,{}^{B_1}L_k^l, \qquad G_2 = \sum_{l=1}^{9} {}^{B_2}X_{3l2}\,{}^{B_2}L_k^l.$$

The values of X_{3l2} are presented in ref. 3. μ_q and μ_{Q_0} are the dipole moments of the CH and C—C bonds,*

*The direction from the C atom of the ring to the C atom of the CH_3 group is taken as the positive direction of μ_{Q_0}.

$\mu_q^{CH_3}$ is the analogous quantity for the CH bonds of the methyl group, and s is the length of the aromatic CC bond.

As has been shown in refs. 4-6, the zeroth-approximation formulas for the components p'_k cannot be used directly for the calculation of intensities. A self-consistent calculation of the latter can be accomplished only if one takes account of the first-approximation corrections. The electro-optical parameters thus obtained must be found from the experimental values of the band intensities in the infrared spectrum. However, such data are lacking for the majority of the toluene bands. Furthermore, the actual determination of the electro-optical parameters for toluene on this basis would be associated with great difficulties on account of the large number of possibilities for the signs of the quantities p'_k.

Therefore, we were forced to make a simplifying assumption: that the difference of the first-approximation electro-optical parameters for toluene from those for benzene and ethane is small; this permitted us to use

Table 1. Values of $c^{\kappa}_{\lambda l}$ in Dimensionless Quantities*

$c^{\kappa}_{\lambda l}$

κ	A_1		B_1			B_2		
λ \ l	$\mu_q^{CH_3}$	μ_q	$\mu_q^{CH_3}$	μ_q	μ_{Q_0}	$\mu_q^{CH_3}$	μ_q	μ_{Q_0}
1	0	0	0	$-\frac{\sqrt{3}}{2\sqrt{2}}\varepsilon$	0	$-\frac{5}{3\sqrt{3}}\varepsilon\sigma_0$	$-\frac{\sigma_H}{\sqrt{3}}[\sigma_H+\varepsilon(\sigma+\sigma_H)]$	$\frac{1}{\sqrt{3}}\varepsilon\sigma_0(2\sigma_0+$
2	0	$-\frac{3}{2\sqrt{2}}\varepsilon$	0	$\frac{\sqrt{3}}{2\sqrt{2}}\varepsilon$	$-\frac{\sqrt{3}}{\sqrt{2}}\varepsilon\sigma_0$	$\frac{5}{3\sqrt{6}}\varepsilon\sigma_0$	$\frac{\sigma_H}{\sqrt{6}}[\sigma_H+\varepsilon(4\sigma+\sigma_H)]$	$-\frac{\sqrt{2}}{\sqrt{3}}\varepsilon\sigma_0(\sigma_0-$
3	0	$\frac{3}{2\sqrt{2}}\varepsilon$	0	0	0	0	$-2\sqrt{2}\,\varepsilon\sigma\sigma_H$	$2\sqrt{2}\,\varepsilon\sigma\sigma_0$
4	0	0	0	0	0	$-\frac{5}{3\sqrt{6}}\varepsilon\sigma_0$	$\frac{5}{\sqrt{6}}(1+\varepsilon)\sigma_H^2$	$\frac{\sqrt{2}}{\sqrt{3}}\varepsilon\sigma_0^2$
5	0	0	0	$\frac{\varepsilon\sigma}{2\sqrt{2}}$	$\frac{\varepsilon\sigma\sigma_0}{\sqrt{2}}$	$-\frac{5}{3\sqrt{3}}\varepsilon\sigma_0$	$-\frac{\sigma_H}{\sqrt{3}}[\sigma_H+\varepsilon(3\sigma+\sigma_H)]$	$\frac{\varepsilon\sigma_0}{\sqrt{3}}(2\sigma_0+$
6	0	0	0	$\frac{3}{2\sqrt{2}}\varepsilon\sigma$	0	0	$-\frac{4}{\sqrt{3}}\varepsilon\sigma\sigma_H$	$\frac{4}{\sqrt{3}}\varepsilon\sigma\sigma_0$
7	$-\frac{8}{3}\varepsilon$	0	0	$-\frac{1}{\sqrt{2}}\left(\frac{\varepsilon\sigma}{2}+\varepsilon+1\right)$	$-\frac{\varepsilon\sigma\sigma_0}{\sqrt{2}}$	$-\frac{2\sqrt{2}}{3\sqrt{3}}(3+5\varepsilon)$	0	$\frac{2\sqrt{2}}{\sqrt{3}}\varepsilon\sigma_0$
8	0	$\frac{\sqrt{3}}{2}\varepsilon\sigma$	0	$-\frac{1}{\sqrt{2}}\left(\frac{3\varepsilon\sigma}{2}+\varepsilon+1\right)$	0	$-\frac{1}{3\sqrt{6}}[3+5\varepsilon(1+3\sigma_0)]$	0	$\frac{\varepsilon\sigma_0}{\sqrt{6}}(1+6$
9	0	$-\frac{\sqrt{3}}{2}\varepsilon\sigma$	0	$\frac{1}{\sqrt{2}}\left[2(1+\varepsilon)+\frac{3}{2}\varepsilon\sigma\right]$	0	$\frac{10}{3\sqrt{3}}\varepsilon$	0	$-\frac{2}{\sqrt{3}}\varepsilon\sigma$
10	0	$\frac{\sqrt{3}}{\sqrt{2}}(\varepsilon\sigma+\varepsilon+1)$	$-\frac{5\sqrt{2}}{3}\varepsilon\sigma_0$	$\frac{\varepsilon\sigma}{2\sqrt{2}}$	$\frac{\varepsilon\sigma_0}{\sqrt{2}}(4\sigma_0+\sigma)$	—	—	—
11	0	$-\frac{\sqrt{3}}{\sqrt{2}}(\varepsilon\sigma+\varepsilon+1)$	$\frac{2\sqrt{2}}{3\sqrt{3}}(3+5\varepsilon)$	0	$-\frac{2\sqrt{2}}{\sqrt{3}}\varepsilon\sigma_0$	—	—	—
12	$\frac{2\sqrt{2}}{3\sqrt{3}}(3+8\varepsilon)$	0	$-\frac{1}{3\sqrt{6}}[3+5\varepsilon(1+3\sigma_0)]$	0	$\frac{\varepsilon\sigma_0}{\sqrt{6}}(1+6\sigma_0)$	—	—	—
13	$\frac{8}{3\sqrt{3}}\varepsilon$	0	$\frac{10}{3\sqrt{3}}\varepsilon$	0	$-\frac{2}{\sqrt{3}}\varepsilon\sigma_0$	—	—	—

*Numerical values are presented in ref. 3.

the numerical values found for them in refs. 6-8. On this assumption, the first-approximation formulas have the form:

$$A_1: \quad \mathbf{p}'_k(0,\ b_k^{A_1},\ 0),$$

$$b_k^{A_1}=\frac{(\mu_q'^{CH_3}+\Delta_1)}{\sqrt{3}}L_k^{13}+\frac{A}{\sqrt{2}}(L_k^4-L_k^5-\sqrt{2}\,L_k^6)+(\mu'_{Q_0}+\Delta_2)L_k^7+$$
$$+\frac{4}{\sqrt{6}}\frac{(\mu_q^{CH_3}+\Delta_3)}{r_0}L_k^{12}+\frac{3}{2\sqrt{2}\,s}\frac{(B+C)}{r_0}(L_k^2-L_k^3)+$$
$$+\frac{\sqrt{3}}{2}\frac{C}{r_0}[L_k^8-L_k^9+\sqrt{2}\,(L_k^{10}-L_k^{11})];$$

$$B_1: \quad \mathbf{p}'_k(b_k^{B_1},\ 0,\ 0)$$

$$b_k^{B_1}=\frac{2}{\sqrt{3}}(\mu_q'^{CH_3}+\Delta_4)L_k^{13}-\sqrt{\frac{3}{2}}\,A(L_k^3+L_k^4)$$
$$-\sqrt{\frac{2}{3}}\frac{(\mu_q^{CH_3}+\Delta_5)}{r_0}L_k^{12}+$$
$$+\frac{\mu_q^{CH_3}}{r_0}\left(G_1+\sqrt{\frac{2}{3}}\,L_k^{11}\right)-\frac{1}{2\sqrt{2}}\frac{(3B+C)}{r_0}(L_k^5+L_k^6)-$$
$$-\frac{C}{\sqrt{2}\,r_0}(L_k^7+L_k^8-L_k^9-L_k^{10})-\frac{G_1}{r_0}(\mu_q-\mu_{Q_0});$$

$$B_2: \quad \mathbf{p}'_k(0,\ 0,\ b_k^{B_2}),$$

$$b_k^{B_2}=\frac{2}{\sqrt{3}}(\mu_q'^{CH_3}+\Delta_4)L_k^9-\sqrt{\frac{2}{3}}\frac{(\mu_q^{CH_3}+\Delta_5)}{r_0}L_k^8$$
$$+\frac{\mu_q^{CH_3}}{r_0}\left(-\sqrt{\frac{2}{3}}\,L_k^7+G_2\right)+$$
$$+\frac{\mu_q}{r_0}(\sqrt{6}\,L_k^4-G_2)+\frac{\mu_{Q_0}}{r_0}G_2.$$

A, B, and C are the electro-optical parameters of benzene, in the first approximation. Δ_1 to Δ_5 are the first approximation corrections. In view of the fact that the expressions for them are cumbersome, we shall not present them in explicit form.

THE NUMERICAL CALCULATION OF THE INTENSITIES

In the numerical calculation of the intensities, the values of the electro-optical parameters from ref. 6 were used: A = −0.48D/A, B = 0.40D, C = 0.34D; also those from refs. 7 and 8:

$$\mu_q'^{CH_3}+\Delta_1=-1.24, \qquad \mu_q'^{CH_3}+\Delta_4=-0.75,$$
$$\frac{(\mu_q^{CH_3}+\Delta_3)}{r_0}=0.23, \qquad \frac{(\mu_q^{CH_3}+\Delta_5)}{r_0}=0.36,$$
$$\frac{\mu_q^{CH_3}}{r_0}=0.26, \qquad \frac{\mu_q}{r_0}=0.60\,\frac{D}{\text{Å}}.$$

The parameter $\mu'_{Q_0}+\Delta_2$ was found from the experimental data for the intensity of the ν = 1211 cm^{-1} band.[9] We did not use the other frequency (ν = 1030 cm^{-1}) on account of the smallness of the form coefficie for the parameter being determined. Two values were found for $\mu'_{Q_0}+\Delta_2$: 0.31 and −2.10D/A. Both values we used in the calculation of the intensities (see Table 2).

The parameter μ_{Q_0} was found from the experimer value for the dipole moment of the whole toluene molecule, μ = 0.34D,[10] and the quantities[6] μ_q = 0.65D and μ

ble 2. Calculated Values of the Integrated Intensities for Toluene, and Experimental ε Values for the Monoalkylbenzenes

$\nu_{expt.}$ (cm^{-1})	ln J (units of J: 10^{-7} cm^2 mol^{-1} sec^{-1}) Expt.[9]	Calculated (for $\mu Q_0 + \Lambda_2$ D/A:) 0.31	−2.10	ε ($cm^2 \cdot mol^{-1}$) (x = cell thickness (mm))[15]
		A_1		
521	—	0.00	0.05	—
786	—	0.00	0.30	—
1004	—	0.00	0.02	—
1030	0.21	0.14	0.21	20 (x = 0.05)
1181	—	0.00	0.00	5 (x = 0.2)
1211	0.25	0.25	0.24	—
1380	—	0.21	0.87	—
1504	—	0.24	0.88	100 (x = 0.01)
1605	—	0.00	0.19	20 (x = 0.01)
2920	—	1.03	0.70	—
3054	—	0.05	0.05	—
3067	—	0.02	0.02	—
3086	—	0.90	0.91	—
		B_1		
346		0.00		—
623		0.00		—
970		0.10		—
1081		0.25		—
1155		0.01		4 (x = 0.2)
1278		0.06		—
1311		0.02		—
1439		0.04		—
1460		0.15		—
1586		0.04		—
2980		1.44		—
3032		0.00		—
3074		1.45		—
		B_2		
217		0.05		—
465		0.24		—
690		1.00		200 (x = 0.005)
730		2.39		—
895		0.06		9 (x = 0.05)
993		0.00		—
1041		0.31		—
1460		0.04		—
2980		1.52		—

29D.[8] The value found for μ_{Q_0} equals 0.03D. Another lue (0.71D) was discarded as being unrealistic.

The intensity was found according to the formula $3mc)(p'_k)^2$. The form coefficients of the vibrations, ich were necessary for the calculation, are presented ref. 11.

The results of the computations are represented in ble 2.

SCUSSION OF THE RESULTS OF THE CALCULATION

It can be seen from Table 2 that, for A_1, the value $_0 + \Delta_2 = -2.10$D/A leads to good agreement with the perimental data[9] on the integrated intensities for the o bands ν = 1030 and 1211 cm^{-1}, and it is to be pre-red to the value 0.31D/A. Quantitative experimental a on the integrated intensities for all the other bands the infrared spectrum of toluene are unknown to us, the computed integrated intensities are in satisfac-y agreement with the numerous experimental data of alitative character.[12-16] Thus, for example, the most ense bands are the bands with the frequencies 690, 730, 1504, and 3074 cm^{-1}, which corresponds to the results of our calculation. For the bands characterized by low intensity, the computed values are also small.

Using the data obtained[17] with regard to the vibrations characteristic in frequency and form, one can find the values for the integrated absorption intensities of the characteristic bands in the spectra of monosubstituted benzenes. It should be noted that this can be done only on condition that constancy of the electro-optical parameters is maintained (for the most essential form coefficients of the vibrations) for a series of these compounds. Thus the data of Table 2 enable one to predict the values of the integrated absorption intensities of the characteristic bands of the monoalkylbenzenes. For an orienting qualitative comparison of the results of the calculation with experiment, data[15] are presented in Table 2 on the values of the absorption coefficient ε at the maxima of the characteristic bands of the monoalkylbenzenes. Comparison shows that the results of the calculation and of experiment are in satisfactory agreement with each other.

In conclusion, I offer my thanks to M. A. Kovner for his interest in this work.

REFERENCES

1. M. V. Vol'kenshtein, M. A. El'yashevich, and B. I. Stepanov, "Molecular Vibrations," vol. 2. State Press for Technical and Theoretical Literature, Moscow, 1949.
2. B. N. Snegirev and M. A. Kovner, Opt. i Spektr. 8, 880 (1960), Optics and Spectroscopy 8, 462 (1960).
3. M. A. Kovner and B. N. Snegirev, Opt. i Spektr. 7, 487 (1959), Optics and Spectroscopy 7, 309 (1959).
4. L. M. Sverdlov, Opt. i Spektr. 4, 697 (1958).
5. L. M. Sverdlov, Opt. i Spektr. 6, 729 (1959), Optics and Spectroscopy 6, 477 (1959).
6. M. A. Kovner and B. N. Snegirev, Opt. i Spektr. 10, 328 (1961), Optics and Spectroscopy 10, 165 (1961).
7. L. M. Sverdlov, Opt. i Spektr. 7, 21 (1959), Optics and Spectroscopy 7, 11 (1959).
8. I. M. Nyquist, I. M. Mills, W. B. Person, and B. L. Crawford, J. Chem. Phys. 26, 552 (1957).
9. R. R. Randle and D. H. Whiffen, Trans. Faraday Soc. 52, 9 (1956).
10. M. V. Vol'kenshtein, "Structure and Physical Properties of Molecules." Academy of Sciences of the USSR Press, Moscow-Leningrad, 1955.
11. M. A. Kovner and B. N. Snegirev, Opt. i Spektr. 9, 170 (1960), Optics and Spectroscopy 9, 90 (1960).
12. N. Fuson, C. Garrigou-Lagrange, and M. L. Josien, Spectrochim. Acta 16, 106 (1960).
13. Landolt-Börnstein, "Zahlenwerte und Funktionen," 2 Teil, "Molekeln." Berlin, 1951.
14. L. J. Bellamy, "Infrared Spectra of Complex Molecules." Wiley, New York, 1954. Foreign Literature Press, Moscow, 1957.
15. "Physico-Chemical Properties of Individual Hydrocarbons." State Press for Technical and Theoretical Literature, Moscow, 1957.
16. W. West, ed., "Application of Spectroscopy to Chemistry." Foreign Literature Press, Moscow, 1959. Interscience, New York.
17. A. M. Bogomolov, Opt. i Spektr. 9, 311 (1960), Optics and Spectroscopy 9, 162 (1960).

VIBRATIONAL SPECTRA OF SILICATES
III. Infrared Spectra of the Pyroxenoids and Other Chain Metasilicates

A. N. Lazarev and T. F. Tenisheva (pp. 584-587)

Received 13 December 1960

The infrared absorption spectra of silicates containing infinite chain anions of the type $[(SiO_3)_n]_\infty$ with n = 3, 5, and 7 have been investigated. Decision about the size of the repeating unit of the chain on the basis of spectroscopic data is shown to be possible.

In a foregoing communication,[1] devoted to the spectra of chain metagermanates and metasilicates with the anions $[(XO_3)_n]_\infty$ (n = 1, 2), it was shown that the "one-dimensional crystal" model enables one to interpret satisfactorily the spectrum in the frequency region of the stretching vibrations of the chain. It was therewith supposed that the number of bands of vibrations of the type ν_s (XOX), which are so located in the spectrum as to be isolated from the bands corresponding to other vibrations of the chains, enables one to judge of the number of linked XO_4 tetrahedra within the repeating unit of the chain. Since the existence of silicate chains containing three, five, and seven tetrahedra within the repeating unit has recently been shown by x-ray structural investigations, it was of interest to examine the infrared spectra of these materials with the purpose of establishing the possibility of determining the structure of such chains by spectroscopic methods.

We have investigated the infrared spectra of wollastonite (β-$CaSiO_3$) (synthetic and natural), rhodonite ((Mn, Ca)SiO_3), and pyroxmangite ((Mn,Fe)SiO_3).*

*The pyroxmangite sample was kindly furnished to us by Kh. S. Mamedov and the wollastonite samples by A. I. Boikova. The rhodonite samples were obtained from the Mineralogical Museum of the USSR Academy of Sciences. Many of the samples of the natural minerals contained a considerable quantity of CO_3 ions, the absorption bands of which can usually be identified quite easily (around 1410-1440, 1060, 870, and 700-710 cm^{-1}). In the curves of Fig. 2, these bands are excluded as far as possible. To identify the bands of the carbonate ion, some rhodonite samples were treated with HCl.

The structure of the silicon-oxygen chains in these silicates is shown schematically in Fig. 1, according to the data of the x-ray structural investigations.[2-4] One may expect that, as the number of silicon-oxygen tetrahedra in the repeating unit of the chain increases, an increase in the number of bands in the frequency region of the ν_s(SiOSi) vibrations will take place. In this connection, the low symmetry of the chains should not impose any limitations on the selection rules. Actually, in the wollastonite spectrum (Fig. 2, Table 1), three narrow bands of medium intensity are observed in the 560-680 cm^{-1} interval; they may probably be ascribed to the three ν_s(SiOSi) vibrations of a chain of the type $[(SiO_3)_3]_\infty$. Transition to the rhodonite spectrum ($[(SiO_3)_5]_\infty$ chains) leads to an increase in the number of frequencies in this region; however, instead of the five bands anticipated in the spectrum, six are observed. It is possible that one of these frequencies originates in an impurity or, which is more probable, that it is produced by a splitting of the internal vibrations of the anion under the influence of interactions in the crystal lattice. Finally, in the spectrum of pyroxmangite with $[(SiO_3)_7]_\infty$ chains, the number of ν_s(SiOSi) bands increases to seven. In the 1100-900 cm^{-1} region in the spectra of all the compounds, there is observed a group of intense bands, in which six or seven maxima can be distinguished; however, a detailed assignment of the numerous close-lying ν_{as}(SiOSi), ν_{as}(O^-S and ν_s(O^-SiO^-) vibration frequencies is hardly possible. The bands near 500 cm^{-1} and lower may be associated with vibrations of the cations and deformation vibrations of the chains.

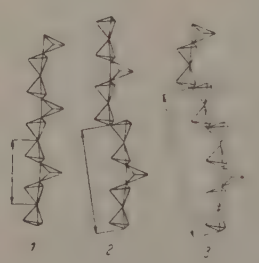

Fig. 1

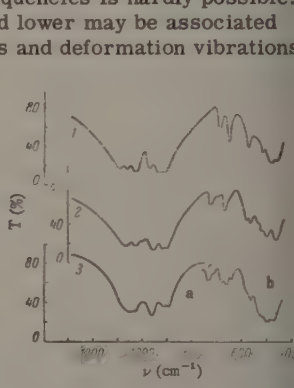

Fig. 2

Fig. 1. Schematic drawing of the silicate chains $[(SiO_3)_n]_\infty$ in various crystals. 1—wollastonite (n = 3). 2—rhodonite (n = 5). 3—pyroxmangite (n = 7).

Fig. 2. Infrared absorption spectra of wollastonite (curve 1), rhodonite (curve 2), and pyroxmangite (Glen Beag, Scotland) (curve 3). Samples: pressed KBr discs of diameter 25 mm and total weight 2 gm. Quantity of substance under study in disc (mg): curve 1—5; curve 2—5; curve 3a—2.5; curve 3b—5.

The structure of bustamite ((Ca,Mn)SiO_3) has not been completely deciphered, but it is supposed (on the basis of the similarity in the parameters of the unit cell) to be like the structure of wollastonite.[5] We have investigated the absorption spectra of a whole series of bustamite samples (obtained from the Mineralogical Museum of the USSR Academy of Sciences and the Museum of the Mining Institute). The spectrum corresponding to the purest samples is presented in Fig. 3 (curve 1) (for the frequency values, see Table 1). In the 750-550 cm^{-1} region there are observed two distinct but quite weak bands on a "shoulder" on the slope of the much stronger absorption around 500 cm^{-1}. One may suppose that these three frequencies, as in the case of wollastonite, testify to the presence of chains of the type $[(SiO_3)_3]_\infty$. At the same

Table 1.* Frequencies in the Infrared Spectra of Metasilicates

Vibration	Compound: Wollastonite β-$CaSiO_3$	Bustamite** $(Ca, Mn)SiO_3$	Pyroxmangite $(Mn, Fe)SiO_3$	Rhodonite $(Mn, Ca)SiO_3$
	Structure of the chain (anion): $[(SiO_3)_3]_\infty$		$[SiO_3]_\infty$	$[(SiO_3)_5]_\infty$
	1087 (vs) vs	1086 (sh, s)	1080 (sh, s) 1063 (vs)	1077 (sh, s) 1050 (vs)
... (O⁻SiO⁻), ... (SiOSi), ... (O⁻SiO⁻)	1056 (vs) 1019 (vs) 964 (vs)	1062 (vs) 979 (vs) 951 (vs)	1023 (vs) 998 (s 954 (vs)	1027 (vs) 959 (vs) 946 (sh?
	925 (vs) 904 (vs)	911 (vs) 872 (vs) 850 (sh, s) 803 (m	916 (vs) 900 (vs)	908 (vs) 890 (s
			720 (m)	732 (m) 710 (sh, w)
... (SiOSi)	680 (m) 642 (m) 566 (m)	660 (m) 619 (m) 560 (sh?)	690 (w) 661 (m) 638 (sh, w) 577 (m) 559 (m)	676 (m) 658 (m) 637 (m) 579 (sh, m) 561 (s)
... (Si—O), ... (M—O)	508 (m) 471 (vs) 452 (vs)	525 (sh?) 510 (vs) 465 (vs) 450 (sh, m)	532 (m) 514 (m) 492 (vs) 458 (vs)	523 (s) 496 (vs) 468 (vs)

*The symbols ν_s and ν_{as} fix the character of the corresponding vibration in the ...lated SiOSi or OSiO group.
Band intensities: vw – very weak, w – weak, m – medium intensity, s – strong, ... – very strong, sh – "shoulder" against the background of a neighboring more intense ...d.
**See Fig. 3, curve 1.

...ie, the intensity distribution of these three bands, which different from the case of wollastonite, and the lack of ...milarity between the spectra of these compounds in the ...00-800 cm^{-1} region apparently indicate substantial dif...rences between the crystal structures of wollastonite ...d bustamite. It has already been noted in the litera...re that these differences probably reduce to a different ...sition of the chains and (or) cations.[5] For more reli...le judgments on the structure of bustamite, an investi...tion of the spectrum of the synthetic product, free ...m impurities (and possessing well-formed crystals), desirable.

The spectrum of a typical sample of natural busta...te, containing a considerable admixture of rhodonite ...d CO_3^{--} ions), as can easily be seen by juxtaposition the spectra, is also presented in Fig. 3 (curve 2), il...strating in particular the convenience of using the 550-...0 cm^{-1} region for purely analytical purposes.

Chains containing three XO_4 tetrahedra per repeating ...it are present in the crystals of certain germanates ...particular, calcium metagermanate ($CaGeO_3$)), as is

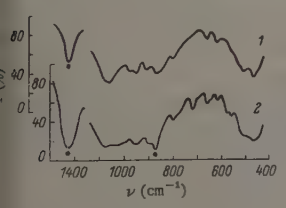

Fig. 3

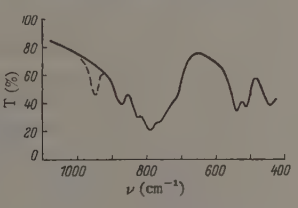

Fig. 4

Fig. 3. Infrared absorption spectra of bustamite ($(Ca,Mn)SiO_3$). Curve 1—sample from Belogorsk; curve 2—sample from Monte Civillina, Italy. Bands of the CO_3 ion are marked by stars. Quantity of substance under study in KBr disc—5 mg.

Fig. 4. Infrared absorption spectrum of $CaGeO_3$. Quantity of substance under study in KBr disc—5 mg.

supposed in the works of Liebau.[6] The absorption spectrum of $CaGeO_3$ is presented in Fig. 4.* Comparison with the spectra of the alkali metal germanates, which have $[(GeO_3)_2]_\infty$ chains,[1] enables one to propose the following frequency assignment, which agrees with the supposition of the existence of chains of the type $[(GeO_3)_3]_\infty$ in this compound (Table 2).

*$CaGeO_3$ was synthesized at 1450°C in a platinum crucible; $CaCO_3$ and GeO_2 were taken in the stoichiometric ratio. The fact that the quantity of impurities was small was established by a microscopic examination conducted by A. I. Boikova. One may suppose that the band around 948 cm^{-1}, shown dotted in Fig. 4, originates in an impurity, since its intensity varied greatly from sample to sample.

A structure of the pseudowollastonite type, i.e., with "triple" $[Ge_3O_9]^{6-}$ rings, has been ascribed to strontium metagermanate ($SrGeO_3$) by Liebau and certain other authors.[6,7] However, the spectrum of $SrGeO_3$ obtained by dehydration of SrH_2GeO_4 at 550°C, as presented in ref. 8, is very close to the spectrum of $CaGeO_3$, which testifies to a chain structure for the anion. One may suppose that Liebau's data relate to the high-temperature form of $SrGeO_3$, which, as will be shown in our next communication, actually does contain Ge_3O_9 rings.

Thus the experimental data which we have obtained apparently confirm the quasi specificity of the 750-550 cm^{-1} frequency region for ν_s(SiOSi) vibrations in silicate chains, and the possibility of determining the structure type of a chain (the number of tetrahedra in the repeating unit) by tabulating the number of bands in this region of the spectrum. However, on considering chains with a large number (five or more) of silicon-oxygen tetrahedra in the repeating unit, the distances between the bands become insignificant (and the intensities of the separate bands diminish), which does not always permit one to delimit the effects produced by interactions within the chains and between them (and the cations).

Table 2.* Frequency Assignment in the Spectra of Germanates

ν_s (GeOGe)	ν_s (O–GeO–), ν_{as} (O–GeO–), ν_{as} (GeOGe)
445 s, 516 s, 542 s (c)	725 sh?, 765 vs, 791 vs, (c. c.), 826 s, 874 s, 894 sh (II)

*See note to Table 1.

REFERENCES

1. A. N. Lazarev and T. F. Tenisheva, Opt. i Spektr. 10, 79 (1961), Optics and Spectroscopy 10, 37 (1961).
2. Kh. S. Mamedov and N. V. Belov, Doklady Akad. Nauk SSSR 107, 463 (1956);
K. Dornberger-Schiff, F. Liebau, and E. Thilo, Acta Crystallogr. 8, 752 (1955).
3. F. Liebau, W. Hilmer, and G. Lindemann, Acta Crystallogr. 12, 182 (1959);
Kh. S. Mamedov, Doklady Akad. Nauk Azerb. SSR 14, 445 (1958).
4. F. Liebau, Acta Crystallogr. 12, 177 (1959).
5. F. Liebau, M. Sprung, and E. Thilo, Z. anorg. u. allgem. Chem. 297, 213 (1958).
6. F. Liebau, Acta Crystallogr. 10, 790 (1957).
7. W. Hilmer, Naturwiss. 45, 238 (1958).
8. G. P. Stavitskaha and Ya. I. Ryskin, Opt. i Spektr. 10, 343 (1961), Optics and Spectroscopy 10, 172 (1961).

VIBRATIONAL SPECTRA AND STRUCTURE OF ENE-YNE SILICO-HYDROCARBONS

T. V. Yakovleva, A. A. Petrov, and M. D. Standnichuk (pp. 588-593)

Received 26 December 1960

The vibrational spectra of four ene-yne silico-hydrocarbons have been studied. The data obtained are compared with the analogous data for similarly constructed ene-yne hydrocarbons. The changes observed in the spectral quantities ν, ρ, and α'_2/α'_1 are explained not only by the increase in the mass of the atom adjoining the triple bond, but also by a qualitative change in the character of this bond—an increase in its force constant.

Investigation of the infrared and Raman spectra of ene-yne hydrocarbons has made it possible to establish a definite relationship between the position and intensity of certain bands and the structure of the hydrocarbons.[1-3]

The vibrational spectra of ene-yne silico-hydrocarbons have not been systematically studied. Only the spectra of triethylsilylbutene-3-yne-1 and certain other ene-ynes containing hydrogen atoms on the silicon atom have been investigated.[4]

We have investigated the vibrational spectra of four ene-yne silico-hydrocarbons and have compared the data obtained with the data for the analogously constructed ene-yne hydrocarbons.[5] The results of the measurements are given in Table 1 and in the Figure.

From a comparison of the spectra presented and the data of another communication,[5] the following conclusions may be drawn.

1. The replacement of the carbon atom adjacent to the triple bond in the ene-yne system by a silicon atom leads to a sharp lowering of the frequency (by roughly 75 cm^{-1} in both the infrared and Raman spectra) and an increase in the intensity of the corresponding band in the infrared spectrum. At the same time, the frequency of the double bond vibrations remains practically unchanged. The intensity of the double-bond band also changes insignificantly: it is high in the Raman spectra and moderate or weak in the infrared spectra. In the Raman spectrum of trimethylsilylvinylacetylene, two lines correspond to the double bond vibration.

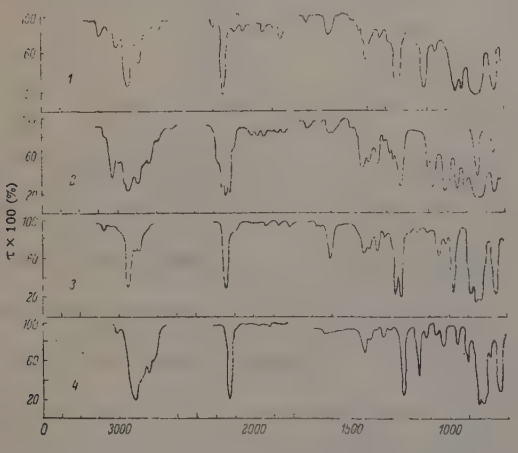

Infrared transmission spectra. 1—1-trimethylsilylbutene-3-yne-1; 2—1-trimethylsilylpentene-3-yne-1; 3—1-trimethylsilyl-3-methylbutene-3-yne-1; 4—1-trimethylsilyl-2-(cyclohexen-1-yl)ethyne.

In the spectra of trimethylsilylpentene-3-yne-1, there are two bands corresponding to the double and to the triple bond; they belong to the cis- and trans-forms of the substance.

2. The well known regularities in the frequencies of the CH deformation vibrations in the 900-1000 cm^{-1} region, which are characteristic for the infrared spectra of various substituted ethylenic groups, also occur in the spectra of the silico-hydrocarbons. The vinyl group is characterized by the frequencies 923 and 956 cm^{-1}, the —CH=CH— group by the frequency 953 cm^{-1}, and the $>C=CH_2$ group by the frequency 887 cm^{-1}. In the Rama spectra, these bands are of very low intensity. In comparison with the hydrocarbons, the first frequency of the vinyl group is raised in the silico-hydrocarbons, the second is lowered.

3. As in the case of the ene-yne hydrocarbons, a CH stretching vibration band around 3100 cm^{-1}, of medium intensity in the infrared spectra and weak in the Raman spectra, corresponds to the terminal methylene group. In the spectra of the silico-hydrocarbons (III) and (IV), this band is absent.

The planar deformation vibration bands around 1410 cm^{-1}, which are especially intense in the infrared spectra, correspond to the methylene group.

4. In the infrared spectra of acetylenic as well as some ene-yne hydrocarbons, variable-intensity bands of unknown origin are observed in the 1700 cm^{-1} region. In the spectra of the ene-yne silico-hydrocarbons, these bands are not detected.

5. In the infrared spectra of the ene-yne hydrocarbons and silico-hydrocarbons containing a vinyl group, a band at 1850 cm^{-1} (an overtone) is observed.

6. In the infrared spectra of the ene-yne silico-hydrocarbons, there is the usual band of the unsymmetrical Si-C stretching vibrations in the 1250 cm^{-1} region.[6] In the Raman spectra, this band has a low intensity.

The intense line in the 620-640 cm^{-1} region in the Raman spectra corresponds to the symmetrical Si—C vibration. This is the only polarized line in the region from 100 to 1500 cm^{-1}. In the spectra of 1,3-dienic silico-hydrocarbons, a band at 602 cm^{-1} corresponds to this vibration.[6]

7. A band around 1200 cm^{-1}, intense in both spectra, corresponds to the tertiary butyl group in the spectra of the ene-yne hydrocarbons; a band around 850 cm very intense in the infrared and weak in the Raman spectra, corresponds to the $(CH_3)_3Si$ grouping in the spectra of the silico-hydrocarbons.[7]

Table 1. Vibrational Spectra of 4 Ene-Yne Silico-Hydrocarbons (Frequencies are given in cm^{-1})

1-trimethylsilylbutene-3-yne-1 (I)		1-trimethylsilyl-3-methyl-butene-3-yne-1 (II)		1-trimethylsilylpentene-3-yne-1 (III)		1-trimethylsilyl-2-(cyclohexen-1-yl)-ethyne (IV)	
Ram.	IR	Ram.	IR	Ram.	IR	Ram.	IR
–	–	–	–	–	–	112 vw	–
176 m	–	157 s	–	133 m	–	135 m	–
–	–	–	–	–	–	190 m	–
212 m	–	210 s	–	214 m	–	215 s	–
–	–	–	–	–	–	270 vw	–
–	–	351 w	–	316 vw	–	332 vw	–
–	–	371 w	–	364 w	–	–	–
386 s	–	385 m	–	385 m	–	379 m	–
–	–	–	–	404 vw	–	–	–
447 vs	–	–	–	457 w	–	457 vs	–
–	–	507 w	–	502 w	–	503 vw	–
–	–	537 vw	–	556 vw	–	535 vw	–
576 m	–	578 vw	–	576 w	–	571 vw	–
–	–	–	–	603 w	–	–	–
640 s	–	635 s	–	627 m	–	619 s	–
–	–	–	–	661 w	–	687 w	–
701 w	703 s	708 w	–	701 w	700 vs	698 w	–
–	–	–	–	724 vw	724 vs	–	–
760 w	758 vs	764 w	760 vs	762 w	760 vs	761 vw	746 s
–	–	–	–	791 vw	–	780 w	789 m
–	–	–	–	–	–	802 vw	–
–	–	835 vw	837 vs	–	–	–	831 vs
845 vw	847 vs	847 vw	–	817 w	843 vs	851 w	856 vs
–	–	875 vw	861 vs	–	–	–	–
929 vw	923 vs	907 vw	893 s	920 vw	–	921 w	908 m
962 vw	956 vs	984 w	978 vs	955 vw	953 vs	974 w	958 m
–	–	–	–	–	995 vs	–	–
–	–	1015 m	1011 w	1015 vw	1015 vs	–	1033 m
–	–	–	1052 m	1039 vw	–	1057 vw	1067 w
–	–	–	–	1082 w	1081 vs	1079 vw	–
1111 w	1109 vs	–	1111 vw	1107 w	1102 m	1108 vw	1118 w
1135 w	–	1142 w	–	1136 w	–	1137 w	1133 m
–	–	–	1163 vw	1147 w	–	–	1159 s
1201 w	–	1207 w	–	1198 w	–	1171 w	–
–	–	–	–	1231 w	–	–	–
1257 w	1252 vs	1257 w	1250 vs	1253 w	1247 vs	1252 vw	1246 vs
–	–	–	–	1264 vw	–	1268 w	–
1292 m	–	1278 m	1273 vs	1286 vw	1285 m	–	–
–	–	1319 w	1327 m	1302 w	1298 w	1302 w	1310 vw
–	1334 m	–	–	–	–	1343 w	1345 w
–	–	1375 w	1366 m	1365 vw	1363 s	1359 vw	–
–	–	1389 m	–	1380 w	1379 m	–	–
–	–	–	–	1401 w	–	–	–
1412 s	1411 s	–	1406 m	1413 w	1405 m	–	–
–	–	–	–	–	1423 m	1432 s	1439 m
–	–	1443 w	1431 m	1446 m	1443 m	1448 m	1454 w
1599 vs	–	–	–	1617 vs	1590 w	–	–
1612 vs	1601 m	1613 vs	1610 m	1632 vs	1610 w	1630 vs	1625 vw
–	1850 m	–	–	–	–	–	–
–	–	–	–	2130 vs	2127 vs	–	–
2147 vs	2151 vs	2150 vs	2149 s	2152 vs	2147 vs	2145 vs	2143 vs
–	–	–	–	2166 m	2167 s	–	–
2790 vw	–	–	–	–	–	2784 vw	2792 vw
–	–	–	–	–	2848 m	2840 w	2833 m
–	–	–	–	–	2878 m	2865 m	2861 s
2900 s	2889 s	2901 s	2898 m	2902 vs	2902 vs	2900 vs	–
–	–	2926 m	2920 m	2914 vs	–	2914 s	2930 vs
2961 s	2945 vs	2963 s	2955 s	2965 vs	2953 vs	2964 s	2948 s
3011 m	3007 m	–	–	3005 m	2999 m	–	–
–	–	3022 m	3023 vw	3032 m	3027 s	3035 vw	3029 w
3104 w	3096 m	3103 m	3093 w	–	–	–	–

Note: Conventional symbols: Ram. – Raman spectrum, IR – infrared spectrum; vs – very strong, s – strong, m – medium, w – weak, vw – very weak.

8. In the long wavelength region, intense bands at and 758 cm^{-1} ($CH_2=CH-C\equiv C-$), at 760 cm^{-1}

$$(CH_2=\underset{\displaystyle CH_3}{\overset{|}{C}}-C\equiv C-),$$

at 700, 724, and 760 cm^{-1} ($CH_3-CH=CH-C\equiv C-$) espond to the ene-yne grouping. The bands of the de- ation vibrations of the acetylenic bond are found in region.

In the infrared spectra of the ene-yne silico-hydro- ons, the intensity of the bands of the triple bond (con- ed with the silicon atom) is significantly greater than e of the double bond. In the Raman spectra, the in- ity of the line of the triple* bond is also greater by a factor of 1.5-2 than that of the double bond.

We further investigated the degree of depolarization (ρ) of the lines of the C≡C, C=C, and Si–C stretching vibrations. The data obtained were used to calculate the quantity α'^2/α'^2_1, which characterizes the shape of the derivative of the polarizability ellipsoid.[5] Since for stretching vibrations one observes a parallelism in the changes of α' and α, the data obtained also characterize the shape of the polarizability ellipsoid of the bond under investigation.

It can be seen from Table 2 that, as the carbon chain of a silico-hydrocarbon is lengthened, the polarizability ellipsoid is elongated, while it is compressed by branching, since the transverse component of the tensor of the

he Russian original, this word reads "double" which appears to be a typographical error.-Translation Editor.

derivative of the polarizability, α_2', increases. Ring formation acts more like a lengthening of the chain than like a branching.

Table 2

Substance	Bond	Frequency (cm^{-1})	ρ	α_2'/α_3'
$(CH_3)_3C-C\equiv C-CH=CH_2$	C≡C	2204	0.355	0.120
	C=C	1611	0.34	0.125
$(CH_3)_3Si-C\equiv C-CH=CH_2$	C≡C	2147	0.365	0.111
	C=C	1612	0.345	0.126
		1599	0.385	0.094
	C—Si	640	0.04	0.592
$(CH_3)_3C-C\equiv C-C(CH_3)=CH_2$	C≡C	2213	0.39	0.085
	C=C	1617	0.295	0.174
$(CH_3)_3Si-C\equiv C-C(CH_3)=CH_2$	C≡C	2150	0.345	0.128
	C=C	1613	0.42	0.065
	C—Si	635	Less than 0.1	—
$(CH_3)_3Si-C\equiv C-CH=CH-CH_3$	C≡C	2152	0.39	0.085
	C≡C	2130	0.43	0.056
	C=C	1632	0.41	0.073
	C=C	1617	0.36	0.115
	C—Si	627	—	—
$(CH_3)_3Si-C\equiv C-C\equiv CH$ (with CH_2-CH_2 ring)	C≡C	2145	0.43	0.056
	C=C	1630	0.445	0.044
	C—Si	619	Less than 0.1	—

Comparison of the quantities α_2'/α_1' for the hydrocarbons and the silico-hydrocarbons show that, as the nature of the atom linked with the triple bond is changed (replacement of carbon by silicon), the ellipsoid of the derivative of the polarizability, and consequently the electron cloud of the triple bond as well, is elongated. It is possible that this is connected with a redistribution of electrons involving the d shell of the silicon atom.

An approximate calculation of the force constants of the triple bond enables us to form a conclusion concerning the causes for the abrupt fall in the stretching vibration frequency of the triple bond on going from the hydrocarbons to the silico-hydrocarbons.

It can be seen from Table 3 that this change in frequency is associated not only with the change in mass of the adjoining atom, but also with a qualitative change the character of the bond—with an increase in the for constant. The reduced mass changes by 25%, and the force constant of the bond changes by roughly 20%.*

*Only the mass of the atom directly connected with th acetylenic grouping was taken into account.

Thus we have arrived by a different path at the conclusion previously formed concerning the qualitati change in the electron cloud of the triple bond on goin from the hydrocarbons to the silico-hydrocarbons.

Table 3

№	System under investigation	Weight of atom A_1	Reduced mass	Frequency (cm^{-1})	Relative coefficient of elasticity	De de
1 2 3 4	C—C≡C—C	12	12	2200	1	
	Si—C≡C—C	28	15	2150	1.19	

REFERENCES

1. A. A. Petrov, Yu. I. Porfir'eva, and G. I. Semenov, Zhur. Obshchei Khim. 27, 1167 (1957).
2. A. A. Petrov, V. A. Kolesova, and Yu. I. Porfir'eva Zhur. Obshchei Khim. 27, 2081 (1957).
3. A. A. Petrov, B. S. Kupin, T. V. Yakovleva, and K. Mingaleva, Zhur. Obshchei Khim. 29, 3732 (1959).
4. A. D. Petrov, S. I. Sadykhzade, and Yu. P. Egorov, Izvest. Akad. Nauk SSSR, Ser. Khim. 722 (1954).
5. T. V. Yakovleva and A. A. Petrov, Opt. i Spektr. 11 594 (1961), Optics and Spectroscopy 11, 320 (1961).
6. Yu. P. Egorov, Izvest. Akad. Nauk SSSR, Ser. Khim 1553 (1960).
7. Yu. Ya. Mikhailenko, "Collection: Analysis and Physico-Chemical Methods of Investigation of Silic Organic Compounds." Leningrad, 1958

DEPOLARIZATION OF RAMAN LINES OF MULTIPLE BONDS OF VINYLACETYLENIC HYDROCARBONS AS RELATED TO THEIR STRUCTURE

T. V. Yakovleva and A. A. Petrov (pp. 594-597)

Received 26 December 1960

Basic regularities in the Raman spectra of vinylacetylenic hydrocarbons of different structure have been examined in an earlier published study[1] carried out with the participation of one of the authors of the present communication. It was established there that the triple bond corresponds to a frequency of about 2100 (the group $HC\equiv C-$) or 2230 and 2330 (the group $-C\equiv C-$) cm^{-1}, and the double bond to a frequency about 1600 ($-CH=CH_2$), 1621 ($>C=CH_2$), or 1616 ($-CH=CH-$) cm^{-1}. In the region of the out-of-plane CH deformation vibrations (900-1000 cm^{-1}) there were observed general regularities related to the structure, as observed earlier for olefins. In the work cited the question of the comparison of the band intensities of both multiple bonds in dependence their position in the chain was also raised; however, could be solved only approximately since photometry the spectra was not carried out and conclusions on th Raman line intensities were made visually.

Having obtained the possibility of using a recordi spectrophotometer for the study of Raman spectra, w repeated the investigation with the purpose of determ more accurately the intensities and degrees of depola zation of the bands corresponding to the multiple bon We have attempted to use the data on the degree of de polarization of the multiple bond lines to study the in ence of the hydrocarbon structure on the character o the electron cloud of the separate multiple bonds. Kn

he degree of depolarization ρ of the characteristic tching vibration band of the double and triple bonds can determine the quantity α'_2/α'_1, characterizing the n of the polarizability ellipsoid with respect to the ear coordinate for the condition that $\alpha'_2 = \alpha'_3$;

$$\frac{\alpha'_2}{\alpha'_1} = \frac{1 - \sqrt{\frac{5\rho}{6-7\rho}}}{2\sqrt{\frac{5\rho}{6-7\rho}} + 1}.$$

The larger the degree of depolarization the smaller quantity α'_2/α'_1 and, accordingly, the more elongated polarizability derivative ellipsoid.

It is known that for stretching vibrations there is a ct connection between changes of the values of α and Therefore, from the magnitude of α'_2/α'_1, one can ment on the form of the polarizability ellipsoid of the studied.

The Raman line frequencies for four hydrocarbons presented in Table 1. The estimate of the line inten- s is approximate since different portions of the tra were recorded using different slits and special surements to estimate the intensities were not made.

Table 1. The Raman Spectra of the Hydrocarbons Investigated*

ne-1- -3	Pentene-3-yne-1	2-methylpentene-1-yne-3	5,5-dimenyl-hexene-1-yne-3	2,5,5-trimethyl-hexene-1-yne-3
0 w	161 vs	186 s	205 s	180 m
	–	–	–	242 vw
	273 vw	263 vw	272 vw	286 w
0 w	334 m	336 w	333 vw	–
8 vw	369 vw	394 w	363 vw	367 vw
	386 vw	–	–	–
	–	–	–	427 vw
8 w	491 m	–	447 w	457 w
	–	–	507 w	503 vw
7 w	527 m	527 w	550 w	558 w
	619 m	–	–	617 vw
2 vw	640 w	633 w	640 w	643 vw
9 vw	–	–	688 w	–
	729 vw	–	–	–
	793 w	765 w	–	796 w
	–	–	826 s	–
	895 w	905 vw	–	903 m
0 vw	–	–	933 m	926 w
	961 w	956 w	998 vw	–
3 vw	1031 w	1013 w	1036 vw	1015 w
	1105 w	–	–	–
4 w	1154 w	1162 vw	1120 w	1156 vw
0 w	–	–	1206 w	1203 m
5 w	1232 m	1217 vw	–	1239 vw
	1274 vw	1267 vw	1271 vw	–
0 m	1291 vw	–	1294 s	–
	1305 m	–	–	1307 vw
2 vw	1345 vw	–	–	–
	1367 vw	1379 w	–	–
9 m	1381 w	1392 m	–	1384 m
1 s	1400 vs	–	1411 s	–
	1445 m	1444 vw	1454 s	1449 m
8 s	1617 vs	1615 vs	1611 vs	1617 s
	1627 vs	–	–	–
9 m	2101 vs	2099 vs	2204 vs	2213 vs
6 vs	–	–	2259 w	–
1 w	–	–	2716 w	2716 w
5 w	–	2786 w	2786 m	2784 s
	–	–	–	2834 vw
9 w	2869 w	2872 vw	2876 m	2868 w
	–	2896 vw	2885 vw	–
1 vs	2921 m	2926 s	2906 m	2716 w
	2948 vw	2961 w	2930 s	2925 s
	–	–	–	2956 w
9 vs	2979 vw	2979 w	2975 vs	2971 s
2 s	3014 w	3023 w	3014 s	3021 w
	3039 w	–	–	–
4 w	–	3100 m	3108 m	3100 w
7 vw	–	–	–	3129 vw
	3300 vw	3315 vw	–	–

he frequencies are in cm^{-1}; the designations of the band intensities are: very weak, w – weak, m – medium, s – strong, vs – very strong.

The lack of correspondence between the given intensity estimate of the series of bands and the literature data is primarily due to the different sensitivity of photographic plates and photomultipliers.

The experimental data obtained have confirmed the conclusion drawn earlier on the greater intensity of bands of the acetylenic bond in comparison with the ethylenic, independent of the molecular weight and structure of the particular hydrocarbon. The intensity of the main characteristic triple bond band is in all cases approximately twice the intensity of the characteristic double bond band. The relative intensity of the band of a triple bond, located at the end of the molecule, is 20-25% higher than the relative intensity of the band of the same bond in the middle of the molecule. The band intensity of the triple bond in the spectrum of hydrocarbon IV is approximately 20% higher than in the spectrum of hydrocarbon III. Possibly this is due to a shift of the electron density along the chain due to the influence of the methyl groups.[2]

In Table 2 are given values of ρ and α'_2/α'_1 for eight hydrocarbons investigated.* In any case, where there are several characteristic frequencies, only the quantities for the basic intense band were considered. The determination of the degree of depolarization of the weak bands has a large associated error due to overlap.

*The experimental data for the vinyl-, vinylethyl-, and vinylpropylacetylenes were obtained earlier by T. V. Yakovleva together with M. V. Vol'kenshtein.

One can draw the following conclusions from the table:

1. In the case of vinylacetylene the degree of depolarization of the band corresponding to the double bond is higher than for the triple bond. In the closest homologues of vinylacetylene the opposite situation is observed. With an increase in the chain length of the normal radical this difference is smoothed out.

2. The form of the polarizability ellipsoid of multiple bonds changes with substitution: the polarizability ellipsoid of the acetylenic bond is elongated, and that of the ethylenic one compressed, and this effect appears significantly stronger for the triple bond.

It does not appear possible to relate in any manner changes in the values of the degree of depolarization of characteristic stretching vibration bands of multiple bonds in the spectra of single hydrocarbons with the character of the substitution and the reactivity.

Table 2. Values of ρ and α'_2/α'_1 for the Hydrocarbons Investigated

Compound	Bond	ν (cm^{-1})	ρ	$\frac{\alpha'_2}{\alpha'_1}$	Ratio of the Band Intensities $\frac{I_{C\equiv C}}{I_{C=C}}$
$HC\equiv C-CH=CH_2$ (I)	C≡C	2097	0.22	0.25	—
	C=C	1593	0.39	0.085	—
$CH_3-C\equiv C-CH=CH_2$ (II) .	C≡C	2236	0.325	0.146	1.7
	C=C	1608	0.255	0.215	—
$HC\equiv C-C(CH_3)=CH_2$ (III)	C≡C	2099	0.285	0.184	1.7
	C=C	1615	0.23	0.25	—
$HC\equiv C-CH=CH-CH_3$ (IV)	C≡C	2100	0.34	0.125	2.5
	C=C	1617	0.315	0.155	—
$C_2H_5-C\equiv C-CH=CH_2$ (V) .	C≡C	2224	0.34	0.125	—
	C=C	1603	0.32	0.145	—
$C_3H_7-C\equiv C-CH=CH_2$ (VI) .	C≡C	2221	0.32	0.154	—
	C=C	1603	0.33	0.135	—
$(CH_3)_3C-C\equiv C-CH=CH_2$ (VII)	C≡C	2204	0.355	0.125	2.8
	C=C	1611	0.34	0.125	—
$(CH_3)_3C-C\equiv C-C(CH_3)=CH_2$ (VIII)	C≡C	2213	0.39	0.085	2.0
	C=C	1617	0.295	0.174	—

The work was performed on a DFS-12 apparatus with a recorder. As a light source we used a DRS-600 low-pressure mercury lamp. A saturated solution of sodium nitrite served as a light filter. To obtain more accurate values of the frequencies the Raman spectra were recorded three times in the region from 4047 to 5100 A, after which we measured the distance between the bands and from the mean values calculated the frequency values using the Hartmann formula.

The degree of depolarization was determined by the two exposure methods and was calculated graphically. We used as polarizers cylinders of polaroid sheet, wrapped around the cell containing the sample being investigated. One of the cylinders transmitted light whose electric vector vibrated parallel to the cell axis, the second perpendicular to this axis. The apparatus was calibrated using the degrees of depolarization of the lines 217 (ρ = 0.85), 313 (ρ = 0.87), and 459 (ρ = 0.04) cm^{-1} of carbon tetrachloride and 606 (ρ = 0.80) and 99 (ρ = 0.05) cm^{-1} of benzene.

REFERENCES

1. A. A. Petrov, V. A. Kolesova, and Yu. I. Porfir'eva Zhur. Org. Khim. 27, 2081 (1957).
2. A. A. Petrov, K. S. Mingoleva, and B. S. Kupin, Doklady Akad. Nauk SSSR 123, 298 (1958).

THE LUMINESCENCE OF ALCOHOLIC SOLUTIONS OF BENZENE AT −196°C

T. V. Ivanova and B. Ya. Sveshnikov (pp. 598-605)

Received 3 December 1960

The phosphorescence and fluorescence spectra of alcoholic solutions of benzene have been investigated at −196°C. The phosphorescence spectrum analysis proposed by Shull and by Sveshnikov and Dikun was confirmed in principle. In agreement with these authors, analysis of the phosphorescence spectrum permits the assertion that the phosphorescent level has either B_{1u} or B_{2u} symmetry, but does not discriminate between the two. The choice is made in the present paper by comparing the phosphorescence and fluorescence spectra of benzene in solution. It is shown that the structures and term schemes of the two spectra differ markedly from each other. It is generally accepted that the fluorescent level has B_{2u} symmetry. Then if the set of vibrations permitting the transition does not depend on the multiplicity of the level, the phosphorescent level must have the symmetry B_{1u}.

INTRODUCTION

At the beginning of 1949, Shull,[1] and also Sveshnikov and Dikun[2] published analyses of the vibrational structure of the phosphorescent spectrum of solutions of benzene in EPA (Shull) and in ethyl alcohol (Sveshnikov and Dikun) at −196°C. One of the basic problems of this analysis was getting information about the lower triplet level of benzene, the transition from which to the normal level is responsible for the phosphorescence.

Prior to 1949, the literature contained completely different opinions about the properties of the triplet (phosphorescent) state of benzene. Thus, Lewis and Kasha,[3] on the basis of their spectroscopic data, proposed that the benzene molecule in the triplet state had a quinoid structure, and this hypothesis found support in the theoretical work of Redlich and Holt.[4] However, the authors of many other theoretical papers on the singlet and triplet levels of benzene[5] considered that the triplet levels of benzene had the same symmetry as the excited singlet levels, so that the difference between the triplet and singlet systems consisted only in a different ordering of the levels. The lower excited singlet (fluorescent) level in benzene has the symmetry B_{2u}, the second B_{1u}, and the top E_u^-.* Calculations show that the triplet level

*A, B, +, and − symbolize respectively six-, three-, two-, and onefold symmetry about an axis perpendicular to the plane of the molecule. The indices 1 and g indicate, respectively, symmetry with respect to 180° rotation about an axis passing through the ring, and to inversion through the center; the indices 2 and u refer to lack of symm with respect to the same transformations. The letter signifies a degenerate level.

$^3E_u^-$ lies between the levels $^3B_{1u}$ and $^3B_{2u}$; however, th calculations do not indicate which of the latter two leve is the lower (phosphorescent).

The work of Shull, Sveshnikov, and Dikun complete refuted the hypothesis of Lewis and Kasha. Analysis o the phosphorescence spectrum of benzene showed that phosphorescence level has the symmetry B_{2u} or B_{1u}. follows from this that the symmetry of the electron cl in the triplet state does not differ from the symmetry one of the excited singlet states of benzene; however, t choice between the two indicated levels turns out to be difficult. Practically all of the vibrations appearing in the phosphorescence spectrum, according to the selec rules for the symmetry group D_{6h}, are permitted both the transition $B_{1u} \rightarrow A_{1g}$* and for the transition $B_{2u} \rightarrow$

*A_{1g} is the symmetry of the normal state of the benze molecule.

under the assumption that the moment of the transitio both cases lies in the plane of the molecule. The only argument that could be used in favor of the B_{1u} level would be the detection in the phosphorescence spectru of the $\nu_0 - \nu_4$ band, where ν_0 is the frequency of the zero-point transition and ν_4 = 685 cm^{-1} is the frequen corresponding to vibration of the benzene molecule wi symmetry B_{2g}. According to the selection rules, the v brations of this symmetry appear in combination with

electronic transition $B_{1u} \leftrightarrow A_{1g}$. In this case, the sition moment is perpendicular to the plane of the zene molecule.

In spite of this, the question of the symmetry of the sphorescent level of benzene is difficult to decide on basis of the presence in the phosphorescence spec- n of one rather weak line, particularly when there is gnificant perturbing influence due to the solvent. In , theoretical investigation shows that in benzene the ely electronic transitions $B_{2u} \leftrightarrow A_{1g}$ and $B_{1u} \leftrightarrow A_{1g}$ forbidden, and the transition moments in both cases in the plane of the molecule. However, this conclu- n applies to gases. In the absorption and fluorescence ctra of crystalline benzene at 20°K obtained by Kronen- ger,[6] and by Broude et al.,[7] the purely electronic sition is fairly clearly seen. It should be pointed out, ever, that the intensity of the bands corresponding to sitions associated with vibrations of symmetry E_g^+ t least an order of magnitude greater than the inten- of the bands produced by the perturbing action of the lium.

Sveshnikov and Ermolaev[8] tried to resolve the ques- of the symmetry of the phosphorescent level of aro- ic compounds by means of polarization experiments. y investigated the dependence of the degree of polari- on of the phosphorescence of dyes on the wavelength he exciting light, and showed that in its polarization racteristic, the phosphorescent level was analogous he second and not to the first excited singlet level.

However, not a single opinion has been voiced so far ut the symmetry of the phosphorescent level of ben- e. Thus, for example, in the recently published theo- cal treatment of Hameka and Oosterhof,[9] the conclu- n based on the calculated values of the transition babilities (emission lifetimes) for $^3B_{1u} \rightarrow {}^1A_{1g}$ and $^3E_u^- \rightarrow {}^1A_{1g}$ is that the phosphorescent level probably has symmetry B_{2u}, rather than B_{1u}. Pesteil and Zmerli[10] ak out even more decisively. These authors present luminescence spectra of crystalline benzene at 20°K ained under continuous excitation. They believe that observed two phosphorescence spectra, one corre- nding to the transition $^3E_u^- \rightarrow {}^1A_{1g}$ and the other to the sition $^3B_{2u} \rightarrow {}^1A_{1g}$. According to their analysis of the ctra, the $^3E_u^-$ level is 38,724 cm^{-1} above the ground el and the $^3B_{2u}$ level is 30,754 cm^{-1} above the ground el; i.e., the first level is not much higher than the rescent level, and the second is about 1100 cm^{-1} her than the phosphorescent level specified in the ers of Shull, Sveshnikov, and Dikun.*

e data of Sveshnikov, Dikun, and Shull on the position he phosphorescent level were recently confirmed by ron et al.[11]

This large difference between the energy values for lowest triplet state of benzene given by Pesteil and erli and those given by other authors results from the that those authors[10] took the first line of the "long elength" phosphorescence spectrum of benzene as ν_8,* where $\nu_8 = 1585$ cm^{-1}. This assumption led them

e vibration designations are given according to Pitzer Scott.[12]

n incorrect spectrum analysis. In the "long wave- th" phosphorescence spectrum the authors[10] "dis- ered" transitions to certain vibrational levels, where or three vibrations occur whose product gives the metry B_{1g}. Among the fundamental vibrations of benzene there are none of symmetry B_{1g}; however, according to the selection rules, a combination of vibrations having the symmetry B_{1g} can appear in benzene in the transition from a B_{2u} level to the ground state for an electric moment perpendicular to the plane of the molecule.

We note in connection with this that the entire analysis of Pesteil and Zmerli seems somewhat strange. We limit ourselves to two comments. In the case of the transition $^3E_u^- \rightarrow {}^1A_{1g}$, to which the authors ascribe the "short wavelength" luminescence, it is completely unclear why the first line is identified with $\nu_0 - \nu_8$. The transition $^3E_u^- \rightarrow {}^3A_{1g}$ is permitted from symmetry considerations, and should produce an intense line corresponding to a purely electronic transition. It is also not clear why the very intense lines in the benzene luminescence spectrum correspond to a transition moment perpendicular to the plane of the molecule.*

*It should be pointed out, however, that in a paper published after that of Pesteil and Zmerli, the latter author[13] rejects the earlier interpretation[10] of the "long wavelength" phosphorescence spectrum and accepts for the "lower" phosphorescent level an energy value close to that found in the papers of Shull and Sveshnikov and Dikun.

The properties of the phosphorescent level of benzene were also taken up at the time of the Faraday Discussions in 1959. Thus, Porter and Wright[14] sought to revive the hypothesis of Lewis and Kasha[3] about the quinoid structure of the benzene molecule in the phosphorescent state, and also the hypothesis of Lewis et al.[15] in which the nuclear configuration corresponding to the phosphorescent state is maintained because of a rigid medium. The authors considered that the phosphorescent and ground states of the benzene molecule not only differed in their spin functions but also appeared to be real isomers of the given substance.

The principal aim of our work was to obtain new evidence in support of the assignment of B_{1u} symmetry to the phosphorescent level. We therefore compared the phosphorescence and fluorescence spectra of frozen alcoholic solutions of benzene. For the transition moment E_u^-, lying in the plane of the molecule,* both transitions

*Except for the aforementioned $\nu_0 - \nu_4$ band, all the bands in the phosphorescence spectrum of benzene are associated with a moment lying in the plane of the molecule.

$B_{1u} \rightarrow A_{1g}$ and $B_{2u} \rightarrow A_{1g}$ can be permitted only by superposing vibrations of symmetry E_g^+ upon the electronic transition. In the benzene molecule, there are four fundamental vibrations having the symmetry E_g^+: $\nu_6(C) = 606$ cm^{-1}, $\nu_8(C) = 1585$ cm^{-1}, $\nu_9(H) = 1178$ cm^{-1}, and $\nu_2(H) = 3060$ cm^{-1}. It was hoped that the vibrations which were active in the molecule in the B_{2u} state (the fluorescent state) would not turn out to be the most active ones for the molecule in the B_{1u} state. Some basis for such an assumption was given by the fact that in the fluorescence spectrum of gaseous benzene, according to Ingold et al.,[16] the most active vibration is ν_6, whereas in the phosphorescence spectrum of benzene solutions at 77°K this vibration is not detected.[1,2]

In connection with this problem, it seemed important to us to study the distribution of energy in the fluorescence and phosphorescence spectra of benzene solutions at low temperatures. In the experiments of Shull and Sveshnikov and Dikun, the phosphorescence spectrum was studied by photographic methods. The present investigation employed a monochromator with photoelectric re-

corder, which permits a more accurate determination of the energy distribution in the emission spectrum, if precautions are taken to conduct the excitation in such a manner that the photochemical reactions observed in frozen solutions of benzene are sufficiently small.

METHOD OF MEASUREMENT

The apparatus for the investigation of fluorescence spectra consisted of a PRK-4 mercury lamp, from whose spectrum the entire region shorter than 2600 A was isolated by means of a double quartz monochromator, a quartz dewar, a quartz test tube containing the solution being investigated, a grating monochromator (1200 lines/mm) blazed for 3300 A in the first order, a photomultiplier, and an M-95 galvanometer. A Becquerel phosphoroscope was used for studying the phosphorescence spectra; the luminescence was excited with the total light from a mercury lamp. In order to avoid absorption and scattering of the exciting radiation and the luminescence by liquid air (nitrogen), the excitation and observation were conducted from the same side with a small angle between the incident and emergent beams. This was achieved through the use of an aluminum mirror.

Before beginning work, the spectral sensitivity curve of the monochromator and photomultiplier combined was accurately determined using a ribbon lamp with a Uviol window* specially calibrated according to temperature.

*The absorption of the Uviol window was measured separately.

Studies of absorption spectra were carried out with an SF-4 photoelectric spectrometer with a modified cell chamber.

RESULTS AND DISCUSSION

Figure 1 shows the fluorescence spectrum and the long wavelength part of the absorption spectrum of an alcoholic solution of benzene at −196°C; Fig. 2 shows the phosphorescence spectrum of the same solution. The positions of the maxima in the fluorescence spectra are given in Table 1.

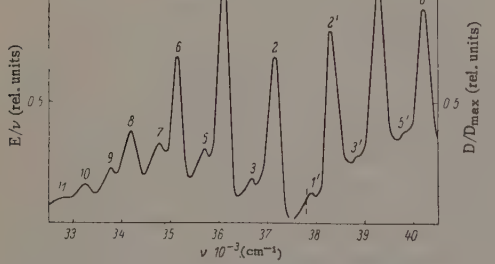

Fig. 1. Fluorescence spectrum and long wavelength part of the absorption spectrum of an alcoholic solution of benzene at −196°C. The broken line indicates the position of the band corresponding to the electronic transition.

Figure 1 and Table 1 show a clear alternation of intense (even-numbered) and weak (odd-numbered) bands in the fluorescence spectrum. The intervals between the strong bands are 1025, 975, 995, and 955 cm^{-1}, and between the weak ones 970, 950, and 990 cm^{-1}.* It is mos

*The intervals between the first and third, and between the ninth and eleventh bands are not indicated here.

natural to assume that these intervals correspond to th totally symmetrical vibration of benzene at 992 cm^{-1}. For the excited benzene molecule, the frequency of this same vibration is 923 cm^{-1}, as is well known. The sep rations between the second and fourth (930 cm^{-1}) and th fourth and sixth (930 cm^{-1}) bands of the benzene absorp tion spectrum agree satisfactorily with this value.

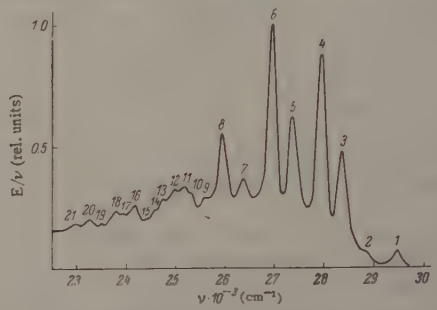

Fig. 2. Phosphorescence spectrum of an alcoholic solution of benzene at −196°C.

According to the selection rule for the transition $A_{1g} \leftrightarrow B_{2u}$, i.e., for the fluorescence and absorption of benzene, the totally symmetrical vibrations can appear in the spectrum only after distortion of the molecule as a result of the nontotally symmetrical vibration of symmetry E_g^+. The frequencies of the fundamental vibration are given above. Since the separation between the first tense band in the fluorescence spectrum and the first i tense band in the absorption spectrum is 1180 cm^{-1} and the term diagrams should be the same for both spectra the vibration to be chosen from the four E_g^+ vibrations given above is ν_6, whose frequency is 606 cm^{-1} in the u excited state and 521 cm^{-1} in the excited state. Hence t frequency of the zero transition $A_{1g} \leftrightarrow B_{2u}$ is 37,780 cr

*We were unable to determine the location of this first band in the fluorescence spectrum because of weak sca tering of the exciting radiation in our apparatus in that region.

The frequency of the purely electronic transition calcu lated in this way in alcoholic solution at −196°C is shif 300 cm^{-1} relative to vapor state.

It can be seen from Fig. 1 that the first absorption band, which should correspond to a purely electronic transition, is displaced to the blue relative to the frequency calculated for this transition. This is probably result of the superposition of the intense second maximum in absorption. We are inclined to attribute the w third maxima in the fluorescence and absorption spect (Fig. 1) to the vibration ν_9 of symmetry E_g^+, the freque of which is 1178 cm^{-1} in the normal state of the molecule.* Ingold and his co-workers did not make use of

*The marked discrepancy between the observed and ca culated frequencies of the transition $\nu_0 - \nu_9$ in the fluorescence spectrum can apparently be explained by the superposition of the intense $\nu_0 - \nu_6$ band.

these vibrations in their interpretation of the fluorescence and absorption spectra of benzene; however, Sp Nordheim, Sklar, and Teller considered it possible to

Table 1. Positions of the Band Maxima in the Fluorescence Spectrum of an Alcoholic Solution of Benzene at −196°C

No.	Intensity*	ν (cm^{-1}) Experimental	ν (cm^{-1}) Calculated	$\Delta\nu$ (cm^{-1})	Corresponds to transition to vibrational level
1	—	Not observed	37780	—	Zero-point
2	s	37175	37174	+ 1	6
3	w	36690	36602	+ 88	9
4	vs	36150	36182	− 32	6 + 1
5	w	35720	35610	+110	9 + 1
6	s	35175	35190	− 15	6 + 2 × 1
7	w	34770	34618	+152	9 + 2 × 1
8	m	34180	34198	− 18	6 + 3 × 1
9	w	33780	33626	+154	9 + 3 × 1
10	w	33225	33206	+ 19	6 + 4 × 1
11	vw	32790	32634	**	9 + 4 × 1
		32750			

*Abbreviations: vw — very weak, w — weak, m — medium intensity, s — strong, sv — very strong.

**Accuracy of determination of the position of the maximum does not exceed ± 40 cm^{-1}.

pret the group of lines near 36,900 cm^{-1} in the fluocence spectrum of gaseous benzene as the transition ν_9 and showed that this hypothesis is strengthened by fact that in heavy benzene, for which ν_9 = 867 cm^{-1}, re is also a group of lines in the region $\nu_0 - \nu_9$.

On the basis of the foregoing, we consider it possible lescribe the formation scheme for the fluorescence ctrum of benzene in alcoholic solution by means of following two series*:

ne absorption spectrum can also be described by these ne series by replacing ν_6 and ν_1 by the vibration frencies in the excited state ν_6' and ν_1'.

$$\nu = \nu_0 - \nu_6 - n\nu_1,$$
$$\nu = \nu_0 - \nu_9 - n\nu_1,$$

ere n = 0, 1, 2, 3.

The bands of the first series are considerably more ense than those of the second series. The most intense d in the fluorescence spectrum corresponds to the nsition $\nu_0 - \nu_6 - \nu_1$.

This sketchy comparison of the phosphorescence and orescence spectra of benzene already convinces us that y do not resemble one another. At the same time, there no reason to say that any of the bands in the phosphoresnce spectrum are due to impurities present in the ginal preparation or created as a result of photochemi- changes in the benzene.

The positions of the calculated and observed maxima the phosphorescence spectrum of benzene are preted in Table 2.

Like Sveshnikov and Dikun and Shull, we shall take observed position of the first phosphorescence band the zero-point transition (frequency 29,510 cm^{-1}).*

veshnikov and Dikun give ν = 29,515 cm^{-1}, Shull gives 29,470 cm^{-1}.

is value is calculated from the location of the fourth nd* as 29,525 cm^{-1}. The second phosphorescence band

should be noted that, in the analysis of the spectrum, concentrated not on the weak first band, corresponding a purely electronic transition, but on the intense rth band, which is interpreted as $\nu_0 - \nu_8$. We feel that the first place it is possible in this way to obtain a re accurate determination of the frequency of the nsition corresponding to the purely electronic transin $^3B_{1u} \rightarrow {}^1A_{1g}$; in the second place, the choice of the

Table 2. Positions of the Band Maxima in the Phosphorescence Spectrum of an Alcoholic Solution of Benzene at −196°C

No.	Intensity*	ν (cm^{-1}) Experimental	ν (cm^{-1}) Calculated	$\Delta\nu$ (cm^{-1})	Corresponds to a transition to the vibrational level
1	m	29510	29525	−15	Zero
2	w	28840	28840	0	4
3	s	28345	28347	−2	9
4	vs	27940	27940	0	8
5	s	27365	27355	+10	9 + 1
6	vs	26950	26948	+2	8 + 1
7	m	26370	26363	+9	9 + 2 × 1
8	s	25955	26355	+15	2 × 8
9	w		25956	−1	8 + 2 × 1
10	w	25595	25584	+9	2 × 9 + 8
11	m	25360	25371	−11	9 + 3 × 1
12	m	24190	25177	+13	9 + 2 × 8
13	w	24970	24964	+6	8 + 3 × 1
14	w	24740	24770	−30	3 × 8
15	vw	24580	24592	−12	2 × 9 + 8 + 1
16	m	24390	24379	+11	9 + 4 × 1
17	w	24245	24285	−40	9 + 2 × 8 + 1
18	w	23930	23972	−42	8 + 4 × 1
19	vw	23780	23778	+2	3 × 8 + 1
20	w	23580	23600	−20	2 × 9 + 8 + 2 × 1
21	w	23270	23293	−23	9 + 2 × 8 + 2 × 1
		23000	22980	−20	8 + 5 × 1

*See notes to Table I.

$\nu_0 - \nu_8$ band as a starting point for all the calculations is justified by the work of Broude and Onoprienko,[17] in which it was shown that in the absorption spectrum of crystals of benzene at 20°K the transitions associated with the purely electronic vibration ν_{1u} undergo splitting (about 40 cm^{-1}), whereas the transitions associated with the nonfully symmetrical C—C vibrations are not split, and also by the works of Bhagavantam and Rao, Broderson and Langseth, and Weigang and Robertson,[18] in which it was shown that, in going from benzene vapor to solution, the frequencies of the C—C vibrations (ν_6, ν_1) do not change, but C—H does change by 10 cm^{-1} (20 cm^{-1} in the excited state).

can be explained only by assuming that it corresponds to the transition $\nu_0 - \nu_4$, as was pointed out by the authors mentioned. If this band were sufficiently intense, the argument over the symmetry of the phosphorescent level could be resolved in favor of B_{1u} rather than B_{2u}. However, this band is unfortunately very weak, and it is always possible to assume that it appears because of solvent interaction.

By analogy with the fluorescence and absorption spectra, it should further be expected that the $\nu_0 - \nu_6$ band would be present in the phosphorescence spectrum. However there is no hint of this band in this spectrum. The third band in the phosphorescence spectrum corresponds to the transition $\nu_0 - \nu_9$. This is the first band in the series $\nu = \nu_0 - \nu_9 - n\nu_1$, where n = 0, 1, 2, 3, 4. The fourth band corresponds to the transition $\nu_0 - \nu_8$. This band ranks second in intensity in the phosphorescence spectrum. It begins the series of intense bands $\nu = \nu_0 - \nu_8 - n\nu_1$, where n = 0, 1, 2, 3, 4, 5; the second band of this series is the most intense one.

In order to explain the origin of the eight remaining bands in the phosphorescence spectrum, we are obliged, like Sveshnikov and Dikun and Shull, to permit transitions in which some ν_8 and ν_9 vibrations participate. Transitions in which any number of ν_8 and ν_9 vibrations participate in any combination are allowed by the selection rules. However, analysis of the spectrum shows that these vibrations combine in a very definite way, and this requires some elucidation.

Thus, the 9th band of the phosphorescence spectrum is impossible to explain in any other way than as $\nu_0 - \nu_8 -$

corder, which permits a more accurate determination of the energy distribution in the emission spectrum, if precautions are taken to conduct the excitation in such a manner that the photochemical reactions observed in frozen solutions of benzene are sufficiently small.

METHOD OF MEASUREMENT

The apparatus for the investigation of fluorescence spectra consisted of a PRK-4 mercury lamp, from whose spectrum the entire region shorter than 2600 A was isolated by means of a double quartz monochromator, a quartz dewar, a quartz test tube containing the solution being investigated, a grating monochromator (1200 lines/mm) blazed for 3300 A in the first order, a photomultiplier, and an M-95 galvanometer. A Becquerel phosphoroscope was used for studying the phosphorescence spectra; the luminescence was excited with the total light from a mercury lamp. In order to avoid absorption and scattering of the exciting radiation and the luminescence by liquid air (nitrogen), the excitation and observation were conducted from the same side with a small angle between the incident and emergent beams. This was achieved through the use of an aluminum mirror.

Before beginning work, the spectral sensitivity curve of the monochromator and photomultiplier combined was accurately determined using a ribbon lamp with a Uviol window* specially calibrated according to temperature.

*The absorption of the Uviol window was measured separately.

Studies of absorption spectra were carried out with an SF-4 photoelectric spectrometer with a modified cell chamber.

RESULTS AND DISCUSSION

Figure 1 shows the fluorescence spectrum and the long wavelength part of the absorption spectrum of an alcoholic solution of benzene at −196°C; Fig. 2 shows the phosphorescence spectrum of the same solution. The positions of the maxima in the fluorescence spectra are given in Table 1.

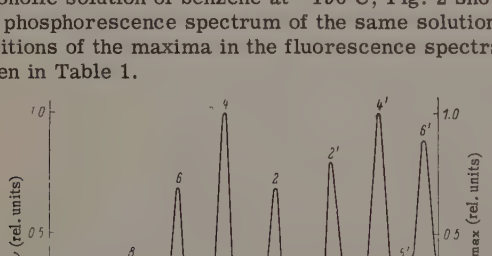

Fig. 1. Fluorescence spectrum and long wavelength part of the absorption spectrum of an alcoholic solution of benzene at −196°C. The broken line indicates the position of the band corresponding to the electronic transition.

Figure 1 and Table 1 show a clear alternation of intense (even-numbered) and weak (odd-numbered) bands in the fluorescence spectrum. The intervals between the strong bands are 1025, 975, 995, and 955 cm^{-1}, and between the weak ones 970, 950, and 990 cm^{-1}.* It is mo

*The intervals between the first and third, and between the ninth and eleventh bands are not indicated here.

natural to assume that these intervals correspond to t totally symmetrical vibration of benzene at 992 cm^{-1}. For the excited benzene molecule, the frequency of thi same vibration is 923 cm^{-1}, as is well known. The sep rations between the second and fourth (930 cm^{-1}) and t fourth and sixth (930 cm^{-1}) bands of the benzene absor tion spectrum agree satisfactorily with this value.

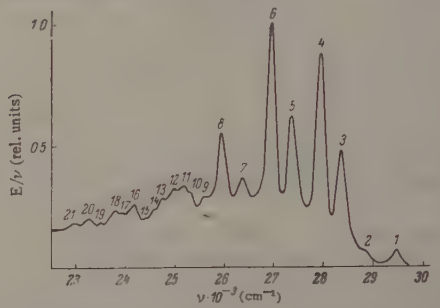

Fig. 2. Phosphorescence spectrum of an alcoholic solution of benzene at −196°C.

According to the selection rule for the transition $A_{1g} \leftrightarrow B_{2u}$, i.e., for the fluorescence and absorption of benzene, the totally symmetrical vibrations can appear in the spectrum only after distortion of the molecule a a result of the nontotally symmetrical vibration of sym metry E_g^+. The frequencies of the fundamental vibratio are given above. Since the separation between the first tense band in the fluorescence spectrum and the first tense band in the absorption spectrum is 1180 cm^{-1} an the term diagrams should be the same for both spectra the vibration to be chosen from the four E_g^+ vibrations given above is ν_6, whose frequency is 606 cm^{-1} in the u excited state and 521 cm^{-1} in the excited state. Hence frequency of the zero transition $A_{1g} \leftrightarrow B_{2u}$ is 37,780 c

*We were unable to determine the location of this first band in the fluorescence spectrum because of weak sca tering of the exciting radiation in our apparatus in that region.

The frequency of the purely electronic transition calcu lated in this way in alcoholic solution at −196°C is shi 300 cm^{-1} relative to vapor state.

It can be seen from Fig. 1 that the first absorptio band, which should correspond to a purely electronic transition, is displaced to the blue relative to the frequency calculated for this transition. This is probably result of the superposition of the intense second maximum in absorption. We are inclined to attribute the w third maxima in the fluorescence and absorption spect (Fig. 1) to the vibration ν_9 of symmetry E_g^+, the frequ of which is 1178 cm^{-1} in the normal state of the molecule.* Ingold and his co-workers did not make use of

*The marked discrepancy between the observed and ca culated frequencies of the transition $\nu_0 - \nu_9$ in the fluo rescence spectrum can apparently be explained by the superposition of the intense $\nu_0 - \nu_6$ band.

these vibrations in their interpretation of the fluores cence and absorption spectra of benzene; however, Sp Nordheim, Sklar, and Teller considered it possible to

Table 1. Positions of the Band Maxima in the Fluorescence Spectrum of an Alcoholic Solution of Benzene at −196°C

No.	Intensity*	ν (cm⁻¹) Experimental	ν (cm⁻¹) Calculated	Δν (cm⁻¹)	Corresponds to transition to vibrational level
1	—	Not observed	37780	—	Zero-point
2	s	37175	37174	+ 1	6
3	w	36690	36602	+ 88	9
4	vs	36150	36182	− 32	6 + 1
5	w	35720	35610	+110	9 + 1
6	s	35175	35190	− 15	6 + 2 × 1
7	w	34770	34618	+152	9 + 2 × 1
8	m	34180	34198	− 18	6 + 3 × 1
9	w	33780	33626	+154	9 + 3 × 1
10	w	33225	33206	+ 19	6 + 4 × 1
11	vw	32790	32634	**	9 + 4 × 1
		32750			

*Abbreviations: vw – very weak, w – weak, m – medium intensity, s – strong, sv – very strong.

**Accuracy of determination of the position of the maximum does not exceed ± 40 cm⁻¹.

pret the group of lines near 36,900 cm⁻¹ in the fluocence spectrum of gaseous benzene as the transition ν_9 and showed that this hypothesis is strengthened by fact that in heavy benzene, for which ν_9 = 867 cm⁻¹, re is also a group of lines in the region $\nu_0 - \nu_9$.

On the basis of the foregoing, we consider it possible lescribe the formation scheme for the fluorescence ctrum of benzene in alcoholic solution by means of following two series*:

e absorption spectrum can also be described by these ne series by replacing ν_6 and ν_1 by the vibration frencies in the excited state ν_6' and ν_1'.

$$\nu = \nu_0 - \nu_6 - n\nu_1,$$
$$\nu = \nu_0 - \nu_9 - n\nu_1,$$

re n = 0, 1, 2, 3.

The bands of the first series are considerably more ense than those of the second series. The most intense d in the fluorescence spectrum corresponds to the nsition $\nu_0 - \nu_6 - \nu_1$.

This sketchy comparison of the phosphorescence and orescence spectra of benzene already convinces us that y do not resemble one another. At the same time, there no reason to say that any of the bands in the phosphoresnce spectrum are due to impurities present in the ginal preparation or created as a result of photochemi- changes in the benzene.

The positions of the calculated and observed maxima the phosphorescence spectrum of benzene are preted in Table 2.

Like Sveshnikov and Dikun and Shull, we shall take observed position of the first phosphorescence band the zero-point transition (frequency 29,510 cm⁻¹).*

veshnikov and Dikun give ν = 29,515 cm⁻¹, Shull gives 29,470 cm⁻¹.

is value is calculated from the location of the fourth nd* as 29,525 cm⁻¹. The second phosphorescence band

should be noted that, in the analysis of the spectrum, concentrated not on the weak first band, corresponding a purely electronic transition, but on the intense rth band, which is interpreted as $\nu_0 - \nu_8$. We feel that the first place it is possible in this way to obtain a re accurate determination of the frequency of the nsition corresponding to the purely electronic transi- n $^3B_{1u} \rightarrow {}^1A_{1g}$; in the second place, the choice of the

Table 2. Positions of the Band Maxima in the Phosphorescence Spectrum of an Alcoholic Solution of Benzene at −196°C

No.	Intensity*	ν (cm⁻¹) Experimental	ν (cm⁻¹) Calculated	Δν (cm⁻¹)	Corresponds to a transition to the vibrational level
1	m	29510	29525	−15	Zero
2	w	28840	28840	0	4
3	s	28345	28347	−2	9
4	vs	27940	27940	0	8
5	s	27365	27355	+10	9 + 1
6	vs	26950	26948	+2	8 + 1
7	m	26370	26363	+9	9 + 2 × 1
8	s	25955	26355	+15	2 × 8
9	w		25956	−1	8 + 2 × 1
10	w	25595	25584	+9	2 × 9 + 8
11	m	25360	25371	−11	9 + 3 × 1
12	m	24190	25177	+13	9 + 2 × 8
13	w	24970	24964	+6	8 + 3 × 1
14	w	24740	24770	−30	3 × 8
15	vw	24580	24592	−12	2 × 9 + 8 + 1
16	m	24290	24379	+11	9 + 4 × 1
17	w	24245	24285	−40	9 + 2 × 8 + 1
18	w	23930	23972	−42	8 + 4 × 1
19	vw	23780	23778	+2	3 × 8 + 1
20	w	23580	23600	−20	2 × 9 + 8 + 2 × 1
21	w	23270	23293	−23	9 + 2 × 8 + 2 × 1
		23000	22980	−20	8 + 5 × 1

*See notes to Table I.

$\nu_0 - \nu_8$ band as a starting point for all the calculations is justified by the work of Broude and Onoprienko,[17] in which it was shown that in the absorption spectrum of crystals of benzene at 20°K the transitions associated with the purely electronic vibration ν_{1u} undergo splitting (about 40 cm⁻¹), whereas the transitions associated with the nonfully symmetrical C–C vibrations are not split, and also by the works of Bhagavantam and Rao, Broderson and Langseth, and Weigang and Robertson,[18] in which it was shown that, in going from benzene vapor to solution, the frequencies of the C–C vibrations (ν_6, ν_1) do not change, but C–H does change by 10 cm⁻¹ (20 cm⁻¹ in the excited state).

can be explained only by assuming that it corresponds to the transition $\nu_0 - \nu_4$, as was pointed out by the authors mentioned. If this band were sufficiently intense, the argument over the symmetry of the phosphorescent level could be resolved in favor of B_{1u} rather than B_{2u}. However, this band is unfortunately very weak, and it is always possible to assume that it appears because of solvent interaction.

By analogy with the fluorescence and absorption spectra, it should further be expected that the $\nu_0 - \nu_6$ band would be present in the phosphorescence spectrum. However there is no hint of this band in this spectrum. The third band in the phosphorescence spectrum corresponds to the transition $\nu_0 - \nu_9$. This is the first band in the series $\nu = \nu_0 - \nu_9 - n\nu_1$, where n = 0, 1, 2, 3, 4. The fourth band corresponds to the transition $\nu_0 - \nu_8$. This band ranks second in intensity in the phosphorescence spectrum. It begins the series of intense bands $\nu = \nu_0 - \nu_8 - n\nu_1$, where n = 0, 1, 2, 3, 4, 5; the second band of this series is the most intense one.

In order to explain the origin of the eight remaining bands in the phosphorescence spectrum, we are obliged, like Sveshnikov and Dikun and Shull, to permit transitions in which some ν_8 and ν_9 vibrations participate. Transitions in which any number of ν_8 and ν_9 vibrations participate in any combination are allowed by the selection rules. However, analysis of the spectrum shows that these vibrations combine in a very definite way, and this requires some elucidation.

Thus, the 9th band of the phosphorescence spectrum is impossible to explain in any other way than as $\nu_0 - \nu_8 -$

$2\nu_9$. Then the 14th is easily explained as $\nu_0 - \nu_8 - 2\nu_9 - \nu_1$, and the 19th as $\nu_0 - \nu_8 - 2\nu_9 - 2\nu_1$. But in spite of everything, it is impossible to find any bands associated with the transitions $\nu_0 - 2\nu_9$ and $\nu_0 - \nu_8 - \nu_9$; i.e., some lines are lacking in the series.

Our observations are probably pertinent to the remaining five bands also. We have interpreted three of them as $\nu_0 - \nu_9 - 2\nu_8 - n_1\nu_1$, where $n_1 = 0, 1, 2$, and two as $\nu_0 - 3\nu_8 - n_1\nu_1$, where $n_1 = 0, 1$. Unfortunately, it is difficult to judge whether the transition $\nu_0 - 2\nu_8$ appears in the spectrum, since its frequency is rather close to the frequency $\nu_0 - \nu_9 - 2\nu_1$. However, we shall assume that, like $\nu_0 - 2\nu_9$, this transition does not appear to any significant extent.

In the papers of Herzberger and Teller,[19] and also in a series of papers by Sponer and other authors,[20] it is pointed out that, in the benzene spectrum, transitions in which some allowed nonfully symmetrical vibrations participate (for example, several E_g^+ vibrations) ought to be considerably weaker than transitions in which fully symmetrical vibrations and one nonfully symmetrical E_g^+ participate.

It seems to us that the foregoing statements are quite correct when there are two or an even number of nonfully symmetrical E_g^+ vibrations (it is known that two nonfully symmetrical E_g^+ vibrations correspond to one fully symmetrical one). In this way, the absence of $\nu_0 - 2\nu_9$ and $\nu_0 - \nu_9 - \nu_8$ can be understood. At the same time, transitions in which an uneven number of E_g^+ vibrations participate can appear with fair intensities.

Comparing the analysis of the fluorescence spectrum of benzene presented earlier with this analysis of the phosphorescence spectrum, we see that the main difference between the structures of the two spectra is the fact that in the first case the most active vibration is ν_6, and in the second, ν_8. Both of these vibrations are vibrations of the carbon skeleton of the molecule and both have the same symmetry. If it is not assumed that the difference in the most active vibrations is connected with the difference in multiplicity of the upper levels in the case of fluorescence and phosphorescence, i.e., if, in agreement with theory, it is assumed that forbidden intercombinations and symmetries can be completely eliminated, then the difference in the most effective vibrations (and thus in the form) of the two spectra is a good indication that the symmetries of the phosphorescent and fluorescent levels are different. Since the identification of the fluorescent level as the $^1B_{2u}$ level is generally accepted, the phosphorescent level must be identified as $^3B_{1u}$. The presence of the $\nu_0 - \nu_4$ band in the spectrum is also evidence for this. If the identification of the phosphorescent level of benzene as $^3B_{1u}$ is made with the reservation that there is a relative lack of interaction between the spin and vibrational functions of the benzene molecule, then it clearly follows from the analysis of the phosphorescence spectrum that the benzene molecule in the phosphorescent state belongs to the symmetry clas D_{6h} and that there can be no question of a quinoid form the molecule (symmetry class V_h).

REFERENCES

1. H. Shull, J. Chem. Phys. 17, 295 (1949).
2. B. Ya. Sveshnikov and P. P. Dikun, Doklady Akad. Nauk SSSR 65, 637 (1949); Zhur. Eksptl. i Teoret. Fiz. 19, 1000 (1949).
3. G. Lewis and M. Kasha, J. Am. Chem. Soc. 66, 210 (1944).
4. O. Redlich and E. Holt, J. Am. Chem. Soc. 67, 1228 (1945).
5. M. Goeppert-Mayer and A. Sklar, J. Chem. Phys. 6 645 (1938);
   A. London, J. Chem. Phys. 13, 396 (1945);
   R. Mulliken and C. Roothaan, J. Chem. Phys. 16, 1 (1948);
   R. Parr and B. Crawford, J. Chem. Phys. 16, 1049 (1948);
   R. Parr, J. Chem. Phys. 17, 725 (1949);
   C. Roothaan and R. Parr, J. Chem. Phys. 17, 1001 (1949).
6. A. Kronenberger, Z. Physik 63, 497 (1930).
7. L. V. Broude, V. S. Medvedev, and A. F. Prikhot'k Zhur. Eksptl. i Teoret. Fiz. 21, 665 (1951); Opt. i Spektr. 2, 317 (1957);
   V. L. Broude and A. F. Prikhot'ko, Zhur. Eksptl. i Teoret. Fiz. 22, 605 (1952).
8. B. Ya. Sveshnikov and V. L. Ermolaev, Doklady Ak Nauk SSSR 71, 647 (1950).
9. H. Hameka and L. Oosterhoff, Mol. Phys. 1, 358 (1
10. P. Pesteil and A. Zmerli, Ann. phys. 10, 1079 (195
11. C. Cupron, R. Lachet, J. Meyer, and A. Rousset, Compt. rend. 250, 3095 (1960).
12. K. Pitzer and D. Scott, J. Am. Chem. Soc. 65, 803 (1943).
13. A. Zmerli, Compt. rend. 245, 1911 (1957).
14. G. Porter and M. Wright, Discussions Faraday Soc 27, 18 (1959).
15. G. Lewis, D. Lipkin, and T. Magel, J. Am. Chem. Soc. 63, 3005 (1941).
16. C. Ingold et al., J. Chem. Soc. 941, 955 (1936).
17. V. L. Broude and M. I. Onoprienko, Opt. i Spektr. 629 (1960), Optics and Spectroscopy 8, 332 (1960).
18. S. Bhagavantam and A. V. Rao, Proc. Indian Acad. Sci. 5, 18 (1937);
   S. Broderson and A. Langseth, Kgl. Danske Videnskab. Selskab, Mat.-fys. Skrifter 1, 1 (1956).
   O. E. Weigang and W. W. Robertson, J. Chem. Phy 30, 1413 (1959).
19. C. Herzberger and E. Teller, Z. physik. Chem. (B 21, 410 (1950).
20. H. Sponer, C. Nordheim, A. Sklar, and E. Teller, J. Chem. Phys. 7, 207 (1937).

THE EFFECT OF HYDROGEN BONDS ON THE LUMINESCENCE OF OXY- AND AMINO-AZO COMPOUNDS

R. N. Nurmukhametov, D. N. Shigorin, Yu. I. Kozlov, and V. A. Puchkov (pp. 606-612)

Received 28 November 1960

The fluorescence spectra of azo compounds of the benzene and naphthalene series were investigated. It was found that the azo compounds acquire the ability to luminesce when substituents able to form intramolecular (=N...H—O—) or intermolecular (=N...H—O—, =N...H—NH—) hydrogen bonds are introduced. O-hydroxyazo compounds fluoresce only in solutions of n-hydrocarbons at T = 77°K; o-aminoazo compounds do not fluoresce either in solution or as powders. O-hydroxy- and some p-hydroxy- and p-aminoazo compounds luminesce as powders at T = 293 and 77°K. Methylation of the hydroxy- and amino groups causes the fluorescence to disappear. An interpretation of the phenomena discovered is given.

In the present paper, the studies of the effects of rious substituents and structural properties on the ctron states of multiatom molecules containing cer- n chromophores begun in ref. 1 have been extended to azo compounds.

There is very little information in the literature on luminescence of azo compounds. Pringsheim[2] notes t among more than 700 azo dyes, there is not a single mple which is known to fluoresce in solution. This fact n be understood on the basis of properties of the chemi- bond in the azo group. It is known that the π-bond be- en the nitrogen atoms has a greater energy value (~50 -cal) than a σ-bond (~30 kg-cal).[3] When the molecules e excited, a loosening of π-bonds takes place, during ich the bond in the —N=N— group is considerably akened. The energy of an absorbed light quantum is her quickly transformed to thermal energy by way of ration of single bonds, or leads to photodecomposition the compound (as occurs with azomethane, for exple).[4]

We have attempted to clarify the conditions for the pearance of fluorescence in azo compounds, and to es- lish the connection between emission spectra and lecular structure. The compounds studied were syn- sized and purified with the aid of methods described the literature. The luminescence of the azo com- unds was studied under different conditions—in neutral lution and in the powdered state, at various tempera- es.

The concentration of the solutions was 5×10^{-4} le/liter, except for compounds VII and VIII (see Table), ich were 10^{-4} mole/liter as a consequence of the poor lubility of these compounds in hexane. The lumines- nce was excited by light from a PRK-2 lamp ($\lambda_{exc.}$ = 5 mμ). The radiation spectra were recorded by a otoelectric technique on an ISP-51 spectrograph with PS-384 photoelectric attachment. An FEU-17 was used the detector. A correction was made for the sensi- ity of the photomultiplier in order to obtain the true tribution of intensity in the spectrum. In the emission rves shown in the figures, intensity is expressed in lative quantum units.

The experiments which were conducted indicated at liquid solutions of the azo compounds do not truly minesce. A number of compounds showed a yellow-red orescence when cooled in solution to 77°K. Several mpounds were observed to fluoresce as powders even room temperature, and the fluorescence increased on cooling. The factor which determines luminescence is the presence of substituents able to form an intra- or intermolecular hydrogen bond (hydroxy- or amino- groups) (see Table). Other substituents exert a secondary effect on the fluorescence, changing the intensity, location, and width of the emission bands, but do not bring on its appearance (these results will be considered in a separate article).

Unsubstituted azobenzene(I) has no luminescence either as powder or in solution. An intense fluorescence appears when an OH- group is introduced on the benzene or naphthalene ring in the position ortho to the azo group; moreover the o-hydroxy-derivatives of the azo compounds in powdered form luminesce even at room temperature (Fig. 1). A thermochromic effect is observed in the case of the powders on cooling to 77°K, and their fluorescence spectra are increased in intensity (see columns 4 and 6 in the Table) and displaced toward shorter wavelengths (column 8). The color of o-hydroxyazobenzene powder changes from red to yellow when cooled; the maximum of the emission band is displaced 35 mμ. The fluorescence spectra of the powders and solutions consist of several broad maxima. The compounds with the highest symmetry have the most spectral structure.

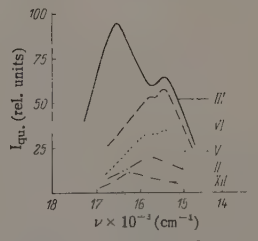

Fig. 1. Emission spectra of azo-compound powders at 20°C, excited by 365 mμ radiation. Curve II: 2-hydroxyazobenzene (× 4); curve III: 1-(benzazo)-naphthol-(2); curve V: 2-(benzazo)-naphthol-(1) (× 3); curve VI: -material VI (see Table) (× 1.5); curve XII: 4-(benzazo)-naphthylamine-(1) (× 10). The scales of some of the curves have been expanded several times for convenience in examination (the factors are shown in parentheses). The true relative intensities of the principal maxima of the emission spectra are given in the Table.

Luminescence Spectra of Azo Compounds as Powders and in Solution

No.	Compound	$T_{melt.}$ (°C)	Powders					Solutions in hexane	
			$T = 293°$ K		$T = 77°$ K		$\Delta\lambda$*** (mμ)	$T = 77°$ K	
			λ* (mμ)	$\frac{I}{I_0}$**	λ* (mμ)	$\frac{I}{I_0}$**		λ* (mμ)	$\frac{I}{I_0}$**
I	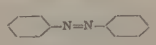	68.5—69.0	none	—	none	—	—	none	—
II	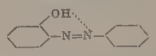	85	634	5	657 636 599 583	6	+35	645 600 581	2
III	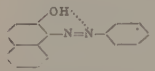	130.5—131	647 605	100	619 587 577	100	+30	635 605 590	25
IV	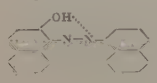	227	In the near infrared region of the spectrum	—	655	4	—	629 619 606 590 578 571 566	40
V	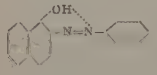	138—139	649 632	11	646 612	23	+5	633 596 586 570	100
VI	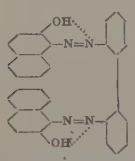	255	646 636	41.5	657 629	41.5	—10	632 605	4
VII	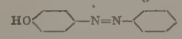	158—159	none	—	587	0.1	—	596	0.2
VIII	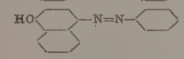	197—197.5	In the near infrared region of the spectrum	—	675	7	—	none	—
IX	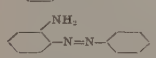	56	none	—	none	—	—	none	—
X	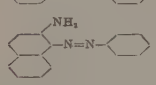	102	none	—	none	—	—	none	—
XI	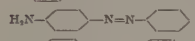	125—126	none	—	none	—	—	none	—
XII	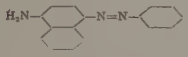	122.5—123.5	614	1	653 613	6.5	—40	none	—
XIII	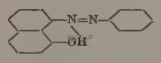	98.5—99.0	none	—	none	—	—	none	—
XIV	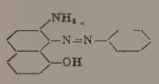	173.0—173.5	none	—	none	—	—	none	—
XV	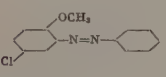	63.5—64.5	none	—	none	—	—	none	—
XVI	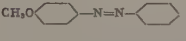	56	none	—	none	—	—	none	—
XVII	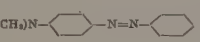	117—118	none	—	none	—	—	none	—

*The locations of the maxima are determined with an accuracy of ± 1 mμ in the green and ± 5 mμ in the red.
**I/I_0 are the ratios of the intensities of the principal maxima (underlined in the Table) in the spectra.
***$\Delta\lambda$ are the displacements of the delta principal maxima of the luminescence spectra of the powders when cooled to T = 77°K.

Of the powders at 77°K, 2-hydroxyazobenzene (II) has the emission spectrum with the most structure (Fig. 2). The spectra of 1-(naphthalene-1-azo)-naphthol-(2)(IV) powder are displaced into the infrared region; consequently, only a part of them could be recorded. In solution (Fig. 3), the spectrum with the most structure (8 bands) was obtained for compound (IV). Vibrational analysis of these spectra is difficult because of the lack of data on the absorption of these compounds under the same conditions, and also because of the fact that the bands are diffuse.

Para-hydroxy-azo compounds [4-oxyazobenzene-(VII), 4-(benzazo)-naphthol-(1) (VIII)] developed a weak luminescence in powders and solutions at 77°K (Figs. 2 and 3). In general the substituted benzazo-naphthalenes

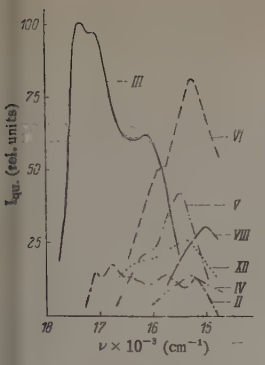

Fig. 2

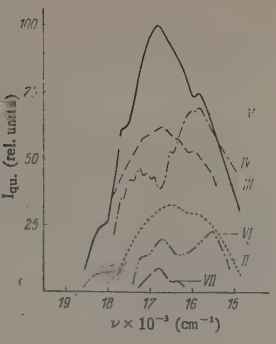

Fig. 3

Fig. 2. Emission spectra of azo-compound powders at 77°K, excited by 365 mμ radiation: Curve II: 2-hydroxyazobenzene (×3.5); curve III: 1-(benzazo)-naphthol-(2); curve IV: 1-(naphthalene-1′-azo)-naphthol-(2) (×3.5); curve V: 2-(benzazo)-naphthol-(1) (×2); curve VI: material VI (see Table) (×2); curve VIII: 4-(benzazo)-naphthol-(1) (×4); curve XII: 4-(benzazo)-naphthylamine-(1) (×4). Curve scales—see note under Fig. 1.

Fig. 3. Emission spectra of solutions of azo compounds in hexane at 77°K, excited by 365 mμ radiation. Curve II: 2-hydroxyazobenzene (×10); curve III: 1-(benzazo)-naphthol-(2) (×2.5); curve IV: 1-(naphthylene-1′-azo)-naphthol-(2) (×1.5); curve V: 2-(benzazo)-naphthol-(1) (×1); curve VI: material VI (see Table) (× 10); curve VII: 4-oxyazobenzene (× 50). Curve scales—see note under Fig. 1.

aving an OH-group in the peri-position to the azo group or example, 1-(benzazo)-naphthol-(8) (XIII) and 1-enzazo)-2-amino-naphthol-(8) (XIV)] do not fluoresce. lethylation of the hydroxy group (replacement of an H om by CH_3) in the ortho- and para- positions [2-methoxy--chlorazobenzene (XV), 4-methoxyazobenzene (XVI)] eads to a disappearance of the luminescence. The intro-uction of a different substituent which can form an H-ond in the azo compound (amino group) exerts a dif-erent influence on the luminescing ability of the mole-ule. Ortho-amino derivatives [2-amino-azobenzene (IX), -(benzazo)-naphthylamine-(2) (X), 1-(benzazo)-2-mino-naphthol-(8) (XIV)] show no luminescence under ny conditions, and 4-(benzazo)-naphthylamine-(1) (XII) luoresces only as a powder.

When the temperature is lowered, the principal max-mum of the spectrum of powder XII is displaced 39 mμ oward the red. Methylation of the amino group located the p-position to the azo group [4-dimethyl-amino-zobenzene (XVI)] causes disappearance of the fluores-ence.

An examination of the luminescence properties of the zo compounds leads to the following conclusions: the zo group corresponds to the long wavelength electronic ransition. Without a hydrogen bridge, this group is rela-ively weakly coupled to the aromatic radicals by a single ond. The absorption of a light quantum leads to a loosen-ng of the bond in the azo group. There is a very high robability of transferring electronic energy by torsional ibration. There is a formation of intramolecular hydro-gen bonds in o-oxy and o-aminoazo compounds. On the basis of a study of the infrared absorption spectra,[5] Shigorin, Bagratishvili, and Postovskii noted that a different kind of hydrogen bond is formed in these azo compounds. Thus, in the ortho-hydroxy derivatives of the azo compounds of the benzene series, the characteristic OH vibrational frequency is reduced to $\nu_{OH} = 3175$ cm^{-1}; in the derivatives of the naphthalene series it is reduced to $\nu_{OH} = 3100$ cm^{-1}. In the case of the o-amino-azo compounds of the naphthalene series $\nu_{NH} = 3225$ cm^{-1} (formation of H-bonds takes place), but in o-aminoazo-benzene, the free N-H frequency appears.

According to the hypothesis developed by one of us,[6] the hydrogen bond (as well as the metallic element bond) in molecules with a conjugated system of bonds is formed as a result of three kinds of interactions: dipole (E_d), acceptor-donor (E_a), and π-electron (E_π); i.e.,

$$E_H = E_d + E_a + E_\pi .$$

In conjugate systems, π-electron interaction plays the determining role in the formation of the H-bond, especially in the excited state of the molecule. However, π-electron interaction plays this role only when the ring formed by means of the hydrogen bond is coplanar with the remaining part of the molecule. Exactly such a plane, quasi-aromatic, six-membered ring is formed in o-hydroxyazo compounds; it is closed by an H-bond and is coplanar with the remainder of the molecule (I).

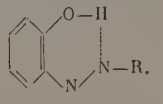

(I)

Here R is a radical of benzene, naphthalene, or their substituents.

The planar character of the structure of such compounds is confirmed by the value of their dipole moments.

The structure of the molecule becomes more rigid as a result of the formation of an additional plane ring with sharing of π-electrons. When the molecule is excited, the hydrogen bond and the additional ring are retained and possibly even strengthened as a consequence of the increase in coupling with the π-electron system, which reduces the probability of deactivation. The strengthening of the skeleton of the molecule, especially the chromophoric —N=N— group included in the new ring, leads to an increase in the lifetime of the excited state of the o-hydroxyazo compound molecules. Fluorescence develops in these compounds because of this condition. It should be noted that metallic element bonds in inner complex azo compounds containing metals are even more effective than the hydrogen bond in increasing luminescence;[7] their effect is similar, however.[8] A hydroxy-group in the peri-position of benzazo naphthalene interacts with the nearest atom and loosens the electron system of the azo group, so that the latter is not included in the ring with the hydrogen bond (II).

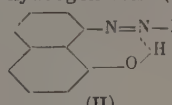

(II)

When the condition of coplanarity is violated in the formation of a hydrogen bond, π-electron interaction is reduced and acceptor-donor interaction plays the primary role. The latter occurs in o-aminoazo compounds with hydrogen bridges

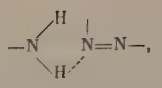

in which the coplanarity conditions are not fulfilled very well. For this reason, a weakening rather than a strengthening of the H-bond takes place during excitation. It may even be broken as a result of the disruption of the acceptor-donor interaction and the difficulty of participation by an NH_2-group in π-electron interaction. This hypothesis is supported by the absence of luminescence in the o-aminoazo compounds. The occurrence of weak luminescence in powders of p-aminoazo compounds and the even weaker luminescence of p-hydroxyazo compounds is explained by the formation of intermolecule H-bridges. The fluorescence of these compounds in solution is either absent altogether or significantly weakened (in the latter case, apparently because of the presence in solution of a certain quantity of molecules associated by means of intermolecular H-bonds). The possibility of forming intra- and intermolecular hydrogen bonds is lost when the OH- and NH_2- groups are methylated and the fluorescence disappears.

The observed characteristics of the fluorescence of the azo compounds indicate that the event of light absorption by the molecule is located primarily in the azo group. The results obtained in this investigation indicate the important role of H-bonds in the processes of transfer and redistribution of energy (both within and between molecules), which determine the luminescence properties of the compounds.

REFERENCES

1. D. N. Shigorin, N. A. Shcheglova, R. N. Nurmukhametov, and N. S. Dokunikhin, Doklady Akad. Nauk SSSR 120, 1242 (1958), Soviet Phys.-Doklady 3, 628 (1958).
2. P. Pringsheim, "Fluorescence and Phosphorescence," p. 335 of Russian edition. Interscience, New York, 1949. Foreign Literature Press, Moscow, 1951.
3. Ya. K. Syrkin and M. E. Dyatkina, "The Chemical Bond and Molecular Structure," p. 288 of Russian edition. State Publishers of Chemical Literature, Moscow, 1946.
4. W. West, ed., "Chemical Applications of Spectroscopy p. 603 of Russian edition. Foreign Literature Press, Moscow, 1954. Interscience, New York, 1956.
5. G. D. Bagratishvili and D. N. Shigorin, Doklady Akad. Nauk SSSR 56, 753 (1954);
G. D. Bagratishvili, Doctoral dissertation, Moscow, 1954.
6. D. N. Shigorin, Izvest. Akad. Nauk SSSR, Ser. Fiz. 14, 395 (1953); Spectrochim. Acta. 14, 198 (1959).
7. E. A. Bozhevol'nov, Izvest. Akad. Nauk SSSR, Ser. Fiz. 24, 762 (1960).
8. D. N. Shigorin, A. N. Rodionov, T. V. Talalaeva, and K. A. Kocheshkov, Doklady Akad. Nauk SSSR 133, 178 (1960).

ON QUENCHING OF FLUORESCENCE IN SOLUTIONS AT LIQUID AIR TEMPERATURE BY IODIDES

L. A. Kiyanskaya and B. Ya. Sveshnikov (pp. 613-616)

Received 9 December 1960

The change in the duration and yield of fluorescence of several fluorescent substances in aqueous-alcohol solutions at −183°C has been studied as a function of iodide concentration. Zelinskii and Kolobkov's hypothesis that halogen-containing compounds quench the fluorescence of solutions at room temperature by increasing the probability of transition of an excited molecule to the metastable state has been shown not to have general significance, and may only be useful in explaining individual cases.

The theory of diffusion fluorescence quenching of solutions contains one important assumption that is not always pointed out. It is assumed that the duration of the quenching is very short in comparison with the time of diffusion, or, in other words, that there is a marked dependence of the probability of quenching on the distance between the molecules. Consequently, the idea of a sharply defined zone of action, inside of which the probability of quenching is close to one and outside of which is equal to zero, has been successfully used in explaining diffusion quenching. The hypothesis that the probability of quenching by extraneous substances (not absorbing the fluorescence) is strongly affected by the distance between the molecules is consistent with the fact that the zone of action in diffusion quenching is shown by calculations to be close to a kinetic sphere.

Experiments on the dependence of quenching on viscosity have furnished cogent evidence in favor of the diffusion theory of fluorescence quenching of solutions by extraneous substances and the sharp dependence of quenching on the distance between the molecules. In several instances, when the diffusion quenching theory is quantitatively obeyed by solutions of low viscosity, quenching is strongly reduced on changing to viscous solutions, and tends to zero for infinite viscosity.

The purpose of this investigation is to examine the extent to which these well known facts agree with the hypothesis of Zelinskii and Kolobkov, according to which the fluorescence quenching of solutions by halogen-containing compounds at room temperature consists in increasing the probability of transition of a molecule to the metastable state. In accordance with this hypothesis, the authors consider that an investigation of the fluorescence quenching action of halides at room temperature is a method for studying the probability of transition of a molecule to the metastable state.

As proof of the stated hypothesis, they refer to their own results and to those of Zhmyreva and Borgman[1] on the quenching of the fluorescence of aqueous-alcohol solutions of phthalimides and naphthalene derivatives by

Change in Duration ($\tau \times 10^{-9}$ sec) and Intensity of Fluorescence (I_f) of Solutions of Several Fluorescent Substances at −183°C as a Function of Iodide Concentration

Substance and concentration (moles/liter)	Additive	Concentration of additive (moles/liter)	τ	J_f	Comments
Fluorescein (3×10^{-6})	—	0	1.5	1	Concentration of NaOH 7.5×10^{-4} mole/liter
	KI	0.39	4.4	3	
	KI	0.78	1.9	2	
Fluorescein (3×10^{-6})	—	0	4.9	1	Concentration of NaOH 0.25 mole/liter
	KI	0.39	4.86	1	
	KI	0.78	4.83	1	
Erythrosine (1×10^{-5})	—	0	2.5		
	KI	0.156	2.5		
	KI	0.39	2.37		
	KI	0.78	2.3		
Eosin (1×10^{-5})	—	0	2.96		
	KI	0.156	2.74		
	KI	0.39	2.73		
	KI	0.78	2.73		
4-acetylamino-N-meyhylphthalmide (1×10^{-4})	—	0	19.5	1*	
	KI	0.78	14.8	0.23	
	NaI+KI	2.95	8.1	0.03	
Quinine bisulfate (1×10^{-4})	—	0	7.4	1	
	KI	0.156	6.25	0.91	
	KI	0.39	6.0	0.83	
	KI	0.78	5.7	0.75	
	KI	1.56	5.1	0.475	
3-aminophthalmide (1×10^{-5})	—	0	16.0	1.0	
	KI	0.156	15.4	0.91	
	KI	0.39	14.9	0.85	
	KI	0.78	13.4	0.73	
Anthracene (1×10^{-4})	—	0	8.8	1.0	
	KI	0.156	7.4	0.89	
	KI	0.39	6.8	0.705	
	KI	0.78	5.7	0.41	

Data of Zelinskii, Kolobkov, Zhmyreva, and Borgman.

iides at −183°. For the group of compounds studied by e four authors, a significant decrease in fluorescence eld and increase in phosphorescence yield is actually served when iodides are added to solutions of the fluoscent substances. The abovementioned authors obrved the phenomena described during fluorescence enching by iodides or bromides, but not during quench- by organic substances. Consequently, they apply their pothesis only to quenching by iodides and bromides and ore the problems connected with the quenching of fluoscence by organic substances.

The increase in phosphorescence yield, i.e., in the obability of transition from the fluorescent to the metaible state under the action of heavy atoms, has been monstrated many times;[2] however, in order to use this echanism to explain the fluorescence quenching of soluns at room temperature, more substantial experimental oof is required. Firstly, it was necessary to study the netics of fluorescence quenching by iodides in cooled lutions.

We studied the quenching effect of iodides on the iorescence of seven substances: two phthalimides, orescein, eosin, quinine bisulfate, and anthracene bilfate, in a mixture of methyl alcohol and water at 83°. The investigation was mainly confined to studying anges in the duration and yield of fluorescence, but in me instances the changes in initial intensity and duran of phosphorescence were also studied.

In initial experiments on the fluorescence quenching fluorescein, it was found that the addition of potassium dide to a solution of the dye containing a small amount alkali (1×10^{-4} mole/liter) has a very peculiar effect—low concentrations of potassium iodide the duration of minescence is increased, and at high concentrations the ration and intensity are diminished rapidly (see Table). the addition of large amounts of alkali (0.25 mole/liter) the solution, all of these phenomena disappear, and the duration of the luminescence is practically unchanged upon adding 0.78 mole/liter of potassium iodide to the solution. Also, the addition of the same amount of potassium iodide has little effect on the fluorescence of eosin and erythrosine solutions.

For the remaining four fluorescent compounds (quinine bisulfate, anthracene bisulfate, and the two phthalimides), the addition of potassium iodide to a solution of the fluorescent substance decreases the duration and yield of luminescence. Furthermore, the duration of luminescence of all the compounds studied varies linearly with increasing quencher concentration, and the yield (with the exception of 3-aminophthalimide) varies superlinearly.

However, the differences between the changes of yield and duration of fluorescence are large only for 4-acetylaminophthalimide; for anthracene and quinine bisulfate they do not exceed three.

We attempted to corroborate the viewpoint of the abovementioned authors by separating the quenching into fluorescent and phosphorescent levels. As indicated in a theoretical article by one of the writers,[3] during excitation periods which are short, compared with the duration of phosphorescence, the initial phosphorescence intensity depends on quenching at the fluorescent level and is independent of quenching at the phosphorescent level.

The fluorescence and phosphorescence yields of cooled solutions of 4-acetylamino-N-methylphthalimide are 0.78 and 0.07 respectively, and the fluorescence yield in the presence of 0.78* mole/liter of quencher is 0.16;

*The concentration specified refers to the calculated volume of the cooled solution.

and, since Zelinskii and Kolobkov believe that fluorescence quenching should be considered as a transition to the phosphorescent state, we expected that for this quencher the initial intensity of phosphorescence should increase about seven times.

Experiments* showed that the initial phosphorescence

*The procedure and equipment were described previously by Mokeeva and Sveshnikov.[4]

intensity of quenched (0.78 mole/liter) solutions of 4-acetylamino-N-methylphthalimide is sixty-five times greater than the initial phosphorescence intensity of the unquenched solution. A study of the laws of phosphorescence attenuation of quenched solutions using a taumeter enabled us to find the cause of this discrepancy. Quenched solutions of 4-acetylamino-N-methylphthalimide, in contrast to unquenched solutions, showed an intense phosphorescence with a duration of the order of 1×10^{-3} sec. Apparently, it exists simultaneously with the phosphorescence having a duration of 0.27 sec, which was found in quenched solutions by Zelinskii, Kolobkov, Zhmyreva, and Borgman.

Thus, on the addition of iodides to a solution of 4-acetylamino-N-methylphthalimide, two metastable states are formed. It is most natural to assume that they are intrinsically different emitting centers, and that in the centers having a shorter duration of luminescence, the iodides are more firmly combined with the fluorescent substance (as a complex compound, for example). The existence of a chemical bond between molecules of the iodine-containing substance and 4-acetylamino-N-methylphthalimide is also suggested by the fact that, according to the results of the abovementioned four authors, an increase in iodide concentration from 0.78 to 2.95 mole/liter does not affect the luminescence yield of

a cooled solution of the given phthalimide, whereas the total luminescence yield of a solution containing 0.78 mole/liter iodide is 2.2 times less than for a solution not containing iodides.

From our brief investigation we draw the following conclusions: The experiments of Zelinskii, Kolobkov, Zhmyreva, and Borgman present additional indisputable confirmation of the well-known hypothesis that the presence of heavy atoms in a solution of a fluorescent substance substantially facilitates intercombination transtions in an excited molecule of the fluorescent substance. One cannot deny that this mechanism operates during the fluorescence quenching of solid solutions by foreign substances, and, judging by the picture of quenching, there are two possible alternatives: the formation of complexes and the influence of distance. However, one cannot apply the second, more interesting case to the quenching of liquid solutions. Actually, from the nature of the dependencies of the change of yield and duration of fluorescence on the quencher concentration, it follows that the quenching action of iodides on anthracene, quinine, and 3-aminophthalimide diminishes relatively slowly as the distance between the molecules of the quencher and the excited fluorescence substance increases. If this quenching mechanism, with the same dependence on distance between the molecules, were fundamental in liquid solutions, then the existence of a marked dependence of quenching on the viscosity of the solvent would be incomprehensible. It is well known that in the quenching of fluorescence by foreign absorbing substances, where it is assumed that the quenching action is inversely proportional to the sixth power of the distance between the excited molecules and molecules of the quencher, the dependence of quenching action on viscosity is very slight.

REFERENCES

1. V. V. Zelinskii and V. P. Kolobkov, Doklady Akad. Nauk SSSR **101**, 241 (1955); Opt. i Spektr. **1**, 560 (1956)
V. V. Zelinskii, V. P. Kolobkov, I. A. Zhmyreva, and V. A. Borgman, Doklady Akad. Nauk SSSR **131**, 781 (1960), Soviet Phys.-Doklady **5**, 324 (1960);
V. P. Kolobkov, Candidate's Thesis, Minsk, 1960;
V. V. Zelinskii, V. P. Kolobkov, and N. I. Kondaraki, Doklady Akad. Nauk SSSR **117**, 391 (1957), Soviet Phys Doklady **2**, 501 (1958).
2. P. Yuster and S. J. Weissman, J. Chem. Phys. **17**, 1183 (1949);
E. Clementy and M. Kăsha, J. Chem. Phys. **26**, 956 (1957).
3. B. N. Sveshnikov, Zhur. Eksptl. i Teoret. Fiz. **18**, 10, 897 (1948).
4. G. A. Mokeeva and B. Ya. Sveshnikov, Opt. i Spektr. **9**, 601 (1960), Optics and Spectroscopy **9**, 317 (1960).
5. B. Ya. Sveshnikov and L. A. Kuznetsova, Opt. i Spektr **4**, 57 (1958).

PHOSPHORESCENCE OF ORGANIC MOLECULES WITH TWO METASTABLE LEVELS

M. E. Khalupovskii (pp. 617-622)

Received 31 December 1960

Phosphorescence spectra of organic phosphors were investigated at various temperatures in different stages of decay. The experimental data are explained by postulating the possibility of two metastable levels in the organic molecule.

The possibility of two metastable levels existing in an organic molecule was demonstrated by Pilipovich and Sveshnikov, who established a difference in the degree of polarization of the long wavelength phosphorescence in various parts of the emission spectrum.[1,2]

Problems connected with the location of metastable levels, their interaction among themselves and with other electronic levels of the radiating molecule were studied by Kato and Koizumi[3] who proposed a model with two metastable levels for the phosphorescence of tripaflavin on silica gel; only nonradiative transitions from both metastable levels were permitted in this model.

Luminescence of tripaflavin on silica gel at room temperature is, as shown by Kato and Koizumi, α-phosphorescence to which the indicated model can be applied in absence of β-phosphorescence. The polarization measurements of Pilipovich and Sveshnikov were, however, made on the β-phosphorescence of fluoresceine in boric acid. Kato and Koizumi's scheme can therefore be considered only as a special case. In order to establish a more general scheme it is necessary to carry out a series of additional investigations with the greatest possible number of compounds and at various temperatures.

The following compounds were investigated in the present work: benzene, naphthalene, phenanthrene, o-phenatroline, α-aminopyridine, diphenylamine, diphenylcarbazide and also gallic, anthranylic, sulfanilic, m-aminobenzoic, and isophthalic acids. Alcohol, ether, acetone, n-heptane, and boric acid were used as solvents. All substances were chemically pure. The purity of solvents was such, that their own luminescence was negligibly small as compared to the luminescence of the corresponding solutions.

The method of measuring spectra (in the initial stage of decay) and decay curves was identical to the method described in ref. 4. Afterglow spectra at various stages of decay were determined in 15 to 20 regions of the spectrum from the initial phosphorescence spectra and from decay curves. The corresponding spectral regions were isolated by a monochromator. The spectral region of the mercury spectrum around 313 mμ was used for excitation. Phosphorescence spectra (immediately after excitation) were measured with a steady excitation, decay curves after a lengthy preliminary excitation.

Phosphors prepared in organic solvents were investigated at liquid oxygen temperature; crystalline compounds and phosphors prepared in boric acid were investigated in the temperature range from −180°C to room temperature.

Phosphorescence spectra of a number of crystalliz

mpounds (p-phenatroline, gallic and isophthalic acids) d also of a number of solutions (α-aminopyridine, di-enylcarbazide and anthranilic acid in alcohol, diphenyl-ine in ether, o-phenatroline in alcohol, ether and boric id) do not undergo, at liquid oxygen temperature, no-eable changes when phosphorescence has decayed ore than 100 times. In this group of phosphors the de-y of individual spectral regions of the phosphores-nce is exponential and the logarithmic decrement of e decay does not depend on the location of the observed gion in the spectrum. Phosphors such as diphenyla-ine and sulfanilic acid crystals, benzene in alcohol and her, m-aminobenzoic acid in boric acid, phenanthrene alcohol, ether, acetone, n-heptane, and boric acid, ose phosphorescence spectra change during the decay ocess, belong to another group.

The change during the decay process in the phos-orescence spectra of crystalline sulfanilic acid and of enanthrene in ether is shown in Fig. 1. As it can be en in the figure, two regions, decaying at a different te, can be separated out in the phosphorescence spec-a of these phosphors (405-460 and 460-540 mμ in the ectrum of sulfanilic acid and 410-450 and 450-570 mμ the phenanthrene spectrum in ether). Phosphores-nce decay proceeds according to an exponential law thin the limits of each one of the indicated regions (ex-pt in a narrow "borderline" section). The duration phosphorescence does not depend on the spectral lo-tion of the observed sections within the limits of each e of the indicated regions. Values of average duration different spectral sections are shown in Table 1. The cay of narrow sections of benzene and naphthalene so-tions is markedly different from an exponential law.

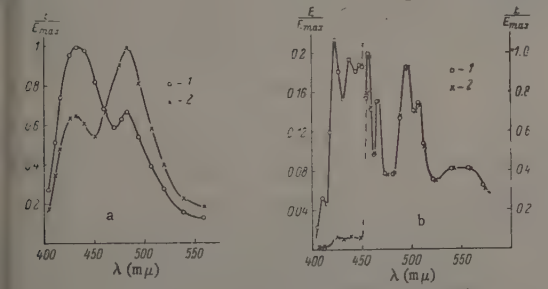

Fig. 1. Change of phosphorescence spectra during decay at liquid oxygen temperature. a—crystalline sulfanilic acid 0.01 sec (1) and 6.9 sec (2) after excitation; b—phenanthrene in ether 0.01 sec (1) and 7.8 sec (2) after excitation.

The nonexponential character of the phosphorescence ecay of benzene in alcohol solution was pointed out in a aper by Dikun et al.[5] In the same reference a difference as noticed in the average duration of the phosphores-ence of an alcohol solution of phenanthrene when ob-erved through a blue and a yellow-green filter (1.6 and .5 sec respectively), which is obviously in good agree-ent with the data of the present paper.

The presence in the phosphorescence spectrum of o regions, decaying at different rates, can be con-dered as an indication of two metastable levels taking rt in the emission.* One of these levels is apparently

Dumartin et al.[11] have observed, at room temperature, o phosphorescence bands in proline and terosine, which ey also explained by the presence of two metastable vels with a forbidden transition between them.

Table 1. Dependence of the Average Duration of Phosphorescence on the Location in the Spectrum of the Observed Section of the Phosphorescence Spectrum at −180°C.

Average wavelength of the spectral region (mμ)		413	423	437	456	465	485	495	508	540	560
Average duration of phosphorescence (sec)	I	1.6	1.6	1.6	3.6	3.6	3.6	3.6	3.6	3.6	3.6
	II	1.2	1.2	1.2	—	—	1.4	1.4	1.4	1.4	1.4

Remarks: I – phenanthrene in ether, II – crystalline sulfanilic acid.

responsible for the regular β-phosphorescence (spectral regions 460-540 and 450-570 mμ in sulfanilic acid and phenanthrene, respectively), and the other for a short wavelength radiation (405-460 and 410-450 mμ, respectively, for sulfanilic acid and phenanthrene), which we will further designate as β'-phosphorescence.

It is shown in Fig. 2 how the relation between β and β' phosphorescence changes with a rise in temperature. It is easy to see that β-phosphorescence is (especially in crystallized substances) much more stable with respect to a rise in temperature. A similar change of phosphorescence spectra with a rise in temperature takes place in isophthalic acid and diphenylamine crystals and in m-aminobenzoic acid in boric acid solution. An entirely different temperature dependence of the duration of phosphorescence in the short and long wavelength regions of the spectrum was moreover found in substances investigated in the crystalline state (Table 2). This also does not fit into a phosphorescence scheme with a single metastable level.*

*An abnormal change of duration in the initial stages of luminescence takes place upon raising the temperature from −140° to −110°. This question will be examined in more detail in the next communication.

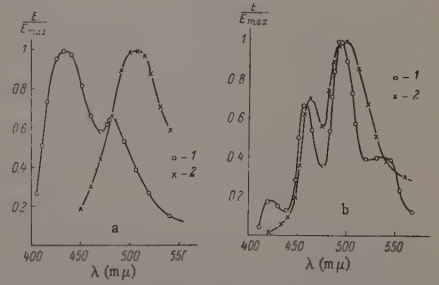

Fig. 2. Influence of temperature on phosphorescence spectra (0.01 sec after excitation). a—crystalline sulfanilic acid at −180°C (1) and −90°C (2); b—phenanthrene in boric acid at −180°C (1) and 20°C (2).

A change in the duration of the afterglow of the β- and β'-phenanthrene phosphorescence in boric acid upon an increase in temperature occurs in the same way, which can be considered as a manifestation of the specific effect of the surrounding medium on the emitting molecule. It is known that the medium plays a very important part in phosphorescence.[6,7] The question arises in this connection whether the formation of the second phosphorescence level is due to an action of the solvent which splits the ground level of the molecule. The afterglow of phenanthrene in various media was studied in order to clarify this question. It was hereby found that only in boric acid has the phosphorescence spectrum a

Table 2. Dependence of the Average Duration of Phosphorescence (in sec) on Temperature

Temperature (°C)	Spectral region (mμ)			
	Sulfanilic acid		Isophthalic acid	
	Near 500	Near 437	Near 500	Near 437
−180	1.4	1.2	2.4	2.4
−170	1.3	1.1	2.0	1.8
−160	1.2	1.0	1.5	1.1
−150	1.1	0.9	1.4	0.5
−140	1.0	0.7	1.1	—
−130	0.9	0.4	1.2	—
−120	1.2	—	1.3	
−110	1.4	—	1.3	—
−100	1.4	—	1.2	
−80	1.4	—	1.2	
−60	1.4	—	0.9	
−40	1.3	—	—	—

less clearly pronounced structure than the spectra in organic solvents. The duration of the phosphorescence and its dependence on the spectral location of the observed region was found to be the same in all solvents used.

The existence of a second phosphorescence band can be caused in particular by the presence of a phosphorescent impurity. In order to clarify this question phenanthrene was subjected to an additional purification by recrystallization from an alcohol solution. No changes were however found in the phosphorescent properties of phenanthrene as a result of such purification. It can hardly be admitted, moreover, that a regular change of the spectra and of the durations of the afterglows upon temperature rise, as well as the peculiar influence of solvents, can be caused by the presence of impurities.

The experimental results can be explained by postulating the possibility of realization of two metastable states in an organic molecule (Fig. 3).

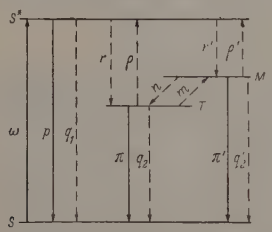

Fig. 3. Possible scheme of phosphorescence formation in the presence of two metastable levels. S and S*—normal levels; M and T—metastable levels. Dashed arrows—nonradiative transitions; full lines—optical transitions.

Let us, for example, examine the phosphorescence decay law at liquid oxygen temperature. Since, at this temperature, the probabilities $\rho = \rho' = 0$ (Fig. 3),[8] we obtain, after designating by N_1 and N_2 the numbers of molecules in levels T and M, the following equations for the rate of decrease of the number of molecules:

$$\frac{dN_1}{dt} = -fN_1 - nN_1 + mN_2,$$

$$\frac{dN_2}{dN} = -f'N_2 - mN_2 + nN_1,$$

where $f = \pi + q_2$, $f' = \pi' + q_2'$.

A solution of this system for given initial conditions has the form[9]:

$$N_1(t) = \left[\frac{f - f' + m - n + 2D}{4D} N_1(0) - \frac{2n}{4D} N_2(0)\right] e^{-\alpha_1 t} + \left[\frac{f' - f + n - m + 2D}{4D} N_1(0) + \frac{2n}{4D} N_2(0)\right] e^{-\alpha_2 t},$$

$$N_2(t) = \left[\frac{f - f' + n - m + 2D}{4D} N_2(0) - \frac{2n}{4D} N_1(0)\right] e^{-\alpha_1 t} + \left[\frac{f - f' + m - n + 2D}{4D} N_2(0) + \frac{2n}{4D} N_1(0)\right] e^{-\alpha_2 t},$$

where $N_1(0)$ and $N_2(0)$ are the numbers of molecules in levels T and M at the instant t, determined by the inequality $\tau_{fl.} \ll t \ll \tau_{phosph.}$[8]

$$\alpha_{1,2} = \frac{1}{2}(f + f' + m + n \pm D),$$

$$D = \frac{1}{2}\sqrt{(f + f' + m + n)^2 - 4(fn + f'm + ff')}.$$

If $m = n = 0$, the metastable states are not mutually interdependent and N_1 and N_2 decrease with time according to exponential laws

$$N_1(t) = N_1(0)\, e^{-ft}, \quad N_2(t) = N_2(0)\, e^{-f't}.$$

If m and n are comparable in order of magnitude to ρ and ρ', the phosphorescence decay will be nonexponential. If, finally, the values of m and n are considerably larger than those of ρ and ρ' (it is in practic sufficient for these values to be a little larger than ρ and ρ', which occurs in the case of conversion along triplet levels, due to an exchange resonance interaction between two molecules[10]), then

$$N_1(t) = Ae^{-\gamma t}, \quad N_2(t) = Be^{-\gamma t},$$

where

$$A = \frac{n}{m+n}[N_1(0) + N_2(0)], \quad B = \frac{m}{m+n}[N_1(0) + N_2(0)],$$

$$\gamma = \frac{n}{m+n} f + \frac{n}{m+n} f',$$

that is, the decay law will be exponential and the logarithmic decrement will be independent of the wavelen of phosphorescence.

The last conclusion is of considerable importance since it shows that the presence in the phosphorescence spectrum of a single band, decaying according to an exponential law, cannot serve as a positive proof of the ab sence of a second metastable level.

The scheme shown in Fig. 3 includes Kato and Koizumi's scheme as a particular case for $r = \rho = \pi = \pi' = 0$.

The present paper resulted from a suggestion of B. Ya. Sveshnikov to whom the author expresses his sin cere gratitude.

REFERENCES

1. V. A. Pilipovich and B. Ya. Sveshnikov, Opt. i Spek 5, 290 (1958).
2. V. A. Pilipovich, Abstracts of Candidate dissertati Minsk, 1958.
3. S. Kato and M. Koizumi, Bull. chem. Soc. Japan 30, 27 (1957).
4. V. A. Pilipovich and B. Ya. Sveshnikov, Opt. i Spek 4, 116 (1958);
G. A. Mokeeva and B. Ya. Sveshnikov, Opt. i Spektr 9, 601 (1960), Optics and Spectroscopy 9, 317 (1960
5. P. P. Dikun, A. A. Petrov, and B. Ya. Sveshnikov, Zhur. Eksptl. i Teoret. Fiz. 2, 601 (1951).

O. G. Zinov'eva, Doklady Akad. Nauk SSSR 68, 265 (1949).
B. Ya. Sveshnikov and A. A. Petrov, Doklady Akad. Nauk SSSR 71, 461 (1950).
B. Ya. Sveshnikov, Zhur. Eksptl. i Teoret. Fiz. 18, 878 (1948).
B. I. Stepanov, "Luminescence of Complex Molecules." Academy of Sciences of the Belorussian SSR Press, Minsk, 1955.
10. V. L. Ermolaev and A. N. Terenin, J. Chem. Phys. 55, 698 (1958);
V. L. Ermolaev, Opt. i Spektr. 6, 642 (1959), Optics and Spectroscopy 6, 417 (1959).
V. L. Ermolaev, I. P. Kotlyar and K. K. Svitashev, Izvest. Akad. Nauk SSSR, Ser. Fiz. 24, 492 (1960).
11. M. Dumartin, R. Lochet, B. Rybak, and A. Rousset, Compt. rend. acad. sci. 244, 2905 (1957).

A STUDY OF THE KINETICS OF THE SENSITIZED EMISSION OF RADIATION DUE TO CERTAIN ADDITIONS IN NAPHTHALENE CRYSTALS

A. M. Bonch-Bruevich, B. P. Kovalev, L. M. Belyaev, and G. S. Belikova (pp. 623-628)

Received 9 December 1960

The duration of photoluminescence decay is measured for naphthalene crystals containing various added activators, with the exciting light absorped either directly by the activator or by the body of the crystal. The results are interpreted from the viewpoint of the exciton mechanism of transferring energy from the lattice of the host material to luminescent centers. It is suggested that the exciton is localized near the activator. An indication is given of the lifetime of the exciton in the localized state, the average diffusion length, and the average time for one diffusion displacement of the exciton in the crystals investigated.

Recent years have witnessed the publication of nu-rous articles describing naphthalene-base mixed crys- used in studying nuclear radiation by the scintilla- method.[1-4] These papers give data on absorption and inescence spectra and on the luminescence yields of stals of naphthalene containing different additives. ortunately, these papers give no systematic data on kinetics of the luminescence.

PERIMENTAL RESULTS

We investigated the photoluminescence of naphthalene stals containing the following additives: (1) anthranilic d (ANA), (2) 1,4-diphenylbutadiene (DPB), (3) 1,6-henylhexatriene-1,3,5 (DPH). With the aid of a GOI se fluorometer,[5] we measured the luminescence de- time of the added activator when the crystal was ex- ed in the absorption band of the host, naphthalene $\lambda_{exc.}$ = 313 mμ), and in the absorption band of the acti- or ($\lambda_{exc.}$ = 365 mμ).

Crystals of naphthalene were grown from melts with erent concentrations of impurities (0.001-2%). The mples were prepared in the form of rectangular 15 × × 10 mm parallelepipeds with optically polished sur- es. All samples were oriented in such a way that the gest plane of the parallelepiped coincided with the 1) cleavage plane of naphthalene. All materials used crystal growing were initially purified by various thods (sublimation at atmospheric pressure, vacuum limation, recrystallization from solution, etc.). Melt- points and spectral characteristics of all these ma- ials agreed with published data.

The process of growing crystals of naphthalene with all concentrations of impurities differs very little m growing crystals of pure naphthalene. With increas- impurity concentration in the melt, the growing of gle crystals of naphthalene becomes complicated (the saic structure of the crystal increases, inclusions appear more frequently). After an impurity has reached a certain limiting concentration in a single crystal of naphthalene, any further increase in the amount of impurity in the melt leads to a cessation of crystal growth. Because of self-purification, the impurity enters the crystal nonuniformly. This nonuniformity is particularly evident along the height of the crystal.

According to present theories,[6] the impurity can enter the crystal in two ways—by forming a true solid solution or by forming an interstitial solid solution. Similarity of shape and dimensions of the host and impurity molecules are necessary and sufficient conditions for the formation of true solid solutions of organic compounds. By comparing projections of models of a naphthalene molecule and molecules of the indicated impurities, one can see that the ANA molecule is geometrically similar to the naphthalene molecule and is capable of replacing it in the naphthalene lattice. DPB and DPH molecules, although they differ strongly from the naphthalene molecule, may possibly be able to replace two naphthalene molecules in the naphthalene lattice and form solid solutions. However, inasmuch as the impurity concentrations in the crystals are small (the inclusion coefficient is ~1/100), x-ray methods do not reveal any change in the crystal lattice constants. However, the reproducible change of the luminescence properties of the mixed crystal gives us reason to believe that we are dealing with a true solid solution. Lattice defects produced by these materials increase in proportion to the increase of impurity concentration in the crystal, and the lattice reaches a state at which any further increase in the amount of impurity in the single crystal does not produce a solid solution.

The true concentration of the activator in the crystal was determined by measuring the absorption of a solution of the material in heptane in the absorption band of the activator (about 330-380 mμ). It turned out that no more than 1/80th of the ANA, 1/40th of the DPB, or 1/60th of the DPH passes into the crystal from the melt. The corresponding maximum concentration of activator

in the crystals does not exceed 0.0002 mole activator/mole host in the case of ANA and 0.0003 mole activator/mole host in the case of DPB or DPH. Considering the molar absorption coefficients of the activators and naphthalene,[7] we find that even for the highest concentration of activator in the crystal (0.0003 mole/mole) absorption by the activator in the 313 mμ region is at least 30 times weaker than absorption by the host. In the 365 mμ region, however, only the activator absorbs.

Figure 1 shows luminescence spectra of the crystals when excited in the absorption bands of the host and activators, respectively. The spectra practically coincide, which indicates the presence of a more or less effective mechanism for the transfer of energy from the lattice to the activator. This process is terminated by the excitation of the activator and its subsequent transition to a normal state, with emission.

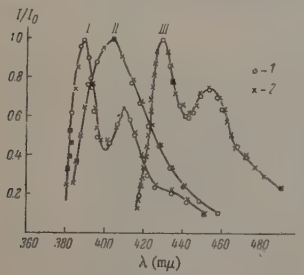

Fig. 1

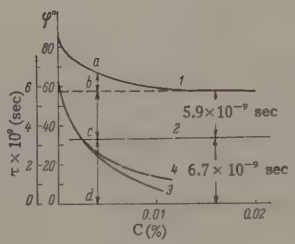

Fig. 2

Fig. 1. Luminescence spectra of naphthalene crystals with different activators. Activator: curve I—diphenylbutadiene; curve II—anthranilic acid; curve III—diphenylhexatriene. $\lambda_{exc.}$ (mμ); 1—365; 2—313.

Fig. 2. Dependence of the luminescence and diffusion times on activator concentration (anthranilic acid). Curve 1—luminescence time for excitation through the host ($\lambda_{exc.}$ = 313 mμ); curve 2—the same for excitation in the activator band ($\lambda_{exc.}$ = 365 mμ); curve 3—measured diffusion time of the exciton; curve 4—diffusion time calculated by formula (1).

Figures 2-4 show the phase shift of the luminescence of the activator relative to the exciting light as a function of activator concentration. It is easy to see that the decay time of the activator for excitation through the host (curve 1) decreases rapidly with increasing concentra-

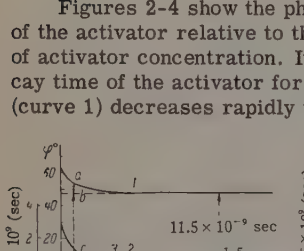

Fig. 3

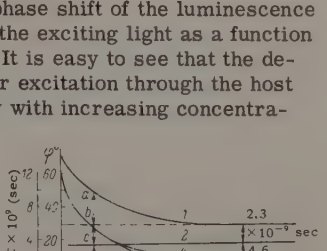

Fig. 4

Fig. 3. Dependence of luminescence and diffusion times on activator concentration (diphenylbutadiene). Curves 1-4, same meaning as Fig. 2.

Fig. 4. Dependence of luminescence and diffusion times on activator concentration (diphenylhexatriene). Curves 1-4, same meaning as Fig. 2.

tion in the region of small concentrations. It then stops depending on concentration, but always remains considerably greater than the natural time of luminescence of the activator (curve 2). Therefore, when excitation takes place through the crystal lattice, the decay time of an activator depends on its concentration and always exceeds the decay time for emission by the pure activator. The measured decay times of the luminescence for photoexcitation are given in Table 1.

Table 1

Activator	Natural duration of activator luminescence (sec)	Duration of luminescence for excitation through the lattice (sec)	
		Low activator concentration	High activator concentration
ANA	$6.7 \cdot 10^{-9}$	$19 \cdot 10^{-9}$	$12.6 \cdot 10^{-9}$
DPB	$1.5 \cdot 10^{-9}$	$16.2 \cdot 10^{-9}$	$13 \cdot 10^{-9}$
DPH	$4.6 \cdot 10^{-9}$	$19.5 \cdot 10^{-9}$	$6.9 \cdot 10^{-9}$

DISCUSSION OF RESULTS

The coincidence of the luminescence spectra obtai by excitation in the host and activator absorption bands and the significant increase in luminescence time for e citation through the host* indicate the presence of a m

*The luminescence of the pure activator (dissolved in heptane) decays with the same τ for $\lambda_{exc.}$ = 313 mμ and $\lambda_{exc.}$ = 365 mμ.

or less effective transfer of energy from the lattice to the activator.

A large amount of theoretical and experimental work[8-19] has been devoted to the question of energy migration in crystals and solutions. Various possible mechanisms of intermolecular energy transfer have been considered. In the majority of experimental investigations, changes in the absorption and luminescence spectra of the hosts and impurities were investigated as a function of the concentration of the latter. Only in refs. 16-18 were there any systematic measurements of the duration of luminescence. This characteristic quantity is very sensitive to the energy transfer mechanism.

In the systems considered there are three possible forms of energy transfer: transfer from naphthalene to naphthalene (N → N), transfer from naphthalene to activator (N → A), and transfer from activator to activator (A → A). The latter process is negligible because of the low concentration of the activator. This is confirmed by the mutual independence of φ_{365} (i.e., τ_{365}) and activator concentration (curves 2 in Figs. 2-4).

The N → A transfer is the final link in the N → N chain (which can be broken either by the emission of radiation by the naphthalene or by the nonradiative loss of energy) and is apparently affiliated with an exciton. The decrease in the average lifetime of the excited host molecules and the high luminescent yield of the activator determined by the energy transfer[16,17] indicate that the transfer does not amount merely to a simple absorption of the host emission by activator molecules. The absence of any connection between the overlapping of the luminescent spectrum of the host and the absorption spectrum of the activator, and the extent of the quenching effect of the activator on the host noted in reference 1 indicate that the transfer is not a resonance transfer.

One can represent the process in the following way upon absorption of light by the lattice of a molecular

ystal, an excited state—an exciton—arises. The motion the exciton in the regular field of the lattice resembles ffusion. The length of the chain of N → N transfers is termined by the probability of a collision with an ac- ator; i.e., by the concentration of the activator and the fective cross section for exciton capture. In the dis- rted field near the activator, the exciton is localized d part of its energy dissipated until it coincides with e excitation level of the activator. It is then finally ptured by the activator. Normal luminescence of the tivator follows. The total measured luminescence ne of the activator is the sum of the exciton diffusion ne (distance ab in Figs. 2-4), the lifetime of the exciton the localized state (distance bc), and the natural lumi- scence time of the activator (distance cd). Therefore, e process of luminescence must be nonexponential and ve several steps.

The nonexponential decay of luminescence can be de- cted directly by measuring the decrease in the per- ntage modulation of the luminescent light in compari- n with the percentage modulation of the exciting light.[20] e corresponding data for one of the activators—anthra- lic acid—are given in Table 2 for one-, two-, and three- ep processes. It is easy to see that the experimental ta agree best of all with the idea of a cascaded three- ep process. Analagous results were obtained for the ner activators.

Table 2

Activator concentration (mole/mole)	Demodulation (measured)	Demodulation (calculated) One-step	Two-step	Three-step
$2 \cdot 10^{-6}$	0.69	0.39	0.61	0.74
$2 \cdot 10^{-5}$	0.79	0.54	0.74	0.82
$8 \cdot 10^{-5}$	0.92	0.75	0.88	0.91
$2.7 \cdot 10^{-4}$	0.93	0.88	0.93	0.93

The time required for energy transfer, i.e., the total etime of the exciton, is determined both by the proper- s of the host and the properties of the activator. The ffusion component can be estimated by the following ethod: Consider the steady state luminescence of the ystal. Let the concentration of free excitons in the ystal equal N, the activator concentration be c, and ν_0 diffusion displacements take place in the average citon lifetime τ_0. The number of exciton-activator collisions'' per unit time will equal $Nc\nu_0/\tau_0$, and the de- ease in the number of excitons in the time dt because natural losses and losses at activator sites is deter- ined by the expression

$$dN = \left(-\frac{N}{\tau_0} - \frac{Nc\nu_0}{\tau_0}\right) dt = -\frac{N}{\tau}\, dt.$$

The dependence of the diffusion component of the ergy transfer time on activator concentration has the rm

$$\tau = \frac{\tau_0}{1 + c\nu_0}. \qquad (1)$$

Figs. 2-4, curves 3 shows the measured values of the citon diffusion time $\tan \varphi_{ab}/\omega$, and curves 4 are hyper- las constructed from formula (1). The parameters of e hyperbolas were determined from the experimental rves: τ_0 is the value extrapolated to zero concentra- on, and ν_0 is the value at a concentration of one-half τ. is easy to see that at higher concentrations, the experi- ental curve falls considerably faster than the hyper- la. This is explained, evidently, by the fact that the number of lattice defects leading to the nonradiative destruction of an exciton increases with activator concentration.

Several parameters of the process of exciton energy transfer obtained from the experimental curves are given in Table 3.

Table 3

Activator	$\nu_0 \times 10^{-3}$ (sec^{-1})	τ_0 (sec)	Time for one diffusion displacement (sec)	Localization time of the exciton (sec)	Average diffusion path of the exciton*
ANA	43.5	$6.5 \cdot 10^{-9}$	$1.5 \cdot 10^{-13}$	$5.9 \cdot 10^{-9}$	66a
DPB	100	$3.2 \cdot 10^{-9}$	$3.2 \cdot 10^{-14}$	$11.5 \cdot 10^{-9}$	315a
DPH	32.2	$12.6 \cdot 10^{-9}$	$4 \cdot 10^{-13}$	$2.3 \cdot 10^{-9}$	180a

*a = average length of one diffusion displacement; i.e., the average distance between naphthalene molecules (a ~ 5 A).

Thus the nonexponential behavior of the luminescence decay and the $\varphi_{313} = f(c)$ curves can be interpreted as resulting from the localization of an exciton near the luminescent center for times the order of $(2 - 10) \times 10^{-9}$ sec. Between formation and localization, the exciton undergoes as many as 10^5 N → N displacements; it stays within a given molecule for approximately 10^{-13} sec and moves a distance of about 100-300 times the lattice constant of the crystal.

REFERENCES

1. J. Birks, Proc. Phys. Soc. (London) **63**, 36, 90, 1944 (1950).
2. G. S. Belikova, L. M. Belyaev, and Kh. V. Protopopov, Symposium of Scintillators and Scintillating Materials, Moscow, 1960.
3. G. S. Belikova and L. M. Belyaev, Kristallografiya **4**, 6, 929 (1959).
4. Yu. V. Naboikin, V. K. Dobrokhotova, and V. V. Uglanova, Izvest. Akad. Nauk SSSR, Ser. Fiz. **24**, 6, 744 (1960).
5. A. M. Bonch-Bruevich, V. A. Molchanov, V. I. Shirokov, and I. V. Karazin, Pribory i Tekh. Ekspt. No. 2, 53 (1959).
6. A. I. Kitaigorodskii, Kristallografiya **2**, 4, 456 (1957).
7. A. E. Gillam and E. S. Stern, "Introduction to Electronic Absorption Spectroscopy in Organic Chemistry." Arnold, London, 1954. Izd. Inostrannoi Lit., Moscow, 1957.
8. S. I. Vavilov and M. D. Galanin, Doklady Akad. Nauk SSSR **67**, 811 (1949).
9. T. Forster, Ann. Physik **2**, 55 (1948); Z. Naturforsch. **4a**, 321 (1949).
10. D. L. Dexter, J. Chem. Phys. **21**, 836 (1953).
11. J. Birks, Phys. Rev. **94**, 1567 (1954).
12. O. Bowen, Proc. Phys. Soc. (London) **A62**, 26 (1949).
13. J. Frank and R. Livingston, Revs. Modern Phys. **21**, 505 (1949).
14. S. C. Ganguly and N. K. Choudbury, Revs. Modern Phys. **31**, 920 (1960).
15. O. Simpson, Proc. Roy. Soc. (London) **A238**, 402 (1957).
16. A. Schmillen, Z. Physik **150**, 123 (1958).
17. M. D. Galanin, Trudy Fiz. Inst., Akad. Nauk SSSR **12**, 3 (1960).
18. O. Knau, Z. Naturforsch. **12a**, 881 (1957).
19. D. C. Northrop and G. Simpson, Proc. Roy. Soc. (London) **A234**, 136 (1956).
20. L. A. Tumerman, Uspekhi Fiz. Nauk **23**, 218 (1947).

INFLUENCE OF EXCITED LIGHT BIREFRINGENCE ON THE LUMINESCENCE POLARIZATION IN MOLECULAR CRYSTALS

N. D. Zhevandrov, V. I. Gribkov, and I. D. Khan-Magometova (pp. 629-635)

Received 26 December 1960

It is shown that in molecular crystals the polarization of luminescence does not depend on the polarization of the exciting light. This independence always exists, even when such complicating factors as birefringence, dichroism, and optical activity are eliminated or accounted for. This phenomenon can be explained by the migration of the excitation energy in the crystals.

One of the authors has previously shown the independence of the degree of luminescence polarization of molecular crystals on the direction of the electric vector of the exciting light.[1,2] If one considers that the molecules from which such crystals are formed (for example anthracene) are highly anisotropic and are regarded as linear oscillators, and that in addition there is usually more than one possible orientation of the molecules in the lattice (often two), then this independence seems at first a paradox.

Actually, if there are two oscillators with different orientation, then, generally speaking, they will always be differently oriented with respect to the electric vector of the exciting light. They will therefore be excited with different probabilities, and the degree of polarization of the light emitted by them will be different. As a result, we should certainly find a dependence of the degree of polarization of all luminescence of a crystal on the direction of the electric vector of the exciting light relative to the oscillators (i.e., relative to the crystal).

Of course, one must also consider the orientation of the crystal itself relative to the axes along which the mutually perpendicular components I_1 and I_2, which define the degree of luminescence polarization

$$P = \frac{I_1 - I_2}{I_1 + I_2},$$

are polarized in the measuring apparatus.

This orientation is very important. Suppose, for example, that the crystal is oriented in such a way that I_1 coincides with the bisector of the angle between the oscillators. It is easy to see that, in this particular case, there would be no dependence of the degree of luminescence polarization on the polarization of the excitation. Actually, differently oriented oscillators will be excited with different probabilities, but the relative projections on the I_1 and I_2 axes will be the same for each oscillator. Consequently, the degree of polarization of all luminescence will always be the same. This is a very unfavorable orientation for detection of a dependence of luminescence polarization on the polarization of the excitation. Calculation shows that the most favorable orientation is the one in which one of the oscillators coincides with one of the axes I_1 or I_2. This orientation should show the sharpest dependence. However, if in an experiment the complete absence of such an orientation were surely established, then there would be no dependence.

One can explain these results if one admits the possibility of the migration of excitation energy in the crystal. If, after the time of the excited state, the excitation energy passes from molecules of one orientation to molecules of another orientation and is uniformly distributed among molecules of all different orientations, then the initial anisotropy created by the exciting light with def polarization will be lost at the instant of emission. Th mechanism of energy transfer need not be considered, has no effect on the result.

The study of luminescence of crystals (particular its polarization) is complicated by birefringence. In r 3, the birefringence of luminescent light was studied i detail. In the present paper, we wish to turn our atten tion to the birefringence of the exciting light. This is important in connection with the problems stated abov It is necessary to find out whether the independence of luminescence polarization and excitation polarization might be due to the splitting of the exciting light in the crystal into two rays with perpendicular electric vectors, rather than to the migration of excitation energy Would not a definite value of the degree of luminescen polarization, no longer depending on the polarization o the incident exciting light, be a consequence of this? I other words, the existence of a definite path difference between components into which the exciting light is sp in the crystal leads to a rotation of the electric vecto of the exciting light. Thus the electric vector, by its r tion, will successively coincide with oscillators of dif ent orientation, and as a result they will all be excited uniformly, independent of the initial orientation of the citing electric vector.

This paper is devoted to an analysis of these circ stances.

First of all, the question of crystal thickness is v important. If one works with very thin single crystals then during the passage of the exciting light through th crystal the path difference will be small and the rotat of the electric vector also correspondingly small. A sufficient condition is $d \cdot \Delta n \ll \lambda$, where d is the crys tal thickness, λ the wavelength, and Δn the differenc the refractive indices for the split components. For e ample, light traveling in a direction perpendicular to surface ab of an anthracene crystal has a refractive i dex (for $\lambda = 436$ mμ) of $n_{\parallel} = 1.97$ for the component p larized parallel to the b-axis and $n_{\perp} = 1.81$ for the ot component.[3,4] Thus $\Delta n = 0.16$. For a plate of thickne d we find $d(0.16) \ll 0.44\,\mu$, i.e., $d \ll 3\,\mu$. This conditi may be regarded as sufficiently well satisfied for thic nesses of 0.1-0.3 μ. In work with microscopic crystal a micropolarimeter[1] this condition was always easily satisfied, since the microplates of the crystals had li dimensions the order of several microns and a thickn less than 0.1 μ. However, for single crystal films gro by sublimation, the thickness of the crystals in sever cases might reach several microns. It is true that se eral materials (for example, anthracene with naphtha cene) form extremely thin films during sublimation. for work with large, thick single crystals, plates of w

e sawed from large blocks and have a thickness of some
n millimeters or more, one must take account of the
ect of birefringence of the exciting light.

It is clear from what has been said that it is neces-
ry to arrange experiments in such a way as to exclude
take into account the indicated effect of birefringence.
e results of such experiments are discussed below.

In essence, one of them consists of the following: The
litting of the exciting light into two components can
d to equally probable excitation of oscillators of two
fferent orientations only in case that these differently
ented oscillators are located symmetrically relative
the axes along which the components of the birefrin-
nce are polarized. There is such symmetry in anthra-
ne,[3] for example. However, there are crystals in which
such symmetry exists. After considering several
ystals at our disposal, we chose stilbene for these ex-
riments.

The orientation of stilbene molecules in their lattice
known from x-ray data.[5] Calculations showed that the
ction containing the bc′ plane is the most convenient
r our purpose. The projection of the oscillators on this
ne appears in Fig. 1. The direction of the electric vec-
rs of the split components in biaxial crystals is de-
rmined by Fresnel's theorem.[6] They lie in planes which
sect the region between planes containing the direction
the ray and one of the optic axes. If the ray lies in the
ne of the optic axes the latter two planes become one.
e of the bisecting planes coincides with this plane; the
er is perpendicular to it. In the stilbene crystal, the
tic axes lie in the plane ab: the a-axis is the bisector
the acute angle between them, and the b-axis is the bi-
ctor of the obtuse angle.[7] For the exciting light inci-
nt perpendicular to the plane bc′, i.e., along the a-axis,
e split rays will be polarized along c′ and along b. As
en in Fig. 1, the projections of the molecular oscilla-
rs are located unsymmetrically relative to these direc-
ns. For investigating the dependence of luminescence
larization on the polarization of the excitation, let us
ose the orientation indicated in Fig. 1 when the pro-
ction of one of the oscillators is vertical (axes I_1 and
vertical and horizontal, respectively). If one excites
luminescence by light polarized along c′ and b, then
is evident that in these cases we must obtain a differ-
t polarization of the luminescence. Calculations show
at, in the first case, the degree of polarization must be
%, and in the second, 73%. The difference is 15%, and
n be realiably detected in an experiment.

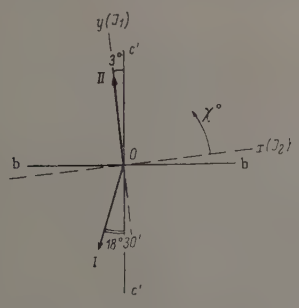

Fig. 1. Projection of the oscillators in a crystal of stilbene on the plane bc′.

Measurements were made on a spectropolarimeter[8]
ich, in this case, is convenient since it permits a de-
ndable isolation of the exciting light. This is extremely
important in such experiments, since the smallest admixture of exciting light can alter the result considerably. The case of stilbene is especially complex because the spectrum lies in the violet and near ultraviolet. Excitation was accomplished with 365 mμ radiation from a PRK-4 lamp. In the luminescence spectrum, the polarization was measured at 395 and 424 mμ. Control experiments were performed without the crystal and with a quartz dispersion plate. The results appear in Fig. 2 from which it is evident that the luminescence polarization does not depend at all on the position of the electric vector of the exciting light. This result can be explained only by the migration of energy.

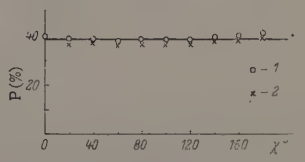

Fig. 2. Dependence of the degree of luminescence polarization of a single crystal of stilbene on the direction (χ°) of the electric vector of the exciting light. Section in the bc′-plane (crystal orientation shown in Fig. 1). λ (mμ): 1 = 395; 2 = 424.

The idea of the other group of experiments is to direct the exciting light along an optic axis of the crystal. In these experiments uniaxial single crystals of benzyl and biaxial single crystals of stilbene were the objects of investigation.

In the elementary cell of a benzyl crystal (hexagonal system) there are three molecules. They are arranged spirally around the axis of highest symmetry, which coincides with the optic axis[9] (this axis is the growth axis of single crystals). Thus in plates sawed perpendicular to the growth axis, the optic axis is normal to the surface of the crystal; and the projections of the molecular oscillators on the surface of the crystal are arranged symmetrically around this axis and make angles of 120° with each other (Fig. 3). It is not difficult to calculate the dependence of the degree of luminescence polarization in the direction of the optic axis on the angle χ which defines the position of the electric vector of the exciting light in a plane normal to the optic axis. The calculated dependence is shown in Fig. 4. Since there is no birefringence of the exciting light when it is propagated along the optic axis, this dependence must be detectable experimentally if there is no migration of excitation energy between molecules.

It is easy to separate the intense green luminescence of benzyl from the exciting light. The measurements were performed on a visible apparatus with a Cornu polarimeter. The results for 365 and 436 mμ exciting light are shown in Fig. 4. Excitation by blue light is of interest in connection with the following optical characteristics of a benzyl crystal[9]: For wavelengths the order of 590 mμ, the crystal is uniaxial positive. Toward the short wavelengths, the birefringence decreases, and at 420 mμ the crystal becomes isotropic. At shorter wavelengths the birefringence changes sign; i.e., the crystal becomes uniaxial negative. Thus, by exciting with 436 mμ light, we work with a practically isotropic crystal.

As is evident from Fig. 4, luminescence polarization is again completely independent of the polarization of the excitation, which can be interpreted only as an indication of the migration of energy in the crystal.

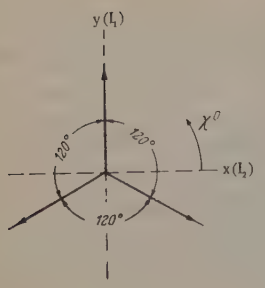

Fig. 3

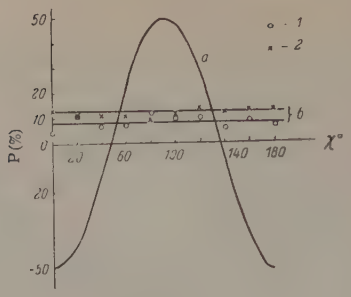

Fig. 4

Fig. 3. Projection of the oscillators in a benzyl crystal on a plane perpendicular to the optic axis.

Fig. 4. Dependence of the luminescence polarization on polarization of the exciting light for benzyl. a—calculated; b—experimental. Slice in a plane perpendicular to the optic axis (orientation shown in Fig. 3). λ_{ex} (mμ): 1 = 436; 2 = 365.

Of course, it is still necessary to consider the fact that benzyl crystals rotate the plane of polarization. However, the magnitude of this effect is insufficient to substantially change the calculated dependence shown in Fig. 4. According to published data,[9] the rotating power for the blue region is about 45° in 1 mm. The crystals used in our experiments were about 0.1 mm thick, and in experiments performed with a micropolarimeter the thickness was of the order of several microns. Thus the rotation was approximately 5° to a fraction of a degree, and may be ignored.

The other objects of similar experiments were biaxial crystals of stilbene, which belong to the monoclinic system and do not possess optical activity.

The position of the optic axes was determined on spherical single crystals on a conoscopic plot[7] for the violet edge of the spectrum. Plates perpendicular to one or the other optic axis were sawed from the spheres. Excitation along the optic axes was accomplished with 365 mμ light. Polarization of the luminescence was measured at 414 mμ. The experiments were performed on a spectropolarimeter. Special attention was paid to the isolation of the exciting light, since in these experiments the exciting light was aimed exactly in the direction in which the luminescence was observed.

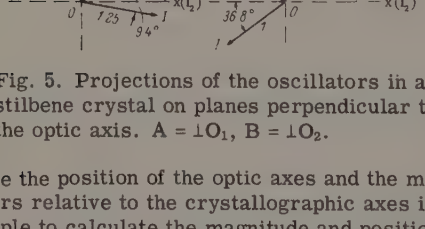

Fig. 5. Projections of the oscillators in a stilbene crystal on planes perpendicular to the optic axis. A = ⊥O_1, B = ⊥O_2.

Since the position of the optic axes and the molecular oscillators relative to the crystallographic axes is known, it is simple to calculate the magnitude and position of the oscillator projections on planes perpendicular to the optic axes. The results are given in Fig. 5, which shows the oscillator positions for each crystal section in the mos favorable orientation (one of the oscillators vertical). The calculations and experimental measurements of po larization dependence were also performed with these orientations. With natural excitation, these two slices gave very different luminescence polarization (−17% a and +42% by calculation, −18% and +30% by experiment so that it is easy to distinguish them.

Curves of luminescence polarization calculated as function of the position of the electric vector of the ex citing light are shown in Fig. 6. It is evident that the c pendence is marked and characteristic. However, the perimental results given in the same figures (dots) as all preceding cases, show complete independence of th luminescence polarization on the polarization of the ex citation, and indicate the migration of energy in the cr tal.

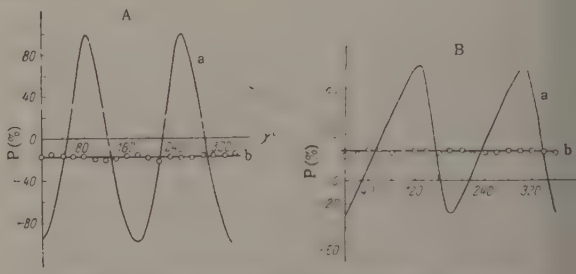

Fig. 6. Dependence of luminescence polarization on the polarization of the exciting light for stilbene. a—calculated; b—experimental. A—slice of the crystal in a plane perpendicular to the optic axis O_1 (orientation shown in Fig. 5A); B—slice perpendicular to the second optic axis O_2 (orientation shown in Fig. 5B).

In the experiments described, there is one compli cating circumstance. We determined the positions of t optic axes for violet light, but excited with radiation i the near ultraviolet. As a consequence of the dispersi of the optic axes, the optic axis for λ = 365 mμ which required might have deviated from the one we found b several degrees. Determination of the axis for ultravi let light by the usual visual method is impossible.

Excitation by means of the 405 mμ mercury line a proved to be impossible, because this wavelength lies near the long wavelength edge of the luminescence spe trum and almost all the luminescence appears in the a Stokes region. In order to be sure that this inaccurac determining the position of the axis useful to us did no affect the result, we performed measurements with th crystal rotated by several degrees (from 2 to 10°). Th is, we propagated the exciting light in directions close the axis for violet light. Nearly fifteen measurements for each slice were made in a cone with an angle up t 20°, which guarantees striking the sought-for optic ax In all cases, complete independence of the luminescen polarization on the polarization of the excitation was f

At first sight, it might appear that even small er rors in determination of the optic axis might have ser effects since it is only exactly along the optic axis tha there is no birefringence. However, it is easy to unde stand that a small error of 1-2°, unavoidable in the ex periment, is unimportant, since birefringence near th optic axis means an insignificantly small path differen and, consequently a negligibly small rotation of the el tric vector of the exciting light.

Finally, it is necessary to take into account the possible effect of dichroism. Even when light is propagated along an optic axis or close to it and the path difference between the split components is very small or completely absent, a rotation of the electric vector is possible if the ratio of intensities of the components changes because of dichroism.

In benzyl, the dichroism in the blue region of the spectrum is small for a slice perpendicular to the optic axis. This is natural because of the high symmetry in the positions of the absorbing molecules. In stilbene, the dichroism at 365 mμ is very small for the ac′ section, but considerable for the bc′ section.[10] In slices perpendicular to the optic axes we have an intermediate case. In order to exclude the possible effect of dichroism, it is necessary to compare the polarization of luminescence in two cases: for excitation by light whose electric vector coincides with the direction of polarization of each split component determined by Fresnel's theorem, i.e., along the c′-axis and perpendicular to it. The calculated value of the luminescence polarization for these cases can be obtained from the theoretical curves of Fig. 6. The values are given in the Table.

Direction of the exciting light	Position of the electric vector of the exciting light	Degree of polarization luminescence (%)
Along one optic axis O_1	$\parallel c'$	−11
	$\perp c'$	+18
Along the second optic axis O_2	$\parallel c'$	−33
	$\perp c'$	+58

It is easy to see that the differences are significant and could certainly be detected experimentally. However, as pointed out above, they are completely absent.

The above evidence indicates that the independence shown by the luminescence polarization of molecular crystals with respect to the polarization of the excitation is an indication of the migration of excitation energy in crystals.

REFERENCES

1. N. D. Zhevandrov, Doklady Akad. Nauk SSSR 88, 677 (1952).
2. N. D. Zhevandrov, Doklady Akad. Nauk SSSR 100, 455 (1955).
3. N. D. Zhevandrov, Izvest. Akad. Nauk SSSR, Ser. Fiz. 20, 553 (1955).
4. I. V. Obreimov, A. F. Prikhot'ko, and I. V. Rodnikova, Zhur. Eksptl. i Teoret. Fiz. 18, 409 (1948).
5. A. I. Kitaigorodskii, "Organic Crystal Chemistry," p. 401. Academy of Sciences Press, Moscow, 1955.
6. F. Pockels, "Lehrbuch der Kristalloptik." Leipzig-Berlin, 1906.
7. V. N. Varfalomeeva and N. D. Zhevandrov, Opt. i Spektr. 5, 571 (1958).
8. N. D. Zhevandrov, V. I. Gribkov, and V. N. Varfolomeeva, Izvest. Akad. Nauk SSSR, Ser. Fiz. 23, 57 (1959).
9. G. S. Chandrasekhar, Proc. Indian Acad. Sci. 39, 243 (1954).
10. V. I. Gribkov, N. D. Zhevandrov, and I. D. Khan-Magometova, Izvest. Akad. Nauk SSSR 24, 740 (1960).

PHOTOLUMINESCENCE OF SOLUTIONS AND CRYSTALS OF GADOLINIUM SALTS

A. N. Zaidel' and G. S. Lazeeva (pp. 636-641)

Received 24 November 1960

The photoluminescence of crystals and solutions of gadolinium salts excited by light from an Fe spark has been investigated. Photochemical damping was observed in solutions of $GdCl_3$. A series of new bands was observed in the luminescence spectrum; the bands were interpreted as a superposition of electronic and vibrational frequencies. It was established that the afterglow times were the same for all bands, and it was shown that thermal equilibrium between the two upper excited states is established during a time which is short in comparison with the lifetime of these states.

Tomaschek and Mehnert[1] were the first to observe photoluminescence in solid gadolinium salts and their solutions; this phenomenon was also observed by Zaidel' and Larionov. The spectra of this luminescence are characterized by a bright narrow band with a maximum at 3110 A and a series of weak bands of which the most important is the band at 3060 A. These bands were assigned to the electronic transitions $^6P_{5/2,\,7/2} \rightarrow {}^8S_{7/2}$ (Fig. 1) which take place inside the 4f orbit of the Gd IV ion.[3] The nature of the weaker bands located in the long wavelength ultraviolet and visible spectrum remained unexplained. Zaidel' and Malakhova[4] showed that the red and yellow bands in the luminescence spectrum belong to the ion Sm IV, which occurs as an impurity in gadolinium preparations. Singh[5] assigned all the long wavelength bands in the luminescence to unidentified natural impurities.

The photoluminescence of gadolinium has a rather long duration ($\tau \sim 10^{-3}$ sec), which in recent times has been used to advantage by a series of authors. Dieke and Hall[6] and also Kondrat'eva and Lazeeva[7] studied the damping of luminescence in crystals and solutions of gadolinium and they observed its exponential character. In a recent paper,[7] an attempt was made to measure τ for the separate bands. However, the sensitivity of the method used in that work was not high enough to permit measurement of the weak band at $\lambda = 3060$ A, and the authors were limited to a rough estimate of $\tau = 10^{-4}$-10^{-3} sec. In these same experiments a reliable value was found for the band at $\lambda = 3110$ A, namely, $\tau = 2 \times 10^{-3}$ sec.

It was, therefore, of interest to make a more detailed study of the luminescence spectrum of the gadolinium ion and also of the nature of the spectrum damping; in par-

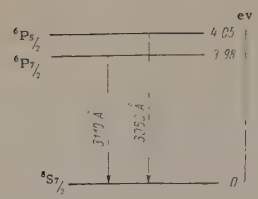

Fig. 1. Energy diagram of the Gd^{3+} levels between which radiative transitions occur.

ticular, it was desirable to establish the value of τ for the 3060 A band. Interest was aroused by the fact that the separation of the $^6P_{5/2}$ and $^6P_{7/2}$ terms amounts to only 0.07 ev and it was, therefore, expected that population equilibrium would be quickly established between these two levels, which should lead to a single value of τ for both bands. In ref. 7 the investigators did not succeed in demonstrating this fact.

Solutions of sulfates and chlorides of gadolinium were prepared by dissolving the purest obtainable gadolinium oxide or hydroxide in corresponding dilute acids. The amount of acid used was slightly in excess of stoichiometric proportions. Crystals of the salts were obtained by carefully evaporating the solution and filtering out the precipitated crystals from the parent solution. Anhydrous sulfates were prepared by baking $Gd_2(SO_4)_3 \cdot 8H_2O$ at 400 to 500°C for 30 min. Anhydrous chlorides were obtained by chlorination of Gd_2O_3 by heating it in vacuo with NH_4Cl; the excess of the latter was then driven off.

A synchronous spark phosphoroscope,[8] consisting of a motor generator with iron electrodes and a maltese cross attached to its axis, served to excite the spectra. The motor generator had a speed of about 300 rpm and, thus, rotation of the maltese cross with respect to the electrodes by 1° corresponded to a short of $\approx 55\,\mu$sec in the time delay between the instant of exposure and the exciting pulse. A step-up transformer whose primary was connected to the motor generator supplied the charge for the spark. The parameters of the high voltage circuit were: L = 0; C = 0.02 μf. The current in the primary of the transformer was 8 to 9 amp; there was a voltage of 10 kv across the secondary.

The spectra were photographed on DK or DN film, and also on Kodak Oa-o plates.

A Hilger E517 quartz spectrograph was used in experiments which did not require high spectral resolution. When fine structure was under investigation, the spectra were photographed using an E488 Hilger spectrograph with average dispersion. The slit width was selected in accordance with the nature of the experiment and varied over the range 10 to 200 μ. Calibration marks were made in the usual way by photographing the iron arc spectrum through a nine step attenuator.

The solutions under investigation were introduced into a small cell cut from a single piece of crystalline quartz. A cell of this type was selected in order to eliminate the effect of phosphorescence from fused quartz and contamination of the solutions which would have occurred if cells with quartz windows glued into them had been used.

The crystals were poured into this same cell. The $Gd_2(SO_4)_3 \cdot 8H_2O$ crystals were spread in a thin layer over the surface of a copper plate cooled by liquid air when observations of the low temperature luminescence were being conducted.

The observations were made through a double win dow made from thin single crystal quartz plates. Silic gel was used as the drying agent.

When the luminescence was excited in this appara the light was so intense that a photograph of the 3110 band could be taken with wide open slit in a matter of few seconds.

EXCITATION AND DAMPING OF THE LUMINESCENCE

As was previously demonstrated, the most effecti region for excitation lies in the vicinity of 2700 to 280 and a spark between iron electrodes turns out to be th optimal source.[9]

During the course of this work, it was noted that t luminescence intensity of the $GdCl_3$ solutions (concent tion ~0.1-1%) decreased as a result of exposure to the light from the iron spark. This phenomenon was very strongly evident in neutral and slightly acidic solution of $GdCl_3$; it was noticeably less evident in solutions wi concentrations of free HCl in the range 10 to 20% and was practically unobservable in gadolinium sulfate sol tions.* This phenomenon was not studied quantitativel

*E. V. Kondrat'eva participated in the experiments on quenching in solutions of $Gd_2(SO_4)_3$.

but it was established qualitatively that exposure to a spark located at a distance of 20 to 33 mm from the ce caused a decrease by tens of times in luminescence w a half hour. By means of experiments with various kin of filters, it was established that the damping effect w evidently produced by that portion of the spectrum whi is located on the short wavelength side of the region o effective excitation (< 2600 A). The luminescence of s lutions which had experienced this damping was not re stored when they were boiled or by addition of HCl or H_2O_2.

The hydroxide which was precipitated from a solu tion which had been "dampened" and then baked until formed Gd_2O_3 produced a solution possessing normal luminescence properties after it was dissolved in HCl Evidently, all possible causes of quenching, with the e ception of photochemical action, were eliminated, but we were still not successful in isolating the mechanis of the phenomenon which leads to a quenching of the luminescence.

It is possible that further studies of the absorptio spectra and of the chemical affinity of the quenched so tions will help to elucidate this phenomenon.

LUMINESCENCE SPECTRA

The luminescence spectra of crystals of hydrous gadolinium sulfate and chloride consists of two princi bands at 3110 and 3060 A which are very narrow even room temperature; each of these bands can be resolv into a series of components. One other narrow double at wavelengths of 3002 and 3005 A was observed in th spectrum of $GdCl_3 \cdot 6H_2O$ for long exposure times. Be cause of the weak intensity of this band, it was not po sible to undertake a study of its characteristics. Bes this, a series of other diffuse bands appear in the spe and after long exposures a complicated spectrum was noticed extending from 3060 to 3700 A.

The luminescence spectra of solutions of these salts re essentially the same as those of the crystals, but the nain bands are more washed out and their fine structure ractically vanishes. The wavelengths of the maxima of he bands and their intensities which were evaluated isually with a 10-point scale are given in the Table. Photographs of the spectra are shown in Figs. 2 through 4.

	Crystals			
	λ (A)	$\Delta\nu$ cm^{-1} $= \lvert\nu - 32130\rvert$	I	Notes
	3052–3058	–	9	Sharp triplet
	3108–3116	–	10	Sharp line consisting of four components
	3083	300	1	Diffuse line
	3091	210	4	" "
	3131	200	4	" "
	3146	340	2	" "
	3177	660	2	Band
	3220–3229	1080–1140	7	Band corresponding to vibrational frequency of the (SO_4) group
	3280	1650	1	Band
	3456–3497	3200–3540	5	Band corresponding to vibrational frequency of the (OH) group
	3002–3005	–	1	Sharp doublet
	3053–3060	–	9	Sharp triplet
	3109–3116	–	10	Sharp line which breaks up into four components
	3079	350	2	Diffuse line
	3095	180	3	" "
	3132	190	4	" "
	3148	360	4	" "
	3170–3183	580–710	5	" "
	3275–3285	1590–1690	4	" "
	3454–3496	3180–3520	7	Band corresponding to vibrational frequency ν (OH)
	3038	–	0	Diffuse line
	3346	–	0	" "
	3407	–	0	" "
	3555	–	0	" "
	Solutions			
	3046–3059	–	9	Diffuse line
	3102–3116	–	10	" "
	3074	370	2	Band
	3094	160	3	"
	3129	200	4	"
	3146	370	3	"
	3173–3190	640–810	2	"
	3214–3223	1050–1130	5	Band corresponding to vibrational frequency of the (SO_4) group
	3279	1660	1	Band
	3432–3492	3020–3520	6	Band corresponding to vibrational frequency of the (OH) group
	–	–		
	3047–3058	–	9	Diffuse line
	3102–3116	–	10	" "
	–	–		
	3095	140	2	Band
	3124	160	3	"
	3144	360	3	"
	3183	750	3	"
	3275–3290	1660–1770	1	"
	3439–3491	3190–3520	6	Band corresponding to vibrational frequency ν(OH).
	–	–	–	–
	–	–	–	–
	–	–	–	–
	–	–	–	–

From the Table and the spectrograms, it is evident hat the spectra of the sulfates and chlorides differ basically from each other.

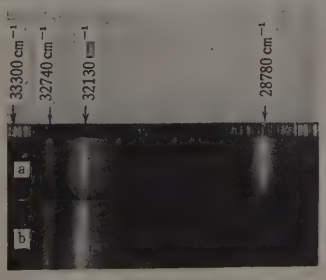

Fig. 2. Fluorescence spectra of gadolinium chloride. a—$GdCl_3 \cdot 6H_2O$; b—aqueous solution of $GdCl_3$.

The band which is separated from the main band (3100 A) by 3350 cm^{-1} attracts one's attention. This band is more intense in aqueous solutions than in the crystals and it is completely absent from solutions of $Gd_2(SO_4)_3$ in concentrated H_2SO_4 and from anhydrous (carefully baked) crystals of $Gd_2(SO_4)_3$ (Fig. 4). It is interesting to note that this band turns up again in the spectra of the sulfates after the anhydrous crystals of $Gd_2(SO_4)$ have been allowed to stand in air for several hours. The separation between this band and the fundamental band is in good agreement with the combination frequency of the valence vibrations of the OH group.[10] Thus, one can conclude that the observed frequency results from the superposition of the electronic transition frequency in the 4f orbits and the vibrational frequency of the OH group.

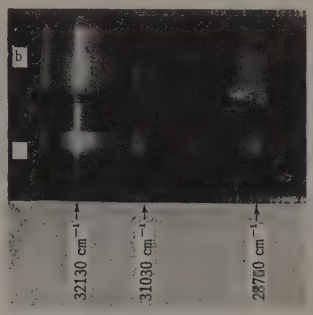

Fig. 3. Fluorescence spectra of gadolinium sulfate. a—$Gd_2(SO_4)_3 \cdot 8H_2O$; b—aqueous solution of $Gd_2(SO_4)_3$.

One can arrive at a similar conclusion when one considers the band separated from the main band by 1100 cm^{-1}. This frequency corresponds to the vibrational frequency of the SO_4'' group.[10] It is observed only in the spectra of solutions and crystals of the sulfate and is completely absent in the chlorides. It is relatively brighter in sulfate crystals than in their solutions; it is brighter in the anhydrous crystals than in hydrous crystals; it is brighter in solutions of $Gd_2(SO_4)_3$ in concentrated H_2SO_4 than in aqueous solutions (Fig. 4).

All these observations lead us to attribute the appearance of this band to the superposition of electronic and SO_4'' ion frequencies.

We did not succeed in identifying the remaining diffuse bands visible in the spectrum. However, a study of the afterglow showed that τ was the same for these bands as for the frequency of electronic transition. This makes it possible to assume that these bands result from superposition of vibrational and electronic transitions. In this connection it is interesting to point out the bands which border directly on the main band and which have a well-defined structure in the crystals and are washed out into a continuum in the solutions. These bands remind one very much of the low frequency spectra observed by Gross and Vuks[11] and it is possible that they are similar in nature.

AFTERGLOW

Although the type of phosphoroscope used by us makes it very difficult to determine the exact value of τ, it is possible to establish with sufficient accuracy whether or not τ is the same for two luminescence bands. For this purpose, it is sufficient to photograph the lumi-

nescence bands. For this purpose, it is sufficient to photograph the luminescence spectra at two different values of delay times and to measure the intensity ratio of the selected bands in both spectra. The ratio will be the same in both spectra of τ is the same and it is very sensitive to a difference in τ for one of the bands. The luminescence spectra of 1% solutions of the chloride and sulfate of gadolinium and of $Gd_2(SO_4)_3 \cdot 8H_2O$ were photographed for two positions of the maltese cross which differed from each other by 35°, which corresponds to a difference in delay time of about 2000 μsec.

The ratio of exposure times was chosen so that the darkening was approximately the same in both spectra. The experiments were made with wide slits in the spectrograph so that the ratio of band intensities could be measured from the darkening at the center of the band. The ratio of darkening, measured in the usual way with a photographic photometer having an accuracy limited to 10%, remained constant for various delay angles. This shows that τ is the same in the two bands to within 10%.

The ratio of intensities of the bands at 3110 and 3060 A was approximately equal to 20 at room temperature. This fact is to be understood on the ground that the populations of the $^6P_{7/2}$ and $^6P_{5/2}$ levels are established by energy exchange between these levels in a time which is short in comparison with the lifetime of the excited state ($\tau \sim 10^{-3}$ sec). Under this condition the radiation which arises from each of the levels will not affect their relative occupancy. The intensity ratio of the two bands will, therefore, be equal to

$$\frac{I_{3060}}{I_{3110}} = \frac{A_{^6P_{5/2}-^8S_{7/2}}}{A_{^6P_{7/2}-^8S_{7/2}}} \cdot \frac{g_{^6P_{5/2}}}{g_{^6P_{7/2}}} \cdot \frac{h\nu_{3060}}{h\nu_{3110}} e^{-\frac{\Delta E}{kT}}; \quad (\Delta E = 0.07 \text{ ev}).$$

The transition probabilities for both bands can be evaluated from absorption spectra studies. Measurements of the intensity ratio of these bands based on absorption have not been made, but one can make an estimate based on the data of refs. 12 and 13; one finds that the absorption bands at 3060 and 3110 are of nearly equal intensity. From this, one obtains a value for the intensity ratio of the luminescence of these bands at room temperature which agrees reasonably well with the experimentally observed value of this ratio. A calculation of the intensity ratio at T = 90° yields a value of $I_{3060}/I_{3110} \sim 10^{-4}$.

Observations of the luminescence spectra of gadolinium sulfates at liquid nitrogen temperature indicated that under these conditions the band at 3060 A is unobservable, which is illustrated in Fig. 5. This is completely in agreement with the assumptions made concerning the establishment of population equilibrium between the two excited levels.

The duration of the excited states of a series of weak luminescence bands in the spectra of the chlorides and sulfates (bands at 3470, 3220, 3180, 3145 A) was also studied. It was established that the decay times of these

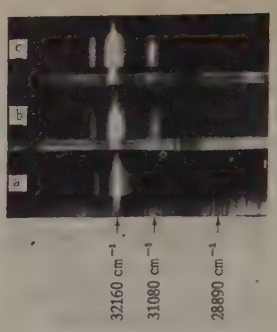

Fig. 4

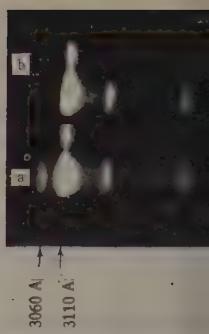

Fig. 5

Fig. 4. Fluorescence spectra of gadolinium sulfate. a—$Gd_2(SO_4)_3 \cdot 8H_2O$; b—anhydrous $Gd_2(SO_4)_3$; c—solution of $Gd_2(SO_4)_3$ in concentrated H_2SO_4.

Fig. 5. Fluorescence spectra of $Gd_2(SO_4)_3 \cdot 8H_2O$. a—T = 290°; b—T = 90°.

bands did not differ appreciably from the decay times of the main electronic transition. This also supports the hypothesis that the indicated bands arise as a result of superposition of vibrational frequencies on the principal transition frequency.

N. V. Kozheurova took part in the experimental work.

REFERENCES

1. R. Tomaschek and E. Mehnert, Ann. Physik (5) **29**, 306 (1937).
2. A. N. Zaidel' and Ya. I. Larionov, Doklady Akad. Nauk. SSSR No. 16, 449 (1937).
3. G. H. Dieke and L. Leopold, J. Opt. Soc. Am. **47**, 9 (1957).
4. A. N. Zaidel' and G. P. Malakhova, Doklady Akad. Nauk SSSR **85**, 591 (1952).
5. S. Singh, Optik No. 2, 133 (1947).
6. G. H. Dieke and L. A. Hall, J. Chem. Phys. **27**, 465 (1957).
7. E. V. Kondrat'eva and G. S. Lazeeva, Opt. i Spektr **8**, 132 (1960), Optics and Spectroscopy **8**, 67 (1960)
8. E. M. Brumberg, Optiko-Mekh. prom. No. 11 (1936
9. A. N. Zaidel', Spectroscopy of rare earth ions in s lution, Doctoral Dissertation, Leningrad, 1944.
10. K. Kohlrausch, "Spectra of Combinatory Scatterin Moscow, 1950.
11. E. F. Gross and M. F. Vuks, J. phys. radium **7**, 11 (1936).
12. W. Prandtl and K. Scheiner, Z. allgem. Chem. **220** 107 (1934).
13. H. Gobrecht, Ann. Physik (5) **28**, 673 (1937).

INTRACRYSTALLINE REACTIONS IN CRYSTALLINE PHOSPHORS AND THE STRUCTURE OF LUMINESCENCE CENTERS

V. V. Osiko (pp. 642-647)

Received 19 November 1960

A study is made of the luminescent properties of the system $|Zn_{100-x}Mn_x|\,|S_{100-y}O_y|$. Using this system as an example, the possibility is demonstrated of a chemical interaction between the different impurity atoms in the crystal lattice of the crystalline phosphor (an intercrystalline reaction). The composition and structure of luminescence centers in crystalline phosphors is discussed, taking into account the part played by intracrystalline reactions.

Crystalline phosphors, as a rule, represent by their structure multicomponent solid solutions of the substitution type. This means that impurity atoms (activators, coactivators, fluxes, uncontrollable contamination) replace the atoms of the host substance at the nodes of the crystalline lattice.

According to crystal chemistry, in the case of multicomponent solid solutions the location of the various atoms at the lattice nodes is arbitrary.[1] On the other hand a series of papers on luminescence published during the past decade describes ideas concerning the formation of various types of associations between impurity atoms in crystalline phosphors. Thus, changes in the luminescence spectra of ZnS:Cu, ZnS:Ag, and ZnS:Sm which are observed when small amounts of oxygen are present in the ZnS lattice are ascribed[2,3] to the formation of activator-oxygen pairs. The specific properties of the phosphor group ZnS:Cu:Ga, ZnS:Cu:In, ZnS:Ag:Ga, and ZnS:Ag:In are explained[4,5] on the basis of a theory of donor-acceptor pairs (Williams, Prener). According to this theory activator-coactivator pairs are formed in crystalline phosphors.

The contents of this paper are devoted to ascertaining the nature and origin of this type of pair in crystals. The author was hoping to obtain an answer to the following typical questions: Is the appearance of interacting pairs determined by the statistical distribution of impurity atoms or is there a chemical interaction between them which leads to their ordered distribution in the crystal?

From this point of view there are marked advantages in replacing the types studied earlier by the system $|Zn_{100-x}Mn_x|\,|S_{100-y}O_y|$, i.e., by a zinc sulfide in whose crystalline lattice part of the zinc atoms have been replaced by manganese atoms and part of the sulfur atoms by oxygen atoms. The impurity atoms (Mn and O) on the one hand and atoms of the host substance (Zn and S) on the other have the same valences and do not differ markedly in their chemical nature. Furthermore, it is possible to have a high concentration of impurity atoms (several molar percent). All of these factors make the system selected suitable for the detection and study of the chemical interaction between the impurity atoms (in this case between atoms of manganese and oxygen).

PREPARATION OF SAMPLES

As raw materials for the phosphor synthesis, we used zinc sulfide and zinc oxide of "luminescence pure" grade (from the "Red Chemist" factory) as well as specially prepared manganese sulfide and oxalate of a high degree of purity. In order to eliminate oxygen, the zinc sulfide was subjected to a preliminary baking in flowing hydrogen sulfide (900°C, 4 hr). The zinc sulfide thus treated had only a very weak reddish luminescence under excitation by light at 365 mμ.

The batch was baked in quartz boats in flowing nitrogen purified of oxygen. As fluxes we used sodium chloride and zinc sulfate of "chemically pure" grade.

The region of phase homogeneity of the system was determined in preliminary experiments. X-ray phase and crystal-optical analyses showed that no less than 6 molar % MnO are dissolved in ZnS at t = 1200°C.

LUMINESCENCE SPECTRA AS FUNCTIONS OF PHOSPHOR COMPOSITION*

*The luminescence spectra were obtained using a UM-2 monochromator, an FEU-27 photomultiplier (which is sensitive in the entire visible range of the spectrum), and an M-21-2 mirror galvanometer.

Experiments repeated many times have shown that the luminescence spectra ($\lambda_{exc.}$ = 365 mμ) of samples containing oxygen (which was introduced in the form of zinc oxide or manganous oxide) are shifted by 5-10 mμ toward longer wavelengths as compared with samples free of oxygen. This result is analogous to the results obtained[2] for ZnS:Cu and ZnS:Ag phosphors. However, the change in the luminescence spectrum cannot by itself serve as a proof that manganese and oxygen atoms are located at adjoining nodes of the crystalline lattice as a result of their chemical interaction. Let us consider separately the possible reasons for the observed spectral shift: (1) A change in the parameters of the zinc sulfide lattice when oxygen is introduced ($r_{O^{2-}}$ = 1.32 A; $r_{S^{2-}}$ = 1.74 A). (2) The fact that in a random distribution an appreciable number of manganese and oxygen atoms are situated close to each other. (3) A regular distribution of manganese and oxygen caused by their chemical interaction. (In this case the number of pairs can be much larger than for a random distribution of atoms.)

Figure 1 shows the luminescence spectra ($\lambda_{exc.}$ = 365 mμ) of phosphors containing different amounts of manganous oxide. (These phosphors were baked at 1000°C.) It is known that when zinc is replaced by manganese, the constant of the zinc sulfide lattice increases[6] ($r_{Mn^{2+}} > r_{Zn^{2+}}$) and the luminescence spectrum is shifted toward longer wavelengths. When oxygen is introduced into the lattice ($r_{O^{2-}} < r_{S^{2-}}$), the lattice constant is de-

creased by a larger amount than it increases when manganese is introduced.[2] We could thus expect that the total change of lattice parameters due to the introduction of both manganese and oxygen in the form of manganous oxide will displace the spectrum toward shorter wavelengths. The data shown in Fig. 1 confirm these considerations: with increase in the content of manganous oxide, the luminescence spectrum is shifted toward shorter wavelengths. Hence the long wavelength shift of the spectrum which we observed upon introducing oxygen into ZnS:Mn cannot be caused by a change in lattice parameters since that effect and the effect whose nature we are trying to ascertain work in opposite directions.

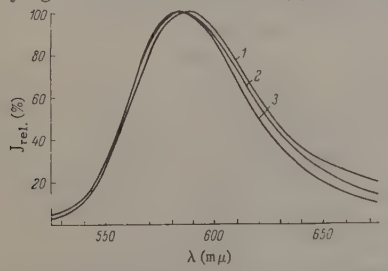

Fig. 1. Displacement of the luminescence spectra of ZnS-MnO phosphors with increase in manganous oxide content. Phosphor composition (in molar %): curve 1—99.5ZnS-0.5MnO; curve 2—99ZnS-1MnO; curve 3—95ZnS-5MnO. Baking atmosphere, temperature (in °C), and duration (in minutes): N_2, 1000, 15. $\lambda_{exc.}$ = 365 mμ.

Let us consider the second possible cause of a long wavelength shift. In the Table we list the values which we have calculated for the probability of finding oxygen atoms at lattice nodes adjoining the positions of manganese atoms. The calculations were carried out using a method described in ref. 7. The calculation shows that the number of closely situated manganese and oxygen atoms is sufficiently large to cause the observed spectral shift. Furthermore, the number of such pairs increases sharply with increasing oxygen content. Figure 2 shows the luminescence spectra ($\lambda_{exc.}$ = 365 mμ, t = 77°K) of samples with different manganese and oxygen content (baking temperature 900°C). As may be seen in the Table, the number of manganese and oxygen atoms located at adjoining lattice nodes increases sharply with increasing concentration of these impurities. The magnitude of the spectral shift is not a monotonic function of manganese and oxygen concentrations. (See Fig. 2.) It also fails to correspond to the data listed in the Table. Analogous results were also obtained for diffuse reflection spectra. Thus the magnitudes of the edge shift in reflection spectra turned out to be practically the same for samples containing 1% and 3%, respectively, of oxygen. (See Fig. 3.)*

*The reflection spectra were obtained using a quartz monochromator, an FEU-19-M photomultiplier, and an M-95 microammeter.

[O]	P_1	P_2
0.3	0.012	0.081
1	0.040	0.274
3	0.115	0.510

[O] is the atomic concentration of oxygen; P_1 and P_2 are the probabilities of at least one oxygen atom being found within the bounds of the first and second coordination ranges, respectively, of the manganese atom.

THE LUMINESCENCE SPECTRA AS FUNCTIONS OF THE BAKING TEMPERATURE OF THE PHOSPHORS

The presence of oxygen in the lattice of the phospho being studied must obviously result in the existence of a least two kinds of manganese centers. In one of these th manganese atoms would be surrounded solely by sulfur atoms, while in the other the manganese atom would hav among its neighbors at least one oxygen atom. This wou be true both in the case of the statistical distribution of oxygen atoms relative to the manganese atoms and in the case where they interact chemically. However, in the ca of chemical interaction, we should observe a functional dependence on temperature of the equilibrium concentrations of the isolated manganese and oxygen atoms and th Mn-O pairs, as required by the laws of chemical thermodynamics.

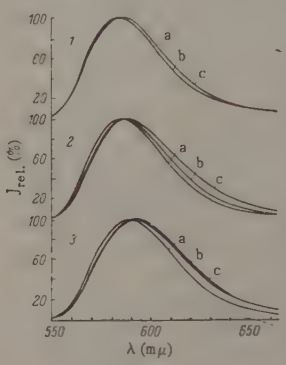

Fig. 2

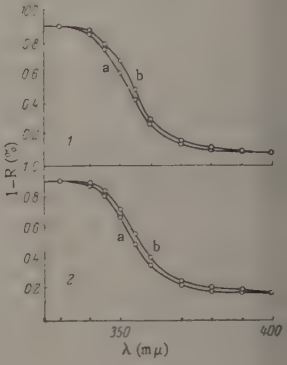

Fig. 3

Fig. 2. Displacement of the luminescence spectra (temperature 77°K) when oxygen is introduced into the phosphors. Phosphor composition (in molar %): curve 1a—99.7ZnS-0.3MnS; curve 1b—99.4ZnS-0.3ZnO-0.3MnS; curve 1c—99.7ZnS-0.3MnO; curve 2a—99ZnS-1MnS; curve 2b—98ZnS-1ZnO-1MnS; curve 2c—98ZnS-1MnO;* curve 3a—97ZnS-3MnS; curve 3b—94ZnS-3ZnO-3MnS; curve 3c—97ZnS-3MnO. Baking conditions, atmosphere, temperature (in °C), and duration (in minutes): 2% NaCl, N_2, 900, 20. $\lambda_{exc.}$ = 365 mμ.

*Translation Editor's Note: Probably should read 99ZnS-1MnO.

Fig. 3. Diffuse reflection spectra of the phosphors. Phosphor composition (in molar %): curve 1a—99ZnS-1MnS; curve 1b—99ZnS-1MnO; curve 2a—97ZnS-3MnS; curve 2b—97ZnS-3MnO.

In the case of random distribution, the number of pairs is temperature independent. Therefore, any expe mentally observed dependence between the position of t luminescence spectrum and the baking temperature of t phosphor would serve as the deciding factor in favor of chemical interaction between manganese and oxygen. Figure 4 shows luminescence spectra of samples, containing 0.5 atomic % of oxygen, which were baked at dif ferent temperatures. It is evident that as the baking te perature is raised, the spectrum is shifted toward sho wavelengths. The shift involved in passing from t = 70

t = 1200°C amounts to 10 mμ. The results of another xperiment are shown in Fig. 5. Samples containing 0.5 tomic % of oxygen were baked at 1000°C. Then part of he phosphors was maintained for four hours at 700°C n flowing nitrogen). The luminescence spectra of samles before and after the additional baking are compared Fig. 5. It is easily seen that, as was to be expected, in his case also the luminescence spectrum varies with the aking temperature.

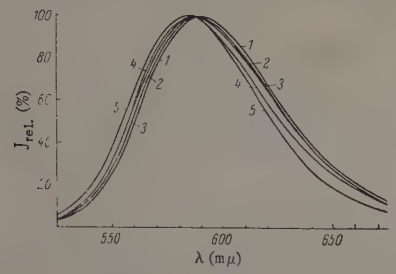

Fig. 4. Luminescence spectra of the 99.5ZnS-0.5MnO phosphor as a function of the phosphor baking temperature. Baking temperature (in (in °C): curve 1—700; curve 2—800; curve 3—900, curve 4—1000; curve 5—1200. Conditions, atmosphere, and duration (in hours) of baking: 2% NaCl, N_2, 1. $\lambda_{exc.}$ = 365 mμ.

The possibility is not excluded that in this case the pectral shift is caused by the polymorphous transition phalerite⇄wurtzite. In order to check this possibility, xperiments analogous to the ones described were carried out on samples free of oxygen. We found that for hese samples a change in baking temperature causes ractically no spectral shift. The data obtained from an -ray analysis agree with this result: The temperature anges within which we observe a maximum variation in he luminescence spectra and those in which the phalerite⇄wurtzite transition occurs according to the ebye diagrams do not coincide.

Thus the spectral shift observed for a change in aking temperature can only be explained on the basis of chemical interaction between manganese and oxygen oms.

ISCUSSION OF RESULTS

Our experiments indicate that the manganese and xygen atoms in the system considered do interact chemially. The equilibrium concentrations of Mn-O pairs and f isolated manganese and oxygen atoms vary with temerature. The higher the temperature, the stronger beomes the shift of the equilibrium towards the side of he dissociation of pairs into isolated atoms. Conversely, he lower the temperature, the higher the equilibrium air concentration.

Let us go back to the structure of luminescence ceners in the system considered. The process of chemical nteraction between manganese and oxygen leads to the ollowing result: In the ZnS:Mn phosphor there are alays centers of at least two kinds (even if the oxygen admixture is slight): manganese centers in which the four eighbors of the manganese atom are all sulfur atoms, nd manganese centers in which at least one of these eighbors is an oxygen atom. The relative concentration f these centers depends on oxygen concentration and on he baking temperature of the phosphor. These two kinds of centers have different properties. Thus the emission band of the Mn-O center is in the region of longer wavelengths than the band of the manganese center isolated from oxygen. The observed ZnS:Mn luminescence is a superposition of the radiation in these two bands. Figure 6 shows the luminescence spectra at two temperatures of observation for an oxygen-containing phosphor.

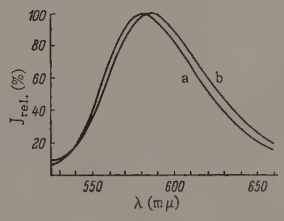

Fig. 5

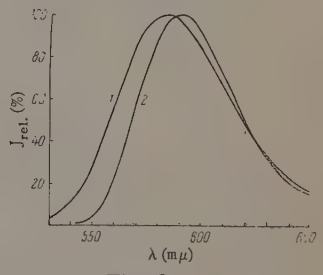

Fig. 6

Fig. 5. Change in the luminescence spectrum of a 99.5ZnS-0.5MnO phosphor after additional baking. Conditions, atmosphere, temperature (in °C), and duration (in minutes) of baking during phosphor preparation: 2% NaCl, N_2, 1000, 15. Curve a—spectrum of prepared phosphor; curve b—spectrum of the same phosphor after additional 4-hr baking at 700°C in an atmosphere of nitrogen. $\lambda_{exc.}$ = 365 mμ.

Fig. 6. Luminescence spectra of a 98ZnS-2MnO phosphor at temperatures of 291 (curve 1) and 77°K (curve 2). Baking atmosphere, temperature (in °C), and duration (in minutes): N_2, 900, 15. $\lambda_{exc.}$ = 365 mμ.

It is easily seen that the narrowing of the spectrum at lowered temperature is sharply asymmetrical. This is not observed in oxygen-free samples. Hence we may conclude that the asymmetry in the narrowing of the composite band is caused by a difference in the temperature dependence of the luminescence yield of the two bands mentioned.*

*A detailed description of the luminescent properties of ZnS:Mn is given in refs. 8 and 9.

It is natural to consider that a chemical interaction between impurity atoms similar to the one revealed here takes place in other systems as well. In principle, such chemical processes can occur also between other atom pairs, both in ZnS and in other crystals. We have called such reactions intracrystalline, i.e., reactions taking place inside of crystals. A study of the regularities of intracrystalline reactions in crystalline phosphors will undoubtedly provide valuable information concerning the chemical composition and structure of luminescence centers and other local formations in the crystals which are responsible for the luminescent properties.

In conclusion the author wishes to express sincere appreciation to M. A. Konstantinova-Shlezinger for her constant interest in this work, discussion of results, and valuable comments.

REFERENCES

1. R. K. Evans, "Introduction to Crystal Chemistry," p. 207. State Chemistry Press, 1948. Cambridge Univ. Press, 1961.

2. F. A. Kröger and J. A. Dikhoff, J. Electrochem. Soc. 99, 144 (1952).
3. Z. A. Trapeznikova, Proc. Fifth All-Union Conf. on Luminescence (Crystaline Phosphors), p. 17. Tartu Univ., Tartu, 1957.
4. E. F. Apple and F. E. Williams, J. Electrochem. Soc. 106, 224 (1959).
5. F. E. Williams, J. Phys. Chem. Solids 12, 265 (1960).
6. F. A. Kröger, "Some Aspects of the Luminescence of Solids," p. 310, Elseviev, New York, 1948.
7. I. Z. Fisher and V. S. Aizenshtat, Uchenye Zapiski Beloruss. Univ., Ser. Fiz. 41, 181 (1958).
8. V. L. Levshin and V. F. Tunitskaya, Opt. i Spektr. 8, 663 (1960), Optics and Spectroscopy 8, 350 (1960).
9. V. L. Levshin and V. F. Tunitskaya, Opt. i Spektr. 9, 223 (1960), Optics and Spectroscopy 9, 118 (1960).

LOCATION OF ENERGY LEVELS IN ZnS-CdS PHOSPHORS

L. Drozd and V. L. Levshin (pp. 648-655)

Received 12 December 1960

The effect of the wavelength of the exciting light on the composition of the luminescence of ZnS-CdS phosphors is studied as well as the change with variation in CdS content of the width of the forbidden band and of the glow curves. The energy level scheme of the ZnS-CdS phosphor is constructed on the basis of the data obtained and of the results of earlier investigations by the authors.

INTRODUCTION

In our preceding papers[1,2] we studied the problem of self-activation of mixed ZnS-CdS phosphors. We established the presence of three different luminescence centers. The centers which emit radiation with the longest wavelength luminescence at all values of the CdS content from 0 to 100% and in the entire temperature range from −195° to +180°C. As the cadmium content is increased, the spectrum of this luminescence (band I) is shifted from the blue to the infrared region. The luminescence centers of the second kind emit a radiation of shorter wavelength; in the absence of cadmium they manifest themselves very weakly. Their luminescence becomes most pronounced for a cadmium concentration equal to 35-50%. As the cadmium content is increased still further, a third band with the shortest wavelength makes its appearance at the expense of the intensity of the second band. This third band becomes most pronounced for a 100% CdS concentration. Bands II and III become noticeable at low temperatures only (below −120° and below −140°C, respectively).

In ref. 2, we also listed some preliminary considerations concerning the nature of the luminescence centers emitting these bands. The first of these was ascribed to the self-activator of zinc sulfide, a cation vacancy, whose nature and surroundings have not yet been established.*

*The idea that the blue luminescence center is a cation vacancy has recently been presented by a series of authors.[5,7] Grillot[4] considers that the centers of blue luminescence are formed by traces of copper which, in amounts less than 2×10^{-7}%, always remains in zinc. Bundel' and Rusanova[8] and others ascribe the blue luminescence to atomic Zn, while Riehl and Ortmann[18] ascribe it to a zinc vacancy connected with oxygen.

The second band was ascribed to a center surrounded by a fully determined amount of cadmium. An increase in CdS content in the lattice up to 35% increases the number of such centers. Furthermore, by changing the internal field of the lattice, it shifts the emission spectrum to the long wavelength side. When cadmium concentration exceeds 35%, centers giving rise to the third emission band begin to appear at the expense of these centers of the second kind. We must assume that in these zinc is fully replaced by cadmium, since their luminescence is most intense in pure CdS. In the present investigation we performed additional experiments in order to confirm this point of view and to clarify the location of energy levels in the ZnS-CdS phosphors.

The experiments were carried out on the same series of ZnS-CdS (2% NaCl) phosphors prepared in the presence of oxygen which were described before.[1,2] The experimental arrangement used in this investigation was also the same as before.

THE EMISSION OF ZnS-CdS PHOSPHORS AS A FUNCTION OF THE WAVELENGTH OF THE EXCITING LIGHT

The previously established[1,2] absence at room temperature of luminescence of the natural CdS activator in the phosphors which we studied is of great importance in ascertaining the luminescence kinetics of the ZnS-CdS phosphors. However, it still remained uncertain whether additional luminescence caused by the embedding of CdS in the crystal lattice could be obtained under excitation by short wavelength radiation corresponding to the fundamental absorption region. In Fig. 1 we show the emission bands at 18°C of phosphors containing 0, 1, 5, 10, and 15 respectively of CdS excited by lines at 365 (circles) and 313 mμ (triangles). For excitation by $\lambda_{exc.} = 313$ mμ, the intensity of luminescence was much weaker. Therefore to compare the shapes of the spectral distribution curves these were normalized according to the intensity at the maximum. It is easily seen that, within the limit of experimental error, the circles and triangles fall on the same curves. The lack of dependence of the spectral distribution curve on the exciting wavelength is an additional confirmation of the fact that the luminescence of the ZnS-CdS phosphors investigated is due solely to one luminescence center and also that the emission bands are not composite.

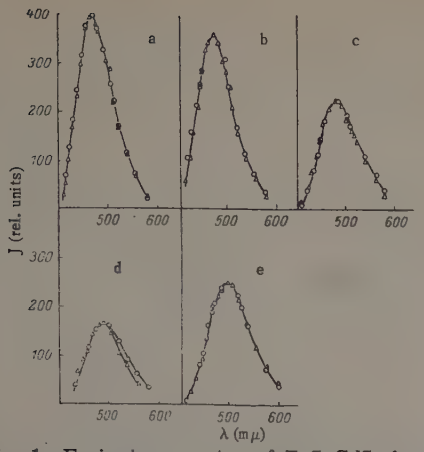

Fig. 1. Emission spectra of ZnS-CdS phosphors at 18°C. CdS content (in %): a—0; b—1; c—5; d—10; e—15. $\lambda_{exc.}$ (in mμ): circles—365; triangles—313.

A different situation is observed when the same phosphors are excited by light with the wavelengths of 313, 365, and 436 mμ, respectively, at a temperature of −195°. The corresponding spectral distribution curves shown in Fig. 2 consist here of two bands. (The curves are normalized according to the same maximum as in Fig. 1.) It is not difficult to see that under excitation by light at 313 mμ a second, shorter wave band becomes apparent even in the spectrum of pure ZnS. This band increases rapidly in intensity with increase in cadmium content (it is weakened for a CdS concentration in excess of 50%). The relative development of band II as compared to band I depends on the wavelength of the exciting light. For a CdS content up to 20%, excitation by light at 313 mμ is favorable to the development of band II. When the CdS content exceeds 20%, better conditions for the excitation of this type of luminescence are obtained using exciting light at 365 mμ. The use of still longer wavelength light at 436 mμ is found to be less effective in all cases. This behavior of band II may be interpreted as a sign

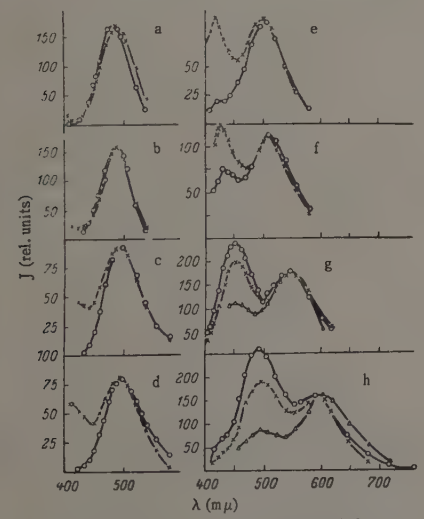

Fig. 2. Emission spectra of ZnS-CdS phosphors at −195°C. CdS content (in %): a—0; b—1; c—5; d—10; e—15; f—20; g—35; h—50. $\lambda_{exc.}$ (in mμ): crosses—313; circles—365; triangles—436.

that the energy levels of its luminescence centers are very close to the valence band. (For a CdS concentration in excess of 20%, the 365 mμ line is very close to the fundamental absorption edge, while the 436 mμ line at all concentrations investigated is an appreciable distance away from the absorption edge of the lattice.)

These experiments confirm our earlier conclusion concerning the existence of a separate luminescence center for bands II, a center which is surrounded by a certain definite amount of CdS. The luminescence of center III belongs to large CdS concentrations. In Fig. 2 it shows up faintly only on the luminescence curve of the ZnS(50%)-CdS(50%) phosphor for $\lambda_{exc.} = 365$ mμ.

Figure 2 shows that the intensity of luminescence of the ZnS-CdS phosphors exhibits in all cases a minimum for a CdS concentration in the neighborhood of 12% and passes through a maximum for a concentration close to 50%. Fridman and one of the present authors have earlier found[14] an analogous variation in the intensity of luminescence of the ZnS-CdS:Cu phosphors at room temperature.

THE WIDTH OF THE FORBIDDEN BAND IN THE ZnS-CdS PHOSPHORS AND THE POSITION OF THE LOCAL HOLE LEVELS

The spacing between the valence band and the bottom of the conduction band is usually taken as being from 3.7 to 4 ev for ZnS and 2.5 ev for CdS phosphors.[3-5] These values are based on the determination of the fundamental absorption edge. We should, however, point out a certain arbitrariness in these values connected first of all with the uncertainty as to the proper definition of the absorption edge and secondly with the inaccuracy in the experimental methods used for its determination.

The edge of the fundamental absorption cannot be determined accurately from reflection experiments, since it is impossible to ascertain exactly either the wavelength corresponding to its onset or the wavelength for which it reaches its full development. Apparently the bottom of the conduction band is strongly washed out. Even in a crystal which does not contain foreign impurities, the absorption edge cannot be sharp due to the effect of imperfection of the lattice itself and to thermal inhomogeneities. This washing out and shift to longer wavelengths is the more pronounced the less pure the ZnS. Depending on the purity of the crystalline ZnS, various authors[9] place the edge of the fundamental absorption band in the range from 330 to 310 mμ. In studying the absorption of evaporated ZnS films, Shalimova[10] placed the absorption edge at 334 mμ, while Arapova[11] found several absorption maxima in the 180-330 mμ region. The determination of the fundamental absorption edge is all the more difficult since its tail is superimposed on the equally washed out absorption region of the centers of deep luminescence of zinc.

It is possible to determine fairly accurately experimentally the wavelength at which absorption reaches half of its maximum value. This is how we determined here the location of the fundamental absorption edge even though this method characterizes only conditionally the width of the forbidden band, giving for it values known to be too low.*

*The first determinations of the fundamental absorption edge of the ZnS-CdS phosphors were carried out by Gisolf[12] and Kröger.[13] While their phosphors differed from ours in the method of preparation, the difference in the position of the fundamental absorption edge turned out to be small.

The values of the absorption are shown in Fig. 3 as differences between the values of the fluxes reflected from a perfectly scattering surface (MgO) and from an infinitely thick layer of ZnS-CdS phosphors with different (large) CdS concentration. The Table (column 4) lists the values obtained in this fashion for $\lambda_{abs.}$, the fundamental absorption edge for phosphors with a CdS content exceeding 50%. Column 6 of the Table lists the corresponding spacings ($E_{sp.}$) between the conduction and valence bands. Taking into account the peculiarities described above of the method used to determine the absorption edge, we may consider these values to be too low by about 0.2-0.3 ev. Almost the same values were obtained from the excitation spectra, i.e., from the determination of the wavelength of the exciting light which corresponds to the maximum intensity of luminescence. This agreement is not remarkable since the method of the excitation spectra also gives values for the interzone spacing which are too low. (This method essentially determines the spacing between the conduction band and the centers located above the valence band.) The wavelengths of optimal excitation $\lambda_{exc.}$ are listed in column 5 of the Table. (The corresponding values of $E_{sp.}$ for phosphors with a CdS content below 50% are given in column 6 in parentheses.)

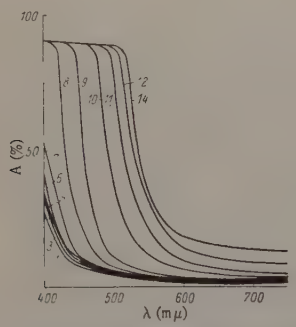

Fig. 3. Location of fundamental absorption edge of ZnS-CdS phosphors at 18°C. CdS content (in %): curve 1—0; curve 3—5; curve 4—10; curve 6—20; curve 7—35; curve 8—50; curve 9—65; curve 10—80; curve 11—90; curve 12—95; curve 14—100.

To determine the positions of the localized hole levels, we may use data from the emission spectra, considering that the magnitude of the emitted quanta characterizes the spacing between the conduction band and the level of the corresponding luminescence center. Two assumptions are possible concerning the origin of the luminescence: (1) A preliminary transition of the electron from the conduction band to one of the excited levels of the center, which is followed by luminescence. (2) A direct recombination with an ionized center, the excitation of the center being produced by the energy released. We consider the second assumption more probable. Obviously, however, the emission spectra in both cases determine only the values of the excitation energy of the luminescence centers, which are smaller than the distances of the hole levels from the conduction band. Therefore, the values of the latter which are obtained from the emission spectra are decreased, while the distances to the valence band are raised in value. The validity of this last conclusion is, however, appreciably lowered by the fact that, as indicated above, we assume the forbidden band itself to be too narrow. (It is decreased by, say, 0.2 ev.) The washed-out appearance of the emission bands may be a consequence both of the smearing in the positions of the excitation levels of the luminescence centers and of the smearing in the positions of the localized hole levels.

Change in the Width of the Forbidden Band and in the Position of the Levels of the Ionized Centers When the CdS Content Is Increased

Phosphor no.	C_{CdS} (wt. %)	C_{CdS} (mol %)	λ_{abs} (mμ)	λ_{exc} (mμ)	E_{sp} (ev)	λ_L (mμ)	E_L (ev)	$E_{sp}-E$ $= E_{cI}$ (e
1	0	0	(346)	342	(3.61)	469	2.63	(0.98
3	5	3.4	—	347	(3.56)	481	2.56	(1.00
4	10	7	—	352	(3.51)	487	2.53	(0.98
5	15	10.7	—	361	(3.41)	498	2.48	(0.93
6	20	14.6	—	368	(3.36)	506	2.44	(0.92
7	35	32.1	—	396	(3.14)	533	2.31	(0.83
8	50	40.3	427	420	2.89	575	2.15	0.74
9	65	55.6	457	443	2.72	616	2	0.72
10	80	73	489	472	2.52	678	1.82	0.70
11	90	85.9	509	494	2.42	718	1.72	0.70
12	95	92.8	518		2.38	742	1.66	0.72
14	100	100	521	516	2.37	760	1.63	0.74

In order to ascertain the value of the average distan between the valence band and the level of the luminescence center of band I, we determined the values of the energy which correspond to the maximum of the emissio spectra (column 8 of the Table). These are the values which characterize the distances between the conduction band and the position of maximum density of the levels o the centers I. If we subtract these quantities from the values of the width of the forbidden band, we find the pos tion of the maximum density of the levels of the centers relative to the valence band. (These values, $E_{sp.} - E_L = E_{cI}$ are given in column 9.) It follows from the data give that the distances between the valence band and the level of the ionized centers turn out to be almost the same fo all samples (8-14) for which E_{cI} was determined by the same method. (This value is on the average 0.72 ev.) This occurs in spite of the large variation in CdS content (from 50 to 100%). At lower values of the CdS content, the position of the levels of the ionized centers was determined as before, but for the width of the forbidden band we took values determined from the excitation curves (column 6). The data on the position of the levels of centers I for phosphors with low CdS content which were obtained by this procedure appear in parentheses in column 9 of the Table. These values are somewhat higher than for phosphors with large CdS content and reveal a more or less systematic behavior in the range from 0.83 to 0.96 ev. (We consider them to be less reliable.) It is clear from the above that the position of th levels of the excited centers relative to the valence band is independent of CdS content if this content exceeds 50% However, at lower CdS content, the levels of these centers move slowly away from the valence band. The slig degree of dependence on CdS content in the position of t levels of the ionized centers confirms the assumption that these levels are formed by cation vacancies.

It is known that many authors (Seitz, Bundel'[18]) ascribe the blue ZnS luminescence to excess Zn atoms. However, the assumption that the ZnS-CdS luminescenc represents atomic zinc radiation which is gradually bei displaced toward longer wavelengths encounters difficul ties, since the latter effect is not to be expected in phos phors with large cadmium content. Of little probability is also the hypothesis that at low cadmium concentrations the luminescence is due to zinc and at high cadmium concentrations to cadmium. It is not in accord wi the perfectly smooth behavior of the displacement of the

axima of the emission spectra when the CdS concentration is increased.[2]

The value which we obtained for the distance of the vels of the blue luminescence centers from the top of e valence band in ZnS is close to the values cited in fs. 4 and 5. It is, however, appreciably higher than the lues determined in ref. 2 using the temperature quench- g method. We ascribe this disagreement to the poor curacy of both methods.

The shift of the luminescence maxima of centers II the short wavelength side relative to the luminescence axima of centers I amounts on the average to 0.47 ev. nce the maximum density of these levels occurs at a stance ~0.25 ev above the valence band for phosphors th high CdS content and at a distance ~0.5 ev for phosors with low CdS content. The maxima of the emission nds of centers III are shifted on the average by 0.79 ev lative to the maximum of bands I. Thus the correspondg levels practically coincide with the top of the valence nd. Hence bands III correspond to centers whose levels e in the immediate vicinity of the valence band. We can d this point of view confirmed in the papers by Grillot ich are devoted to a study of the luminescence of pure iS at low temperatures.[15] As already noted, bands III e very weak and arise at low temperatures at a CdS ntent in excess of 50%.

E POSITION OF THE LOCALIZED ELECTRON LEVELS

In order to study the positions of the localized elecn levels in the ZnS-CdS phosphors, we investigated the w curves of their first principal band. The phosphors re excited for 10 min while being cooled with liquid rogen. The heating was started 1 min after the stop excitation and was carried out at a rate of 13°/min. e intensity of luminescence was measured using the U-17 and FEU-22 photomultipliers. The emission of first band was isolated by means of light filters which re changed for changes in the emission spectrum. In ating the results of the observations we introduced rrections to allow for differences in filter transmission the luminescence from different samples and in photoultiplier sensitivity to the transmitted radiation.

The glow curves obtained are shown in Fig. 4. The nal maxima at −165 and −110° are observed for pure nS. The introduction of CdS leads to the following reults:

1. The total light sum stored is greatly decreased: r C_{CdS} equal to 0, 5, 10, 15, 20, and 35%, respectively, it amounts correspondingly to 1.00, 0.92, 0.79, 0.61, 0.59,* and 0.18.

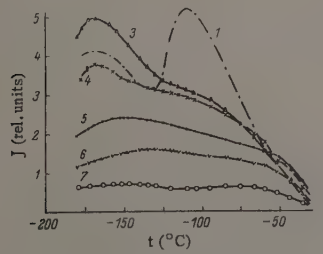

Fig. 4. Glow curves of inactivated ZnS-CdS phosphors. CdS content (in %): curve 1—0; curve 3—5; curve 4—10; curve 5—15; curve 6—20; curve 7—35.

*Translation Editor's Note: Probably a misprint for 0.39.

2. The localized electron levels become washed out, gradually forming an almost uniform band in the range from −180 to −25°.

3. In studying the data of Fig. 4 more closely, we can see that in the concentration range investigated (up to 35% CdS) the group of levels at −165° is strongly smeared out. In the same range of concentrations the group of levels at −110° is first sharply displaced toward lower temperatures and then disappears completely. Instead a crowding of levels appears at −50°.

The decrease in the light sums may be due to the following causes: (a) A decrease in the number of localization spots. (b) Nonradiative recombinations with liberated holes at the localization spots (external quenching). (c) The development of internal quenching of the recombination luminescence. All three causes may act simultaneously.

Noteworthy is the difference in the effect of the introduction of CdS on luminescence under excitation and on phosphorescence. Thus the change in luminescence yield under excitation is mainly connected with the formation of lattice irregularities produced by the transition of the phosphor from the sphalerite to the wurtzite type and does not proceed monotonically. [It has a minimum at ~10% CdS content. (See Fig. 2.)] On the other hand, the decrease in light sum values with increasing CdS content proceeds monotonically and at a considerably faster rate.

The data available are so far insufficient to establish the principal cause, among those listed above, for the decrease in the storing ability of the phosphors. The latter is, however, certainly connected with the appearance of a large number of lattice defects caused by Cd ions. A similar decrease in storing ability is observed in ZnS phosphors as a result of the appearance of internal deformations when the crystals are crushed.[16,17]

THE APPEARANCE OF THE BAND SCHEME OF THE ENERGY LEVELS OF ACTIVATORLESS ZnS-CdS PHOSPHORS

Figure 5 shows data characterizing the relative positions of the energy levels of ZnS-CdS phosphors. The CdS content is plotted along the horizontal axis, the energy levels along the vertical one.

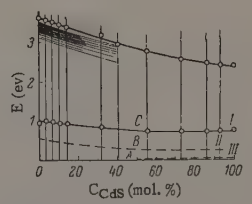

Fig. 5. Energy level scheme for the localized electron and hole levels in ZnS-CdS phosphors. The position of the levels of phosphors with different CdS content is measured along the ordinate axis. The vertical lines correspond to the phosphors investigated. The energy level scheme was constructed from the positions of the levels of these phosphors.

For $C_{CdS} < 50\%$, the density of localized electron levels near the conductivity band reflects qualitatively the values of the light sum obtained when the corresponding levels are vacated. For $C_{CdS} = 15\%$, the localized electron levels fill almost uniformly the top of the forbidden band, while for C_{CdS} below 15% they split up into individual systems.

The emission corresponding to bands I, II, and III, respectively, occurs as the result of the following transitions: I. The electrons move from the conduction band to the C levels of the centers of the first kind. II. The electrons move to the B levels of the centers of the second kind. III. The electrons move to the A levels of the centers of the third kind located in the immediate vicinity of the top of the valence band. The disappearance of bands II and III when the temperature rises above −130° is caused by the transition of holes from levels A and B to levels C through the valence band. The position of levels C is established more certainly than that of levels A and B. No great accuracy is claimed for the numerical values characterizing the positions of the levels in the given scheme.

REFERENCES

1. L. Drozd, Izvest. Akad. Nauk SSSR, Ser. Fiz. 23, 1300 (1959).
2. L. Drozd and V. L. Levshin, Opt. i Spektr. 10, 773 (1961), Optics and Spectroscopy 10, 408 (1961).
3. V. L. Levshin and V. F. Tunitskaya, Opt. i Spektr. 9 223 (1960), Optics and Spectroscopy 9, 118 (1960).
4. E. Grillot, J. phys. radium 17, 624 (1956).
5. P. F. Brown, J. Electronics 2, 154 (1956).
6. J. S. Prener and F. E. Williams, J. phys. radium 17 667 (1956).
7. J. S. Prener and D. J. Weil, J. Electrochem. Soc. 106, 409 (1959).
8. A. A. Bundel' and A. I. Rusanova, Izvest. Akad. Nau SSSR, Ser. Fiz. 13, 173 (1949).
9. M. N. Alentsev, Opt. i Spektr. 1, 240 (1956).
10. K. V. Shalimova, Doklady Akad. Nauk SSSR 80, 587 (1951); Izvest. Akad. Nauk SSSR, Ser. Fiz. 15, 638 (1951).
11. E. Ya. Arapova, Proc. Seventh Conf. on the Lumines cence of Crystalline Phosphors, Tartu, 1959, p. 358
12. J. H. Gisolf, Physica 6, 84 (1939).
13. F. A. Kröger, Physica 6, 369 (1939).
14. V. L. Levshin and S. A. Fridman, Zhur. Fiz. Khim. 8, 1277 (1935).
15. E. Grillot and M. Bancie-Grillot, Izvest. Akad. Nau SSSR, Ser. Fiz. 22, 1356 (1958).
16. V. L. Levshin and I. V. Veits, Zhur. Eksptl. i Teore Fiz. 20, 411 (1950).
17. V. L. Levshin and B. D. Ryzhikov, Izvest. Akad. Na SSSR, Ser. Fiz. 25, 362 (1961).
18. N. Riehl and H. Ortmann, "La luminescence des co cristallins anorganiques," p. 12. Paris, 1956.

SEPARATING THE SELENIUM BAND IN THE SPECTRA OF SULFIDE-SELENIDE PHOSPHORS

A. A. Bundel', Z. I. Guretskaya, and M. N. Noskova (pp. 656-660)

Received 15 December 1960

A study of the ZnS-ZnSe phosphors at −196, +20, and +120°C under conditions where the intensity of excitation varies by a factor of 30, as well as a study of the afterglow spectra, show the existence of two bands in the spectra of these phosphors, namely, a zinc band and a band connected with the introduction of the selenide. At room temperature and for an increase of the ZnSe content in the sample to 10% there is a gradual suppression of the zinc band by the selenium band. When the ZnSe content is made to exceed 10%, there is a smooth displacement of the now solely remaining selenium band toward longer wavelengths. A study of the spectra at −196°C shows the presence of the luminescence centers of the blue zinc band up to a ZnSe content of 75%.

An earlier supposition[1] stating that in mixed ZnS-ZnSe phosphors zinc selenide plays the part of a modifier which displaces the emission band of self-activated ZnS toward longer wavelengths can now no longer be considered correct. The spectral distribution curves for the sulfide-selenide phosphors given by Bundel',[2] Leverenz,[3] and Klasens[4] show that a special band in the green region appears when small amounts of selenide are introduced into ZnS.

One of the authors[2] who studied the self-activated ZnS-ZnSe phosphor observed the appearance in the spectrum of a second maximum caused by the selenium band. Leverenz records only a slight asymmetry of the spectral curve for a ZnSe content of from 5 to 10 mol. %.

The problem of the existence and properties of a characteristic selenium band are of great interest in ascertaining the nature of the activator principle in self-activated zinc sulfide and sulfide-selenide phosphors. We have therefore carried out an investigation of the luminescence spectra of the ZnS-ZnSe phosphors for a ZnSe content varying from 0 to 75% under different conditions of excitation: The intensity of excitation was varied by factors of 4 and 30, respectively, and the temperature was varied from −196° to +120°C.*

*The phosphors were prepared from ZnS and ZnSe. Th latter was obtained from ZnS and SeO_2. In order to remove ZnO, the substance was treated with an acid and analyzed for Zn, Se, and S content. The phosphor conte is indicated throughout in % by weight. The spectra we obtained with a UM-2 monochromator with an FEU-19 photomultiplier. Excitation was carried out using light from a PRK-2 lamp with a UFS-2 filter and a regulate power supply.

Figure 1 shows spectra obtained at room temperare with the sample 15 cm away from the lamp. (The rves are normalized according to the maximum.) irves 1 and 4 of Fig. 2 show the positions of the maxa of the spectral curves and the intensities at the maxa, respectively, as functions of the ZnSe content in the osphor. The spectra obtained when the intensity of extation was decreased by factors of 4 and of 30 are not produced here. (They are similar in appearance to the rves of Fig. 1; however, the maxima of the curves are gularly displaced toward longer wavelengths when the tensity of excitation is decreased.)

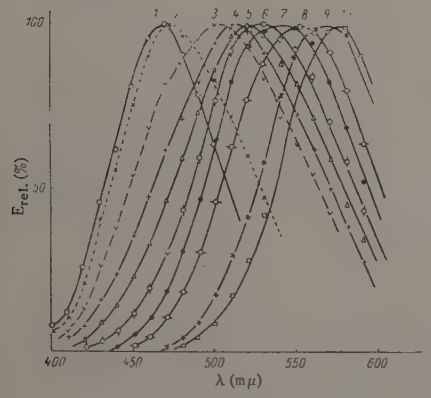

Fig. 1. Luminescence spectra of ZnS-ZnSe phosphors at +20°C. Selenide content (in %): curve 1—0; curve 2—1; curve 3—3; curve 4—5; curve 5—8; curve 6—10; curve 7—20; curve 8—30; curve 9—50; curve 10—75. Excitation by PRK-2 lamp; distance to phosphor, 15 cm.

Curves 2 and 3, respectively, of Fig. 2 give the posions of the spectral maxima as functions of composition der the conditions specified above. Curves 5 and 6 of g. 2 characterize the intensity variation at the maxium under the same conditions of excitation.

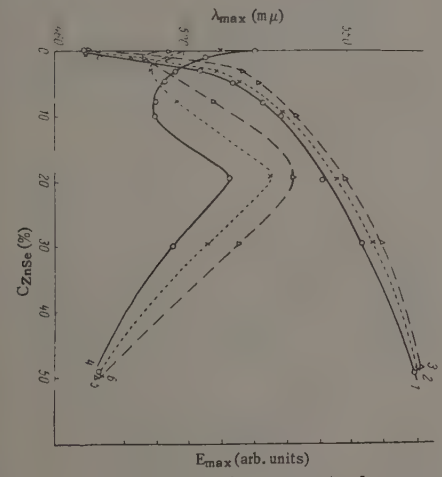

Fig. 2. The positions of the spectral maxima (curves 1-3) and the intensities at the maximum (curves 4-6) in ZnS-ZnSe phosphors as functions of the ZnSe content at +20°C for different excitation intensities. Excitation intensity: curves 1 and 4—J; curves 2 and 5—J/4; curves 3 and 6—J/30.

The spectral curves resemble the spectra of phosphors with a single activator for all values of the excitation intensity. However, the displacement of the maxima with increasing selenide content (Fig. 2) does not proceed uniformly. Small additions of ZnSe (up to 10%) cause large shifts of the maxima. Thus for a phosphor with a 10% ZnSe content, the maximum of the band is displaced by 600 A relative to that of the pure ZnS, while further additions each of 10% of ZnSe displace the maximum each time by about 100 A.

With increasing ZnSe content the intensity at the maximum (see curve 4 of Fig. 2) first decreases (up to 10% ZnSe), then increases again (approximately to 20% ZnSe), then begins again to decrease.

In the range of concentrations from 1 to 10% ZnSe, the luminescence yield (measured by the area under the luminescence curve) remains constant within the limits of experimental error. Only when the selenide content exceeds 10% do the yield and the intensity at the maximum vary proportionately. This is due to the fact that in the concentration range from 0 to 10% ZnSe, the width of the spectrum increases markedly, reaching a maximum for a selenide content between 3 and 5%. The width of the band remains constant for a selenide content in excess of 10%.

The anomalies which we pointed out in the shift of the maxima and in the change in width of the spectral distribution curve forced us to the following assumption: For a ZnSe concentration range from 0 to 10%, two bands appear in the spectrum at room temperature. These are not separated, due to the closeness of the maxima and relatively large width. The selenium band is brought clearly into evidence in spectra obtained at a raised temperature when the zinc band suffers temperature quenching. As an example we show in Fig. 3 the spectra obtained at room temperature and at +120°C from two samples. These spectra correspond to strong excitation (the distance from the lamp is 15 cm).

In phosphors containing from 1 to 20% ZnSe, a rise in temperature shifts the maximum by 25-30 mμ toward longer wavelengths. The largest displacement occurs in phosphors with a ZnSe content of 1 to 10%. (See Fig. 3, curves 1 and 2.) This is precisely the range of concen-

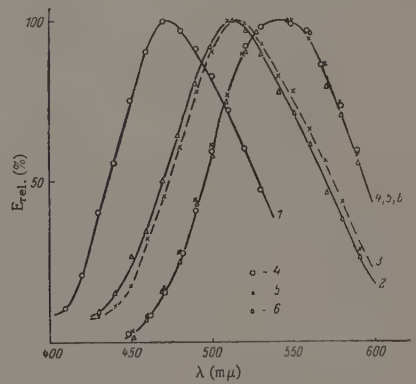

Fig. 3. The selenium band made apparent in the spectra of ZnS-ZnSe phosphors (maximum excitation). Content of ZnSe: curves 1, 2, and 3—1%; curves 4, 5, and 6—20%. Type of emission and temperature (in °C): curves 1 and 4—luminescence (20); curves 2 and 5—luminescence (120); curves 3 and 6—afterglow (20).

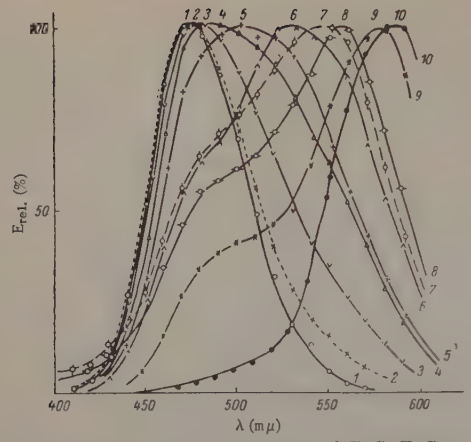

Fig. 4. Luminescence spectra of ZnS-ZnSe phosphors at −196°C at maximum excitation. Content of ZnSe (in %): curve 1—0; curve 2—1; curve 3—3; curve 4—5; curve 5—8; curve 6—10; curve 7—20; curve 8—30; curve 9—50; curve 10—75.

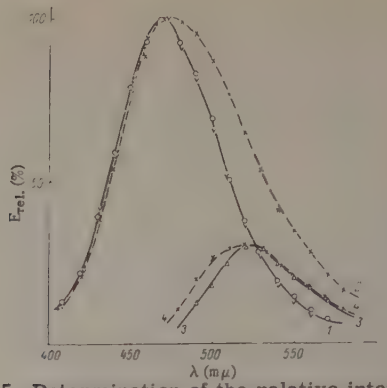

Fig. 5. Determination of the relative intensities of the zinc and selenium bands in the spectrum of a ZnS-ZnSe phosphor. Curve 1—ZnS:Zn; curve 2—ZnS(99%)-ZnSe(1%) at 20°C and for weak excitation; curve 3—difference in the ordinates of curves 1 and 2; curve 4—ZnS(99%)-ZnSe(1%) at 120°C (normalized according to the maximum of curve 3).

trations in which the abovementioned anomalies in the spectra obtained at room temperature forced us to assume the existence of two bands.

In phosphors with a ZnSe content in excess of 20%, the spectra obtained at room temperature and at +120°C practically coincide. (See Fig. 3, curve 4.)

Thus, studies at a raised temperature confirm the existence of a new band in the spectrum of ZnS-ZnSe phosphors. This band is specifically tied in to the introduction of the selenide. It is possible to bring out the long wavelength band which exists in the spectrum of self-activated ZnS-ZnSe phosphors at room temperature as well, by observing the afterglow spectra. We obtained afterglow spectra in ZnS-ZnSe phosphors with a ZnSe content up to 30%. (For larger amounts of the selenide, the duration of the afterglow falls sharply.) In order to observe the afterglow spectra, we used the Wood phosphoroscope. The spectrum was recorded 0.5 sec after the termination of excitation.

The results for phosphors containing 1 and 20% respectively, of ZnSe are shown in Fig. 3 (curves 3 and 4). The same figure shows, for the sake of comparison, the spectra of these respective phosphors obtained at room temperature under strong excitation as well as at a raised temperature. It is easily seen that at 1% ZnSe concentration the afterglow spectra and the spectra obtained at +120°C coincide within the limits of experimental error and consist of a single selenium band. For the 20% ZnSe concentration there is a complete coincidence of all the spectra, i.e., those obtained at 120°C, at room temperature during excitation, and in the afterglow. This indicates that, starting with 20% ZnSe, the spectrum consists only of a single selenium band already at room temperature.

Figure 4 shows the spectra of the ZnS-ZnSe phosphors at liquid nitrogen temperature (−196°C), which have been normalized according to the maximum.

It is easily seen that two bands are clearly pronou in the spectrum. The zinc band is still much apparent 50% ZnSe, and traces of it appear even at 75% selenide content.

As indicated earlier,[5,6] at −196°C the maximum of the zinc band is shifted toward longer wavelengths. In our experiments the displacement amounts to about 6 (See Fig. 4.) A comparison of curves 9 and 10 of Figs. and 4 shows that the selenium band is also shifted towa longer wavelengths. The best separation of the bands a low temperature is caused by a stronger displacement the selenium band (by 10 mμ).

The results described above indicate that two banc exist in the spectrum of the ZnS-ZnSe phosphors, nam a zinc band and a band specifically connected with the troduction of the selenide. The spectral curves with si gle maxima observed under orginary conditions may b separated out into components, the intensities of which may be determined. For this purpose the data given above concerning the shape and position of the two ban may be used. (See Fig. 5.)

REFERENCES

1. L. Wesch, Chem. Ber. 7, 3 (1942).
2. A. A. Bundel', Doctoral Dissertation, Moscow State Univ., 1956.
3. H. W. Leverenz, "An Introduction to Luminescence of Solids," Wiley, New York, 1950.
4. H. A. Klasens, J. Electrochem. Soc. 100, 72 (1953).
5. G. R. Fonda, J. Opt. Soc. Am. 12, 917 (1952).
6. L. Drozd, Izvest. Akad. Nauk SSSR., Ser. Fiz. 23, 1300 (1959).

OPTICAL PROPERTIES OF BERYLLIUM IN THE INFRARED SPECTRAL REGION

I. N. Shklyarevskii and R. G. Yarovaya (pp. 661-666)

Received 26 December 1960

The optical constants, Hall constant, and static conductivity of vacuum-deposited layers of beryllium were measured in the 0.8-11 μ region at 290 and 82°K. It was found that the properties of beryllium in the indicated spectral region are determined entirely by free current carriers. Using the formulas of the normal skin effect, and taking account of the quantum character of the interaction of free carriers with the infrared radiation, the concentration, effective mass, and frequency of collisions among carrier particles were determined. It was shown that the temperature dependence of the optical properties of beryllium is determined by the frequency of these collisions.

Most of the experimental metallo-optical investigations of the last several years have been devoted to checking the theory of the anomalous skin effect. It is natural that metals with high conductivity (copper, silver, gold and aluminum) were selected as objects for such investigations. The anomalous nature of the skin effect in these metals is well defined, even at room temperature. In order to compare the anomalous skin effect with the theory, it is essential that the effective frequency of electron collisions be negligible compared to the frequency of the electromagnetic oscillations. It seems that, for a number of metals, this condition is not met in the infrared region of the spectrum. However, if the skin effect in which a metal is normal, it is still possible, in principle, to determine the electronic characteristics even when the electron collision frequency is not low.

This work is dedicated to the determination of the optical characteristics of beryllium according to the theory of normal skin effect.

EXPERIMENTAL RESULTS

Nontransparent layers of beryllium were prepared by the vacuum evaporation of beryllium from a tungsten crucible. Beryllium, purified by repeated vacuum distillation, served as the starting material.

Optical measurements in the 0.8-11 μ region were obtained with a ZMR-2 monochromator according to the Avery[1] method. The radiation incident on the sample was first linearly polarized at an azimuth of 45°. This eliminated the polarization effect of the equipment.[2] The indices of refraction μ and absorption $\mu\chi$ were calculated analytically by the method of Noskov et al.[3]

The mean values of μ and $\mu\chi$ for several samples are given in Table 1. The corresponding dispersion curves are given in Fig. 1, in which the optical constants measured at room temperature are marked by open circles. Measurements of the optical constants of beryllium obtained by other polarization methods[4,5] gave identical results. Over the entire region of the spectrum investigated, the indices of refraction were measured with an accuracy of 7-12% and the indices of absorption, with an accuracy of 5-7%.

Table 1

λ (μ)	μ	$\mu\chi$	λ (μ)	μ	$\mu\chi$
0.8	2.7	2.8	4	5.0	12.2
0.9	2.7	2.9	5	6.85	14.3
1.2	2.4	3.5	6	8.0	15.4
1.5	2.4	4.7	7	9.1	17.1
2	2.5	5.8	8	11.0	19.1
2.5	2.75	7.25	9	11.4	18.6
3	3.45	9.0	10	11.9	20.0
3.5	3.9	10.8	11	11.9	21.1

A cryostat which has been described previously[6] was used for the low temperature measurements. At 82°K, the shape of the dispersion curves remains the same, except at the longest wavelengths, where some decrease in the index of refraction is observed. This decrease, however, does not exceed the limits of error of the measurements (dark circles on Fig. 1).

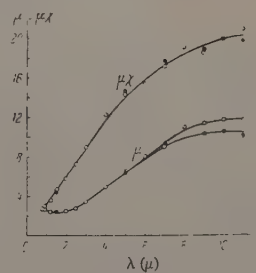

Fig. 1

Using the same samples, the Hall constant R_x and the static conductivity σ_0 were measured. The measurements were performed by means of compensating circuits which eliminate the influence of contacts. The following values were obtained: $R_x = 5.6 \times 10^{-3}$ cgsm and $\sigma_0 = 1.3 \times 10^4$ ohm^{-1} cm^{-1} (hole-type conductivity).

PRELIMINARY REMARKS

In order to draw any conclusions from the dispersion curves concerning the electron properties of metals, it is first necessary to explain qualitatively whether they are determined by free carriers or whether an internal photoeffect occurs. It is more convenient to start from the calculated dependence of the real component of the dielectric constant on $1/\omega^2$ (Fig. 2, curve 1), and the dependence of the absorption A on ω^2:

$$\mathrm{Re}\,\varepsilon = \mu^2 - (\mu\chi)^2, \tag{1}$$

$$A = \frac{4\mu}{(\mu + 1)^2 + (\mu\chi)^2}. \tag{2}$$

The depth of field penetration for beryllium ($\delta = \lambda/2\pi\mu\chi$) is approximately 8×10^{-6} cm. The mean free path of the holes in the beryllium monocrystal, as de-

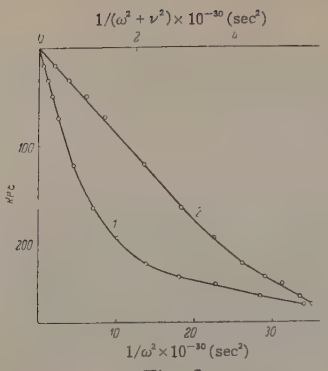

Fig. 2

termined by galvanomagnetic measurements,[7] is 1×10^{-5} cm. A significantly shorter path length can be expected in a film, due to its high degree of disperseness. Consequently, an intermediate skin effect occurs. Therefore, the formulas of either the normal or the anomalous skin effect can be used with equal justification.

For the normal skin effect, the following expressions are valid for free carriers in the infrared:

$$\mathrm{Re}\,\varepsilon = \varepsilon_0 - \frac{4\pi Ne^2}{m^*(\omega^2+\nu^2)}; \qquad (3)$$

$$A = \frac{2\nu}{\sqrt{\frac{4\pi Ne^2}{m^*}}}, \qquad (4)$$

where ε_0 is the static dielectric constant of the metal, N is the concentration of current carriers, ω is the frequency of the incident radiation, ν is the total frequency of electron collisions, m* is the effective mass, and e is the electron charge.

For typical metals, $\nu^2 \ll \omega^2$ in the infrared region. Re ε is therefore a linear function of $1/\omega^2$. Evidently, the absorption A does not depend on the frequency, but a linear dependence of A on ω^2 can be expected, if the quadratic dependence of the collision frequency on the frequency of the infrared radiation is taken into consideration. This dependence, found by Gurzhi[8] and Pitaevskii,[9] can be written

$$\nu = \nu_{\mathrm{coll.}} + \nu_0^{ee}\left(\frac{\hbar\omega}{2\pi kT}\right)^2, \qquad (5)$$

where

$$\nu_{\mathrm{coll.}} = \nu^{ed} + \nu^{ef} + \nu_0^{ee}, \qquad (6)$$

and ν^{ed} and ν^{ef} are the frequencies of the electron collisions with defects and phonons respectively, and ν_0^{ee} is the classical frequency of collisions among the electrons themselves. It is seen from Fig. 3 that such a dependence is observed for beryllium.

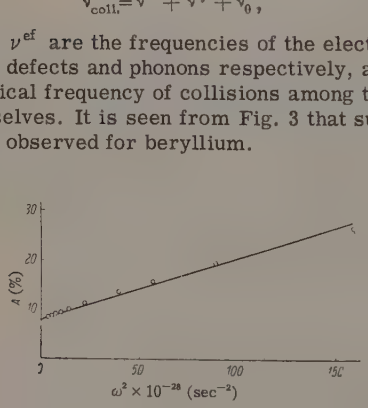

Fig. 3

For Re ε, the linear dependence occurs in the sh wavelength region of the spectrum investigated. With creasing wavelength, this dependence changes fairly rapidly into another straight line with a much lower s It can be shown that this trend of Re ε follows qualita tively from expression (3) if ν is comparable to ω a if they are connected by relation (5). There are there good grounds for believing that the observed dispersi curves of beryllium are determined by the free curre carriers.

A comparison of the present values of the Hall co stant and static conductivity with the published data is very difficult, due to the large differences among the sults of different authors. Apparently both quantities are strongly dependent on the purity of the beryllium. Our value of R_x is 5.6×10^{-3} cgsm. The same quanti according to Borovik's[7] data is 7.7×10^{-3}; earlier re sults[10] give 2.4×10^{-3}. The disagreement among data the conductivity of beryllium is just as great. Howeve in refs. 7 and 11, better agreement was obtained at 0° 29×10^4 and 27.9×10^4 ohm^{-1} cm^{-1} respectively. Th conductivity of the films of beryllium investigated is more than twenty times smaller. As will be shown la this divergence is fully explained by the sharp decrea in the free path carriers in the film caused by its hig degree of disperseness.

DETERMINATION OF MICROCHARACTERISTICS O BERYLLIUM

Without any assumptions about the magnitude of t frequency of electron collisions, this frequency can b calculated in the following manner. The imaginary co ponent of the dielectric constant can be calculated fro the experimental values of μ and $\mu\chi$.

$$\mathrm{Im}\,\varepsilon = 2\mu\cdot\mu\chi = \frac{4\pi Ne^2\nu}{m^*(\omega^2+\nu^2)\omega}.$$

It is easy to see that if $\varepsilon_0 \ll 4\pi Ne^2/m^*(\omega^2+\nu^2)$, (7) divided by (3) and multiplied by ω gives the follo expression for the collision frequency

$$\frac{2\mu\cdot\mu\chi\omega}{\mu^2-(\mu\chi)^2} = \nu = \nu_{\mathrm{coll.}} + \nu_0^{ee}\left(\frac{\hbar\omega}{2\pi kT}\right)^2.$$

Expression (8) as a function of ω^2 should give a straight line, which at $\omega = 0$ gives the value of $\nu_{\mathrm{coll.}}$; slope permits us to find ν_0^{ee}. For beryllium, the real component of ε becomes zero at $\lambda \approx 0.7\,\mu$; for calcul the frequency of collisions, we therefore used data be ginning at $2.5\,\mu$ (this permitted us to neglect ε_0). The corresponding dependence is given in Fig. 4. The col sion frequencies appear to be: $\nu_{\mathrm{coll.}} = 3.6 \times 10^{14}$ sec^{-1} $\nu_0^{ee} = 3.1 \times 10^{13}$ sec^{-1}. When $\lambda \approx 5\,\mu$, $\omega = \nu_{\mathrm{coll.}}$. The as sumption that $\nu \approx \omega$, which was based on the qualitati examination of the dispersion curves, appears to be c rect.

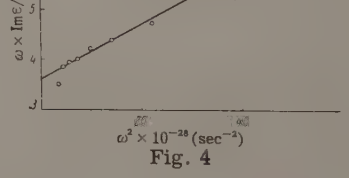

Fig. 4

Figure 2 (curve 2) shows the dependence of Re ε on $/(\omega^2 + \nu^2)$. The small deviation from linearity observed the longest wavelengths may be caused by a small de- ation of the skin effect from its normal character. he shape of the curves in Figs. 2 and 3 indicates the ab- nce of any internal photoeffect over the entire spectral gion investigated.

The ratio N/m*, as determined from the slope of ne 2 of Fig. 2, is 1.9×10^{49} gm^{-1} cm^{-3}. On the other nd, the concentration of carriers found from Hall's con- ant is $N = 1.1 \times 10^{22}$ cm^{-3}; this gives $m^*/m = 0.64$. Our easurements of the Hall constant and optical constants beryllium in the infrared permitted us to calculate a mber of microcharacteristics, which are presented in able 2.

Table 2

N/m* × 10^{-49} (gm^{-1} cm^{-3})	N × 10^{-22} (cm^{-3})	m*/m	$\nu_0^{ee} \times 10^{-13}$ (sec^{-1})	$\nu_{coll.} \times 10^{-14}$ (sec^{-1})
1.9	1.1	0.64	3.1	3.6

ISCUSSION OF THE RESULTS

On the basis of a measurement of the electronic heat pacity, a value of $m_t^*/m = 0.46$ was obtained in ref. 12. owever, it must be remembered that it is only when the ermi surface of a given metal is a sphere that the effec- ve mass entering into optical characteristics generally incides with m_t^*, which is determined from the elec- onic heat capacity.[13] In the opposite case, the ratio $^*/m^*$ can be either smaller or greater than unity, de- nding on the degree of zone overlapping and on the isotropy of the Fermi surface. Since the optical and ectronic heat capacity measurements were made on fferent samples, the m_t^*/m^* value cannot be considered gnificant. However, for beryllium, whose conductivity due only to the overlapping of zones, the inequality $^*/m^* < 1$ must be satisfied.

The very low temperature dependence of the optical nstants of beryllium is understandable, if the values $\nu_{coll.}$ and ν_0^{ee} obtained above are taken into considera- on. Since $\nu_0^{ee} \sim (kT)^2$,[8] the frequency-dependent term in does not change with temperature. In $\nu_{coll.}$, not only ^{e} but ν^{ef} also appears to be temperature dependent. he shape of this function in the infrared depends on the elation between the temperature of the experiment and e Debye temperature of the metal. The Debye tempera- re of beryllium is $\theta = 1000°$, so that both temperatures, 90° and 82°K, are considerably lower than θ. At $\hbar\omega \gg$ $\gg kT$, $\nu^{ef} = 0.4\nu_0^{ef}(\theta)$, where $\nu_0^{ef}(\theta)$ is the classical fre- uency of electron-phonon collisions at the Debye tem- erature. Considering that in the case investigated $^{ed} \gg \nu^{ef}$ (as is seen by comparing the values of σ_0 for monocrystal of beryllium and the film investigated), it becomes evident that the temperature dependence of the optical properties is completely determined by the change in ν_0^{ee}. However, this term is only about 10% of $\nu_{coll.}$. Consequently, a temperature dependence can be observed only for the longest wavelengths, where $\nu_{coll.} \gg \nu_0^{ee}(\hbar\omega/2\pi kT)^2$.

Since we know the values of $\nu_{coll.}$ and N/m*, which were determined from optical measurements, the static conductivity of beryllium can be calculated from the following formula

$$\sigma_0 = \frac{Ne^2}{m^*\nu_{coll.}}. \qquad (9)$$

Of course, the frequency of electron-phonon collisions is different in static and high frequency fields. In the former, it is simply equal to the classical frequency $\nu_0^{ef}(T)$; in the latter, as previously indicated, it is $\nu^{ef} = 0.4\nu_0^{ef}(\theta)$. However, remembering that for a layer of beryllium $\nu^{ed} \gg \nu^{ef}$, we can neglect the difference in ν^{ef}. The value of the static conductivity calculated from formula (9) is in excellent agreement with the measured value. This permits us to state that the current carriers in beryllium are similarly scattered by defects in both static and high frequency fields. The results obtained also confirm our assumption that the very low conductivity of the beryllium film can be explained by the large number of disturbances in the periodicity of the lattice.

REFERENCES

1. D. G. Avery, Proc. Phys. Soc. **B65**, 425 (1952).
2. I. N. Shklyarevskii, A. A. Avdeenko, and V. G. Padalka, Opt. i Spektr. **6**, 528 (1959), Optics and Spectroscopy **6**, 336 (1959).
3. L. A. Afanas'eva, M. M. Noskov, and V. I. Cherepanov, Fiz. Metal. i Metalloved., Akad. Nauk SSSR, Ural. Filial **1**, 566 (1955).
4. G. K. T. Conn and G. K. Eaton, J. Opt. Soc. Am. **44**, 477 (1954).
5. I. N. Shklyarevskii and V. K. Miloslavskii, Opt. i Spektr. **3**, 361 (1957).
6. V. G. Padalka and I. N. Shklyarevskii, Opt. i Spektr. **9**, 119 (1960), Optics and Spectroscopy **9**, 63 (1960).
7. E. C. Borovik, Doct. diss., Fiz. Tekh. Inst., Akad. Nauk SSSR (1954).
8. R. N. Gurzhi, Cand. diss., Fiz. Tekh. Inst., Akad. Nauk SSSR (1957).
9. L. P. Pitaevskii, Zhur. Eksptl. i Teoret. Fiz. **34**, 947 (1958), Soviet Phys.-JETP **7**, 655 (1958).
10. A. Ciccone, Nuovo cimento **10**, 339 (1933).
11. F. Grueneisen and H. Adenstadt, Ann. Physik **32**, 211 (1938).
12. R. W. Hill and P. L. Smith, Phil. Mag. Ser. 7, **44**, 636 (1953).
13. M. H. Cohen, Phil. Mag. Ser. 8, **3**, 762 (1958).

THE SENSITIVITY THRESHOLD FOR OPTICAL ABSORPTION ANALYSIS OF THE COMPOSITION OF LIQUID OR GASEOUS MIXTURES

A. O. Sall (pp. 667-671)

Received 16 December 1960

The problem of the sensitivity threshold for optical absorption analysis of the composition of liquid or gaseous mixtures (which is based on the absorption of radiation by the component to be determined in the mixture) is discussed. Examples of calculations are given.

The sensitivity threshold for the absorption analyzer (the minimum detectable change in concentration of the analyzed component in the mixture) depends on the spectral intensity of the source of radiation, the sensitivity of the receiver, and the scheme of measurement, as well as on the absorption spectrum of the analyzed component. Let us formulate the dependence of the sensitivity threshold on the parameters characterizing the principal construction design of the absorption meter and on the parameters characterizing the intensity of absorption of the radiation by the analyzed component.

The minimum registrable change in the radiation beam in a double-beam absorption analyzer of liquid or gaseous mixtures exceeds the sensitivity threshold of the radiation receiver which is used in it. This can be explained in the first place by the uncontrollable random and unequal changes in the compared beams of radiation. These changes are caused by fluctuations in the voltage of the outside source of energy, by changes in the surrounding temperature, and by aging of the elements of the absorption meter during the time elapsing between periodic checks on it, as well as by the fluctuation in the number of quanta entering the receiver. The residual zero signal in the absorption meters on blocking off the beams also limits their sensitivity. Besides, the scheme of measurements in the automatic self-recording absorption meter usually involves limitations which make it impossible to measure small changes in the beam when the background radiation is intense. Therefore the ratio of the minimum registrable change in the radiation beam traversing the analyzed mixture to the magnitude of one of the two compared beams may be put equal to $\sqrt{\gamma^2 + \alpha^2}$, where γ is the ratio of the sensitivity threshold to the magnitude of one of the radiation beams, while α is a numerical coefficient which characterizes the magnitude of a possible unequal change in the compared beams and takes into consideration the possibility of registering small changes in the beam on the background of the compared beams.[1] Let us define the sensitivity threshold Δc of the absorption meter as such a change in the concentration of the component to be determined in the analyzed mixture for which the corresponding relative decrease in the beam traversing the analyzed mixtures equals $\sqrt{\gamma^2 + \alpha^2}$. The absorption coefficient $\kappa(\nu)$ of the analyzed component depends on the selection of the frequency ν. If, in carrying out the analysis, we select only a narrow region of the spectrum in which the absorption coefficient of the analyzed component has its maximum value equal to $\kappa_{max.}$, we obtain $\kappa_{max.} L \Delta c = \sqrt{\gamma^2 + \alpha^2}$ where L is the length of the path of the beam in the absorption chamber. In order to generalize this expression to the case of a nonmonochromatic beam, let us multiply the right side by the coefficient b, then

$$\Delta c = \frac{b\sqrt{\gamma^2 + \alpha^2}}{\kappa_{max.} L},$$

where

$$b = \frac{\kappa_{max.} \int J s d\nu}{\int J \kappa s d\nu}.$$

Here $J(\nu)$ is the spectral intensity of the compared beams and $s(\nu)$ is the spectral sensitivity of the receiver.

The length of the path L in the layer of the analyz mixture and the parameter α are determined by the d sign and construction of the absorption meter and do n depend on the absorption spectrum of the analyzed com ponent. The ratio γ depends on the intensity of the sou of radiation and the sensitivity threshold of the receiv The parameter b, as we shall see later, depends esse tially on the design and construction of the absorption meter. Its dependence on the absorption spectrum of t analyzed component is much less important. The expression (1) has a sufficiently simple form and for all practical purposes its utilization for the investigation problems concerned with the sensitivity threshold of th absorption meter does not meet any serious obstacles. This will become evident from a study of the following examples.

Example 1. To begin with, let us calculate the sen tivity threshold for the infrared spectrophotometer wit monochromator which is being used for the analysis of gases. If the radiation traversing the analyzed mixture on its way to the receiver were contained in a narrow spectral interval considerably smaller than the line wi of the analyzed component, then, neglecting the existen in the beam of any ballast radiation dispersed by the monochromator, we would have b = 1. As the width of spectral interval is increased, the value of b is increa For the quantitative estimate of the value of b, the wid of the spectral interval determined by the monochroma may be conveniently evaluated according to the formul

$$(\Delta\nu)_{mon.} = [J(\nu') s(\nu')]^{-1} \int J(\nu) s(\nu) d\nu,$$

in which the integration is over the whole spectral inte val determined by the monochromator (ν' is the wave number corresponding to the center of the most intens absorption line). If the distance between the lines is c siderably greater than $(\Delta\nu)_{max.}$ then, using the well kn Lorentz formula for the contour of the absorption band we obtain

$$b = \frac{\kappa_{max.} \int J s d\nu}{J(\nu') s(\nu') \int \kappa d\nu} \approx \frac{(\Delta\nu)_{mon.}}{\int_{-\infty}^{+\infty} \frac{(\Delta\nu)_L^2 dx}{x^2 + (\Delta\nu)_L^2}} = \frac{(\Delta\nu)_{mon.}}{\pi (\Delta\nu)_L},$$

where $(\Delta\nu)_L$ is the half-width of the absorption band.

Taking $(\Delta\nu)_{max.} = 1\ cm^{-1}$ and $(\Delta\nu)_L = 0.1\ cm^{-1}$ we find $b \approx 3$.

Example 2. Let us determine the numerical value of the coefficient b for an optico-acoustical gas analyzer.[2-4] To decrease the sensitivity threshold in the double-beam absorption meter with $\gamma \ll \alpha$ it is necessary to decrease γ_0. Hence the nonselective absorption of radiation is decreased by means of the window and the wall of the radiation receiver chamber of the optico-acoustical receiver.[1] Also, the product of the depth of the radiation receiving chamber and the concentration of the absorbing component in it and the maximum value of the absorption coefficient $\kappa_{max.}$ is made less than unity. In this case for the spectral sensitivity of the optico-acoustical receiver, taking into consideration the radiation by the gas and by the walls of the radiation receiving chamber[5] we have:

$$s(\nu) \approx 1 - e^{-\kappa w} + s_2(\nu) \approx \kappa w - 0.5(\kappa w)^2 + s_2(\nu),$$

where w is the product of the length of the path of the beam in the radiation receiving chamber of the optico-acoustical receiver and the concentration of the analyzed component in it, while $s_2(\nu)$ is the spectral sensitivity determined by the absorption of radiation by the walls of the radiation receiving chamber.[5] Making use of this relationship and expression (2) we obtain

$$b \approx \frac{\kappa_{max.}\left[\left(\int J\kappa d\nu\right) w + \left(\int Js_2 d\nu\right)\right]}{\left(\int J\kappa^2 d\nu\right) w - 0.5\left(\int J\kappa^3 d\nu\right) w^2}$$

$$\approx b_0\left[1 + \left(\frac{\int Js_2 d\nu}{\int J\kappa d\nu}\right)\frac{1}{w} + 0.5\left(\frac{\int J\kappa^3 d\nu}{\int J\kappa^2 d\nu}\right) w\right]$$

$$\geq b_0\left[1 + \sqrt{\frac{2}{b_0(1-\delta_0)}\left(\frac{\kappa_{max.}\int Js_2 d\nu}{\int J\kappa d\nu}\right)}\right] \qquad (4)$$

where

$$b_0 = \frac{\kappa_{max.}\int J\kappa d\nu}{\int J\kappa^2 d\nu}, \qquad (5)$$

$$\delta_0 = 1 - \left(\int J\kappa^2 d\nu\right)^2\left(\int J\kappa d\nu\right)^{-1}\left(\int J\kappa^3 d\nu\right)^{-1}. \qquad (6)$$

The minimum value b_0 appearing on the right side of the inequality (4) corresponds to the

$$w \approx \sqrt{\frac{2\left(\int Js_2 d\nu\right)\left(\int J\kappa^2 d\nu\right)}{\left(\int J\kappa d\nu\right)\left(\int J\kappa^3 d\nu\right)}}. \qquad (7)$$

If the absorption band of the analyzed component consisted of the lines of equal intensity, then, assuming that the contours of the band follow the dispersion formula of Lorentz, we would have

$$b_0 \approx \frac{\kappa_{max.}\int \kappa d\nu}{\int \kappa^2 d\nu} \approx \frac{\int_0^\infty \frac{(\Delta\nu)_л^2}{(\Delta\nu)_л^2 + x^2} dx}{\int_0^\infty \left[\frac{(\Delta\nu)_л^2}{(\Delta\nu)_л^2 + x^2}\right]^2 dx} = 2. \qquad (8)$$

The absorption band, however, actually consists of lines of different intensities. In addition to the most intense line in the center, of which the absorption coefficient equals $\kappa_{max.}$, there exist in the band a large number of weak lines. This leads to an increase in the value of the coefficient b_0. For diatomic and linear polyatomic molecules the numerical value of the coefficient b_0 still does not usually exceed 3-4.[1]

As was indicated by the approximate calculations, the numerical value of δ_0 for diatomic and linear polyatomic molecules usually lies between 0.4 and 0.5. The spectral sensitivity $s_2(\nu)$ may be made considerably smaller than 10^{-5}.[5] In this case usually $\kappa_{max.}\int Js_2 d\nu \ll \int J\kappa d\nu$. Taking into consideration this inequality and utilizing the numerical values obtained above for δ_0 and b_0 we obtain $b \approx b_0$. In other words, the decrease in the sensitivity of the gas analyzer due to the ballast absorption by the walls of the radiation receiving cylinder may in practice be completely excluded. In the same way, the effect of the ballast absorption by the window of the radiation receiving cylinder, as well as the effect of the admixtures of the interfering components which are found in the optico-acoustical receiver, may be excluded.[5]

Example 3. Let us evaluate the sensitivity threshold of the optico-acoustical gas analyzer designed for the estimation of carbon monoxide. Taking into consideration that for carbon monoxide $\kappa_{max.}/b \approx 0.02\ (mm\%\ CO)^{-1}$, and taking $\gamma \ll \alpha = 10^{-3}$,[4,6] and $L = 100$ mm we obtain $\Delta c = 5 \times 10^{-4}\%CO$.

Example 4. The ability of the optico-acoustical receiver of radiation, which is used in the gas analyzer, to select the region of the spectrum necessary for the analysis may be quantitatively evaluated as follows. Let us select a monochromator such that in its utilization in the absorption meter with the nonselective receiver, the numerical value of b would be the same as for the optico-acoustical gas analyzer. Let us determine the magnitude of $(\Delta c)_{mon.}$ that will satisfy this condition. Using expression (3) we shall obtain $(\Delta\nu)_{mon.} = b\pi(\Delta\nu)_L$. Thus, in the abovementioned sense, the optico-acoustical receiver of radiation may be looked upon as a spectroscopic instrument with $(\Delta\nu)_{o.a.i.} = b\pi(\Delta\nu)_L$. Putting $b = 4\pi$, $(\Delta\nu)_L = 0.1\ cm^{-1}$, we find $(\Delta\nu)_{o.a.i.} \approx 1.2\ cm^{-1}$.

Example 5. Using expressions (1) and (2) it is possible to estimate quantitatively the dependence of the sensitivity threshold on the intensity of absorption of radiation by the analyzed component. Let us first discuss the case when $\gamma \gg \alpha$. Using (1) and (2) it may be shown that the sensitivity threshold in this case is inversely proportional to $\int J\kappa s d\nu$. If within the limits of the absorption band of the analyzed component useful in the analysis the magnitude $J(\nu)s(\nu) \approx$ const., then the sensitivity threshold is inversely proportional to $\int \kappa d\nu$, where the integration is carried over the limits of the selected spectral interval. This takes place, for example, in the case of infrared gas analyzer with gaseous moldulation.[5,6]

In the other limiting case when $\gamma \ll \alpha$ the sensitivity threshold is proportional to the ratio $b/\kappa_{max.}$. The absorption coefficient $\kappa_{max.}$ for the various analyzed components in various regions of the spectrum has numerical values differing from each other by several orders of magnitude. As we have seen above, with a rational selection of the optical design and construction of absorption meter the coefficient b usually lies within the limit from unity to several units. Therefore, in the first approximation, we may consider the sensitivity threshold to be inversely proportional to the maximum value of the absorption coefficient, within the accuracy of one order of magnitude.

Example 6. Let us now investigate the dependence of the sensitivity threshold on the duration of measurement t (the duration of analysis). With an increase in the length of the path of the beam L in the working chamber, the volume V_p of the latter becomes so large in the limit that the duration of the analysis t is determined by the time necessary for the practically complete replacement

of the analyzed mixture in the working chamber. The time t and the volume consumption W of the analyzed mixture per unit of time must be such that the product Wt must be at least several times greater than V_p. Let us define $h = WtV_p^{-1}$. For ordinary chambers with a single path in the beam, V_p is approximately equal to the product of the surface area of the window S and L. In the industrial automatic self-recording double-beam absorption meters, the length of whose working chambers is not too large, $\gamma \ll \alpha$ usually.[1] Since α and h in this case are practically independent of t, the sensitivity threshold is inversely proportional to t. Taking $S = 3$ cm^2, $\kappa_{max.}/b = 0.02$ (mm%)$^{-1}$; $h = 5$, $W = 0.5$ liter/min, $\alpha = 10^{-3}$, and $t = 1$ min we shall obtain $L = Wt(hS)^{-1} = 300$ mm and $\Delta c = 10^{-3}/0.02 \times 300 \approx 2 \times 10^{-4}$%. In order to increase the sensitivity of the absorption meter the analyzed mixture is compressed.[7] This may be taken into account in the calculation of the sensitivity threshold by multiplying $\kappa_{max.}$ by a corresponding number (in the first approximation by the same number as the factor for the increase in pressure). With a pressure of the analyzed mixture of the order of 10 atm, taking $L = 10^4$ mm,[7] $\gamma \approx \alpha \approx 10^{-3}$, $\kappa_{max.}/b = 0.2$ (mm%)$^{-1}$, we have $\Delta c \approx 10^{-6}$%. However, the analysis in this case lasts for several tens of minutes.[7] Thus, a considerable increase in the sensitivity of the gas analyzer is accompanied by a significant increase in the duration of measurement.

In single-beam absorption meters with modulation of the quantity of the analyzed component in the path of the beam,[5] $\gamma \gg \alpha$ usually. The length of the path of the beam L increases practically proportionally with the volume of the chamber V_p, i.e., proportionally with t. With an increase in t the value of γ decreases usually inversely proportionally to $\sqrt{t}$. Therefore, the sensitivit threshold is inversely proportional to $t^{1.5}$.

Example 7. Let us now find the condition for maximum sensitivity in a double-beam absorption meter. With sufficiently small L, $\gamma \ll \alpha$ usually. In this case an increase in L results in a decrease of the sensitivity threshold Δc which is inversely proportional to L. In the other limiting case of such large L that $\gamma \gg \alpha$, an increase in L results in a faster increase of γ. At the same time Δc increases with the increase in L (proportionally with the ratio γ/L). Therefore, the maximur sensitivity of the absorption meter corresponds to such a value of L for which γ is of the same order of magnitude as α.

REFERENCES

1. A. O. Sall, Priborostroenie No. 9, 12 (1956).
2. M. L. Veingerov, Doklady Akad. Nauk SSSR **19**, 687 (1938); Zavodskaya Lab. **13**, 426 (1947).
3. I. V. White, J. Opt. Soc. Am. **32**, 285 (1942).
4. V. A. Pavlenko, Modern gas analyzers, in "Collection New Thermo-Energetical Instruments and Regulators State Scientific Technical Press for Machine Construction Literature, 1953; Zavodskaya Lab. **20**, 7 (1954).
5. A. O. Sall, Zhur. Tekh. Fiz. **29**, 330 (1959), Soviet Phys.-Tech. Phys. **4**, 295 (1959).
6. A. O. Sall, Opt. i Spektr. **6**, 394 (1959); Optics and Spectroscopy **6**, 247 (1959).
7. Proc. Instr. Soc. Am. **2**, 97, 103 (1956).
8. Ya. I. Gerlovin and P. V. Slobodskaya, Zavodskaya Lab. **25**, 303 (1959); Opt. i Spektr. **7**, 105 (1959), Optic and Spectroscopy **7**, 63 (1959).

THEORY OF THE SELECTIVITY OF OPTICAL ABSORPTION ANALYZERS FOR THE COMPOSITION OF GASEOUS OR LIQUID MIXTURES. I

A. O. Sall (pp. 672-678)

Received 24 September 1960

Results are presented of an investigation of the selectivity of absorption analyzers for the composition of mixtures of gases or liquids which are based on the absorption of radiation by the component to be determined in the analyzed mixture. Various methods of increasing the selectivity of nondispersive analyzers are discussed.

INTRODUCTION

The principle of the simplest double-beam absorption analyzer (see the diagram) consists of the following. The radiation from the source 1 is directed with the aid of reflectors 2 into two beams in one of which there is a working cell 3 filled with the mixture to be analyzed and in the other a comparison cell 4 filled with a standard mixture. The radiation having traversed both cells falls on the radiation receiver 6 which reacts to the difference in intensity of these two beams. If, in the mixture to be analyzed, the component which is being determined and which absorbs the radiation is absent, the compared beams have equal intensity and the pointer on the registering instrument 7 connected to the receiver reads zero. If the working cell is filled with the mixture to be analyzed, containing the component to be determined which absorbs the radiation, the receiver detects the difference of the compared beams and the magnitude of the detected signal is read directly on the dial graduated in units of concentration of the analyzed component.[1-9]

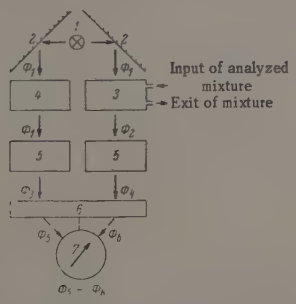

A schematic diagram of the differential absorption meter. The magnitudes of the radiation fluxes in different regions of the optical system are as follows:

$$\Phi_1 = \int_0^\infty I d\nu; \quad \Phi_2 = \int_0^\infty I e^{-\chi_M u_M} d\nu;$$

$$\Phi_3 = \int_0^\infty I e^{-\chi_M V_M} d\nu;$$

$$\Phi_4 = \int_0^\infty I e^{-\chi u - \chi_M u_M - \chi_M V_M} d\nu;$$

$$\Phi_5 = \int_0^\infty I e^{-\chi_M \Gamma_M} s d\nu;$$

$$\Phi_6 = \int_0^\infty I e^{-\chi u - \chi_M u_M - \chi_M V_M} s d\nu$$

The absorption analysis of mixtures of gases or liquids is often complicated by the presence in such mixtures of other components which are not being determined ("interfering components") but which also absorb radiation. To decrease the effect of variation in the composition of these components in the mixture on the results of analysis it is possible to make use of a spectral dispersion of the radiation beams which are being used for analysis in the laboratory instruments. The increase in selectivity of industrial infrared nondispersive absorption gas analyzers is achieved by means of a selective optico-acoustical receiver of the radiation or by means of a selective gas radiation source.[10,11] The application of the negative optico-acoustical effects for the analysis of gases[12-14] also results in an increased selectivity. In the ultraviolet and visible regions of spectra use is being made of selective gaseous discharge sources or of selective optico-acoustical receivers.[1,6,15] For the realization of selective analysis it is possible to modulate with a definite frequency the spectral intensity of both beams in that region of the spectra in which the analyzed component is absorbing. Such intensity modulation of the beam is achieved by a change in the number of molecules of the analyzed component in its path.[16] A periodic change in the thickness of the layer of the analyzed component found in the path of both beams may be attained by placing in their paths, besides the working cell and the comparison cell, also modulating cells with movable reflecting walls.[17] Vibrations of a thin reflecting elastic plate completely or partially made of a magnetic material are induced with the aid of an electromagnet by passing through its coil alternating electric current. With an increase in the magnetic field the plate is attracted by the electromagnet and with a decrease of the magnetic field it returns to its equilibrium position. The thickness of the layer of gas between the reflecting surface and the window is correspondingly changed.

For filtering of the beams (with the purpose of increasing the selectivity of the absorption meter) filter cells 5 (see the diagram), filled with a mixture of the interfering components, are also placed in the path of the beams.[2,4,7,20,21]

I. COEFFICIENT OF SELECTIVITY

Let us in the beginning discuss the magnitude of the error introduced by a change of the composition of the interfering components in the mixture. Let ν be the frequency, $I(\nu)$ the spectral intensity of the beams (identical in both beams of the analyzer), $s(\nu)$ the spectral sensitivity of the receiver, and $\kappa(\nu)$ the natural absorption coefficient of the analyzed component. Let u be the product of the concentration C of the analyzed component in the mixture and the length L of the working cell; let $\kappa_M(\nu)$

be the natural absorption coefficient of the interfering component, u_M the product of concentration C_M of the interfering component in the mixture and the length L of the working cell, and V_M the product of the concentration of the interfering component in the filter cell and its length. The selectivity of the absorption analyzer, whose principal scheme is represented in the diagram, may be estimated in the following way: having differentiated with respect to C and C_M the value of the signal

$$\int_0^\infty I e^{-\varkappa u - \varkappa_M u_M - \varkappa_M V_M} \, s d\nu,$$

resulting in the radiation receiver from the working beam, it is possible to find such values of ΔC and ΔC_M which result in the identical changes in the output signal of the radiation receiver. Let us define the coefficient of selectivity by the following expression

$$\frac{\Delta C_M}{\Delta C} = \frac{\int_0^\infty I e^{-\varkappa u - \varkappa_M u_M - \varkappa_M V_M} \varkappa s d\nu}{\int_0^\infty I e^{-\varkappa u - \varkappa_M u_M - \varkappa_M \Gamma_M} \varkappa_M s d\nu}. \qquad (1.1)$$

The formula given above holds equally for the absorption meter which measures directly the difference in intensity of the two beams as well as for the compensational absorption meter in which, with the help of a monitoring system and an optical shutter connected to it, the intensities of the beams are maintained equal to one another. The coefficient of selectivity does not depend on the type of the scale (linear or nonlinear) of the recording device of the absorption meter or on its construction or design.

If the monochromatic beam of radiation used for the analysis is so narrow that the specific absorption coefficients of the analyzed and the interfering components may be considered constant within the spectral interval used, then the formula (1.1) reduces to

$$\frac{\Delta C_M}{\Delta C} = \frac{\varkappa(\nu)}{\varkappa_M(\nu)}. \qquad (1.2)$$

In case the beam is not monochromatic, the selectivity coefficient depends on the concentration of the analyzed component in the mixture as well as on the length of the working cell. Let us discuss these relationships.

If the absorption spectra of the analyzed and of the interfering components do not in practice overlap but within the limits of the spectrum of the interfering component Is $\neq 0$, then with $\varkappa_M u_M \ll 1$ the relation (1.1) reduces to

$$\frac{\Delta C_M}{\Delta C} = \frac{1}{n} \cdot \left(\frac{\Delta C_M}{\Delta C}\right)_{u=0}. \qquad (1.3)$$

where

$$\left(\frac{\Delta C_M}{\Delta C}\right)_{u=0} = \frac{\int_0^\infty I e^{-\varkappa_M V_M} \varkappa s d\nu}{\int_0^\infty I e^{-\varkappa_M V_M} \varkappa_M s d\nu}, \qquad (1.4)$$

$$n = \frac{\int_0^\infty I e^{-\varkappa_M V_M} \varkappa s d\nu}{\int_0^\infty I e^{-\varkappa_M V_M - \varkappa u} \varkappa s d\nu}. \qquad (1.5)$$

The ratio of the integrals given in (1.4) represents the coefficient of selectivity which would have resulted with $\varkappa u \ll 1$. If the output signal of the radiation receiver is plotted versus the concentration of the analyzed component in the mixture,[18] then the coefficient[17] n may be determined as the ratio of the slope of the tangent at the origin of the scale (u = 0) to the slope of the tangent for that value of u for which the coefficient of selectivity is to be found. Let us call this ratio "the coefficient of nonlinearity of the absorption curve." The magnitude of n permits one to estimate quantitatively the deviation of the absorption curve from a straight line. Since the numerical value of the coefficient of nonlinearity increases with an increase in the concentration of the analyzed component in the mixture, the minimum selectivity will be observed at the end of the scale of the absorption meter. It can be shown that, in the case of strongly overlapping spectra, the coefficient of selectivit is also at its minimum at the end of the scale of the absorption meter. Therefore, the symbol C in formula (1.1) will be referred to in the future as standing for the maximum composition of the analyzed component in the mixture corresponding to the end of the scale of the analyzer. Let us investigate the dependence of the coefficien of selectivity on the length L of the working cell. As follows from formulas (1.3) and (1.5), with an increase in the length of the working cell (for a given concentration C) the coefficient of nonlinearity n increases while the coefficient of selectivity decreases. This may also take place under certain conditions and even for large values of u_M, when $1 - e^{-\varkappa_M u_M} \neq \varkappa_M u_M$. For example, if the absorption of the radiation by the interfering component follows a square-root law and $v_M \geq 5u_M$, then, as indicated by calculations made for an unselective source and radiation receiver, the error introduced by using formula (1.3) does not exceed several percent. In this case, with an increase in the length of the working cell the coefficient of selectivity also decreases. In the other limiting case, when $V_M \ll u_M$, $\varkappa u \ll 1$, while u_M is sufficientl large, the coefficient of selectivity increases with an increase in L.

In the case when the absorption spectra of the analyzed and the interfering components are completely superposable, the differentiation of the expression (1.1) with respect to L and with the condition that $\varkappa_M u_M \ll 1$ leads to the relationship

$$\frac{1}{\left(\frac{\Delta C_M}{\Delta C}\right)} \frac{d}{dL}\left(\frac{\Delta C_M}{\Delta C}\right)_{u_M = u = 0} = \frac{\int_0^\infty I e^{-\varkappa_M V_M} \varkappa_M (\varkappa - \bar{\varkappa}) s d\nu}{\int_0^\infty I e^{-\varkappa_M \Gamma_M} \varkappa_M s d\nu} C - \frac{\int_0^\infty I e^{-\varkappa_M \Gamma_M} \varkappa (\varkappa_M - \bar{\varkappa}_M) s d\nu}{\int_0^\infty I e^{-\varkappa_M V_M} \varkappa s d\nu} C_M, \qquad (1.6)$$

where

$$\bar{\varkappa} = \frac{\int_0^\infty I e^{-\varkappa_M \Gamma_M} \varkappa^2 s d\nu}{\int_0^\infty I e^{-\varkappa_M \Gamma_M} \varkappa s d\nu}; \quad \bar{\varkappa}_M = \frac{\int_0^\infty I e^{-\varkappa_M \Gamma_M} \varkappa_M^2 s d\nu}{\int_0^\infty I e^{-\varkappa_M \Gamma_M} \varkappa_M s d\nu}. \qquad (1.7)$$

If the absorption spectra overlap only weakly then one may take

$$\int_0^\infty I e^{-\varkappa_M \Gamma_M} \varkappa_M \varkappa s d\nu \ll \int_0^\infty I e^{-\varkappa_M \Gamma_M} \bar{\varkappa}_M \bar{\varkappa} s d\nu$$

and

$$\int_0^\infty Ie^{-\varkappa_M V_M \varkappa \varkappa_M} s\,d\nu \ll \int_0^\infty Ie^{-\varkappa_M V_M \varkappa \varkappa_M} s\,d\nu.$$

The right side of expression (1.6) in this case will be reduced to the difference $(\overline{\kappa}_M C_M - \overline{\kappa} C)$. Thus, with an increase in L the coefficient of selectivity decreases at low values of C_M ($C_M\overline{\kappa}_M C_M < \overline{\kappa} C$) and increases at large values of C_M ($\overline{\kappa}_M C_M > \overline{\kappa} C$).

In the simplest case, when within the spectral limits of absorption of the analyzed and interfering components one may consider Is to be approximately constant, then in the absence of filters with the interfering component ($V_M = 0$) and for sufficiently small values of C_M the relations (1.6) and (1.7) are simplified to the following form

$$\frac{1}{\left(\frac{\Delta C_M}{\Delta C}\right)} \frac{d}{dL}\left(\frac{\Delta C_M}{\Delta C}\right)\Big|_{u=0} = \frac{\int_0^\infty (\varkappa - \overline{\varkappa})\,\varkappa_M d\nu}{\int_0^\infty \varkappa_M\, d\nu} C, \qquad (1.8)$$

where

$$\overline{\varkappa} = \frac{\int_0^\infty \varkappa^2 d\nu}{\int_0^\infty \varkappa d\nu}. \qquad (1.9)$$

The specific absorption coefficient $\kappa(\nu)$ depends on the wave number. For some completely definite value of the wave number the absorption coefficient $\kappa(\nu)$ attains the maximum value, $\kappa_{max.}$. The magnitude of $\overline{\kappa}$ expressed by the relation (1.9) is obtained by averaging $\kappa(\nu)$ within the limits of a certain spectral interval. Therefore, $\overline{\kappa} < \kappa_{max.}$. The integrand function in the numerator of expression (1.8) is the product of $\kappa_M(\nu)$ and of the difference $[\kappa(\nu) - \overline{\kappa}]$. Depending on the value of the wave number this difference may be positive or negative. For the wave numbers corresponding to those regions of the spectrum in which the analyzed component absorbs radiation with the greatest intentisy, $[\kappa(\nu) - \overline{\kappa}] > 0$. In the spectral regions where the analyzed component absorbs comparatively weakly, $[\kappa(\nu) - \overline{\kappa}] < 0$. If the absorption spectra of the analyzed and of the interfering components are superposed in such a way that the function $\kappa_M(\nu)$ is practically different from zero only in that region of the spectrum in which for the analyzed component $\kappa(\nu) < \overline{\kappa}$, then with an increase in the length of the working cell the coefficient of selectivity is decreased. The case of the function $\kappa_M(\nu)$ being different from zero only in that region of the spectrum where $\kappa(\nu) > \overline{\kappa}$ has not as yet been encountered in practice. In absorption meters with selective gas radiation sources or with selective optico-acoustical radiation receivers, when C_M is small the coefficient of selectivity is also usually decreased by an increase in L.

II. NONDISPERSIVE METHODS OF INCREASING SELECTIVITY

Let us discuss in some detail the nondispersive methods of increasing the selectivity. First, let us investigate the dependence of the coefficient of selectivity on the magnitude of V_M (on the product of the concentration of the interfering component in the filter cells and their length). In the more important practical case when $u \ll 1$ and $\kappa_M u_M \ll 1$ the formula (1.1) reduced to

$$\frac{\Delta C_M}{\Delta C} = \frac{\int_0^\infty Ie^{-\varkappa_M V_M \varkappa} s\,d\nu}{\int_0^\infty Ie^{-\varkappa_M V_M \varkappa_M} s\,d\nu}. \qquad (2.1)$$

If the absorption spectra of the interfering and analyzed components practically do not overlap while V_M is not very large, then

$$\frac{\Delta C_M}{\Delta C} = n_M \left(\frac{\Delta C_M}{\Delta C}\right)_{V_M=0}, \qquad (2.2)$$

where

$$\left(\frac{\Delta C_M}{\Delta C}\right)_{V_M=0} = \frac{\int_0^\infty I\varkappa s\,d\nu}{\int_0^\infty I\varkappa_M s\,d\nu}, \qquad (2.3)$$

$$n_M = \frac{\int_0^\infty I\varkappa_M s\,d\nu}{\int_0^\infty Ie^{-\varkappa_M V_M \varkappa_M} s\,d\nu}. \qquad (2.4)$$

The physical significance of the coefficient n_M consists of the following. Let us suppose that with the aid of the absorption analyzer we are determining the composition of the interfering component in an analyzed mixture in which the product of the length of the working cell and the concentration of the component equals V_M; then if the functional curve of the output signal of the receiver is plotted against the concentration of the interfering component, the ratio of the slope of the tangent to this curve at the origin of the scale to that of the slope of the tangent at the end of the scale will be equal to n_M. The formula (2.2) holds only in that case when the product $\kappa_M V_M$ is smaller than unity within the limits of the most intense part of the absorption spectrum of the analyzed component. For sufficiently large values of V_M it is important to take into consideration the overlap of the absorption spectra of the analyzed and of the interfering component. In the case of overlap of the absorption spectra, differentiating (2.1) with respect to V_M, we obtain

$$\frac{1}{\left(\frac{\Delta C_M}{\Delta C}\right)} \frac{d}{dV_M}\left(\frac{\Delta C_M}{\Delta C}\right)\Big|_{V_M=0}$$

$$= \int_0^\infty I\varkappa\,(\overline{\varkappa}_M - \varkappa_M)\,s\,d\nu \left[\int_0^\infty I\varkappa s\,d\nu\right]^{-1}, \qquad (2.5)$$

where $\overline{\kappa}_M$ is defined by formula (1.7).

The algebraic sign of the integral in the numerator depends on the sign of the difference $[\overline{\kappa}_M - \kappa_M(\nu)]$. This difference has a negative sign for those values of the wave numbers for which the absorption of the radiation by the interfering component occurs most intensely and has the positive sign in the regions of the spectrum corresponding to weak absorption of radiation by the interfering component. Therefore, if the absorption spectrum of the analyzed component lies principally in the region of the spectrum in which the interfering component absorbs relatively weakly, i.e., $\kappa_M > \overline{\kappa}_M$, then the introduction in the path of the beams of filter cells filled with the interfering component increases the coefficient of selectivity. This is exactly what takes place in practice.

Let us next investigate how the coefficient of selectivity of the infrared absorption meter is changing when a nonselective radiation receiver is replaced by a selective optico-acoustical receiver. For the absorption meter with the nonselective receiver with practically the same spectral sensitivity within the limits of the spectra of the analyzed and of the interfering components, we obtain

$$\left(\frac{\Delta C_M}{\Delta C}\right)_{\text{nonselect.}} \approx \frac{\int_0^\infty I e^{-x_M \Gamma_M x} d\nu}{\int_0^\infty I e^{-x_M \Gamma_M x_M} d\nu}.$$

The spectral sensitivity $s(\nu)$ of the selective optico-acoustical receiver under particular conditions[19] may be made to be practically proportional to $\kappa(\nu)$. In this case we have for the coefficient of selectivity of the optico-acoustical gas analyzer

$$\left(\frac{\Delta C_M}{\Delta C}\right)_{\text{select.}} \approx \frac{\int_0^\infty I e^{-x_M \Gamma_M x} \kappa^2 d\nu}{\int_0^\infty I e^{-x_M \Gamma_M x x_M} d\nu}. \qquad (2.6)$$

From this it follows that

$$\left(\frac{\Delta C_M}{\Delta C}\right)_{\text{select.}} - \left(\frac{\Delta C_M}{\Delta C}\right)_{\substack{\text{non} \\ \text{select.}}} \approx \left(\frac{\Delta C_M}{\Delta C}\right)_{\text{nonselect.}} \cdot \frac{\int_0^\infty I e^{-x_M \Gamma_M x_M (\bar{x} - x)} d\nu}{\int_0^\infty I e^{-x_M \Gamma_M x_M} \kappa d\nu},$$

where $\bar{\kappa}$ is defined by formula (1.7).

If the absorption spectra of the analyzed and interfering components are so far separated that, within the limits of the principal part of the spectrum of the interfering component, the condition $\kappa(\nu) < \bar{\kappa}$ is obeyed, then the replacement of the nonselective receiver in the infrared absorption meter by the selective optico-acoustical receiver leads to an increase of the coefficient of selectivity. This case is usually observed in practice. On the other hand, the case of a decrease in the coefficient of selectivity following the replacement of the unselective receiver by the selective optico-acoustical receiver (which would have taken place if within the limits of the principal part of the spectrum of the interfering component the condition $\kappa(\nu) > \bar{\kappa}$ were obeyed) has not as yet been observed in practice.

If, within the limits of the absorption spectra of the analyzed and interfering components, the spectral intensity is practically identical then the expression (2.6) will become

$$\frac{\Delta C_M}{\Delta C} \approx \frac{\int e^{-x_M \Gamma_M x} \kappa^2 d\nu}{\int e^{-x_M \Gamma_M x x_M} d\nu}. \qquad (2.7)$$

Integration in this case is not performed from 0 to ∞ but over the finite spectral interval of the wave numbers which is used in the analysis.

The expression obtained is also approximately correct in the case when, in the absorption meter with the unselective receiver, the selective gas source is being used, while the spectral intensity of the radiation from that source is practically proportional to $\kappa(\nu)$. If in the absorption gas analyzer based on the utilization of the negative optico-acoustical effect one assumes that in the first approximation the heat exchange by radiation between the optico-acoustical cell and the refrigerator is proportional to $\kappa(\nu)$, then for the coefficient of selectivity one also obtains the formula (2.7).

It is important to note that the expressions (2.6) and (2.7) hold only for such double-beam absorption meters in which only one of the compared beams (the working beam) passes through the analyzed mixture (see diagram).

To be assured of the maximum selectivity of the nondispersive absorption meter one must conform to a series of special conditions which will be investigated in the second part of this work.

REFERENCES

1. M. L. Veingerov, Doklady Akad. Nauk SSSR **19**, 687 (1938).
2. K. F. Luft, Z. tech. Physik **24**, 97 (1943).
3. M. L. Veingerov, Zavodskaya Lab. No. 4, 426 (1947).
4. K. F. Luft, Angew. Chem. B59, 2 (1947).
5. V. Ts. Williams, Uspekhi Fiz. Nauk **37**, 183 (1949).
6. V. M. Chulanovskii, "Introduction to Molecular Spectroscopic Analysis." State Technical and Theoretical Press, Moscow, Leningrad, 1951.
7. V. A. Pavlenko, "Collection: New Thermoenergetical Industrial Instruments and Regulators," p. 70. State Scientific-Technical Press for Machine Construction Literature, 1953.
8. H. H. Shumilovskii and A. A. Sokolov, Automat. i Telemekh. **14**, 328 (1953).
9. N. A. Slovokhotova, Zavodskaya Lab. No. 7, 835 (1954
10. A. O. Sall and S. B. Stanevich, Opt. i Spektr. **7**, 256 (1959), Optics and Spectroscopy **7**, 162 (1959).
11. A. O. Sall, Opt. i Spektr. **7**, 576 (1959), Optics and Spectroscopy **7**, 355 (1959).
12. M. L. Veingerov, Ya. I. Gerlovin, and H. A. Pankrato Opt. i Spektr. **1**, 1023 (1956).
13. M. L. Veingerov, A. A. Sivkov, and E. V. Malykh. Opt i Spektr. **2**, 283 (1957).
14. P. I. Bresler, Opt. i Spektr. **5**, 220 (1958).
15. Ya. I. Gerlovin, Opt. i Spektr. **7**, 571 (1959), Optics and Spectroscopy **7**, 352 (1959).
16. K. F. Luft, Rev. opt. **33**, 501 (1954).
17. A. O. Sall, Zhur. Tekh. Fiz. **29**, 330 (1959), Soviet Phys.-Tech. Phys. **4**, 295 (1959).
18. A. O. Sall, Priborostroenie No. 6, 14 (1956).
19. A. O. Sall, Priborostroenie No. 9, 12 (1956).
20. V. A. Pavlenko, "Collection: Thermoenergetical and Chemicotechnological Instruments and Regulators," p. 96. State Scientific-Technical Press for Machine Construction Literature, 1956.
21. Iiři Ianăč, Infračerveně Analyză tory. Prague, 1959.

SHORT COMMUNICATIONS

AN OSCILLOGRAPHIC METHOD OF STUDYING OPTICAL EXCITATION FUNCTIONS

I. P. Zapesochnyi and A. I. Dashchenko (pp. 679-681)

Received 11 January 1961

Recent years have seen a considerable increase in interest in the experimental determination of the effective excitation cross sections of atoms and molecules, including the study of optical excitation functions. An important advance was the introduction of photoelectric methods, using photomultipliers[1] to replace photographic recording of excited lines and bands. In the work described in ref. 1, and in much similar work, the experimental curves describing the excitation functions of individual atomic lines or diatomic molecular bands were constructed from individual points. Therefore, where detailed study was required of the shape of the excitation function of some line or band, a large number of very time-consuming measurements was necessary (while the life of an excitation tube is usually short).

This raises the problem of improving the photoelectric method of studying excitation functions to obtain continuous experimental curves (excitation functions) without measuring individual points. Two possibilities are open: firstly, the use of an electronic recording potentiometer, the secondly, the use of a cathode ray oscillograph. Frish and Yakhontova first used recorders in experiments on the excitation of helium by electron collision.[2]

The present paper describes an experiment using an oscillograph. We consider this method of obtaining excitation functions to have several advantages: (1) It is possible to obtain almost instantaneous photographs of the shape of the excitation function for any available range of exciting electron velocities; (2) it is possible to isolate as rapidly as desired an arbitrarily narrow portion of the experimental curve by extending it over the whole oscillograph screen so as to clarify different fine details of the excitation functions; (3) photographs of the excitation functions are obtained and stored as records.

We used a setup consisting of an excitation tube, an MS-3 monochromator, and a detector to investigate the possibility of using an oscillograph in studying optical excitation functions. The construction of the excitation tube and the method of filling it were similar to those described earlier (in ref. 3, for example). The tube power supply provided an extra sawtooth voltage applied to the control anode, or alternatively could be used as an ordinary power supply. The horizontal sweep generator of an EO-6 oscillograph provided the saw-tooth voltage. The ordinary power supply of the tube was used for heating the oxide cathode of the electron beam, to determine the monochromaticity of the beam, to find the relationship between the strength of the electron current in the gas under study and the potential of the control anode and other characteristics of the excitation tube. The detector was an FEU-17 photomultiplier with an EO-7 cathode ray oscillograph.

The excitation functions were displayed on the oscillograph as follows. The sawtooth voltage from the sweep generator, applied to the control anode of the excitation tube, gave a periodic variation of the tube electron velocity and hence a corresponding variation in the radiation intensity of the line under study. This change in intensity caused a corresponding periodic change in the photomultiplier output current, which in turn led to a periodic change in the load resistor voltage which was recorded by the oscillograph. If the horizontal sweep of the oscillograph is synchronized with the sawtooth voltage applied to the excitation tube control anode, a curve is seen on the oscillograph screen, describing the change in radiation intensity of a given line in one cycle. But during this cycle the control anode potential passes through all values from zero to some value V. Therefore, the curve seen on the oscillograph screen represents the excitation function of the line in the electron energy range from zero to V. The oscillograph pattern was photographed with a camera using a "Yupiter 8" objective (f/2) on Dk film with sensitivity 350 GOST* units.

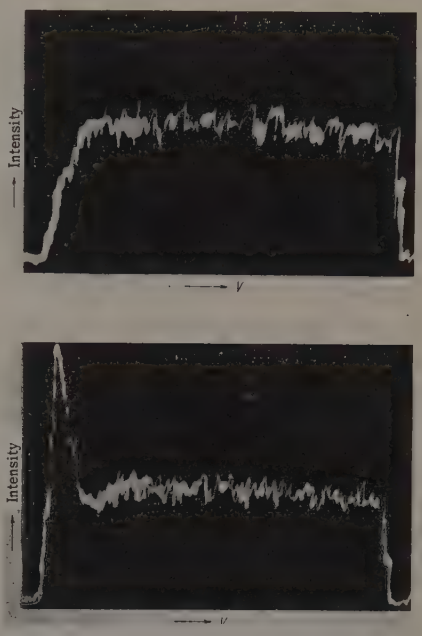

Oscillograms of the excitation functions of mercury lines: top—λ4078 A; bottom—λ5461 A.

*All-Union State Standard.

The exposure time was 1/25 sec.

An isolating condenser in the oscillograph input circuit prevents the photomultiplier and oscillograph from recording the constant background light. This is convenient since it eliminates the necessity of carefully darkening the room.

The Figure shows excitation function oscillograms obtained in the electron energy range 0 to 70 ev for two

atomic mercury lines with upper levels of different multiplicities. The mercury pressure in the excitation tube was 2×10^{-3} mm Hg, the electron current density was about 10^{-3} amp/cm^2, and the scatter in electron energy was about 1 ev.

As these oscillograms show, the curves obtained have the shape typical of the excitation function for singlets (a gently sloping maximum) and for triplets (a sharp maximum with a spike close to the excitation voltage of the system).

When the accelerating voltage is increased in the range of velocities (energies) used, the current in the mercury vapor also increases slightly, which accounts for the slower decrease of the curves after the maxima in the photographs, by comparison with earlier results.[3]

We will continue the development of this new method of observing optical excitation functions, and our next steps will be to remove the defects of the preliminary experiments by filtering out the photomultiplier dark current, constructing a more stable sawtooth generator, eliminating the effect of the electron current increase on the excitation function shape, and increasing the detector sensitivity.

REFERENCES

1. S. E. Frish and I. P. Zapesochnyi, Doklady Akad. Nauk SSSR **95**, 971 (1954);
I. P. Zapesochnyi, Nauch. Zapiski Uzhgorodsk. Univ. **18**, 147 (1957);
I. P. Zapesochnyi and S. M. Kishko, Doklady Akad. Nauk SSSR **134**, 311 (1960), Soviet Phys.-Doklady **5**, 1008 (1961).
2. S. E. Frish and V. E. Yakhontova, Opt. i Spektr. **4**, 402 (1958).
3. I. P. Zapesochnyi, Vestnik Leningrad. Univ. No. 11, 67 (1954).

NONSELECTIVE OPTICO-ACOUSTIC RADIATION DETECTORS WITH ELECTRODYNAMIC MICROPHONE

N. A. Pankratov (pp. 681-683)

Received 21 January 1961

The threshold sensitivity of a nonselective optico-acoustic detector is limited by pressure fluctuations within its gas cell. The magnitude of the fluctuations depends on the dimensions of the cell, the frequency at which observations are made, and the type of gas in the cell.[1] The greatest sensitivity of the cell occurs at low modulation frequencies, of the order of 10-14 cps. To realize the cell's threshold sensitivity it is necessary that the sensitivity of the microphone used with it be sufficiently great and the noise sufficiently small, i.e., the condition

$$\sqrt{\overline{\Delta p_{\text{fl.}}^2}} \times U_{\text{M}} \geq \sqrt{\overline{\Delta V_{\text{M}}^2}},$$

must hold, where $\sqrt{\overline{\Delta p_{\text{fl.}}^2}}$ is the rms value of the pressure fluctuation in some band of frequencies of width Δf centered at the frequency f, U_M is the sensitivity of the microphone at this frequency, and $\sqrt{\overline{\Delta V_{\text{M}}^2}}$ is the rms noise of the microphone without the cell.

From published works[2,3] it is known that resonance electrodynamic microphones have high sensitivity and will detect gas pressure fluctuations at the resonant frequency. In a selective detector, as was shown earlier,[3] the limiting sensitivity of the cell can be realized with such a microphone. It is of interest to set up a nonselective detector with a resonance electrodynamic microphone and estimate its sensitivity. Such detectors were first set up by Veingerov and Luchin,[4] and subsequently improved by Spiro.

The construction of the detector is shown in Fig. 1 and consists of the following. The modulated radiation flux passes through an infrared-transparent window 1 and is absorbed by a very thin aluminum film 2 deposited on a thin organic substrate. The film is clamped between two aluminum rings 3. From the action of the radiation, temperature pulses arise in the film and the gas. As a result, pressure pulses act on the membrane 4 of the

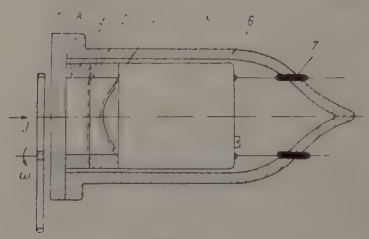

Fig. 1

microphone 5. The entire detector is enclosed in a glass or metal envelope 6 which protects the microphone from outside acoustical influences. Electrical contact with the microphone is achieved by leads inserted through metal tubes 7 in the glass envelope. The junction between the entrance window and the envelope is sealed with OK-50 epoxy cement. Air is evacuated from the envelope by a tube not shown in Fig. 1; after filling the envelope with gas to the necessary pressure the tube is sealed. A duct 8 serves to equalize the pressure between the volumes on both sides of the membrane during slow temperature variations in the envelope resulting from ambient temperature variations.

The distance from the radiation-absorbing film to the window and to the membrane was the same and equal to 1 mm. To increase the absorption of incident radiation the microphone membrane was coated with a reflective aluminum film. Then that part of the radiation previously transmitted through the absorbing film is reflected from the membrane back to the absorbing film.

A type of specially built electrodynamic resonance microphone with a movable coil, whose construction is shown in Fig. 2, was used. The coil 1 has a diameter of 7.5 mm and is cemented to a corrugated styrene membrane 2, whose thickness is 20 μ. On oscillation of the

membrane the coil oscillates in the magnetic gap formed by the yoke 3 and the pole end 4. A permanent magnet 5 serves as the source of the magnetic field. The ends of the coil wires are cemented to the membrane and brought out through a special sleeve in the rear wall of the microphone.

Various types of microphones differed from each other by the diameter of the membrane, body, and microphone magnet. In the detectors described here microphones were used with body diameter 22 mm, the diameter of the active surface of the membrane was 6 mm, the resonant frequency in open space was 600-700 cps, the coil resistance 180 ohms, and the dynamic impedance at the resonant frequency of the order of 1000-1200 ohms. The sensitivity of such microphones in open space with a load of 10^6 ohms was 7-8 mv/bar. When the microphone was set in the detector cell its resonant frequency was somewhat raised, since the elasticity of the gas in the volume in front of the membrane was added to the elasticity of the membrane.

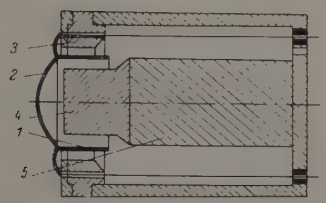

Fig. 2

The signal from the detector was fed to an amplifier with a transformer input. The amplifier bandpass was 20 cps with a resonance filter, and significantly less when a synchronous detector was used in the amplifier. During operation the amplifier was carefully screened; to reduce pickup, battery power was used.

Tests of the detectors were likewise made with a standard 28IM amplifier with a bandpass of the order of 00 cps. This amplifier has relatively low gain and is powered from the line, so the level of interference in it s somewhat higher than in the first amplifier.

Detector tests were made in the following way. A radiant flux from a Hefner lamp was directed through the diaphragm of the detector, whose exposed area was 80 mm^2. The output of the detector was measured and its noise was then determined. Likewise, measurements were made for other detectors with different gases filling the cell and with different gas pressures in the cell.

From the experimental results it was established that with a modulation frequency of 730 cps and an amplifier bandwidth of 20 cps (this corresponds to the amplifier time constant of 0.012 sec) the radiant flux corresponding to the rms noise of the detector if 5×10^{-8} watt and with a bandwidth of 0.15 cps, 3.5×10^{-9} watt. The specific sensitivity of the detector was 0.4 mv/mw. The air pressure within the envelope was 400 mm Hg. At atmospheric pressure the resonant frequency of the microphone was 780 cps and the rms noise was likewise equal to approximately 5×10^{-8} watt. When the cell was filled with helium at the same pressure the radiant flux corresponding to the rms noise was 3.5×10^{-8} watt with a bandwidth of 20 cps.

Thus the rms noise of the cell with helium is 1.4 times less than with air. This is explained, obviously, by the fact that the heat capacity of helium is less than the heat capacity of air.

Because of the high modulation frequency the sensitivity appeared uniformly distributed over the surface, as opposed to a detector working at a low modulation frequency, for example, a detector with an optical microphone.[1]

It is interesting to compare the rms noise of detectors with electrodynamic microphones with the noise of detectors with optical microphones, operating at a modulation frequency of 10 cps, since in both cases the noise is determined by pressure fluctuations. If we convert the rms noise of the amplifier to a lower frequency, assuming that it varies in inverse proportion to $\omega^{1/2}$, and convert to an area of 3 mm diameter, then with an amplifier bandwidth of 0.15 cps we find about 4×10^{-11} watt, i.e., the same noise as for detectors with an optical microphone.

In conclusion it should be mentioned that, although the detector here described is inferior in threshold sensitivity to detectors with optical and condensor microphones, it has extremely small inertia and a large sensitive area; it is distinguished by the simplicity of its construction and the stability of its operation. As a consequence of the small inertia it can be effectively used for rapid recording of spectra and other such tasks. Also, the large sensitive area of the detector is useful in cases where the flux can not be collected onto a small surface or where it is necessary to measure the intensity of radiant energy of long wavelength.

The author thanks M. L. Veingerov for interest and guidance in the work.

REFERENCES

1. N. A. Pankratov, Optiko-Mekh. Prom. Nos. 1, 3, 7 (1960).
2. M. L. Veingerov, Doctoral diss., State Optical Institute, Leningrad, 1940.
3. N. A. Pankratov, Opt. i Spektr. 8, 109 (1960); Optics and Spectroscopy 8, 53 (1960).
4. S. M. Luchin, Zhur. Tekh. Fiz. 16, 1115 (1946).

A CROSSED-DISPERSION SPECTROGRAPH BUILT ON A NEW OPTICAL DESIGN

K. I. Tarasov (pp. 683-686)

Received 21 February 1961

A high-dispersion spectrograph usually allows only small portions of the spectrum to be photographed. The use of diffraction gratings operating in the higher orders (an echelette) enables one, on the one hand, to increase the range which can be taken in by a single exposure, and, on the other hand, to obtain a higher dispersion, proportional to the order of the spectrum. Separation of the orders can be accomplished by the introduction of an additional dispersing element (a prism or a second diffraction grating, operating in the first order), the dispersion of which is directed perpendicular to the dispersion of the echelette; in this case the spectrum appears in the form of several rows of spectral lines, each of the rows corresponding to some one order of the spectrum. With the correct choice of the blaze angle of the echelette, the maximum energy concentration corresponds to the middle of each row of the spectrum.

In crossed-dispersion instruments, a correct choice of the optical design is of decisive importance. The use of lens optics is inappropriate, since it is associated with distortion of the focal surface in two directions. The use of spherical mirrors is always associated with the presence of astigmatism. In the first approximation, both asigmatic focal surfaces are spheres whose radius of curvature depends on the position of the aperture stop (or iris),[1] the role of which is usually filled by the aperture of the dispersing element. There are certain positions of the iris for which each of the focal surfaces goes over into a plane. For rays lying in the meridional section of the beam, this takes place at iris-to-mirror distances equal to approximately 0.85 f and 3.15 f (f is the focal length of the camera objective); for rays lying in the sagittal section, it takes place when the iris is located at the mirror and when the iris lies at a distance of 4 f from the mirror.

The setup at the distance 0.85 f is most frequently used. In this case, the astigmatic focals at the edge of the plate are directed along the spectral lines (with slight bending); at the center of the plate, these focals are directed across the spectral lines, but their length is small enough not to cause significant line broadening. It is inappropriate to apply such a setup in the case of crossed dispersion, since, in consequence of the considerable height of the spectral image on the plate, on the one hand the angles between the directions of the astigmatic focals and the spectral lines at the edges of the plate increase considerably, and on the other hand the value of the transverse astigmatism for lines lying on a vertical passing through the middle of the plate increases.

The formulas derived by the author[1] show that, when the iris is set up in a plane passing through the center of curvature of the camera mirror, the magnitude of the astigmatism and coma is constant over the whole field of view. The astigmatic focals are parallel to one another over the whole surface of the photographic plate and may be made to coincide with the direction of the spectral lines. The astigmatism, furthermore, may be compensated by setting up a cylindrical lens not far from the entrance slit of the spectrograph, and the coma by the use of a Z-shaped design. With such a placement of the iris, the field has its maximal curvature, the radius of curvature being equal to the focal length of the mirror and—which is interesting—being the same for both astigmatic surfaces. The curvature of the field may be adequately corrected by placing a planoconvex lens near the photographic plate. Spherical aberration remains, but it also can be corrected by placing a meniscus in the divergent beam of the collimator; for relative apertures of the order of 1:15 and less, and with a focal length of the order of 1 meter for the collimator and camera objectives, this correction is superfluous.

The optical design proposed by the author is represented in Fig. 1. If, instead of the photographic plate 13 a photographic film is used, then the lens 12 is not put in place, but rather the film itself is bent into a cylindrical surface. On the basis of this design and the technical requirements of the instrument as drawn up by V. K. Prokof'ev, M. M. Kler, and A. K. Rusanov, the technical assignment has been worked out; in accordance with the latter, an experimental model of the instrument, coded STE-1, has been designed by L. F. Belugin.

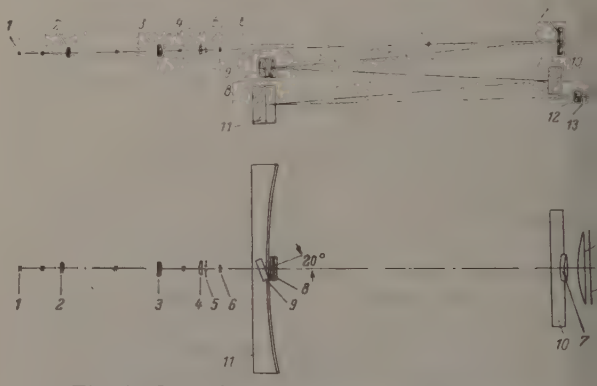

Fig. 1. Optical design (above—vertical section, below—view from above). 1—light source; 2, 3, 4—lenses of the condensing system; 5—entrance slit; 6—cylindrical lens; 7—collimating mirror; 8—prism; 9—echelette; 10—plane mirror, which serves to reduce the dimensions of the apparatus; 11—camera mirror; 12—lens to correct the curvature of the field; 13—photographic plate.

Laboratory tests of the experimental model have shown that it has good image quality. In Fig. 2 a spectrogram of the well-known group of iron lines at 3099.897-3099.971-3100.304-3100.666 A, taken with a 5 μ slit at a arc current of 2 amp, is shown, and in Fig. 3 a spectrogram of the lines Cr 2512.40 and Fe 2512.363; the latter pair of lines is at the limit of resolution. The real resolving power at 2512 A amounts to 60,000 (for photography on slide plates), which corresponds to a linear resolution of 93 lines/mm.

The comparatively large relative aperture of the

Technical Data for the STE-1 Instrument

Row no. of the spectrum	Order of the spectrum	Spectral range (A)		Linear dispersion (A/mm)	Theoretical resolving power
		Plate 180 mm long	Film 240 mm long		
With quartz optics and a diffraction grating with 600 lines/mm					
1	5	2200–2700	2200–2820	3.8	165000
2	4	2520–3375	2375–3500	4.7	132000
3	3	3360–4500	3165–4500	6.4	99000
With glass optics and a diffraction grating with 300 lines/mm					
1	5	4500–5400	4500–5640	7.6	82500
2	4	5040–6750	4750–7000	9.4	66000
3	3	6720–9000	6330–9000	12.8	49500

Note: Focal length of the mirror objectives: collimator – 901.5 mm; camera – 807.2 mm. elative aperture 1:15. Dimensions of the photographic plate 13 × 18 cm; dimensions of e film 12 × 24 and 3.5 × 24 cm. Working height of entrance slit 5 mm (M. M. Kler's 10- ep attenuator may be inserted). Height of the three rows of the spectrum 24 mm. Dimen- ns and weight of the instrument without track 960 × 720 × 350 mm and 95 kg.

TE-1 instrument, 1:15 (existing instruments of the same ispersion have 1:35-1:40), and the high image quality nsure a considerably shorter exposure than in other in- truments, which simplifies the analysis of samples which urn out quickly. The physical light speed of the STE-1 the wavelength interval 2900-3265 A has been com- ared with the light speed of the DFS-13 spectrograph on he basis of the exposures necessary to photograph weak ines, since only for them is there any point in raising he light speed of the instrument. Naturally, in this con- ection the exposures depend on the quality of the image iven by the instrument. For a DFS-13 instrument with n image quality somewhat below average, the exposure as 6 times as great as for the STE-1 at the same cur- ent (4 amp) and the same slit width (10 μ). For another FS-13 instrument with satisfactory image quality, the xposure was only 3-4 times as great as for the STE-1. ince it is reasonable to compare exposures for instru- ents not only at the same dispersion, but also (which s more important) at the same resolving power, the lit in the STE-1 was widened to 15 μ in order to obtain the same resolution as with the DFS-13. In this case, the exposure for the DFS-13 proved to be 12-16 times as great as the exposure for the STE-1.

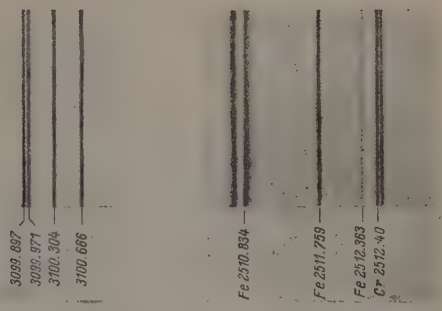

Fig. 2 Fig. 3

Fig. 2. Spectrogram of a group of Fe lines (magnification 75).
Fig. 3. Spectrogram of Cr and Fe lines (magnification 75.)

On the basis of the new optical design, as tested on the STE-1 instrument, and with the availability of serial echelettes which give good image quality in 5-10 orders, compact spectrographs can be constructed with resolution no worse than in the DFS-13, but with considerably greater light speed. The same optical design can be applied in quantometers, where it will give a possibility of obtaining considerably greater light fluxes than the Paschen-Runge design, and consequently of reaching farther into the ultraviolet.

REFERENCE

1. K. I. Tarasov, Opt. i Spektr. 8, 723 (1960), Optics and Spectroscopy 8, 380 (1960).

RELATION BETWEEN THE FREQUENCIES OF N—H SYMMETRIC AND ANTISYMMETRIC VIBRATIONS IN THE MOLECULES OF PRIMARY AMINES

Yu. S. Varshavskii (pp. 686-688)

Received 22 February 1961

In the work of Bellamy and Williams[1] a linear relation was assumed between the values of the frequencies of symmetric and antisymmetric N—H vibrations in primary amino groups:

$$\nu_s = 0.876\nu_a + 345.5 \ (\text{cm}^{-1}). \quad (1)$$

Figure 1 shows the difference δ (between ν_s, calculated from Eq. (1), and the experimental value, see Table, plotted against the frequencies of the antisymmetric vibrations. As shown in Fig. 1, the discrepancy associated with the use of Eq. (1) has a regular character and increases with increasing ν_a. Within the limits of the restricted series of related compounds included in the Table, Eq. (1) can be improved by a change in the numerical values of the constants. Thus, the equation*

$$\nu_s = 0.667\nu_a + 1075 \quad (2)$$

gives a better description of the reduced data than does the Bellamy-Williams equation. In principle, however, neither one of these equations can be considered satisfactory. For this reason we will not use directly the quantities ν_a and ν_s but rather their difference ($\Delta\nu$) and their average (ν_{av}): It is obvious that (1) and (2) imply a linear relationship between $\Delta\nu$ and ν_{av}:

$$\Delta\nu = p\nu_{av.} - q. \quad (3)$$

The solution of the equations resulting from a valence-bond model,[2] by the approximation of substituting the mean frequency $[\frac{1}{2}(\nu_a^2 + \nu_s^2)]^{1/2}$ for the arithmetic average value of the frequency ν_{av}, leads to the equation

$$\Delta\nu = \frac{m_H(2\sin^2\theta - 1)\nu_{av.}}{m_N + m_H}, \quad (4)$$

*Obtained by the method of least squares.

Frequencies of Valence Vibrations of N—H in Molecules of the Type X—C_6H_4—NH_2, Calculated from Eqs. (1) and (2)

Substituent X	ν_a (cm^{-1})	ν_s (cm^{-1}) Exptl. From ref. 3	ν_s (cm^{-1}) Calc. By (1)	ν_s (cm^{-1}) Calc. By (2)
para-NH_2	3453	3376	3370	3378
para-CH_3	3469	3388	3384	3389
meta-NH_2	3478	3395	3392	3395
meta-CH_3	3475	3393	3389	3394
H	3478	3395	3392	3395
para-F	3473	3394	3387	3391
para-Cl	3482	3398	3396	3397
para-Br	3484	3399	3397	3399
para-I	3487	3398	3400	3401
meta-Cl	3489	3401	3401	3402
meta-Br	3489	3401	3401	3402
meta-NO_2	3495	3407	3406	3406
para-CH_3CO	3501	3410	3412	3410
para-NO_2	3508	3413	3418	3415

where θ is one-half the valence angle H-N-H in the amino group, and m_H and m_N are the atomic masses of hydrogen and nitrogen.

Equation (4) shows that in the case of a constant valence angle, the value of $\Delta\nu$ changes proportionally to ν_{av}, i.e., for θ = constant, the last term in (3) is absent (q = 0). In the case $\theta \neq$ constant, the nature of the relationship between $\Delta\nu$ and ν_{av} appears more complicated and takes the form of the dependence between θ and ν_{av}. The linear equation (3) with $q \neq 0$ corresponds to a special form of the latter dependence, namely,

$$\sin^2\theta = m - \frac{n}{\nu_{av.}} \qquad (5)$$

[In frequencies, from (1) m = 1.49, n = 2760.] Equation (5) represents the conditions compatible with the Bellamy-Williams formula for the valence bond theory.

The experimental data[3-5] presented in Fig. 2 encompass a wide range of conditions of the amino group (from aliphatic amines to amides of carboxylic acids) and show that the relationship between $\Delta\nu$ and ν_{av} (and, therefore, between ν_s and ν_a) cannot be satisfactorily approximated by a linear equation over a sufficiently wide frequency interval

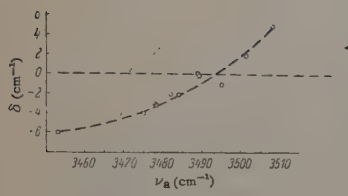

Fig. 1

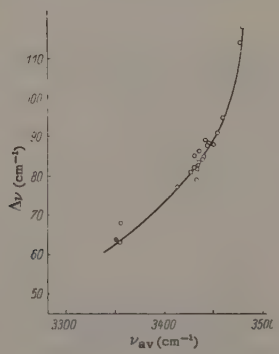

Fig. 2

Fig. 1. Discrepancy δ between the value of ν_s, calculated from the Bellamy-Williams equation, and the experimental value.
Fig. 2. Relationship between the frequency difference $\Delta\nu$ for primary amines and the average frequency (according to refs. 3, 4, and 5).

The increase in ν_{av} and the corresponding increase in the force constant f_{N-H} reflect the increasing fraction of s-orbitals in the N—H bonds,[4,6] which occurs in the change from aliphatic amines to aromatic amines and further to acid amides. However, the increasing s-character of the bonds involving the nitrogen atom results in an increase in the valence angle H-N-H. The determination of the value of θ from the data of Fig. 2 by the use of Eq. (4) shows that in going from aliphatic amines to amides of carboxylic acids the angle H-N-H increases from around 108° to around 120°. Calculation from Eq. (5), with constants calculated in Eq. (1), gives for this same series an increase in the H-N-H angle from around 110° to around 113°. Thus, the Bellamy-Williams equation evidently does not make sufficient allowance for the dependence of θ on ν_{av}. It should be noted that Eq. (1) leads to the condition $d^2(\Delta\nu/\nu_{av})/d\nu_{av}^2 < 0$, while from the experimental data it follows (Fig. 2) that this derivative is actually positive.

The change in the force constant f_{N-H} reflects a change not only in the type of hybridization of the bond, but also in the magnitude of effective charge on the nitrogen atom.[2,6] This implies that f (and, consequently, ν_{av}) is a function of at least two variables (s-character and charge), whereas the angle θ is defined by only one (namely the first) of these variables. A calculation of the influence of effective charge thus casts doubt not only on the linearity of Eq. (4), but also on the existence of a well-defined relationship between $\Delta\nu$ and ν_{av}, i.e., between ν_s and ν_a. In particular, this relates to coordination compounds, in the formation of which there occurs a disturbance of the relationship normally existing in free amines between changes in electron density on the nitrogen atom and its valence state.[7,8] A series of examples of coordinating amines which do not conform to the Bellamy-Williams equation is presented in that publication.[1] The authors[1] assume that the nonapplicability of Eq. (1) is caused by the formation on the amino group of unsymmetrical hydrogen bonds, and they suggest the use of Eq. (1) as an appropriate criterion. It seems clear from these statements that their assumption cannot be accepted as proved. Linear equations of the type of Eqs. (1) and (2) can be used for interpolation within the limits of not too broad classes of related compounds and this is the extent of their importance.

REFERENCES

1. L. J. Bellamy and R. L. Williams, Spectrochim. Acta 9, 341 (1957).
2. J. W. Linnett, Trans. Faraday Soc. 41, 223 (1945).
3. S. Califano and R. Moccia, Gazz. chim. ital. 86, 1014 (1956).
4. W. J. Orville Thomas, A. E. Parsons, and C. P. Ogd J. Chem. Soc. 1047 (1958).
5. L. Bellamy, "Infrared Spectra of Complex Molecules p. 247. Foreign Literature Press, Moscow, 1957. 2n ed., Wiley, New York, 1958.
6. R. E. Richards, Trans Faraday Soc. 44, 40 (1948).
7. M. S. Barvinok and Yu. S. Varshavskii, Zhur. Neorg. Khim. 6, 851 (1961).
8. M. S. Barvinok, Yu. S. Varshavskii, and L. K. Putse Zhur. Neorg. Khim. 6, 1125 (1961).

COMPARISON OF SPECTRAL INTENSITIES OF THE HYDROGEN AND DEUTERIUM RADIATION

S. I. Levikov and L. P. Shishatskaya (pp. 689-691)

Received 19 April 1961

The work described in this article consisted of a mparison of intensities of three Balmer lines, of the ntinuum, and of the band emission spectrum of hydro- n and deuterium obtained under completely identical nditions of excitation by an electrical discharge. At e same time we utilized new deuterium lamps of two pes which we have recently constructed: DSFU-3 with traviolet transmitting windows and DLF-25 with lithium oride windows. They were compared with the standard drogen lamps of similar types—the HSFU-3 lamps om the SF-4 spectrophotometer)[1] and HLF-25 lamps om the vacuum spectrograph SP-66). Deuterium was tained by the electrolysis of heavy water in a special cuum apparatus. In order to obtain maximum intensity emission in the ultraviolet region of the spectrum round 2500 A and in the region 1608-1610 A) optimal essures of the gases in the lamps were selected. For uterium the optimum pressure was found to be 5 mm and for the hydrogen 3.5-4.0 mm Hg. The latter value in good agreement with the data found in foreign lit- ature[2] for hydrogen lamps of similar construction and wer. The selected pressures resulted in more or less e same drop in potential between the electrodes in all e lamps. With a discharge current of 0.3 amp it was the order of 80 volts. The lamps were operated from electronic stabilizers EPS-86 (from the spectropho- meters SF-4).

All the measurements were made with the help of o instruments: for the visible and long wavelength ul- aviolet regions of the spectrum (down to 2150 A) the ectrophotometer SF-4 was used, and for the short velength ultraviolet region (down to 1460 A) the mono- romator instrument SP-41 was utilized. As a measure intensity of emission in the first case the numerical lues of the reciprocals of the square of the width of e entrance slit in SF-4 were used, and in the second se—the registered values of an electrical device, ich were proportional to the current in the photomul- plier. The comparison of the effectiveness of emission as made in the following sequence: the Balmer lines ere measured first, followed by the long wavelength gion of the ultraviolet spectrum (3600-2150 A) and ally by its short wavelength region (2500-1460 A).

The Lines of Balmer Series. The intensities of three nes in the emission spectra from the deuterium lamps SFU-3 and DLF-25 and the hydrogen lamps HSFU-3 and LF-25 were measured on the spectrophotometer SF-4. was found that these lines were somewhat more in- nse in deuterium than in hydrogen. The average values the results of the measurements for all of the above- entioned lamps are shown in the Table.

Balmer lines	Wavelength (A)		Ratio of intensities of deuterium to hydrogen lines
	Hydrogen lamp	Deuterium lamp	
Red	6562.846	6561.063	1.29
Blue	4861.322	4859.992	1.11
Violet	4340.458	4339.27	1.37

The Long Wavelength Region of the Ultraviolet Spectrum. On the same instrument and for the same lamps, measurements of the distribution of intensities of the continuous ultraviolet emission were carried out in the 3600-2150 A spectral region. For this series of measurements the intensity of the emission by the HSFU-3 and HLF-25 lamps at 2500 A was conditionally taken to be 100% and the intensity of emission of deuterium and hydrogen as well as of other wavelengths were measured in relation to it. Figure 1 shows two curves characterizing the dependence of the intensity of continuous emission by deuterium and hydrogen on the wavelength. It is easy to see that deuterium is more effective than hydrogen in this region of the spectrum and that its percentage superiority in the intensity of emitted radiation is the greater the shorter the wavelength of the emission. Thus, if for λ = 2200 A deuterium is more effective than hydrogen by 50-60%, it is only more effective by 30% in the 3600 A region.

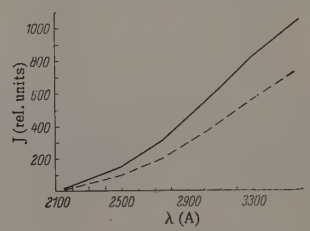

Fig. 1. Dependence of the relative intensity of emission by deuterium (solid line) and by hydrogen (broken line) on wavelength in the long wavelength region of the ultraviolet spectrum.

The Short Wavelength Region of the Ultraviolet Spectrum. Comparison of the intensities of ultraviolet emission in the 2500-1460 A interval for the lamps of types HLF-25 and DLF-25 was carried out on the monochromator of the SP-41 instrument. As in the previous case, the intensity of emission of the hydrogen lamps at 2500 A was conditionally taken to be 100% and the intensities of emission of deuterium and hydrogen, as well as of the other wavelengths, were determined with respect to it. Based on the averages of the experimental data, two curves were constructed illustrating the dependence of the emission of deuterium and hydrogen on the wavelength (Fig. 2). It is seen from this figure that deuterium is more effective than hydrogen not only in the 3600-2150 A region but even in the region further out in the ultraviolet (almost down to 1710 A). However, starting from a wavelength of 2220 A and shorter this greater effectiveness of the heavy isotope is rapidly lowered, and at around 1700 A both gases have practically the same intensity of emission. In the region of shorter wavelengths, up to the limit of the region investigated by us (1460 A), deuterium loses its greater effectiveness in the intensity of emission.

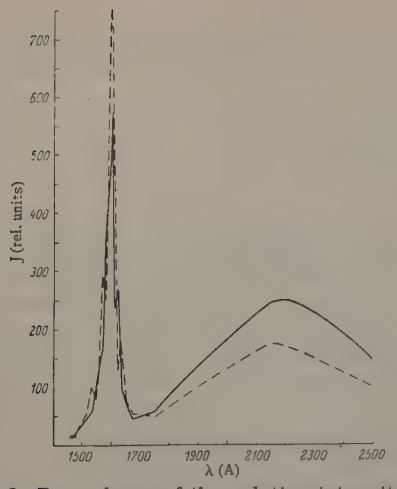

Fig. 2. Dependence of the relative intensity of emission by deuterium (solid line) and by hydrogen (broken line) on wavelength in the short wavelength region of the ultraviolet spectrum.

The results obtained in this work allow us to make the following conclusions.

1. The lamps enclosed in the bulbs carrying ultraviolet transmitting windows and therefore designed for the work in the near ultraviolet region (down to 2200 A must be constructed with deuterium filling. It must be noted that the advantage of deuterium over hydrogen in this case is especially important because the greatest superiority of deuterium in intensity was found to be near the limit of spectral transparency of the ultraviol transmitting window on the bulb. Therefore, the utiliza tion of deuterium lamps in spectral instruments will n only increase the accuracy of measurements but will also somewhat shift the working spectral ranges of the instruments towards the shorter wavelength region. T justifies the replacement of hydrogen HSFU-3 lamps b the new DSFU-3 lamps in the SF-4 spectrometers. Th experiments which have been carried out show that the DSFU-3 lamps are completely analogous to the old HS lamps as far as their durability and stability are concerned.

2. In many cases it is sensible to also fill with de terium those lamps whose bulbs are equipped with the fused quartz or sapphire windows.

3. The lamps with fluorite and lithium fluoride wi dows designed for the vacuum ultraviolet region shoul still be filled with ordinary hydrogen.

REFERENCES

1. S. I. Levikov and L. P. Shishatskaya, Opt. i Spektr. 688 (1959), Optics and Spectroscopy 6, 446 (1959).
2. O. Kern, Z. angew. Physik 12, 536 (1954).

CALCULATION OF THE C=O STRETCHING VIBRATION FREQUENCY FOR Cis- AND GAUCHE ISOMERS OF MOLECULES OF THE TYPE $ClCH_2-C\overset{O}{\underset{R}{}}$

V. G. Boitsov and Yu. Ya. Gotlib (pp. 691-693)

Received 24 April 1961

In studies made by Bellamy, Thomas, Norman, and Williams[1-3] dedicated to the investigation of infrared spectra of a number of compounds containing carbonyl groups, it was noted that these compounds have one absorption band in the solid state, corresponding to the C=O stretching vibration, whereas in the liquid state the spectra in the same frequency range show two bands; the shorter wavelength component of the doublet corresponds to the band observed in the solid state. It was shown that the relative intensity of the longer wavelength band increases at the expense of the intensity of the shorter wavelength band when the temperature rises and when there is a change from a less polar solvent to a more polar one.

It was suggested that the appearance of the long wavelength band in the liquid state was related to the presence of a second rotational isomer, and that the isomer associated with the higher frequency must be a more polarized form of the molecule. The latter assumption was related to the fact that solvents of high dielectric constant favor the more polar forms of rotational isomers.[3] In particular, the cis-form of chloracetophenone is more polar, where the chlorine atom is in the cis-position with respect to the oxygen atom. Thus, in refs. 1 and 2, a higher carbonyl frequency was associated with the cis-form and a lower frequency was associated with the gauche form (see Figure). In the opinion of several authors[1,2] the greater C=O frequency associated with the more polar form was related to the presence of induced intramolecular forces and dipole moments which alter the polarity of the C=O bond and thus influenced the carbonyl frequency.

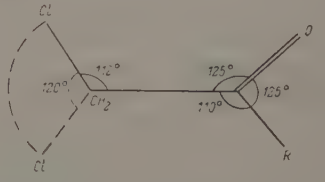

It seems natural, however, before relating the frequency shift during transition from the cis- to the gauche isomer with a change in the nature of the interactions in the magnitude of the force constants, to make sure that a similar shift cannot be obtained with the same force constants and a variation in the mechanics of vibration of two types of isomers. Reference 4 gives results of calculations of the relationship between skeletal vibration frequencies of $ClCh_2COCl$ and $BrCH_2COCl$ and the ang

rotation of the C—Cl bond around the CH_2—C bond, om which it is evident that the C=O frequency gradually creases during the change from a trans-position to a s-position between the halogen and the oxygen atom. he calculations were made on the assumption of the ass of the CH_2-group being concentrated in the C atom. roceeding from an analogous model we studied the re- tionship of the C=O stretching vibration frequency of a olecule of the type $ClCH_2-C\lessdot^{O}_{R}$ to the mass of the oup R (see Figure), the length of the C—R bond, and e force constants $F_{R...O}$ and $F_{C...R}$, which characterize e interaction of the group R with C and O atoms that e not bonded directly to it. The problem was solved th a Urey-Bradley potential field in which the potential nction for the given molecule has the form:

$$V=\frac{1}{2}[Kr_R+t_1^2(F'_{OR}+F'_{CR})+s_1^2(F_{OR}+F_{CR})](\Delta r_R)^2$$

$$\frac{1}{2}[Kr_C+s_0^2(F_{CR}+F_{OC}+F_{CCl})+t_0^2(F'_{CR}+F'_{OC}+F'_{CCl})](\Delta r_C)^2$$

$$+\frac{1}{2}[Kr_{Cl}+F'_{CCl}t_1^2+F_{CCl}s_1^2](\Delta r_{Cl})^2+\frac{1}{2}(Kr_O+F'_{OR}t_0^2+F_{OR}s_0^2$$

$$+F'_{OC}t_0^2+F_{OC}s_1^2)(\Delta r_O)^2$$

$$+\frac{1}{2}[H_{CCl}-F'_{CC}s_0s_1+F_{CCl}t_0t_1](\sqrt{r_{Cl}r_C}\Delta\alpha_{C-Cl})^2$$

$$+\frac{1}{2}(H_{OC}-F'_{OR}s_0s_1+F_{OC}t_0t_1)(\sqrt{r_Or_C}\Delta\alpha_{OC})^2$$

$$+\frac{1}{2}(H_{CR}-F'_{CR}s_0s_1+F_{CR}t_0t_1)(\sqrt{r_Cr_R}\Delta\alpha_{CR})^2$$

$$+\frac{1}{2}(H_{OR}-F'_{OR}s_0s_1+F_{OR}t_0t_1)(\sqrt{r_Or_R}\Delta\alpha_{OR})^2$$

$$F_{OR}s_0s_1-F'_{OR}t_0t_1)(\Delta r_O)(\Delta r_R)+(F_{CR}s_0s_1-F'_{CR}t_0t_1)(\Delta r_C)(\Delta r_R)$$

$$F_{OC}s_0s_1+F'_{OC}t_0t_1)(\Delta r_C)(\Delta r_O)+(F_{CCl}s_0s_1-F'_{CCl}t_0t_1)(\Delta r_C)(\Delta r_{Cl})$$

$$+\rho_1(F'_{OR}t_0s_1+F_{OR}s_0t_1)\sqrt{r_Or_R}(\Delta r_O)(\Delta\alpha_{OR})$$

$$+\rho_2(F'_{OR}t_1s_0+F_{OR}s_1t_0)\sqrt{r_Cr_R}(\Delta r_R)(\Delta\alpha_{OR})$$

$$+\rho_3(F'_{CR}t_0s_1+F_{CR}s_0t_1)\sqrt{r_Rr_C}(\Delta r_C)(\Delta\alpha_{CR})$$

$$+\rho_4(F'_{CR}t_1s_0+F_{CR}s_1t_0)\sqrt{r_Cr_R}(\Delta r_R)(\Delta\alpha_{CR})$$

$$+\rho_5(F'_{OC}t_0s_1+F_{OC}s_0t_1)\sqrt{r_Or_C}(\Delta r_C)(\Delta\alpha_{CO})$$

$$+\rho_6(F'_{OC}t_1s_0+F_{OC}s_1t_0)\sqrt{r_Cr_O}(\Delta r_O)(\Delta\alpha_{CO})$$

$$+\rho_7(F'_{CCl}t_0s_1+F_{CCl}s_0t_1)\sqrt{r_{Cl}r_C}(\Delta r_C)(\Delta\alpha_{CCl})$$

$$+\rho_8(F'_{CCl}t_1s_0+F_{CCl}s_1t_0)\sqrt{r_Cr_{Cl}}(\Delta r_{Cl})(\Delta\alpha_{CCl}).$$

re

$$\rho_1=\sqrt{\frac{r_R}{r_O}},\quad \rho_2=\sqrt{\frac{r_O}{r_R}},$$

$$\rho_3=\sqrt{\frac{r_R}{r_C}},\quad \rho_4=\sqrt{\frac{r_C}{r_R}},$$

$$=\sqrt{\frac{r_O}{r_C}},\quad \rho_6=\sqrt{\frac{r_C}{r_O}},\quad \rho_7=\sqrt{\frac{r_{Cl}}{r_C}},\quad \rho_8=\sqrt{\frac{r_C}{r_{Cl}}},$$

ere r_R, r_O, r_C, r_{Cl} are the equilibrium lengths of the rresponding bonds

$$s_0=\frac{(r_O-r_R\cos\alpha_{OR})}{a},\quad s_0=\frac{r_C-r_R\cos\alpha_{CR}}{b},$$

$$s_1=\frac{r_R-r_O\cos\alpha_{OR}}{a},\quad s_1=\frac{r_R-r_C\cos\alpha_{CR}}{b},$$

$$t_0=\frac{r_R\sin\alpha_{OR}}{a},\quad t_0=\frac{r_R\sin\alpha_{CR}}{b},$$

$$t_1=\frac{r_O\sin\alpha_{OR}}{a},\quad t_1=\frac{r_C\sin\alpha_{CR}}{b}\ \text{и т. д.},$$

where a, b, c, d are the distances between the atoms which are not bonded directly (correspondingly O...R, C...R, C...O, C...Cl). The angles between the bonds were assumed to be the following: Cl—CH_2—C = 112°; CH_2—C=O = 125°; CH_2—C—R = 110°; O=C—R = 125°. The values for the force constants were taken from ref. 4. The force constants were varied from maximum to minimum values for atoms not bonded directly; this data also was taken from ref. 4. The results of the calculations are shown in the Table, from which it follows that the frequency corresponding to the cis-form is always greater than that corresponding to the gauche form for compounds of the type under study. For the case $m_R = m_{Cl}$ and $r_R = r_{Cl}$ we obtain 1760 cm^{-1} for the cis-form and 1743 cm^{-1} for the gauche form, which is in good agreement with the results from ref. 4. For $m_R = m_C$ and $r_R = r_C$ we obtain 1757 cm^{-1} for the cis-form and 1745 cm^{-1} for the gauche form, which agrees well with the relationships established by Bellamy[3] and contradicts those of Mizushima.[5] Thus the shift in C=O stretching vibration frequency which we observed experimentally for the change from the cis- to the gauche isomer of compounds of the type $ClCH_2-C\lessdot^{O}_{R}$ may be explained by the assumption of unchanged force constants and a variation in kinematic coefficients. Thus, from the observed value of frequency shift in the type of vibration studied, it is still not possible to draw any definite conclusions about changes in properties of the bonds (polarity, polarizability, etc.)

m_R	r_R (A)	$F_{O...R}$	$F_{C...R}$	ν (cm^{-1}) Cis-form (calc.)	Gauche form (calc.)	Cis-form (exptl.)	Gauche form (exptl.)
12	1.54	0.4	0.4	1757	1745	1745 [3]	1725 [3]
		0	0	1721	1715		
72	2.93	0.4	0.4	1749	1734		
		0.1	0.1	1714	1706	1697 [1]	1682 [1]
		0.1	0	1720	1710		
		0	0	1712	1709		
35	1.77	1	1	1724	1697		
		1	0.1	1745	1733	1814 [1]	1780 [1]
		0.4	0.4	1760	1743		
		0.1	0.1	1734	1712		

REFERENCES

1. L. J. Bellamy and L. C. Thomas, J. Chem. Soc. 3704 (1956).
2. J. R. Norman, Can. J. Chem. 36, 1020 (1958).
3. L. J. Bellamy and R. L. Williams, J. Chem. Soc. 4294 (1957).
4. S. Nakagawa, S. Schishima, K. Kuratani, T. Miyazawa, T. Simanouchi, and S. Mizushima, J. Chem. Phys. 20, 1720 (1952).
5. S. Mizushima, T. Simanouchi, T. Miyazawa, and I. Ichishima, J. Chem. Phys. 21, 815 (1953).

EXCITON RELAXATION TIMES IN MOLECULAR CRYSTALS

A. S. Selivanenko (p. 694)

Received 9 May 1961

When light interacts with a crystal, excitons may be formed in the latter, with a momentum equal to that of the light wave (see refs. 1 and 2, for example). In general, the kinetic energy of such an exciton is not equal to the mean thermal energy of the crystal. The exciton will therefore come into thermal equilibrium with the crystal by interacting with lattice vibrations.

When the minimum of the exciton band does not coincide with the value of the exciton momentum, which is equal to zero, and the band is sufficiently wide (that is, its width $\Delta\varepsilon \gg kT$), we can easily estimate the relaxation time or the time required to establish thermal equilibrium between the exciton and the phonons. A similar problem has been solved for electrons in a semiconductor.[3] The equations for the scattering probability of an exciton by phonons are well known.[4] As in ref. 3 the problem reduces to the solution of the kinetic equation*:

*In Eq. (1), for simplicity we have immediately dropped the term describing the diffusion current of electrons in energy space. It was shown in ref. 3 that in estimating the relaxation time from states with energy $\varepsilon \gg kT$, it is permissible to confine one's attention to the term describing spontaneous emission of phonons.

$$\frac{\partial f(\varepsilon)}{\partial t} = \frac{1}{p}[G(\varepsilon) f(\varepsilon)]. \qquad (1)$$

Here, $f(\varepsilon)$ is the distribution function of the exciton over energy ε and p is the exciton momentum.

$$G(\varepsilon) = \frac{a^3\mu}{(2\pi)^2\hbar^4}\int_0^{2p} \frac{\pi e^4}{4\hbar} \cdot \frac{1}{\Omega_{qj}} \cdot F \cdot 36q^2a^2 \cdot \hbar\Omega_{qj} q dq, \qquad (2)$$

where a is the lattice constant, μ is the effective mass of the exciton, e is the electronic charge, and Ω_{qj} is the lattice vibration frequency with momentum q of the j-th branch,

$$F \approx \frac{3}{M}\left[\frac{\pi\hbar\gamma}{m\omega}\right]^2 \frac{1}{a^3}.$$

In the last equation, γ is the oscillator strength of the electronic transition with frequency ω for the exciton, m is the mass of an electron and M is the mass of the whole molecule in the crystal. By carrying out the necessary calculations, we arrive at the differential equat

$$\frac{dE}{dt} = -BE^{\frac{3}{2}}.$$

In Eq. (3) E is the mean energy of the relaxing exciton and

$$B = 420\sqrt{2}\,\frac{\mu^{\frac{5}{2}}}{Mm^2}\,\frac{e^4}{(\hbar\omega)^2}\,\gamma^2\,\frac{1}{a^3},$$

with the same notation as before. By solving Eq. (3) we can determine the relaxation time. For an estimate we will put $m \sim \mu \sim 10^{-27}$ gm; $\hbar\omega \sim 2$ ev; $\gamma \sim 0.1$; $a \sim 7 \times 1$ cm; $M \sim 10^{-22}$ gm. Then the relaxation time of an exci from energy $E \gg kT$ to thermal (room temperature) $E \sim kT$ is $\sim 5 \times 10^{-10}$ sec.

Finally, we note that Eq. (3) agrees with Eq. (7) in ref. 3 to within the value of the constant B. For an exciton, however, the relaxation rate is independent of th type of lattice vibration, since the exciton charge is ze and its interactions with optical and acoustical phonons are identical.

The author thanks O. N. Krokhin and Yu. M. Popov for valuable discussions.

REFERENCES

1. H. Haken, Uspekhi Fiz. Nauk **68**, 565 (1959); Fortsc Physik **6**, 271 (1959).
2. I. I. Hopfield, Phys. Rev. **112**, 1555 (1958).
3. O. N. Krokhin and Yu. M. Popov, Zhur. Eksper. i Teoret. Fiz. **38**, 1589 (1960), Soviet Phys.-JETP **11** 1144 (1961).
4. V. M. Agranovich and Yu. V. Konobeev, Opt. i Spekt **6**, 242 (1959), Optics and Spectroscopy **6**, 155 (1959)

ANOMALOUS RATIO OF THE HFS COMPONENT INTENSITIES OF INDIUM LINES

Yu. I. Turkin and M. P. Chaika (p. 695)

Received 9 June 1961

The anomalous values of the hyperfine structure (hfs) ponent intensities of thallium, mercury, and cadmium s have been investigated in refs. 1-4. A comparison ll observed data led us to conjecture that an analogous ct might occur for all hfs component terms having a ilar structure. Such an anomaly was actually detected erimentally in the hfs of the indium resonance line.

The light source used consisted of a liquid air-cooled ow cathode 6 mm in diameter and 20 mm long, con- ing metallic indium. The current was varied between nd 190 ma. The line structure was recorded by ns of a spectrometer with a Fabry-Perot etalon.

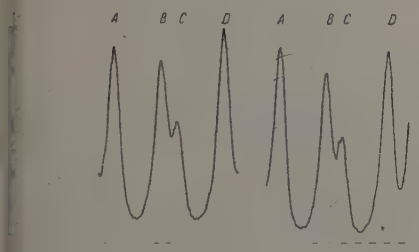

Hyperfine structure of the 4101.8 A indium line. Current (in ma): a—50; b—10.

The relative hfs component intensities of the 4101.8 A indium line ($6s^2S_{1/2}$-$5p^2P_{1/2}$) should be as A : B : C : D = 1 : 0.67 : 0.36 : 1, according to the corresponding transition probabilities. We observed this ratio at relatively small current values. As the current was increased above 20 ma, the hfs component intensities deviated appreciably from this ratio. The most pronounced change was observed for the outside components A and D, which had the same initial intensity (see the Figure). The initial term corresponding to this line ($6s^2S_{1/2}$) cannot be responsible for the observed anomaly, in view of the relative hfs component intensities of In I 4511 A, which corresponds to the same upper level ($6s^2S_{1/2}$).

The violation of the hfs intensity rule in the case of the indium line is much less serious than in the case of Tl I 3775.7 A. This is a consequence of the larger F-values of the sublevels of the indium ground state.

REFERENCES

1. S. Frisch, Z. Physik 68, 758 (1931).
2. E. Lau and O. Reichenheim, Naturwissenschaften 20, 49 (1932).
3. H. Schüler and J. Keyston, Z. Physik 67, 433 (1931).
4. Yu. I. Turkin, Opt. i Spektr. 7, 10 (1959), Optics and Spectroscopy 7, 5 (1959).

ANNOUNCEMENT

THE JOURNAL OF QUANTITATIVE SPECTROSCOPY AND RADIATIVE TRANSFER*

*Translation editor's note: this Announcement has been corrected and brought up to date by the Editor of JQSRT.

Since September 1961, Pergamon Press Ltd. (Head- ón Hill Hall, Oxford, England) has published a new rnational journal, The Journal of Quantitative Spec- copy and Radiative Transfer. Articles may be pub- ed therein in English, French, and German as well Russian. Papers dealing with the following subjects a preferred publication outlet in JQSRT: theoretical experimental determinations of f-numbers or ab- te intensities for atomic and/or molecular systems; retical and experimental studies on spectral line shapes and widths; emissivities of heated gases, liquids, and solids; flame temperatures and flame emissivities; emission of radiation from heated gases, liquids, and solids and long-range detection of radiating sources; quantitative spectroscopic techniques for environmental studies, particularly those related to rocket flights and satellite exploration; shock-tube studies in which the emphasis is on quantitative spectroscopy; radiant energy emission from plasmas; etc.

Complete series of issues and separate issues of the journal Optika i Spektroscopiya (Optics and Spectroscopy) for the years 1956, 1957, 1958, 1959, and 1960 are available for sale. Orders including payment should be directed to the bookstore "Books-by-Mail," Bol'shoi Cherkasskii per., d 2/10, Moscow.

AKADEMKNIGA

Sixth Year of Publication

The Journal is published monthly, 2 volumes per year (six issues in each volume).

SPECTROSCOPIC INVESTIGATION OF A HIGH FREQUENCY DISCHARGE IN NEON

O. P. Bochkova, L. P. Razumovskaya, and S. E. Frish (pp. 697-705)

Received 16 March 1961

The optical and electrical characteristics of the electrodeless high frequency (hf) discharge in neon at a frequency of 6 Mc were investigated by the reabsorption and two-probe methods. Investigations were made in discharge tubes 3.5, 12, 40, and 60 mm in diameter, and 130 to 300 mm long. Data were obtained on the populations of the $2p^5 3sX$ and $2p^5 3pY$ levels in neon as a function of pressure and electron concentration. Measurements of electron and gas temperatures were made. Processes leading to the formation and destruction of atomic excited states are discussed. The hf discharge is compared with the direct current discharge.

INTRODUCTION

The high frequency discharge has been widely used of late as a light source for various optical investigations and the spectral analysis of gases.[1,2] It therefore seemed of interest to study the mechanism of atomic excitation in this type of discharge.

The electrical characteristics of the hf discharge at frequencies of from 1 to 10 Mc have been studied by many authors,[3-5] but as a rule, these observations were not supplemented by optical measurements. On the other hand, Harrison's[6] recent spectroscopic investigations of the hf discharge in helium were not accompanied by electrical measurements of any kind. In the present paper, an attempt is made to conduct simultaneous spectroscopic and electrical measurements, and to compare then with each other, as well as with the results of measurements in the positive column of the dc discharge.

SPECTROSCOPIC MEASUREMENTS

The studies of the spectroscopic characteristics of the electrodeless hf discharge in neon were conducted with cylindrical discharge tubes made of molybdenum glass. These tubes were 3.5, 12, 40, and 60 mm in diameter, and 130 to 300 mm long. The hf voltage was supplied to the external electrodes of the tube by a 6 Mc oscillator (350 watts). The 60 mm diam tube had sealed-on windows and was 130 mm long. The external electrodes were cylindrical and were fitted loosely onto the ends of the discharge tubes which were connected to a high-vacuum apparatus of the usual type; the mercury vapors were frozen out in liquid air traps. The investigations were conducted with natural neon which contained no more than 0.3% helium; the remaining impurities (O_2, H_2, N_2) did not exceed 10^{-3}%.

The measurements were made in the visible (red) part of the spectrum. The population of lower levels $2p3s\,^3P_{0,1,3}$ and $^1P_1$ of neon (Fig. 1) was determined by the method of reabsorption which was used in its simplest form, in which the length of the absorbing column is changed by reflecting the light from a mirror placed behind the tube.[6,7] The reabsorption measurements in the 3.5, 12, and 40 mm diam tubes were made across the emitting column; in the 60 mm diam tube—end on. As we have shown previously, measurements of reabsorption made along and across the discharge tube agreed within experimental error.

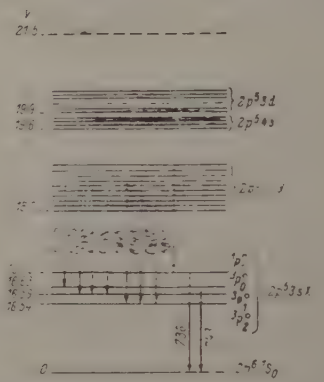

Fig. 1. Diagram of the main levels in neon (Ne I).

In calculating the concentration of the excited at we used Ladenburg's[8] values for the oscillator stren The absolute value of the oscillator strength of Ne 6 was assumed to be 0.5. This value cannot be conside exact and differs greatly from the results of Griffith measurements.[9] However, we feel that Griffiths' val too low, and believe that Ladenburg's value $f_{6402} = 0.$ approximately correct. Thus, it should be kept in m that the absolute values of the concentrations of exci atoms are accurate only as to the order of magnitud The relative values of the concentrations of the exci atoms of neon are more accurate since the relative of the oscillator strengths f of neon lines are known fairly well.

All optical measurements were made with the I spectrograph, using a camera with a focal length of 270 mm. The grating monochromator was made in t NIFI Experimental Workshops of Leningrad State Un versity (600 grooves/mm, ruled area 65 × 75 mm, 600 mm). The line intensity measurements were ma the photoelectric method, using an FEU-19, a bridge amplifying circuit, and a microammeter. Only the s called "strong" discharge was studied.[10]

The gas temperature, which is needed for calcu ting the concentration of excited atoms by the reabs tion method, was determined by the Doppler width o lines. For this purpose, we recorded the profiles of lines λ 6096, 5852, and 6304 A with the aid of 15, 25 30 mm Fabry-Perot etalons. In measuring the Dopp width of the lines, a correction was made for the br

g due to reabsorption.[11] The profiles of the neon are asymmetric because of the presence of the isotope Ne^{22}. In order to avoid the error resulting from the half-width of the line was determined using the stortted half of the profile. The temperature values ned did not exceed 300-600°K and, so far as we could changed little with changing excitation conditions. A ll increase in temperature (approximately 100°) was rved when the gas pressure in the tube increased. A ease in tube diameter from 60 to 12 mm caused an ease in temperature of approximately 150°. In calting the concentration of excited atoms, the temture was assumed to be 500°K in all cases.

Next, the absolute intensities of several neon lines e measured by comparison with the radiation of a rated ribbon filament lamp. The effect of reabsorpwas taken into consideration. Using the intensities determined, the concentrations of the excited atoms e upper $2p^53pY$ levels were found.

The results of the concentration measurements of the ed neon atoms are given below, along with a comparwith probe measurement data.

BE MEASUREMENTS

Along with the optical measurements, and under the e discharge conditions, the electron temperature T_e he electron concentration n_e were measured by the probe method. For this purpose, molybdenum probes nm in diameter and 5 mm long were sealed into the the probes were placed at the center of the tubes eir axes, the distance between the probes being 15 . The electron temperature T_e was determined from robe characteristics by the method of Johnson and er,[12] and the electron concentration n_e according gan and Perel',[13,14] calculated for the cases of low medium pressures, respectively.

The electron temperature T_e and electron concenon n_e were measured in discharge tubes of various eters and at different pressures and power levels. results of these measurements are given in Figs. The generator power is given in arbitrary units of pling" of the hf circuit with the electrodes of the harge tube. A change of the coupling from one to ten esponds to a linear increase of the total current

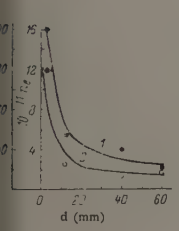

Fig. 2

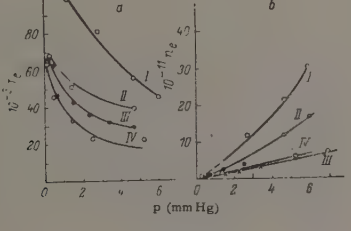

Fig. 3

Fig. 2. Dependence of the electron temperature T_e (curve 1) and electron concentration n_e (curve 2) on the diameter of the discharge tube. Coupling = 6; pressure = 1.3 mm Hg.

Fig. 3. Dependence of electron temperature T_e (a) and electron concentration n_e (b) on pressure. Tube diameters (in mm): curves I—3.5; curves II—12; curves III—40; curves IV—60. Coupling = 6.

(conductance current plus displacement current) and the voltage. Under the conditions of our experiments, the voltage at the tube electrodes ranged from 400 to 1500 volts; the total current ranged from 100 to 500 ma. It was not known what fraction of the total current should be attributed to the current passing through the luminous gas plasma. The degree of ionization of the plasma in no case exceeded 10^{-2}%.

The measurement of the electron concentration at various degrees of coupling of the hf circuit with the tube electrodes permits us to eliminate the "coupling" as a parameter characteristic of the discharge, and instead to consider the dependence of the concentration of excited atoms on n_e alone.

As the diameter of the discharge tube increases the electron temperature T_e and electron concentration n_e decrease. For small diameters this decrease is rapid (Fig. 2), but for $d > 20$ mm, T_e and n_e depend only slightly on tube diameter.

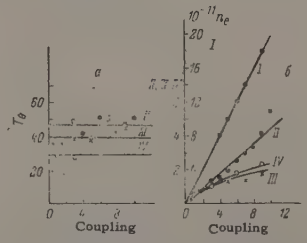

Fig. 4. Dependence of electron temperature T_e (a) and electron concentration n_e (b) on degree of coupling. Tube diameters (in mm): curve I—3.5; curves II—12; curves III—40; curves IV—60. Pressure p = 1.3 mm Hg.

A similar dependence of T_e and n_e on tube diameter was observed by Zaitsev and Yankovskaya in a dc discharge.[15]

Figures 3 and 4 show T_e and n_e as a function of gas pressure and the degree of coupling between the hf circuit and the electrodes. As the pressure increases, the electron temperature decreases and n_e increases. When power is increased by changing the coupling, the electron concentration increases but the electron temperature remains constant, within experimental error.

Figure 5 shows the electron temperature T_e and electron concentration n_e in the positive column of a dc discharge as a function of current in a 30 mm diam tube. It can be seen that the electron temperature T_e decreases somewhat with increasing current density at low currents. The electron concentration n_e increases with increasing current density, the rate of increase being larger, the higher the gas pressure in the tube. These results agree well with the numerous measurements of T_e and n_e obtained in the dc discharge by other authors.[14-16]

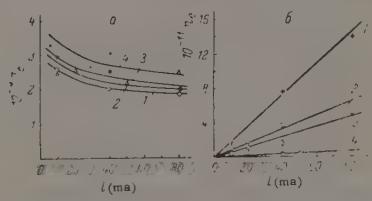

Fig. 5. Dependence of electron temperature T_e (a) and electron concentration n_e (b) on current in a dc discharge at various pressures p (mm Hg): curves 1—4.6, curves 2—2.1; curves 3—1.1; curves 4—0.7.

CONCENTRATION OF EXCITED ATOMS

The results of concentration measurements of excited neon atoms in a hf discharge for the $2p^5 3sX$ and $2p^5 3sY$ levels are given in Figs. 6 to 8. Figure 6 shows the dependence of the concentration of excited atoms on pressure in discharge tubes with diameters of 3.5, 12, and 60 mm. As the pressure changes, the concentration of excited atoms shows a maximum in all tubes, which is in agreement with the observations of other authors in the dc discharge.[17] This maximum occurs at somewhat higher pressures for the $2p^5 3pY$ levels than for the $2p^5 3sX$ levels.

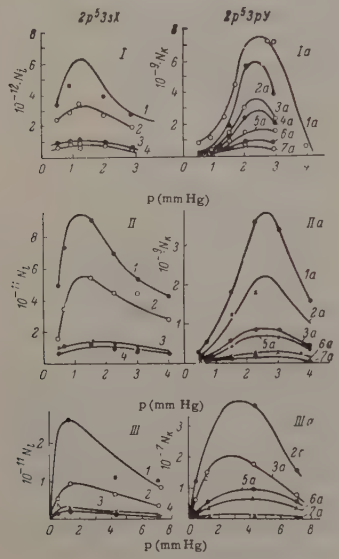

Fig. 6. Dependence of concentration N_i, N_k of excited neon atoms on pressure in tubes of various diameters (d). I, Ia—d = 3.5 mm, coupling = 8; II, IIa—d = 12 mm, coupling = 9-10; III, IIIa—d = 60 mm, coupling = 6. Levels: curves 1—$^3P_2$; curves 2—$^3P_1$; curves 3—$^1P_1$; curves 4—$^3P_0$; curves 1a—$^3S_1$; curves 2a—$^3D_2$; curves 3a—$^1D_2$; curve 4a—$^3P_2$; curves 5a—$^3D_1$; curves 6a—$^3P_1$; curves 7a—$^1S_0$.

In a narrow tube with a diameter of 3.5 mm, a stable discharge appears only at relatively high degrees of coupling between the hf circuit and the external electrodes; under these conditions the electron concentration is greater than 10^{12} cm^{-3}.

The metastable $2p^5 3s^3P_2$ level is the most densely populated in all of the tubes. The metastable $2p^5 3s^3P_0$ level is populated less densely—to about the same degree as the emitting level $2p^5 3s^1P_1$. For all cases except the $2p^5 3pY$ levels in a narrow tube, it is very characteristic that the increase in concentration of excited atoms with increasing electron concentration is retarded at high electron concentrations. The retardation occurs earlier in wider tubes. The population of the $2p^5 3s^3P_2$ and $2p^5 3s^3P_1$ levels in tubes of 12 mm diam even shows a decrease at electron concentrations $n_e > 3 \times 10^{11}$ cm^{-3}. The population of the $2p^5 3pY$ levels in the same tube increases approximately as the square of n_e at low electron concentrations ($n_e < 2 \times 10^{11}$ cm^{-3}).

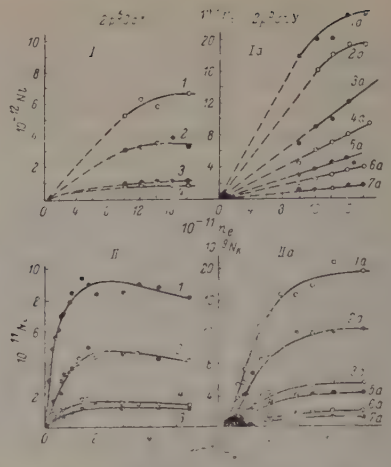

Fig. 7. Dependence of concentrations N_i, N_k of excited neon atoms on electron concentration n_e in tubes with various diameters. Pressure p = 1.3 mm Hg. I, Ia—d = 3.5 mm; II, IIa—d = 12 mm. For curve designations see Fig. 6. The dependence of the concentration of excited atoms on electron concentration n_e at 1.3 mm Hg is given in Fig. 7.

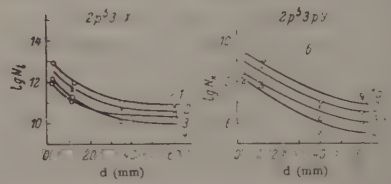

Fig. 8. Dependence of concentrations N_i, N_k of excited neon atoms on tube diameter d, pressure p = 1.3 mm Hg, coupling = 6. Levels: curve 1—$^3P_2$; curve 2—$^3P_1$; curve 3—$^3P_0$; curve 4—$^1P_1$; curve 1a—$^3D_2$; curve 2a—$^1D_2$; curve 3a—$^3P_1$; curve 4a—$^1S_0$.

Figure 8 shows the concentration of excited neon atoms in the states $2p^5 3sX$ and $2p^5 3pY$ as a function of the diameter of the discharge tube. The discharge was produced at the same neon pressure p = 1.3 mm Hg and at the same coupling of the hf circuit with the electrode. It can be seen that the population of all levels increases rapidly with decreasing tube diameter (the ordinate scale is logarithmic!). The population of the $2p^5 3pY$ levels increases faster. While the population of the $2p^5 3pY$ levels in a 60 mm tube is 3 or 4 orders of magnitude smaller than the population of the $2p^5 3sX$ levels, this ratio is only approximately two orders of magnitude smaller in a 3.5 mm tube.

For comparison, we give the results of measurements of concentration of excited neon atoms in the dc discharge. Figure 9 gives the concentration of excited atoms in the $2p^5 3sX$ and $2p^5 3pY$ states as a function of electron concentration in the positive column of a dc discharge. The data are given for pressures of 0.6 and 1 mm Hg. The $2p^5 3s^3P_2$ level is the most densely populated of all the $2p^5 3sX$ levels, just as it is in the hf discharge. The population of the $2p^5 3s^3P_0$ level is lowest at a pressure of 4.5 mm Hg and at low current densities; it is up to three times smaller than the population of the $2p^5$

. As the current density increases, the population e $2p^53s^1P_1$ level increases, and for $n_e > 8 \times 10^{11}$ is larger than the population of the $3p^53s^3P_0$ level. .6 mm Hg, the population of the $2p^53s^1P_1$ level is ller than that of the $2p^53s^3P_0$ level over the whole e of electron concentrations investigated. The dif- nce in behavior of the $2p^53sX$ and $2p^53pY$ levels is ficant; for the former, at high n_e there is a retarda- of the growth (and even a decrease) in the concentra- of excited atoms with increasing n_e, in both the dc harge and the hf discharge. However, the concentra- of the excited atoms in the $2p^53sY$ states increases n_e over the whole range of electron concentrations stigated; at low pressure (p = 0.6 mm Hg) the in- se is linear.

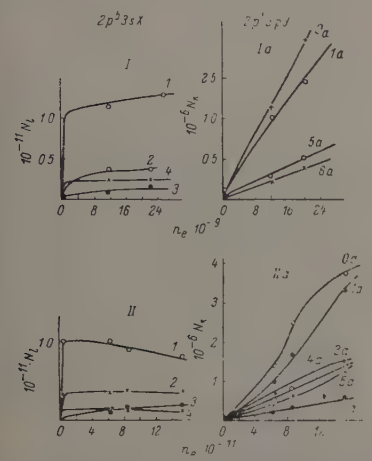

Fig. 9. Dependence of concentrations N_i, N_k of excited neon atoms on electron concentra- tion n_e in a dc discharge. Pressure: I, Ia— p = 0.6 mm Hg; II, IIa—p = 4.5 mm Hg. Tube diameter d = 3.5 mm. Designation of curves: curve 0a—$^3D_3$; for the remainder, see Fig. 6.

The population of the $2p^53sY$ levels is four to five rs of magnitude lower than the population of the sX levels. Thus the high levels are less densely lated in the dc discharge than in the hf discharge. The above data on the populations of levels are in a l agreement with investigations of the dc discharge.[17]

USSION OF RESULTS

Comparison of the electrical and optical characteris- of the hf discharge in neon shows that a hf discharge haracterized by a high concentration of excited atoms. reabsorption of radiation is observed even at low ssures and current densities. In narrow tubes, the re- rption is noticeable for lines whose lower levels are relatively high levels belonging to the electron con- ration $2p^53p$.

Nevertheless, the absolute concentrations of the ted atoms are three or four orders of magnitude r than the equilibrium concentration corresponding temperature equal to the electron temperature. ations from equilibrium are also indicated by the that the concentration ratios of the excited states in $2p^53sX$ states differ greatly from the ratios of the esponding statistical weights of the levels (at high tron temperatures, the concentration ratio should be close to the ratio of the statistical weights of the levels). The ratios of the statistical weights of the $2p^53s^3P_2$, $^3P_1$, $^3P_0$, and $^1P_1$ levels are 5:3:1:3. However, according to the experimental data, the populations of the $^3P_0$ and $^1P_1$ levels are almost equal under most conditions, and the population of the $^3P_1$ level is higher than that of the $^1P_1$ level. The $^3P_2$ level is the most densely populated. It can also be seen from these data that there is no significant difference between the populations of the emitting and the metastable levels.

For a stationary process, the population of each of the levels N_i is determined by the condition that the number of excitation processes ΔN_i equal the number of destruction processes $\Delta N_i'$ per unit time.[18] Under our conditions the levels are populated essentially through the following processes: (1) direct and steplike excitation by collisions of the first kind with electrons; (2) transitions between the levels due to the collisions of the second kind with electrons and atoms; (3) spontaneous transitions from higher levels; (4) absorption of emission. The depolation of levels is due essentially to the following processes: (1) spontaneous emission; (2) transition to higher levels due to collisions of the first kind with electrons; (3) transition between the levels due to collisions of the second kind with electrons and atoms; (4) triple collisions; (5) collisions with the walls. We shall neglect the latter, since the mean free path under our conditions is considerably smaller than the radius of the discharge tube.

A quantitative estimation of the processes of excitation and deactivation is not possible because of lack of sufficient data on transition probabilities and effective cross sections for collision. Nevertheless, some qualitative conclusions can be made and compared with the results of other authors.

First of all, it should be noted that the small difference between the populations of the emitting $2p^53s^1P_1$, $^3P_1$ levels and the metastable $2p^53s^3P_0$, $^3P_2$ levels can be explained by two factors, in agreement with the Phelps' data[19]: by the "imprisonment" of the λ 736 and λ 743 A resonance radiation and by collisions of the second kind with atoms and electrons producing transitions between the metastable and emitting levels. The "imprisonment" of the resonance radiation leads to an increase in the mean lifetime of the emitting states $^1P_1$ and $^3P_1$; the collisions of the second kind lead to a decrease in the lifetime of the metastable states $^3P_0$ and $^3P_2$. As a result, the mean lifetimes become equalized, and since the number of the excitation processes per unit time do not differ appreciably for these four levels ($2p^53s^3P_{0,1,2}$, $^1P_1$), their populations do not differ much from each other.

Next we shall consider the dependence of the population of levels on electron concentration n_e. The number of excitation processes due to collisions of the first kind with electrons is proportional to n_e for direct excitation, and to n_e^2 for steplike excitation. At low pressures and current densities, the concentration of the excited atoms is proportional to the number of acts of excitation. We may expect, then, that $N_i \approx n_e$ for the $2p^53sX$ levels and $N_k \sim (an_e + bn_e^2)$ for the $2p^53pY$ levels. Actually, these relationships do hold at low electron concentrations n_e. The quadratic dependence of the concentration of excited atoms in $2p^53pY$ states on n_e permits determination of the ratio of the effective cross sections Q_{0i} and Q'_{ik} corresponding to the transitions $2p^6\ ^1S_0 \rightarrow 2p^53pY$ and $2p^53sX \rightarrow 2p^53pY$ (Fig. 1). We have approximately

$$N_k \sim N_0 n_e f_1(T_e) Q_{0i} + N_i n_e f_2(T_e) Q'_{ik}, \qquad (1)$$

where N_0 is the concentration of atoms in the $2p^6\ ^1S_0$ state, N_i is the concentration of atoms in the $2p^5 3sX$ state, and $f_1(T_e)$ and $f_2(T_e)$ are functions of the electron temperature.[18] An estimation according to formula (1) leads to the result that, for neon, Q'_{ik} is approximately two orders of magnitude larger than Q_{0i}. The calculation was made on the assumption of a Maxwell velocity distribution for electrons. However, for neon there is a deviation from the Maxwell distribution, according to data of Kagan and Lyagushchenko[20]: the curve for the velocity distribution of electrons in the range of high velocities decreases considerably faster than according to Maxwell's law. Then the ratio Q'_{ik}/Q_{ik} will be smaller.

Taking account of this deviation from the Maxwell velocity distribution for electrons is very important in comparing data on the excitation of atoms with data on electron temperatures measured by the probe method. The reason for this is as follows: The deviations from the Maxwell distribution are noticeable mainly at higher velocities, i.e., in the "tail" of the distribution curve. Probe characteristics, on the other hand, are determined by electrons whose velocities are close to the most probable velocity. As a result of this, the "tail" of the distribution has little effect on the form of the probe characteristics, or, consequently, on the observed value of the electron temperature T_e. The excitation of neon levels, the critical potentials for which are large, is due mainly to the "tail" of the distribution curve. Thus the deviations from Maxwell's law may have little effect on probe characteristics, but at the same time may strongly influence the process of excitation of neon atoms.

This situation is well illustrated by the experimental data. When the pressure increases, there is a large change in the mean electron energy and velocity distribution. At the same time, this also affects the electron temperature T_e which decreases with the increasing p (Fig. 3), as well as the concentration of the excited atoms, which shows a pronounced maximum with increasing pressure (Fig. 6).

The mean electron energy shows little dependence on electron concentration: the electron temperature T_e as determined by the probe method shows almost no dependence on n_e (Fig. 4). On the other hand, the atomic concentrations, as mentioned before, show saturation and even decrease with increasing n_e (Fig. 7). This dependence of N_i on n_e cannot be explained by destructive collisions with electrons: according to Phelps' data,[19] the destruction of the $2p^5 3s\ ^3P_2$ level occurs practically only because of collisions of the second kind with neutral atoms; according to the experimental data, the $2p^5 3s\ ^3P_2$ level displays the same dependence on n_e as other $2p^5 3sX$ levels do. The saturation and the decrease in the concentration of excited atoms can be explained by a change in the electron velocity distribution. As n_e increases, the ratio E/p in the gas-discharge plasma also increases (E is the field strength). According to the calculations of Kagan and Lyagushchenko, an increase of E/p in neon leads to a considerable decrease in the relative number of fast electrons. As a result, the increase in the number of excited atoms at the $2p^5 3sX$ level is retarded, in spite of the increase in the electron concentration n_e. This phenomenon is less pronounced for the $2p^5 3pY$ levels, because for them the steplike excitation plays an important role.

In conclusion, it should be noted that the well-known properties of the hf discharge explain its applicability in the spectral analysis of gases. The conditions of excitation in the hf discharge can easily be varied by changing the pressure, discharge current, and diameter of the discharge tube. This permits the choice of the most advantageous condition of luminescence for each particular spectral-analytical problem. A high "effective" temperature can be realized in narrow discharge tubes, making it possible to excite small amounts of impurities which are difficult to excite in the presence of easily excited major components.

REFERENCES

1. W. F. Meggers and F. O. Westfall, J. Research Nat. Bur. Standards **44**, 447 (1950).
2. A. T. Forrester, K. A. Gundmundsen, and P. O. Johnson, J. Opt. Soc. Am. **46**, 339 (1956).
3. Kh. A. Dzherpetov and G. M. Pateyuk, Zhur. Eksp. i Teoret. Fiz. **28**, 343 (1955).
4. S. M. Levitskii and I. P. Shashurin, Radiotekh. i Elektron. **4**, No. 8, 1238 (1959).
5. V. V. Avramov and Kh. A. Dzherpetov, Vestnik Moskov. Univ. No. 3, 55 (1960).
6. J. A. Harrison, Proc. Phys. Soc. **73**, 841 (1959).
7. S. E. Frish and O. P. Bochkova, Vestnik Leningr. Univ. No. 16, 40 (1961).
8. R. Ladenburg, Revs. Modern Phys. **5**, 243 (1933); Uspekhi Fiz. Nauk **14**, 726 (1934).
9. J. H. E. Griffiths, Proc. Roy. Soc. **143**, 588 (1933).
10. L. P. Razumovskaya and O. P. Bochkova, Opt. i Spektr. **9**, 271 (1960), Optics and Spectroscopy **9**, (1960).
11. L. M. Biberman and E. M. Novodvorskaya, Dokl. Akad. Nauk SSSR **106**, 35 (1956).
12. E. O. Johnson and L. Molter, Phys. Rev. **80**, 58 (1950).
13. Yu. M. Kagan and V. I. Perel', Doklady Akad. Nauk SSSR **91**, 1321 (1953).
14. V. M. Zakharova, Yu. M. Kagan, K. S. Mustafin, V. I. Perel', Zhur. Tekh. Fiz. **30**, 442 (1960), Soviet Physics-Tech. Phys. **5**, 411 (1960).
15. A. A. Zaitsev and E. I. Yankovskaya, Doklady Akad. Nauk, SSSR **21**, 562 (1940).
16. A. A. Zaitsev, Zhur. Eksptl. i Teoret. Fiz. **8**, 56 (1930).
17. H. Kopfermann and R. Ladenburg, Z. Physik **48**, (1928); ibid. **65**, 167 (1930).
18. S. E. Frish, Uspekhi Fiz. Nauk **61**, 461 (1957).
19. A. V. Phelps, Phys. Rev. **99**, 1657 (1955); ibid **11** 1011 (1959).
20. Yu. M. Kagan and P. Lyagushchenko, Zhur. Tekh. Fiz. **31**, 445 (1961), Soviet Phys.-Tech. Phys. **6**, (1961).

THE USE OF THE METAL MOLECULAR MODEL IN THE CALCULATION OF THE INFLUENCE OF MOLECULAR VIBRATIONS ON FORBIDDEN TRANSITIONS

A. M. Meleshina (pp. 706-712)

Received 2 January 1961

The method of calculating the influence of molecular vibrations on electronic states proposed by the writer some time ago was applied using the metal model. The value obtained for the oscillator strength of the forbidden 2600 A band of benzene, produced by the E_g^+ vibration, agreed satisfactorily with the experimental value.

A number of writers have calculated the influence of ecular vibrations on electronic states, using various roximate methods. In the present paper, we attempt xamine this question using the metal molecular model wish to see whether it is feasible in principle to apply method proposed to the case of the metal model. For calculation, we will therefore use one of the simplest ie models of the benzene molecule, suggested by kenshtein and Borovinski.[1]

Before considering this specific case, let us make e general observations. Suppose we have a molecule n electrons and N nuclei (or atomic residues). We he normal coordinate Q represent the vibration of the ci, assuming that the vibrational state may be repre- ed by the known wave function $\Phi(Q)$, which satisfies equation

$$\hat{\mathcal{H}}_{\text{vib.}}\,\Phi(Q) = E_{\text{vib.}}\,\Phi(Q), \tag{1}$$

re

$$\hat{\mathcal{H}}_{\text{vib.}} = -\frac{\hbar^2}{2M}\frac{\partial^2}{\partial Q^2} + U^0_{\text{vib.}}$$

$U^0_{\text{vib.}}$ is the potential energy of the oscillator.

Without allowing for the influence of vibration, the tronic wave function $\psi(\bar{r}_1, \ldots, \bar{r}_n)$ satisfies Schrö- er's equation

$$\hat{\mathcal{H}}_0\psi = E_0\psi, \tag{2}$$

re

$$\hat{\mathcal{H}}_0 = -\frac{\hbar^2}{2\mu}\sum_{\nu=1}^{n}\nabla_\nu^2 + U_0(\bar{r}_1, \ldots, \bar{r}_n),$$

which U_0 depends on the separation of the electrons the distances between the electrons and the fixed lei.

Schrödinger's equation, neglecting the interaction be- n electrons and vibrations, is written

$$(\hat{\mathcal{H}}_0 + \hat{\mathcal{H}}_{\text{vib.}})\,\psi(\bar{r}_1, \ldots \bar{r}_n)\,\Phi(Q) = (E_0 + E_{\text{vib.}})\,\psi\Phi. \tag{3}$$

We will now examine the interaction between the ions of the nuclei and the electrons.

Schrödinger's equation for the molecule in any given rational state is written

$$\left[-\frac{\hbar^2}{2\mu}\sum_\nu \nabla_\nu^2 - \frac{\hbar^2}{2M}\frac{\partial^2}{\partial Q^2} + U(\bar{r}_1, \ldots \bar{r}_n, Q)\right]$$

$$\times \Psi(\bar{r}_1, \ldots \bar{r}_n, Q) = E\Psi(\bar{r}_1, \ldots \bar{r}_n, Q). \tag{4}$$

The following observations may be made in regard ie potential $U(\bar{r}_1, \ldots, \bar{r}_n, Q)$: First, we note that in y of the small amplitudes of the nuclear vibrations, interaction energy between electrons and nuclei

$$U_1 \equiv \sum_k \sum_\nu \frac{e_k e_\nu}{r_{k\nu}(Q)}$$

may be expanded into the series

$$U_1 = U_1^0 + \left(\frac{\partial U_1}{\partial Q}\right)_0 Q + \ldots. \tag{5}$$

where

$$Q\left(\frac{\partial U_1}{\partial Q}\right)_0 = Q\sum_k\sum_\nu \frac{e_k e_\nu}{r^3_{k\nu}(0)}$$

$$\times\left[(x_\nu - x_k^0)\,\xi_k + (y_\nu - y_k^0)\,\eta_k^0 + (z_\nu - z_k^0)\,\zeta_k\right], \tag{6}$$

$$\xi_k \equiv \frac{\partial x_n}{\partial Q}, \quad \eta_k \equiv \frac{\partial y_k}{\partial Q}, \quad \zeta \equiv \frac{\partial z_k}{\partial Q}$$

and x_k^0, y_k^0, z_k^0 are the coordinates of the k-th nucleus in the absence of vibration.

Expression (6) has the form of a dipole potential multiplied by Q. For the benzene molecule, for example,[2] the energy of this interaction for the ω = 606 cm^{-1} vibration is $\sim 1.6 \times 10^{-3}$ erg. On the other hand, the vibrational energy difference which leads to the emission of a quantum ω = 606 cm^{-1} is 1.2×10^{-13} erg. Thus the correction in calculating the energy of interaction of electrons with vibrations is of the same order as the vibrational energy itself. Obviously, if we assume Eq. (3) to be valid, and calculate the vibrational states, we start with the experimental value of the vibrational frequency, and must assume that the influence of potential (6) on the vibrational states has already been taken into account in Eq. (1). This last may be said of the electronic energy as well, if the exact form of the potential is not given in Eq. (3) (which always happens in practice as a result of the multibody nature of the problem). Taking all this into account, we will assume hereinafter that in Eq. (4)

$$U(\bar{r}_1, \ldots \bar{r}_n, Q) = U_0(\bar{r}_1, \ldots \bar{r}_n) + U^0_{\text{vib.}}\ ; \quad E = E_0 + E_{\text{vib.}}.$$

Equation (4) is now rewritten in the form

$$\left(-\frac{\hbar^2}{2\mu}\sum_\nu \nabla_\nu^2 - \frac{\hbar^2}{2M}\frac{\partial^2}{\partial Q^2} + U_0 + U^0_{\text{vib.}}\right)\Psi(\bar{r}_1, \ldots \bar{r}_n, Q)$$

$$= (E_0 + E_{\text{vib.}})\,\Psi(\bar{r}_1, \ldots \bar{r}_n, Q). \tag{7}$$

We will seek a solution of Eq. (7) in the form:

$$\Psi(\bar{r}_1, \ldots \bar{r}_n, Q) = \psi(\bar{r}_1, \ldots \bar{r}_n)\,\Phi(Q)\,[1 + F(\bar{r}_1, \ldots \bar{r}_n, Q)]. \tag{8}$$

Substituting (8) into (7) and taking (3) into account, we obtain an equation for the determination of $F(\bar{r}_1, \ldots \bar{r}_n, Q)$:

$$\sum \nabla_\nu^2 F + \lambda \frac{\partial^2 F}{\partial Q^2} + 2\lambda \left(\frac{\Phi'}{\Phi} + \frac{1}{\psi} \frac{\partial \psi}{\partial Q} \right) \frac{\partial F}{\partial Q} + \lambda \left(\frac{1}{\psi} \frac{\partial^2 \psi}{\partial Q^2} + \frac{\Phi'}{\Phi} \frac{1}{\psi} \frac{\partial \psi}{\partial Q} \right) F = -\lambda \frac{1}{\psi} \frac{\partial^2 \psi}{\partial Q^2} - \lambda \frac{\Phi'}{\Phi} \frac{1}{\psi} \frac{\partial \psi}{\partial Q}, \quad (9)$$

where $\lambda \equiv \mu/M$.

The explicit form of Eq. (9) depends on the values of Φ and ψ.

We now turn to the specific case of benzene. When the metal model is used, in contrast to the Goeppert-Mayer and Sklar approximation which we adopted in the earlier paper,[3] the wave function of the electron does not appear in the form of linear combinations of atomic functions. For this reason, the method we will choose for solving Eq. (9) will differ from that used in ref. 3.

As we said above, we have used the model of ref. 1. According to this model, a molecule is a one-dimensional closed potential box with a flat bottom, the rectilinear hexagon of benzene being replaced by a circle of circumference $2\pi R = 6l$, where $l = 1.39$ A. The position of the electron on the circle is defined by the angle θ or the length of the arc r (Fig. 1). The energy levels $\varepsilon_2 = \varepsilon_3$ correspond to the wave function

$$\psi_2 = (6l)^{-1/2} \exp\left(i \frac{2\pi}{6} r \right)$$

$$\psi_3 = (6l)^{-1/2} \exp\left(-i \frac{2\pi}{6} r \right),$$

and the levels $\varepsilon_4 = \varepsilon_5$ to the functions

$$\psi_4 = (6l)^{-1/2} \exp\left(2i \frac{2\pi}{6} r \right)$$

and

$$\psi_5 = (6l)^{-1/2} \exp\left(-2i \frac{2\pi}{6} r \right).$$

Transitions $2 \rightarrow 4$ and $3 \rightarrow 5$ give the observed "allowed" band, and transitions $2 \rightarrow 5$ and $3 \rightarrow 4$ are forbidden. The vibration of the atoms removes the degeneracy and changes the electronic wave functions, so that the corresponding matrix element of the dipole moment may differ from zero. According to ref. 1, the $2 \rightarrow 5$ transition gives the 2050 A line and the $3 \rightarrow 4$ transition gives the 2600 A line.

Fig. 1

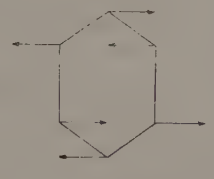

Fig. 2

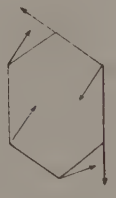

Fig. 3

The weak line 2600 A appears as a result of the influence of the E_g^+ vibration ($\omega = 606$ cm^{-1}), the form of which is shown in Fig. 2 (cf. for example refs. 4 and 6). The radial and tangential displacements of the k-th nucleus are designated as $\rho_k Q$ and $\sigma_k Q$, respectively. Then for our vibration, $\rho k/\rho = 0, -1, 1, 0, -1, \gamma$ and $2\sigma_k/\sigma = -2, 1, 1, -2, 1, 1$, where, according to ref. 6, $\rho = 0.9$, $\sigma = -0.25$.

In accordance with considerations of symmetry, the benzene vibration $\omega = 1569$ cm^{-1} (Fig. 3) should also remove the prohibition against transition $3 \rightarrow 4$. It has been found experimentally, however, that this spectra line is either completely absent or very weak. (For t vibration $\rho = 0.44$; $\sigma = 0.52$.)

To allow for vibrational deformation of the molecule in the model,[1] we divide the circle forming the perimeter of the molecule into six equal parts in acco ance with the position of the carbon atoms (Fig. 1). W represent the deformation of the benzene ring as a lengthening of the corresponding arc of the circle.

We introduce coordinates x_k defining the position the electron on the sector between the k-th and (k + 1) C atoms. In the deformed case, this coordinate may b written in the form

$$x_k = \frac{r - (k-1)\, l - \varepsilon_k Q}{l + (\varepsilon_{k+1} - \varepsilon_k) Q},$$

where

$$\varepsilon_k = \frac{1}{2} \rho_k + \frac{\sqrt{3}}{2},$$

and $0 \leq x_k \leq 1$.

In our case, according to (8), $\Psi = \Phi(Q)\psi(x)[1 + F(x,Q)]$, where F is the function sought. As the wave function of the electron, without allowing for the influence of vibration, we take the function

$$\psi^{(\nu)} = (6l)^{-1/2} e^{i\beta_\nu r},$$

where $\beta_1 \equiv -2\pi/6l$, $\beta_2 \equiv 2(2\pi/6l)$. In the new coordina x_k, the $\psi^{(\nu)}$ functions appear as the set of functions

$$\psi_k^{(\nu)} = (6l)^{-1/2} \exp\left\{ i\beta_\nu \left[x_k l + (k-1)\, l + \varepsilon_k Q \right] \right\} \approx (6l)^{-1/2} e^{i\beta_\nu l(k-1)} \cdot e^{i\beta_\nu l \varepsilon_k}.$$

The usual continuity conditions must be fulfilled at the boundaries of the sectors.

Letting $F_k \equiv F(x_k)$, we obtain the following equatio from which F_k may be found:

$$\frac{\partial^2 F_k}{\partial x^2} \{ 1 + \lambda [\varepsilon_k + (\varepsilon_{k+1} - \varepsilon_k)]^2 \} + \lambda l^2 \frac{\partial^2 F_k}{\partial Q^2} + \frac{\partial F_k}{\partial x} \cdot l \Big\{ \lambda(\varepsilon_{k+1} - \varepsilon_k) \times [\varepsilon_k + (\varepsilon_{k+1} - \varepsilon_k) x_k] + 2 \frac{\psi_k'}{\psi_k} - 2\lambda [\varepsilon_k + (\varepsilon_{k+1} - \varepsilon_k) x_k] \frac{\Phi'}{\Phi} + 2\lambda [\varepsilon_k + (\varepsilon_{k+1} - \varepsilon_k) x_k]^2 \frac{\psi_k'}{\psi_k} \Big\} + \frac{\partial^2 F_k}{\partial Q^2} l^2 \Big\{ 2\lambda \frac{\Phi'}{\Phi} - 2\lambda [\varepsilon_k + (\varepsilon_{k+1} - \varepsilon_k) x_k] \frac{\psi_k'}{\psi_k} \Big\} + 2\lambda F_k l^2 \Big\{ [\varepsilon_k + (\varepsilon_{k+1} - \varepsilon_k) x_k]^2 \frac{\psi_k''}{\psi_k} + (\varepsilon_{k+1} - \varepsilon_k) [\varepsilon_k + (\varepsilon_{k+1} - \varepsilon_k) x_k] \frac{\psi_k'}{\psi_k} - [\varepsilon_k + (\varepsilon_{k+1} - \varepsilon_k) x_k] \frac{\Phi'}{\Phi} \cdot \frac{\psi_k'}{\psi_k} \Big\} = 0.$$

Here the following conditions must be fulfilled:

$$F_k(1) = F_{k+1}(0); \quad \left(\frac{\partial F_k}{\partial x_k} \right)_{x_k = 1} = \left(\frac{\partial F_{k+1}}{\partial x_{k+1}} \right)_{x_{k+1} = 0}.$$

Let us seek F_k in the form of a power series in that is,

$$F_k = f_{1k}\varepsilon_k + g_{1k}\varepsilon_{k+1} + f_{2k}\varepsilon_k^2 + g_{2k}\varepsilon_{k+1}^2 + h_k \varepsilon_k \varepsilon_{k+1} + \ldots,$$

which gives a system of equations of the following for

$$\frac{\partial^2 f_{1k}}{\partial x_k^2}+\lambda l^2\frac{\partial^2 f_{1k}}{\partial Q^2}+2\frac{\partial f_{1k}}{\partial x_k}l\frac{\psi'}{\psi}$$

$$+2\lambda l^2\frac{\partial f_{1k}}{\partial Q}\frac{\Phi'}{\Phi}=2\lambda l^2\frac{\Phi'}{\Phi}\frac{\psi'}{\psi}(1-k_k), \qquad (11a)$$

$$\frac{\partial^2 g_{1k}}{\partial x_k^2}+\lambda l^2\frac{\partial^2 g_{1k}}{\partial Q}+2\frac{\partial g_{1k}}{\partial x_k}l\frac{\psi'}{\psi}$$

$$+2\lambda l^2\frac{\partial g_{1k}}{\partial Q}\frac{\Phi''}{\Phi}=2\lambda l^2 x_k\frac{\Phi'}{\Phi}\frac{\psi'}{\psi} \qquad (11b)$$

d so on. For f_{1k} and g_{1k}, conditions of type (10) are itten.

The matrix element for the transition from the state $= \Phi_1\psi_1(1 + F_1)$ to the state $\Psi_2 = \Phi_2\psi_2(1 + F_2)$ takes the rm:

$$\frac{M}{e}=\int \Phi_2^*\psi_2^*(1+F_2^*)\,r\Phi_1\psi_1(1+F_1)\,d\tau dQ$$

$$\approx l\sum_k\left[\int_0^1 \Phi_2^*\psi_{2k}^*F_{2k}^*\,r\Phi_1\psi_{1k}dx_k dQ+\int_0^1 \Phi_2^*\psi_{2k}^*\,r\Phi_1\psi_{1k}F_{1k}dx_k dQ\right].$$

Introducing $\theta_k = \theta_1 + (k - 1)(2\pi/6)$ and assuming that $= R\cos\theta$, $y = R\sin\theta$, and using the explicit form of we obtain the following expressions for the compo- nts of the dipole moment:

$$\frac{z}{}=\frac{R}{12}\sum_k e^{i(\beta_1-\beta_2)l(k-1)}\left\{e^{\frac{2\pi i}{6}(k-1)}\int_0^1 e^{i\left[(\beta_1-\beta_2)l+\frac{l}{R}\right]x}\Phi_2^*F_{2k}^*\Phi_1 dxdQ\right.$$

$$-e^{-\frac{2\pi i}{6}(k-1)}\int_0^1 e^{i\left[(\beta_1-\beta_2)l-\frac{l}{R}\right]x}\Phi_2^*F_{2k}^*\Phi_1 dxdQ$$

$$+e^{\frac{2\pi i}{6}(k-1)}\int_0^1 e^{i\left[(\beta_1-\beta_2)+\frac{l}{R}\right]x}\Phi_2^*F_{1k}\Phi_1 dxdQ$$

$$\left.-e^{-\frac{2\pi i}{6}(k-1)}\int_0^1 e^{i\left[(\beta_1-\beta_2)l-\frac{l}{R}\right]x}\Phi_2^*F_{1k}\Phi_1 dxdQ\right\}. \qquad (12)$$

e expression for M_y/e differs from (12) by the factor and the + signs before the second and fourth integrals. re F_{1k} and F_{2k} are corrections obtained from the in- ence of vibration in the normal state

$$\Phi_1(Q)=(Q_0\sqrt{\pi})^{-1/2}e^{-\frac{Q^2}{2Q_0^2}}$$

d the first excited state

$$\Phi_2(Q)=(2Q_0\sqrt{\pi})^{-1/2}e^{-\frac{Q^2}{2Q_0^2}}\cdot 2\frac{Q}{Q_0}$$

spectively $[Q_0 = (h/M\nu_{vib.})^{1/2}]$

Let us look at the solution of Eqs. (10), when $\Phi = \Phi_1$. this case

$$\frac{\Phi'}{\Phi}=-\frac{Q}{Q_0^2},\quad \frac{\psi'}{\psi}=i\beta_1 l.$$

e will attempt to solve Eqs. (10) in the form:

$$\left.\begin{aligned} f_k&=Q\left(\frac{A_k}{\varepsilon_k}e^{\gamma_1 x}+\frac{B_k}{\varepsilon_k}e^{\gamma_2 x}+\varphi_f(x)\right),\\ g_k&=Q\left(\frac{C_k}{\varepsilon_k}e^{\gamma_1 x}+\frac{D_k}{\varepsilon_k}e^{\gamma_2 x}+\varphi_g(x)\right),\end{aligned}\right\} \qquad (13)$$

ere

$$\gamma=-i\beta l\pm\sqrt{-\beta^2 l^2+\frac{2\lambda l^2}{Q_0^2}},$$

and A_k, B_k, C_k, and D_k are determined in accordance with the conditions of (10), from the equations

$$A_k e^{i\gamma_1}+B_k e^{i\gamma_2}+\varepsilon_k\varphi_f(1)=A_{k+1}+B_{k+1}+\varepsilon_{k+1}\varphi_f(0), \qquad (14a)$$

$$i\gamma_1 A_k e^{i\gamma_1}+i\gamma_2 B_k e^{i\gamma_2}+\varepsilon_k\varphi_f'(1) \qquad (14b)$$

$$=i\gamma_1 A_{k+1}+i\gamma_2 B_{k+1}+\varepsilon_{k+1}\varphi_f'(0)$$

and similarly for C_k and D_k.

As expression (12 does not actually contain the A_k, B_k, etc., but only linear combinations of them in the form

$$A^{\pm}\equiv\sum_k(-1)^{k-1}e^{\pm\frac{2\pi i}{6}(k-1)}$$

and so on, by multiplying (14) by $(-1)^{k-1}\exp[(2\pi i/6)(k-1)]$ and adding all of Eq. (14a) and all of Eq. (14b), we obtain two equations for determining each of the pairs A^+ and B^+ etc. Introducing the designations

$$\varepsilon^{\pm}\equiv\sum_k(-1)^{k-1}e^{\pm\frac{2\pi i}{6}(k-1)}\varepsilon_k,$$

we obtain

$$A^{\pm}=\varepsilon^{\pm}\frac{\gamma_2\left[e^{\mp\frac{2\pi i}{6}}\varphi_f(0)+\varphi_f(1)\right]-\left[e^{\mp\frac{2\pi i}{6}}\varphi_f'(0)+\varphi_f'(1)\right]}{(\gamma_1-\gamma_2)\left(e^{\gamma_1}+e^{\mp\frac{2\pi i}{6}}\right)},$$

$$B^{\pm}=\varepsilon^{\pm}\frac{\gamma_1\left[e^{\mp\frac{2\pi i}{6}}\varphi_f(0)+\varphi_f(1)\right]-\left[e^{\mp\frac{2\pi i}{6}}\varphi_f'(0)+\varphi_f'(1)\right]}{(\gamma_2-\gamma_1)\left(e^{\gamma_2}+e^{\mp\frac{2\pi i}{6}}\right)} \qquad (15)$$

and similarly for $C^{\pm}$ and $D^{\pm}$. Here

$$\varphi_f(x)=i\beta(1-x)+\frac{\beta_1^2Q_0^2}{\lambda l},\quad \varphi_g(x)=i\beta_1 x-\frac{\beta_1^2Q_0^2}{\lambda l}.$$

Let us look at Eq. (11), if $\Phi = \Phi_2$:

$$\frac{\partial^2 f_{1k}}{\partial x^2}+\lambda l^2\frac{\partial^2 f_{1k}}{\partial Q^2}+2i\beta_2 l\frac{\partial f_{1k}}{\partial x}$$

$$+2i\lambda l^2\left(\frac{1}{Q}-\frac{Q}{Q_0^2}\right)\frac{\partial f_{1k}}{\partial Q}=2i\lambda l^2\beta_2(1-x)\left(\frac{1}{Q}-\frac{Q}{Q_0^2}\right),$$

$$\frac{\partial^2 g_{1k}}{\partial x^2}+\lambda l^2\frac{\partial^2 g_{1k}}{\partial Q^2}+2i\beta_2 l\frac{\partial g_{1k}}{\partial x}+2\lambda l^2\left(\frac{1}{Q}-\frac{Q}{Q_0^2}\right)=2i\lambda l^2\beta_2 x\left(\frac{1}{Q}-\frac{Q}{Q_0^2}\right),$$

$$f_{1k}(x,Q)=Q\left[i\beta_2(1-x)+\frac{A_{1k}}{\varepsilon_k}e^{\gamma_1' x}+\frac{B_{1k}}{\varepsilon_k}e^{\gamma_2' x}+\frac{\beta_2^2Q_0^2}{\lambda l}\right]$$

$$+\frac{1}{Q}\left[\frac{A_{1k}'}{\varepsilon_k}e^{\gamma_1' x}+\frac{B_{1k}'}{\varepsilon_k}e^{\gamma_2' x}-\frac{\beta_2^2Q_0^4}{\lambda l}\right.$$

$$\left.+\frac{2\lambda l}{\gamma_1'^2+2i\beta_2 l\gamma_1'}\frac{A_{1k}}{\varepsilon_k}e^{\gamma_1' x}-\frac{2\lambda l^2}{\gamma_2'^2+2i\beta_2 l\gamma_2'}\frac{B_{1k}}{\varepsilon_k}e^{\gamma_2' x}\right], \qquad (16)$$

where

$$\gamma_1'=-i\beta_2 l\pm\sqrt{-\beta_2^2l^2-\frac{2\lambda l^2}{Q_0^2}},$$

$$\gamma_2'=-i\beta_2 l\pm\sqrt{-\beta_2^2l^2-\frac{2\lambda l^2}{Q_0^2}},$$

and A_{1k}, B_{1k}, A'_{1k}, and B'_{1k} are determined from the boundary conditions. Using designations analogous to

those introduced above, we obtain

$$A_1'^{\pm} = \frac{1}{(x_2 - x_1)\left(e^{x_1} + e^{\mp\frac{2\pi i}{6}}\right)}\left[x_2 \frac{\beta_2^2 Q_0^4}{\lambda l}\varepsilon^{\pm}\left(1 + e^{\pm\frac{2\pi i}{6}}\right)\right.$$
$$+ A_1^{\pm}(x_1 - \gamma_1')\frac{2\lambda l^2}{\gamma_1'^2 + 2i\beta_2 l\gamma_1'}\left(1 + e^{\gamma_1'}\right)$$
$$\left. + B_1^{\pm}(x_2 - \gamma_2')\frac{2\lambda l^2}{\gamma_2'^2 + 2i\beta_2 l\gamma_2'}\left(1 + e^{\gamma_2'}\right)\right],$$

$$B'^{\pm} = \frac{1}{(x_1 - x_2)\left(e^{x_1} + e^{\mp\frac{2\pi i}{6}}\right)}\left[x_1 \frac{\beta_2^2 Q_0^4}{\lambda l}\varepsilon^{\pm}\left(1 + e^{\mp\frac{2\pi i}{6}}\right)\right.$$
$$+ A_1^{\pm}(x_1 - \gamma_1')\frac{2\lambda l^2}{\gamma_1'^2 + 2i\beta_2 l\gamma_1'}\left(1 + e^{\gamma_1'}\right)$$
$$\left. + B_1^{\pm}(x_1 - \gamma_9')\frac{2\lambda l^2}{\gamma_2'^2 + 2i\beta_2 l\gamma_2'}\left(1 + e^{\gamma_2'}\right)\right].$$

$A_1^{\pm}$ and $B_1^{\pm}$, are obtained from formula (15), where γ is replaced by γ' and β_1 by β_2. Similar expressions are obtained for $g_{1k}(x,Q)$.

We obtained the expressions F_k containing the lowest powers of ε. To determine the terms f_{2k}, g_{2k}, h_k, etc., it is easy to construct equations like those in (11), with f_{1k} and g_{1k} entering into these equations. We will not demonstrate the convergence of the method here, but it seems permissible to assume at this point that the functions which appear as coefficients at higher powers of ε are several orders of magnitude smaller than f_1 and g_1.

Thus, for example, for f_{2k} we obtain the equation

$$\frac{\partial^2 f_{2k}}{\partial x^2} + \lambda l^2 \frac{\partial^2 f_{2k}}{\partial Q^2} + 2\lambda l^2 \frac{\Phi'}{\Phi}\frac{\partial f_{2k}}{\partial Q} + 2\lambda \frac{\psi_k'}{\psi_k}\frac{\partial f_{2k}}{\partial x} = 2\lambda l^2 \frac{\Phi'}{\Phi}\frac{\psi'}{\psi}(1 - x) f_{1k}$$
$$+ 2\lambda l \frac{\Phi'}{\Phi}\frac{\partial f_1}{\partial x} - 2\lambda l^2 (1 - x)\frac{\psi'}{\psi},$$

in which the left side exactly coincides with the left side of Eq. (11a) and the average of the right side is two orders smaller; this also gives a smaller order for f_{2k} in comparison with f_{1k}. Thus we will consider it possible in the expression F_k to limit ourselves to the lowest pow of ε.

Substituting the expressions for F_{1k} and F_{2k} into formula (12), removing the elementary integrals, and substituting the numerical values of variables corresponding to the vibration $\omega = 606\ cm^{-1}$ ($M = -73.37 \times 10^{-24}$ r, $Q_0 = 2.7 \times 10^{-10}$ cm, $\lambda = 1.4 \times 10^{-5}$),[3] and value l and β from ref. 1 as well, we obtain

$$\frac{|M|^2}{e^2} = 17.46 \cdot 10^{-20}.$$

The oscillator strength is

$$f = \frac{8\pi^2 \mu \cdot \nu_{2n}}{3h}\frac{|M|^2}{e^2} = 4 \cdot 10^{15}\frac{|M|^2}{e^2} = 0.7 \cdot 10^{-3}.$$

The experimental value is $f_{exp.} = 1.6 \times 10^{-3}$.

The result obtained shows that the method of calcu lating the influence of the nuclear vibrations on the elec tronic state used in this paper may be applied within th limitations of the metal model. It should be mentioned that our use of the simplest variant of the model makes it impossible to give sufficiently accurate consideration to the form of the vibrations, so that we obtain an f of same order of magnitude for the vibration $\omega = 1598$ cm as for $\omega = 606\ cm^{-1}$, whereas experimentally it is considerably smaller.

REFERENCES

1. M. V. Vol'kenshtein and L. A. Borovinski, Doklady Akad. Nauk USSR **85**, 787 (1958).
2. J. N. Murrell and J. A. Pople, Proc. Phys. Soc. **69**, 245 (1956).
3. A. M. Meleshina, Opt. i Spektr. **9**, 564 (1960), Optics and Spectroscopy **9**, 299 (1960).
4. G. Herzberg, "Molecular Spectra and Molecular Structures. Vol. 2. Infrared and Raman Spectra of Polyatomic Molecules." 2nd ed., Van Nostrand, Princeton, New Jersey, 1945. Foreign Literature Press, Moscow, 1949.
5. O. Craig, J. Chem. Soc. **59**, (1950).
6. O. Sponer and O. Herzfeld, Z. Physik **133**, 41 (1952).

CALCULATION OF THE HYPERFINE STRUCTURE OF MOLECULAR ROTATIONAL SPECTRA

K. K. Svidzinskii (pp. 713-723)

Received 7 January 1961

On the basis of the technique of irreducible tensor operators, a theory of the hyperfine structure of the rotational spectra of molecules in the ground nondegenerate electronic state is put forward. In order to simplify the evaluation of the hyperfine interactions of three identical nuclei, a method is proposed which permits one to make use of the transposition invariance of the Hamiltonian.

TRODUCTION

The ground electronic state of the great majority of olecules is nondegenerate. Molecules of the symmetric otor type in the $^1\Sigma$ ground electronic state belong to this ass, as do also molecules of the asymmetric rotor type the singlet electronic state. The theory of the magtic dipole interaction of the nuclei in such molecules as been most fully examined in refs. 1 and 2, and the adrupole interaction in ref. 3. However, calculation of e hyperfine structure of molecular spectra with the recision accessible to modern experimental methods, easured in hundreds of cycles per sec, is quite a comex task even in the case of the simplest molecules.[4,5]

The task of calculating the hyperfine structure of olecular spectra may be simplified to a considerable tent through application of the mathematical techniques angular momentum theory,[6,7] which is the purpose of e present article as well.

Application of the technique of irreducible tensor erators[8] leads to the conclusion that all the matrix eleents of the hyperfine interactions can be expressed by eans of combinations of the Wigner 3n-j symbols[7]—the ndamental quantities which figure in angular momenm theory. Their connection with the Clebsch-Gordan d Racah coefficients, and also the choice of phases for e irreducible tensor operators, are presented below in e Appendix. Extensive tables of the 3n-j symbols and the quantities associated with them are in existence. he most complete bibliography on this question is contined in the book, ref. 6.

THE HAMILTONIAN OF THE HYPERFINE INTERACTIONS

The energy of the hyperfine interaction of a nucleus ith the field of the molecule may be written in the form an expansion in multipole moments

$$\mathcal{H} = \sum_{\lambda} \left(m^{(\lambda)} \cdot M^{(\lambda)}\right) = \sum_{\lambda} \sum_{\mu=-\lambda}^{\lambda} (-1)^{\lambda-\mu} m_{\mu}^{(\lambda)} M_{-\mu}^{(\lambda)}. \qquad (1.1)$$

For even λ, the quantities $M_\mu^{(\lambda)}$ denote the operars of the static electric multipole moments of the ucleus and are defined by the expressions

$$M_{\mu}^{(\lambda)} = \int r^{\lambda} Y_{\mu}^{(\lambda)}(\theta, \varphi)\, \rho_n(r, \theta, \varphi)\, dv_n \qquad (\lambda = 2n), \qquad (1.2)$$

hile for odd λ they are the operators of the static magtic multipole moments of the nucleus:

$$M_{\mu}^{(\lambda)} = \int r^{\lambda} Y_{\mu}^{(\lambda,\lambda)}(\theta, \varphi) \cdot \mathbf{j}_n(r, \theta, \varphi)\, dv_n, \qquad (\lambda = 2n+1), \qquad (1.3)$$

where ρ_n and $\mathbf{j}_n$ are the charge and current densities in the nucleus and $Y_\mu^{(\lambda)}(\theta, \varphi)$ and $Y_\mu^{(\lambda,\lambda)}(\theta, \varphi)$ are the scalar and vector spherical functions (see Appendix). The origin of the spherical coordinate system r, θ, φ is taken at the center of mass of the nucleus. The operators of the electric and magnetic multipoles of the molecule are defined analogously in terms of the molecular charge density ρ_m and current density $\mathbf{j}_m$:

$$m_{\nu}^{(\lambda)} = \int r^{-(\lambda+1)} Y^{(\lambda)}(\theta, \varphi)\, \rho_m(r, \theta, \varphi)\, dv_m, \qquad (\lambda = 2n), \qquad (1.4)$$

$$m_{\nu}^{(\lambda)} = \int r^{-(\lambda+1)} Y_{\nu}^{(\lambda,\lambda)}(\theta, \varphi)\, \mathbf{j}_m(r, \theta, \varphi)\, dv_m, \qquad (\lambda = 2n+1). \qquad (1.5)$$

The value of the energy for the 2^λ-pole interaction $(m^{(\lambda)}M^{(\lambda)})$ is proportional to $(r_n/r_a)^\lambda$, where r_n and r_a are the average distances which characterize the distribution of charges and currents in the nucleus and the atom respectively. Since $r_n/r_a \approx \sqrt{Z} \times 10^{-4}$ (Z is the atomic number),[9] then in molecules containing heavy nuclei hexadecapole ($\lambda = 4$) and octupole ($\lambda = 3$) interactions, as well as quadrupole ($\lambda = 2$) and dipole ($\lambda = 1$) interactions, may prove to be appreciable.

The molecular multipoles are to be averaged over the ground electronic and vibrational states of the molecule, taking account of the perturbation of the electronic orbital moment in a rotating molecule.[10] To the second approximation of perturbation theory, the average values of the electric multipoles do not depend on the rotational state, and the averaged magnetic multipole may be represented in the form of two components:

$$m_{\nu}^{(\lambda)} = m_{\nu}^{(\lambda)}(\mathbf{J}) + m_{\nu}^{(\lambda)}(\mathbf{I}). \qquad (1.6)$$

The first of these takes account of the contribution of convection currents to the magnetic multipole and is proportional to the rotational moment of the molecule, J. It follows from symmetry considerations that the operator $m_\nu^{(\lambda)}(J)$, represented in the form of products of irreducible tensors, must be expressed in terms of two "molecular g-factors," $G_\nu^{(\lambda,\lambda\pm1)}$:

$$m_{\nu}^{(\lambda)}(J) = \left[J^{(1)} \times G^{(\lambda;\,\lambda+1)}\right]_{\nu}^{(\lambda)} + \left[J^{(1)} \times G^{(\lambda;\,\lambda-1)}\right]_{\nu}^{(\lambda)}. \qquad (1.7)$$

The quantities $G_\nu^{(\lambda;k)}$ are real irreducible tensors of rank $k = \lambda \pm 1$ and, in the approximation under consideration, do not depend on the rotational state of the molecule. Explicit expressions for them, taking account of the Thomas precession, are represented in ref. 11. The second component of (1.6) represents the contribution of the "spin" currents of the nuclei. If we consider the distribution of the dipole moments of the nuclei to be a point distribution, then this operator may be converted to the form:

$$m_\nu^{(\lambda)}(I) = \sqrt{\lambda(2\lambda+3)} \sum_i \mu_0 g_i I_i \cdot r^{-(\lambda+2)} Y_\nu^{(\lambda+1,\lambda)}(\theta_i, \varphi_i), \quad (1.8)$$

where μ_0 is the nuclear magneton, I_i and g_i are the spin moment and the g factor of the i-th nucleus, and r_i, θ_i, φ_i are the coordinates of the i-th nucleus relative to the nucleus being examined.

The "spin" electron currents will not contribute to the magnetic multipole, since we are neglecting the influence of excited nonsinglet electronic states.[9] For the same reason, we do not allow for the effects of penetration of electrons into the nucleus.

II. THE FUNDAMENTAL MATRIX ELEMENTS

The rotational wave functions of a molecule of the symmetric rotor type coincide, except for a normalizing factor, with the elements of the matrix of finite rotations [F. R. (5.2)].*

*We shall introduce a special designation for references to Fano and Racah's book.[8] For example, [F. R. (5.2)] denotes a reference to formula (5.2) of that book.

$$\langle \varphi\theta\psi \mid JKM\rangle = \left(\sqrt{\frac{2J+1}{8\pi^2}}\right)^{\frac{1}{2}} D^{(J)}_{KM}(\psi, \theta, \varphi), \quad (2.1)$$

where K and M are the projections of the vector J on the molecular and the laboratory z-axes respectively; φ, θ, and ψ are the Eulerian angles. The rotational energy of a molecule of the asymmetric rotor type is characterized by the quantum numbers $J\tau$, where $\tau = J, J-1, \ldots, -J$, and by the corresponding wave function

$$\langle \varphi\theta, \psi \mid J\tau M\rangle = \left(\sqrt{\frac{2J+1}{8\pi^2}}\right)^{\frac{1}{2}} \sum_{K=-J}^{J} D^{(J)}_{KM}(\psi, \theta, \varphi) \cdot (JK \mid J\tau). \quad (2.2)$$

The procedure for finding the wave functions of an asymmetric rotor, $(JK \mid J\tau)$, has been well studied,[2] and we shall consider them as known. Therefore, all further investigation will be carried out only for molecules of the symmetric rotor type, assuming that the transition from the representation JKM to the representation $J\tau M$ can always be accomplished with the help of the well-known formulas of transformation theory.

For the matrix elements of the operator $m_\mu^{(\lambda)}$, which is given in the laboratory coordinate system, we may write, on the basis of the Eckart-Wigner theorem [F. R. (14.4)],

$$\langle JKM \mid m_\mu^{(\lambda)} \mid J'K'M\rangle = (-1)^{J-M} \begin{pmatrix} J' & J & \lambda \\ M' & -M & \mu \end{pmatrix} (JK \| m^{(\lambda)} \| J'K'), \quad (2.3)$$

where the second factor is the Wigner 3-j symbol (see Appendix).

To evaluate the reduced matrix element $(JK \| m^{(\lambda)} \| J'K')$, let us project the operator $m_\mu^{(\lambda)}$ onto the molecular coordinate system:

$$m_\mu^{(\lambda)} = \sum_{\nu=-\lambda}^{\lambda} m_\nu^{(\lambda)} D^{(\lambda)}_{\nu\mu}(\psi, \theta, \varphi). \quad (2.4)$$

When the operator $m_\nu^{(\lambda)}$ does not depend on the variables which describe the rotational state, as in the case of the operators (1.8) and (1.4), the reduced matrix element can be evaluated directly with the help of (2.1), (2.3), and formula (4.6.2) of ref. 7:

$$(JK \| m^{(\lambda)} \| J'K) = (-1)^{J-K} [(2K+1)(2J'+1)]^{1/2} \times \begin{pmatrix} J' & J & \lambda \\ K & -K & \nu \end{pmatrix} m_\nu^{(\lambda)}. \quad (2.5)$$

This expression does not apply to the operator $m_\nu^{(\lambda)}(J)$, which, according to (1.7), is proportional to J, but it is valid for the operators $G_\nu^{(\lambda;k)}$. The reduced matrix element of the operator $m_\nu^{(\lambda)}(J)$ is to be evaluated according to formula [F. R. (15.15)], taking into account that [F. R. (14.9)]

$$(J \| J^{(1)} \| J) = i[J(J+1)(2J+1)]^{1/2}. \quad (2.$$

We obtain as our result

$$(JK \| m_\nu^{(\lambda)}(J) \| J'K') = (-1)^{\lambda+J'-K} (J \| J^{(1)} \| J) [(2\lambda+1)(2J+1)(2J'+1)]^{1/2} \times \left[\begin{Bmatrix} \lambda & J & J' \\ J & \lambda+1 & 1 \end{Bmatrix} \begin{pmatrix} J' & J & \lambda+1 \\ K' & -K & \nu \end{pmatrix} G_\nu^{(\lambda;\lambda+1)} + \begin{Bmatrix} \lambda & J & J' \\ J & \lambda-1 & 1 \end{Bmatrix} \begin{pmatrix} J' & J & \lambda-1 \\ K' & -K & \nu \end{pmatrix} G_\nu^{(\lambda;\lambda-1)} \right]. \quad (2.$$

The reduced matrix element of the nuclear multipo is usually defined in terms of the "magnitude of the nuclear multipole moment"

$$\langle M^{(\lambda)} \rangle = \langle Im_I = I \mid M^{(\lambda)} \mid Im_I = I \rangle. \quad (2.$$

where I is the nuclear spin, while it follows from the Eckart-Wigner theorem that

$$(I \| M^{(\lambda)} \| I) = \frac{[(2I-\lambda)!(2I+\lambda+1)!]^{1/2}}{(2I)!} \langle M^{(\lambda)} \rangle. \quad (2.$$

In the representation $JKIFM_F$, where $\mathbf{F} = \mathbf{J} + \mathbf{I}$ and M_F is the projection of the vector F on the laboratory z-axis (associated with the nucleus), the matrix elemen for the energy of the 2^λ-pole interaction equals [F. R. (15.6)]

$$(JKIF \mid (m^{(\lambda)} \cdot M^{(\lambda)}) \mid J'KIF) = (-1)^{\lambda+J'+I+F} \begin{Bmatrix} \lambda & J & J' \\ F & I & I \end{Bmatrix} (JK \| m^{(\lambda)} \| J'K') (I \| M^{(\lambda)} \| I). \quad (2.1$$

where the second factor if the Wigner 6-j symbol (see Appendix). When there are hyperfine interactions of se eral nuclei in the molecule, the matrix elements are evaluated in the representation $JKI_1F_1I_2FM_F$, where I_1 is the spin of the first nucleus, $\mathbf{F}_1 = \mathbf{J} + \mathbf{I}_1$, I_2 is the spin of the second nucleus (whose interaction is being computed), and $\mathbf{F} = \mathbf{F}_1 + \mathbf{I}_2$. Then

$$(JKI_1F_1I_2F \mid (m^{(\lambda)} \cdot M^{(\lambda)}) \mid J'K'I_1F_1'I_2F) = (-1)^{\lambda+F_1'+I_1+F} \begin{Bmatrix} \lambda & F_1 & F_1' \\ F & I_2 & I_2 \end{Bmatrix} (JKI_1F \| m^{(\lambda)} \| J'K'I_1F_1) (I_2 \| M^{(\lambda)} \| I_2 \quad (2.1$$

For the evaluation of the next to last matrix element, formula [F. R. (15.7)] is to be used; this gives

$$(JKI_1F \| M^{(\lambda)} \| J'K I_1F_1') = (-1)^{J+I_1+F_1'+\lambda} [(2F_1+1)(2F_1'+1)] \begin{Bmatrix} \lambda & J & J' \\ I_1 & F_1' & F_1 \end{Bmatrix} (JK \| m^{(\lambda)} \| J'K'). \quad (2.1$$

We note that, in the first approximation of perturba tion theory, the splitting brought about by a 2^λ-pole inte action is characterized by a definite interval rule pertaining to a given λ, which, according to (2.10), is described by the function $\begin{Bmatrix} \lambda\, J\, J \\ F\, I\, I \end{Bmatrix}$, which also contains within itself the selection rules $2I, 2J \geq \lambda$. Since the 6- symbols represent, in their own way, a complete set of functions in the sense of an interval rule (the orthogona ity property), then it is easy to derive the constant for 2^λ-pole interaction to a first approximation from a give set of experimental levels E(JIF), namely [F. R. (16.8)]

$$(JK\|m^{(\lambda)}\|JK)(I\|M^{(\lambda)}\|I)$$

$$= \sum_{F=|J-I|}^{F=J+I} (-1)^{\lambda+I+J+F}(2\lambda+1)(2F+1)\begin{Bmatrix}\lambda & J & J\\ F & I & I\end{Bmatrix} F(JIF). \quad (2.13)$$

However, in higher approximations of perturbation ory, the 2^{λ}-pole interaction contains intervals of a ltipolarity λ' which is different from λ. To derive corrections of multipolarity λ', the product of the responding 6-j symbols may be represented in the m:

$$\begin{Bmatrix}\lambda & J & J''\\ F & I & I\end{Bmatrix}\begin{Bmatrix}\lambda & J' & J''\\ F & I & I\end{Bmatrix}$$

$$+\sum_{\lambda'=0}^{2\lambda}(-1)^{\lambda'+I+J''+F}\begin{Bmatrix}\lambda' & J & J''\\ F & I & I\end{Bmatrix} a\begin{pmatrix}\lambda' & J & J''\\ \lambda & J' & I\end{pmatrix}, \quad (2.14)$$

ere

$$a\begin{pmatrix}\lambda' & J & J''\\ \lambda & J' & I\end{pmatrix} = (-1)^{2I+J+J''}(2\lambda'+1)\begin{Bmatrix}\lambda' & J & J\\ J' & \lambda & \lambda\end{Bmatrix}\begin{Bmatrix}\lambda' & I & I\\ I & \lambda & \lambda\end{Bmatrix}. \quad (2.15)$$

THE ELECTRIC INTERACTIONS

The magnitude of the quadrupole interaction ($\lambda = 2$) molecules amounts to 10^6-10^8 cps.[2] The correction m the second perturbation-theory approximation for rational levels amounts to a value of the order of 10^4-^{5} cps, while the third-approximation corrections may ove to be comparable, in order of magnitude, to the xadecapole interaction ($\lambda = 4$) and to amount to a few ndred cycles per sec.

In the spectroscopic literature, definitions[9] have en adopted for the quadrupole constants which are con-cted with $\langle M^{(2)}\rangle$ and $m_0^{(2)}$ by the relations

$$\left.\begin{aligned} eQ &= -2\langle M^{(2)}\rangle,\\ eq &= -2m_0^{(2)}.\end{aligned}\right\} \quad (3.1)$$

The diagonal matrix element of the quadrupole in-raction, as computed according to formulas (2.10), 9), and (2.5),

$$\frac{eQq}{4}(-1)^{J-K}\begin{pmatrix}J & J & 2\\ K & -K & 0\end{pmatrix}\left[\frac{(2I+3)(2I+2)(2I+1)}{2I(2I-1)}\right]^{1/2}(2J+1)$$

$$\times(-1)^{J+I+F}\begin{Bmatrix}2 & J & J\\ F & I & I\end{Bmatrix}, \quad (3.2)$$

incides, naturally, with the known result (Bardeen and wnes[3]) if for

$$\begin{pmatrix}J & J & 2\\ K & -K & 0\end{pmatrix}\text{and}\begin{Bmatrix}2 & J & J\\ F & I & I\end{Bmatrix}$$

substitute their analytical expressions.[7]

The correction of multipolarity λ ($0 \leq \lambda \leq 4$) brought ut by quadrupole interaction, in the second approxi-tion of perturbation theory, equals

$$\Delta E_2^{\lambda} = (-1)^{\lambda+J+I+F}\begin{Bmatrix}\lambda & J & J\\ F & I & I\end{Bmatrix} A_{JK}^{\lambda}, \quad (3.3)$$

ere

$$A_{JK}^{\lambda} = \sum_{J'K'}'(2J+1)(2J'+1)\,a\begin{pmatrix}\lambda & J & J\\ 2 & J' & I\end{pmatrix}$$

$$\cdot\left[\begin{pmatrix}J' & J & 2\\ K & -K & \nu\end{pmatrix}\right]^2\frac{(eQ)^2|m_{\nu}^{(2)}|^2}{4(E_{JK}-E_{J'K'})}, \quad (3.4)$$

l the quantity

$$a\begin{pmatrix}\lambda & J & J\\ 2 & J' & I\end{pmatrix}$$

is defined by the expression (2.15).

In the third approximation, it is reasonable to write down the correction of hexadecapole character, which proves to be equal to

$$\Delta E_3^4 = (-1)^{J+I+F}\begin{Bmatrix}4 & J & J\\ F & I & I\end{Bmatrix} B_{JK}^4, \quad (3.5)$$

where

$$B_{JK}^4 = \left[\frac{(2I+3)(2I+2)(2I+1)}{2I(2I-1)}\right]^{1/2}$$

$$\times\left\{\sum_{J'K'}'\sum_{J''K''}'(-1)^{K+K'+K''}(2J+1)(2J'+1)\right.$$

$$\times(2J''+1)\,b(IJ;\,J'J'')\begin{pmatrix}J'' & J' & 2\\ K'' & -K' & \nu_2\end{pmatrix}\begin{pmatrix}J' & J & 2\\ K' & -K & \nu_1\end{pmatrix}$$

$$\times\begin{pmatrix}J & J'' & 2\\ K & -K & \nu_3\end{pmatrix}\frac{(eQ)^3 m_{\nu_1}^{(2)} m_{\nu_1}^{(2)} m_{\nu_3}^{(2)}}{8(E_{J'K'}-E_{JK})(E_{J''K''}-E_{JK})}$$

$$\left.-(-1)^K(2J+1)^2\begin{pmatrix}J & J & 2\\ K & -J & 0\end{pmatrix}\right\}$$

$$\times\sum_{J'K'}'b(IJ;\,JJ')\left[\begin{pmatrix}J' & J & 2\\ K' & -K & \nu\end{pmatrix}\right]^2\left.\frac{(eQ)^3 m_0^{(2)}|m_{\nu}^{(2)}|^2}{16(E_{J'K'}-E)^2}\right\}, \quad (3.6)$$

and

$$b(IJ;\,J'J'') = \sum_{\varkappa=0}^{4}(-1)^{J+J''+2I}9\begin{Bmatrix}J & J & 4\\ 2 & \varkappa & J''\end{Bmatrix}\begin{Bmatrix}I & I & 4\\ 2 & \varkappa & I\end{Bmatrix}a\begin{pmatrix}\varkappa & J & J''\\ 2 & J' & I\end{pmatrix}. \quad (3.7)$$

The energy of the hexadecapole interaction equals, in the first approximation,

$$E_1^4 = m_0^{(4)}\langle M^{(4)}\rangle(-1)^{J-K}\begin{pmatrix}J & J & 4\\ K & -K & 0\end{pmatrix}$$

$$\times\left[\frac{(2I+5)(2I+3)(2I+1)(I+1)(I+2)}{(2I-3)(2I-1)(I-1)I}\right]^{1/2}$$

$$\times(2J+1)\cdot(-1)^{J+I+F}\begin{Bmatrix}4 & J & J\\ F & I & I\end{Bmatrix}. \quad (3.8)$$

IV. THE MAGNETIC INTERACTIONS

The two components which make up the magnetic multipole of the molecule (1.6) generally are of the same order of magnitude in the case of dipole interaction ($\lambda = 1$), which is associated, as a rule, with an energy of 10^5-10^6 cps. Only in exceptional cases can octupole interaction ($\lambda = 3$) amount to a quantity of the order of tens of cycles per sec, on account of the contribution to $m_v^{(3)}(J)$ of electrons located close to the nucleus. It is sufficient to evaluate the energy of the magnetic interactions in the first approximation of perturbation theory.

The Hamiltonian term

$$\mathcal{H}_{\lambda}(J) = -(m_{\nu}^{(\lambda)}(J)\cdot M^{(\lambda)}), \quad (4.1)$$

as follows from (2.10) and (2.7), gives a contribution

$$(JKIF|\mathcal{H}_{\lambda}(J)|JK'IF) = (-1)^{I+F+K}\cdot\begin{Bmatrix}\lambda & J & J\\ F & I & I\end{Bmatrix}$$

$$\times\frac{[(2I-\lambda)!\,(2I+\lambda+1)!]^{1/2}}{(2I)!}\left[\frac{(2\lambda+1)\lambda}{\lambda+1}\right]^{1/2}$$

$$\times(2J+1)[J(J+1)(2J+1)]^{1/2}\cdot\left[\begin{Bmatrix}J & J & \lambda+1\\ 1 & \lambda & J\end{Bmatrix}\begin{pmatrix}J & J & +1\\ K' & -K & \nu\end{pmatrix}\right.$$

$$\left.\times G_{\nu}^{(\lambda;\,\lambda+1)}+\begin{Bmatrix}J & J & \lambda-1\\ 1 & \lambda & J\end{Bmatrix}\begin{pmatrix}J & J & \lambda-1\\ K' & -K & \nu\end{pmatrix}G_{\nu}^{(\lambda;\,\lambda-1)}\right]M_{\lambda} \quad (4.2)$$

where M_λ, in agreement with ref. 12, denotes the magnitude of the multipole moment, which is connected with (3.8) by the relation

$$M_\lambda = -i\sqrt{\frac{\lambda+1}{\lambda}}\langle M^{(\lambda)}\rangle. \tag{4.3}$$

For dipole interaction, formula (4.2) gives essentially Henderson's result[13]

$$\begin{aligned}&(JKIF\,|\,\mathscr{H}_1(J)\,|\,JKIF)\\ &=\mu_n g\left[G^{(1;\,0)}-\frac{1}{\sqrt{10}}\left(\frac{3K^2}{J(J+1)}-1\right)G_0^{(1;\,2)}\right]\\ &\times\frac{1}{2}[F(F+1)-J(J+1)-I(I+1)],\end{aligned} \tag{4.4}$$

where M_1 has been taken to equal $\mu_n gI$. The spin-spin interaction energy of nuclei with spins I_0 and I_1, according to (1.6), may be written in the form

$$\mathscr{H}_1(I_0\cdot I_1)=\sqrt{10}\,\mu_n^2 g_0 g_1 r_1^{-3}\left(I_0^{(1)}\cdot\left[Y^{(2)}(\theta_1,\varphi_1)\times I_1^{(1)}\right]^{(1)}\right), \tag{4.5}$$

where r_1, θ_1, and φ_1 are the spherical coordinates of the nucleus with spin I_1. In the representation $JKI_1F_1I_0FM_F$ (where $\mathbf{F}_1=\mathbf{J}+\mathbf{I}_1$, $\mathbf{F}=\mathbf{F}_1+\mathbf{I}_0$), the matrix elements of the Hamiltonian (4.5) can be evaluated according to formulas (2.10) and [F. R. (15.9)], which leads to the result

$$\begin{aligned}&(JKI_1F\,I_0F\,|\,\mathscr{H}_1(I_0\cdot I_1)\,|\,JK'I_1F_1'I_1F)=\sqrt{30}\,\mu_n^2 g_0 g_1 r_1^{-3}Y_\nu^{(2)}(\theta_1,\varphi_1)\\ &\times(-1)^{J-K}(2J+1)\begin{pmatrix}J & J & 2\\ K' & -K & \nu\end{pmatrix}\\ &\times\left[I_0(I_0+1)(2I_0+1)\,I_1(I_1+1)(2I_1+1)\,(2F_1+1)(2F_1'+1)\right]^{1/2}\\ &\times(-1)^{F_1'+I_0+F}\begin{Bmatrix}1 & F_1 & F_1'\\ F & I_0 & I_0\end{Bmatrix}\cdot\begin{Bmatrix}I_0 & F_1 & I\\ I_0 & F_1' & I\\ 1 & 1 & 2\end{Bmatrix},\end{aligned} \tag{4.6}$$

where the three-row quantity is the Wigner 9-j symbol.[7]

To evaluate the spin-spin interaction in the representation $IKI_1I_0IFM_F$ (where $\mathbf{I}=\mathbf{I}_1+\mathbf{I}_0$), it is convenient to write the Hamiltonian (4.5) in the form

$$\mathscr{H}_1(I_0\cdot I_1)=\sqrt{6}\,\mu_n^2 g_0 g_1 r_1^{-3}\left(Y^{(2)}(\theta_1,\varphi_1)\cdot\left[I_1^{(1)}\times I_0^{(1)}\right]^{(2)}\right). \tag{4.7}$$

Then

$$\begin{aligned}&(JKI_1I_0IF\,|\,\mathscr{H}_1(I_0\cdot I_1)\,|\,JKI_1I_0I'F)=\sqrt{30}\,\mu_n^2 g_0 g_1 r_1^{-3}Y_\nu^{(2)}(\theta_1,\varphi_1)\\ &\times(-1)^{I+F+K}(2I+1)\begin{pmatrix}J & J & 2\\ K' & -K & \nu\end{pmatrix}\left[I_0(I_0+1)\,I_1(I_1+1)\right]^{1/2}\\ &\times(2I_1+1)(2I_0+1)\begin{Bmatrix}2 & J & J\\ F & I' & I\end{Bmatrix}\begin{Bmatrix}I_1 & I_0 & I\\ I_1 & I_0 & I'\\ 1 & 1 & 2\end{Bmatrix}.\end{aligned} \tag{4.8}$$

For the diagonal elements of (4.6) and (4.8), the evaluation of the corresponding 9-j symbols may be simplified with the help of the formula

$$\begin{aligned}\begin{Bmatrix}j_1 & j_2 & j\\ j_1 & j_2 & j\\ 1 & 1 & 2\end{Bmatrix}&=\frac{(-1)^{2j}}{5\begin{Bmatrix}j & j & 2\\ 1 & 1 & j\end{Bmatrix}}\left[\begin{Bmatrix}j_1 & j_2 & j\\ 1 & j & j_2\end{Bmatrix}\begin{Bmatrix}j_2 & j_1 & j\\ 1 & j & j_1\end{Bmatrix}\right.\\ &\left.+\frac{(-1)^{j_1+j_2+j+1}}{3(2j+1)}\begin{Bmatrix}j & j_1 & j_2\\ 1 & j_2 & j_1\end{Bmatrix}\right],\end{aligned} \tag{4.9}$$

which can be obtained by the use of the known properties of the 9-j symbol.[7] If the nuclear spins are the same, $I_1=I_0=j$, then the 9-j symbol appearing in (4.9) can also be simplified

$$\begin{aligned}\begin{Bmatrix}j & j & I\\ j & j & I'\\ 1 & 1 & 2\end{Bmatrix}&=\frac{(-1)^{2\lambda}}{5\begin{Bmatrix}1 & 1 & 2\\ I' & I & \lambda\end{Bmatrix}}\left[\begin{Bmatrix}j & j & I'\\ 1 & \lambda & j\end{Bmatrix}\begin{Bmatrix}j & j & I\\ 1 & \lambda & j\end{Bmatrix}\right.\\ &\left.+\delta_{II'}\frac{(-1)^{2j+I+1}}{3(2I+1)}\begin{Bmatrix}I & j & j\\ 1 & j & j\end{Bmatrix}\right],\end{aligned} \tag{4}$$

where $\lambda=(I+I')/2$. We note that this 9-j symbol also contains the selection rules $\Delta I=I'-I=0,\pm2$.

V. IDENTICAL NUCLEI

In the case when the values of the hyperfine interaction energy of several nuclei in the molecule do not differ sufficiently markedly from one another, it is impossible, given the intermediate momenta, to introduce such a representation (such as $JKI_1F_1I_2F$, where $\mathbf{F}_1=\mathbf{J}+\mathbf{I}_1$, $\mathbf{F}=\mathbf{F}_1+\mathbf{I}_2$, or JKI_1I_2IF, where $\mathbf{I}=\mathbf{I}_1+\mathbf{I}_2$, $\mathbf{F}=\mathbf{J}+\mathbf{I}$) that the nondiagonal elements of the hyperfine splitting energy should be small in comparison with the diagonal ones. However, if the nuclei are identical, the procedure for diagonalization with respect to the intermediate momenta may be significantly simplified by going over to a representation in which the spin functions of the identical nuclei are characterized by a particular type of symmetry and by a total spin equal to I.

Such a representation may be denoted by $JKj^3\alpha_s IF$, where j is the spin of each of the identical nuclei, α_s denotes a type of irreducible representation of the group of the transpositions of n identical nuclei, and the index s numbers the row of the irreducible representation when it is not one-dimensional. Since α_s and F are integrals of motion, the only quantum number with respect to which diagonalization is to be carried out in this representation is I.

We shall limit our examination to the case of three identical nuclei. This case is most characteristic for those molecules which have been the objects of investigation by microwave gas spectroscopy and which contain identical nuclei. The group of the transpositions of three identical nuclei is isomorphic with the appropriate point symmetry groups, C_{3v} or D_3, of the molecules.[14] It is characterized by the following three irreducible representations: a totally symmetric one A_1, an antisymmetric one A_2, and a two-dimensional one E. The matrix elements $(j,j^2(L)I\,|\,j^3\alpha_s I)$, where L is the intermediate momentum, which takes on the values

$$|I-j|\leqslant L\leqslant\min\{2j,\ I+j\}$$

for the case of the antisymmetric representation $\alpha=$ coincide with the genealogical coefficients [F. R. (chap. 13)]. The method for finding the genealogical coefficients may be generalized in an obvious way to the case of a transition to an arbitrary irreducible representation of the transposition group. As a result, the following expression is obtained for the desired transition matrix

$$(j,\ j^2(L)\,I\,|\,j^3\alpha_s I)=\frac{\left(L\,\middle|\,P_s^{(\alpha)}(I)\,\middle|\,L'\right)}{\sqrt{\left(L_0\,\middle|\,P_s^{(\alpha)}(I)\,\middle|\,L_0\right)}}\,. \tag{}$$

The matrices of the projection operators $P_s^{(\alpha)}$ in the representation j,j(L)I which correspond to $\alpha_s=A_1$, A_2, $E_{1,2}$ may be chosen to be real and may be written in the form:

$$\begin{aligned}&\left(L\,\middle|\,P^{(A_1)}(I)\,\middle|\,L'\right)\\ &=\frac{1}{3}D(2j,\ L)\left[\delta(L,\ L')+2D(L,\ L')\,C(j^3I;\ LL')\right],\end{aligned} \tag{}$$

$$\left(L\left|P^{(A_2)}(I)\right|L'\right)$$

$$=\frac{1}{3}D(2j+1,\ L)\ [\delta(L,\ L')+2D(L,\ L')\,C(j^3I;\ LL')], \quad (5.3)$$

$$\left(L\left|P_1^{(E)}(I)\right|L'\right)$$

$$=\frac{2}{3}D(2j,\ L)\ [\delta(L,\ L')-D(L,\ L')\,C(j^3I;\ LL')], \quad (5.4)$$

$$\left(L\left|P_2^{(E)}(I)\right|L'\right)$$

$$=\frac{2}{3}D(2j+1,\ L)\ [\delta(L,\ L')-D(L,\ L')\,C(j^3I;\ LL')]. \quad (5.5)$$

In the latter formulas, aside from the Kronecker nbol $\delta(L,L')$, the symbols

$$D(n,\ n')=\begin{cases}1, \text{ when } (-1)^n=(-1)^{n'}\\ 0, \text{ when } (-1)^n=-(-1)^{n'},\end{cases} \quad (5.6)$$

also

$$C(j^3I;\ LL')=(-1)^L[(2L+1)(2L'+1)]^{1/2}\begin{Bmatrix}j & j & L\\ j & I & L'\end{Bmatrix}. \quad (5.7)$$

e been introduced.

The numerical values of the coefficients in (5.7)*

anslation Editor's Note: The original cites (6.2) but s appears to be a misprint for, we believe, (5.7).

the cases j = 1 and 3/2 have been presented by us ef. 11.

The matrix elements of the nuclear multipole in the resentation $j^3\alpha_s Im_I$ can be evaluated with the help of) and [F. R. (15.7)]:

$$(j^3a_sI\|M^{(\lambda)}\|j^3a_sI')=\frac{1}{3}(-1)^{j-I}\Delta(\lambda ja_s;\ II')(j\|M^{(\lambda)}\|j), \quad (5.8)$$

re

$$\Delta(\lambda ja_s;\ II')=3(-1)^{\lambda+I+I'}[(2I+1)(2I'+1)]^{1/2}$$

$$\times\sum_L(-1)^L(j^3a_sI|j,\ ^2(L)\ j)\begin{Bmatrix}\lambda II'\\ Ljj\end{Bmatrix}(j,\ j^2(L)\ I'|j^3a_sI'). \quad (5.9)$$

A somewhat more complex expression is obtained he evaluation of the spin-spin interaction for the op- tor $[j^{(1)}\times j^{(1)}]^{(2)}$, which enters into the Hamiltonian ype (4.7). To evaluate it, we make use of [F. R. (15.7), 12)], which leads to the result

$$3(j^3a_sI\|[j^{(1)}\times j^{(1)}]^{(2)}\|j^3a_sI')$$

$$=(-1)^{j+I+1}\sqrt{5}\ j(j+1)(2j+1)\,\sigma(ja_s;\ II'), \quad (5.10)$$

re

$$\sigma(ja_s;\ II')=[(2I+1)(2I'+1)]^{1/2}$$

$$\sum(-1)^LD(L,L')[(2L+1)(2L'+1)]^{1/2}(j^3a_sI|j,\ j^2(L)\ I)\begin{Bmatrix}2II'\\ jL'L\end{Bmatrix}$$

$$\times\frac{3(2L+1)\begin{Bmatrix}jjL'\\ 1\lambda j\end{Bmatrix}\begin{Bmatrix}jjL\\ 1\lambda j\end{Bmatrix}+(-1)^{3j+L+1}\begin{Bmatrix}Ljj\\ 1jj\end{Bmatrix}}{5(2L+1)\begin{Bmatrix}2LL'\\ \lambda 11\end{Bmatrix}}$$

$$\times(j,\ j^2(L')\ I'|j^3a_sI'). \quad (5.11)$$

In the latter expression, $\lambda = (L + L')/2$, and the nbol D(L,L') has been introduced to simplify the cal- ation of the selection rules for ΔL.

The coefficients $\Delta(\lambda j\alpha_s;II')$ and $\sigma(j\alpha_s;II')$ enable one xpress the matrix elements of the Hamiltonian of ee identical nuclei in terms of the appropriate matrix ments of one of the identical nuclei. Numerical tables of them are presented in ref. 11 for the cases j = 1 and 3/2.

To evaluate the hyperfine interaction energy, molecular wave functions which take account of the nuclear statistics should be used. Below we write out the appropriate vectors of the molecular states in the representation $IKj^3\alpha IF$, omitting the nonessential index M_F:

$$|JKj^3A_{1,2}IF)=\frac{1}{\sqrt{2}}\{|JKj^3A_{1,2}IF)$$

$$\pm(-1)^{I+v+2j}|J-Kj^3A_{1,2}IF)\}, \quad (5.12)$$

$$|JKj^3EIF)=\frac{1}{2}\{|JKj^3E,\ JF)-|JKj^3E_2IF)\}$$

$$+\frac{1}{2}(-1)^{I+v+2j}\{|J-Kj^3E_1IF)+|J-Kj^3E_2IF)\}. \quad (5.13)$$

The expression (5.12) corresponds to the case when K is a multiple of 3, the expression (5.13) to the case when K is not a multiple of 3. The upper sign in the right-hand side of (5.12) is to be taken for A_1, the lower for A_2. The quantum number v has been introduced in case account is taken of inversion doubling; v = 0 or 1 respectively for the lower (symmetric) and the upper (antisymmetric) inversion states.

The matrix element of the hyperfine interaction energy of the identical nuclei, of the form (4.8),* equals

*Translation Editor's Note: The original cites (1.8) but this we believe to be a misprint for (4.8).

$$(JKj^3A_{1,2}IF|H_\lambda|JKj^3A_{1,2}I'F)=\Delta(\lambda jA_{1,2};\ II')$$

$$\times(-1)^{\lambda+j+I+F}\begin{Bmatrix}\lambda II'\\ FI'I\end{Bmatrix}(JK\|m^{(\lambda)}\|JK)(j\|M^{(\lambda)}\|j). \quad (5.14)$$

for the case when K is a multiple of 3. Here account is taken of the fact that

$$(JK\|m^{(\lambda)}\|JK)=(J-K\|m^{(\lambda)}\|J-K) \quad (5.15)$$

and that $(JK\|m'^{(\lambda)}\|J\text{-}K)$ reverts to zero for $\lambda < 6$. For the case when K is not a multiple of 3, a result somewhat different from (5.14) is obtained:

$$(JKjEIF|H_\lambda|JKj^3EI'F)=(-1)^{\lambda+j+I+F}\begin{Bmatrix}\lambda II'\\ FI'I\end{Bmatrix}(j\|M^{(\lambda)}\|j)$$

$$\times\Big[\alpha(J,I')(JK\|m^{(\lambda)}\|JK)+(-1)^{I+v+2j}\beta(I,I')$$

$$\times\Big(JK\Big\|\frac{1}{2}(m^{(\lambda)}+m^{(\lambda)+})\Big\|J-K\Big)\Big], \quad (5.16)$$

where

$$\left.\begin{aligned}\alpha(II')&=\frac{1}{2}[\Delta(\lambda jE_1;\ II')+\Delta(\lambda jE_2;\ II')],\\ \beta(II')&=\frac{1}{2}[\Delta(\lambda jE_1;\ II')-\Delta(\lambda jE_2;\ II')].\end{aligned}\right\} \quad (5.17)$$

An analogous expression may be obtained on the basis of (5.8) for the spin-spin interaction of the group of identical nuclei with some other nucleus.

The term in (5.16) which is proportional to $\beta(II')$ for K = 1 may be different from zero for quadrupole and magnetic interactions of nuclei situated off the axis of the molecule. It describes the additional shift which has been observed in the inversion spectra of ordinary[15] and deuterated[16] ammonia in the form of a splitting of those hyperfine structure lines which correspond to transitions between levels with K = 1.[17] Analogously, we obtain for the spin-spin interactions of the identical nuclei

$$(JKj^3A_{1,2}IF \mid H_1 (j \cdot i) JKj^3A_{1,2}I'F) = \frac{\sqrt{3}}{2} (\mu_n g)^2 r^{-3} (-1)^{F+K-j}$$

$$\times \sigma (jA_{1,2};\ II') \sqrt{j(j+1)(2j+1)(2I+1)} \begin{pmatrix} II2 \\ K-K0 \end{pmatrix} \begin{Bmatrix} 2II \\ FI'I \end{Bmatrix}, \quad (5.18)$$

$$(JKj^3EIF \mid H_1 (j \cdot i) \mid JKj^3EI'F) = \sqrt{30} (\mu_n g)^2 r^{-3} \sqrt{j(j+1)(2j+1)(2I+1)}$$

$$\times (-1)^{\bar{H}+K-j} \begin{Bmatrix} 2II \\ FI'I \end{Bmatrix} \left[\frac{1}{2} \sigma (II') \begin{pmatrix} II2 \\ K-K0 \end{pmatrix} - \delta_{k,1} (-1)^{I+s+2j} \right.$$

$$\left. \times \sqrt{\frac{3}{2}} \tau (I, I') \begin{pmatrix} II2 \\ 11-2 \end{pmatrix} \right], \quad (5.19)$$

where r is the distance between the identical nuclei, and

$$\left.\begin{aligned} \sigma (II') &= \tfrac{1}{2} [\sigma (jE_1;\ II') + \sigma (jE_2;\ II')], \\ \tau (II') &= \tfrac{1}{2} [\sigma (jE_1,\ II') - \sigma (jE_2;\ II')]. \end{aligned}\right\} \quad (5.20)$$

APPENDIX

In the present work, the designations proposed by Wigner and adopted in ref. 7 are used for the 3n-j symbols. The 3-j symbol is connected with the Clebsch-Gordan coefficient and the $\overline{V}$-coefficient [F. R.] by the relations

$$\begin{pmatrix} j_1 j_2 j_3 \\ m_1 m_2 m_3 \end{pmatrix} = \frac{(-1)^{j_1 - j_2 - m_3}}{\sqrt{2j_3+1}} (j_1 j_2 j_3 - m_3 \mid j_1 m_1 j_2 m_2)$$

$$= (-1)^{j_1+j_2+j_3} \overline{V} \begin{pmatrix} j_1 j_2 j_3 \\ m_1 m_2 m_3 \end{pmatrix}. \quad (A.1)$$

The 6-j symbol coincides with the $\overline{W}$-coefficient [F. R.] and is connected with the Racah coefficient[7] by the relation

$$\begin{Bmatrix} j_1 j_2 j_3 \\ l_1 l_2 l_3 \end{Bmatrix} = \overline{W} \begin{pmatrix} j_1 j_2 j_3 \\ l_1 l_2 l_3 \end{pmatrix} = (-1)^{j_1+j_2+l_1+l_2} W (j_1 j_2 l_2 l_1;\ j_3 l_3). \quad (A.2)$$

The 9-j symbol is connected with the Fano designation by the relation

$$\begin{Bmatrix} j_1 j_2 j_3 \\ k_1 k_2 k_3 \\ l_1 l_2 l_3 \end{Bmatrix} = X \begin{pmatrix} j_1 j_2 j_3 \\ k_1 k_2 k_3 \\ l_1 l_2 l_3 \end{pmatrix}. \quad (A.3)$$

The phases of the irreducible tensor operators are chosen in such a way that the operator is self-adjoint in the sense of [F. R.], i.e.,

$$T^{(\lambda)+}_{\mu} = (-1)^{\lambda-\mu} T^{(\lambda)}_{-\mu} \quad (A.4)$$

The Eckart-Wigner theorem is written in the form

$$\langle jm \mid T^{(\lambda)}_{\mu} \mid j'm' \rangle = (-1)^{j-m} \begin{pmatrix} j' j \lambda \\ m' - m\mu \end{pmatrix} (j \| T^{(\lambda)} \| j'), \quad (A.5)$$

while

$$(j \mid T^{(\lambda)+} \mid j') = (-1)^{j-j'-\lambda} (j \| T^{(\lambda)} \| j). \quad (A.6)$$

We make use of the scalar spherical functions $Y^{(1)}_m(\theta,\varphi)$, which differ from the usual[14] $Y_{1m}(\theta,\varphi)$:

$$Y^{(l)}_m (\theta, \varphi) = i^l \sqrt{\frac{4\pi}{2l+1}} Y_{lm} (\theta, \varphi) = i^l D^{(l)}_{0,m} (0, \theta, \varphi). \quad (A.7)$$

The vector spherical functions, defined as

$$Y^{(l,\lambda)}_{\mu} (\theta, \varphi) = \sum_{m} (l1\lambda\mu \mid lm1\nu) Y^{(l)}_{m} (\theta, \varphi) e_{\nu}, \quad (A$$

are self-adjoint irreducible tensors of rank λ, and

$$Y^{(l,\lambda)*}_{\mu} (\theta, \varphi) = (-1)^{\lambda-\mu} (\theta, \varphi). \quad (A$$

The spherical basis vector e_μ is defined in correspondence with (A.4)

$$e_{\pm 1} = \frac{1}{\sqrt{2}} (e_y \pm i e_x), \quad e_0 = i e_z, \quad (A.$$

so that

$$T^{(1)}_{\mu} = (\mathbf{T} \cdot \mathbf{e}_{\mu}), \quad \mathbf{T} = \sum_{\mu=1,0,-1} T^{(1)}_{\mu} e^{*}_{\mu}. \quad (A.$$

In conclusion, the author would like to express his gratitude to N. G. Basov for his attention to the work and for valuable advice. The author is also grateful to A. M. Baldin and A. M. Prokhorov for useful discussions of a number of questions connected with the present work.

REFERENCES

1. R. L. White, Revs. Modern Phys. **27**, 276 (1955).
2. C. H. Townes and A. Schawlow, "Microwave Spectroscopy." McGraw-Hill, New York, 1955. Foreign Literature Press, Moscow, 1959.
3. J. Bardeen and C. H. Townes, Phys. Rev. **73**, 647 (1948).
4. G. R. Gunter-Mohr, C. H. Townes, and J. H. Van Vleck; Phys. Rev. **94**, 1191 (1954).
5. J. P. Gordon, Phys. Rev. **99**, 1253 (1955).
6. A. P. Yutsis, I. B. Levinson, and V. V. Vanagas, "Mathematical Techniques of Angular Momentum Theory." GI PNL Litovsk. SSR, Vilna, 1960.
7. A. R. Edmonds, "Angular Momentum in Quantum Mechanics." Princeton Univ. Press, 1957.
8. U. Fano and G. Racah, "Irreducible Tensorial Sets" Academic Press, New York, 1959.
9. N. F. Ramsey, "Molecular Beams." Oxford Univ. Press, 1956.
10. J. H. Van Vleck, Revs. Modern Phys. **23**, 213 (1951)
11. N. G. Basov and K. K. Svidzinskii, Otchet Fiz. Inst. Akad. Nauk (Report of the Physics Institute, Academy of Sciences), 1960.
12. C. Swartz, Phys. Rev. **97**, 380 (1955).
13. R. S. Henderson and J. Van Vleck, Phys. Rev. **74**, 1066 (1948).
14. L. D. Landau and E. M. Lifshits, "Quantum Mechanics: Nonrelativistic Theory." State Technical Press, Moscow-Leningrad, 1948. Addison Wesley, Reading, Mass., 1958.
15. G. R. Gunter-Mohr, R. L. White, A. L. Schawlow, W. E. Good, and D. K. Coles, Phys. Rev. **94**, 1184 (1954).
16. G. Herrman, J. Chem. Phys. **29**, 875 (1959).
17. E. Condon and G. H. Shortley, "Theory of Atomic Spectra." Cambridge Univ. Press, 1935. Foreign Literature Press, Moscow, 1949.

VIBRATIONAL SPECTRA OF THE B_2O_3 AND B_2S_3 MOLECULES

V. M. Tatevskii, G. S. Koptev, and A. A. Mal'tsev (pp. 724-729)

Received 2 January 1961

A calculation of the vibrational spectra of the $B_2^{10}O_3$, $B_2^{11}O_3$, $B^{10}B^{11}O_3$, $B_2^{10}S_3$, and $B_2^{11}S_3$ molecules has been made, and the erroneousness of the calculations of White and his collaborators has been established. It is shown that the bands observed at 1302 and 742 cm^{-1} in the infrared emission spectrum of the vapors over boric anhydride are to be assigned to the spectrum of the liquid phase and not to that of the B_2O_3 molecule. The 993 cm^{-1} band in the spectrum of boron sulfide is also to be assigned to the spectrum of the liquid phase.

At the present time, on account of the great experi-ıtal difficulties associated with the high boiling points óric anhydride and boron sulfide, the vapor spectra hese compounds are little known. On the basis of ctron-diffraction[1] and spectroscopic[2,3] data, it may be sidered as established that, in the gas phase, the B_2O_3 ecule has bent planar structure (C_{2v} symmetry) and a bipyramidal one (D_{3h} symmetry) as was previously epted.[4,5] The B_2S_3 molecule has an analogous struc-.[6] Using the bent model and selecting reasonable ce constants as a basis for estimation, one can carry a calculation of the vibrational spectrum of the B_2O_3 B_2S_3 molecules and can compare it with the existing erimental data. We have carried out such a calcula- for the B_2O_3 molecule,[7] but the results obtained do agree with the data of White et al.[3] who observed, in infrared emission spectrum of the vapors over boric ydride, three bands at 2040, 1302, and 742 cm^{-1}, which assigned to the antisymmetric vibrations of the B=O B—O bonds and the O—B=O angle respectively.

The contradiction comes down basically to the fact in our calculations the frequency of the antisymmetric ration of the B—O bond amounted to about 900 cm^{-1}, the 1302 cm^{-1} frequency, which was assigned by those hors[3] to that type of vibration, was not obtained as a ult of the calculations even when the force constants e varied within quite wide limits. Our attempt to pute the vibrational frequencies from the force con-nts presented in ref. 3, or, conversely, to determine force constants from the frequencies led to absurd ults. This permits us to consider that there is an er- in the calculations of ref. 3.

Comparison of the 1302 and 742 cm^{-1} bands ob-ved in the emission spectrum of the vapors over B_2O_3 h the 1316 and 720 cm^{-1} bands in the reflection spec-m of liquid boric anhydride,[8] as well as the fact that s impossible to obtain a 1302 cm^{-1} band by calculation, us to the conclusion[9] that these two bands belonged to particles of liquid B_2O_3, which were observed[3] in the m of a mist at the ends of the heater. Thus, of the ee experimentally observed bands, only the 2040 cm^{-1} d can be assigned to the spectrum of the B_2O_3 mole-e in the gas phase. A similar situation is observed in spectrum of the vapors over B_2S_3.[10,11]

In order to have a correct idea of the vibrational ctra of the B_2O_3 and B_2S_3 molecules and to use them uture for the calculation of thermodynamic functions the assignment of experimental frequencies, we have ried out a calculation, more detailed than before, of vibrational spectra of the $B_2^{10}O_3$ and $B_2^{11}O_3$ molecules, have also newly computed the spectra of $B^{10}B^{11}O_3$, S_3, and $B_2^{11}S_3$, starting from the values of the one experimental frequency and the force constants estimated from the data for related compounds.

CALCULATION OF THE VIBRATIONAL SPECTRUM OF THE $B_2^{10}O_3$ AND $B_2^{11}O_3$ MOLECULES

The two molecules under consideration each have nine normal vibrations which belong to four symmetry types: $4A_1 + 3B_1 + 1A_2 + 1B_2$. All the vibrations (with the exception of A_2) are allowed in the infrared and Raman spectra. The A_2 vibration is allowed only in the Raman spectrum. In the calculation of the vibration frequencies, we used the coordinates presented in the Figure for the changes in the internuclear distances and valence angles; here D = r(B=O), d = r(B—O), $\alpha = \angle$B—O—B, $\beta = \angle$O—B=O (in the plane of the molecule), and $\gamma = \angle$O—B=O (out of the plane of the molecule).

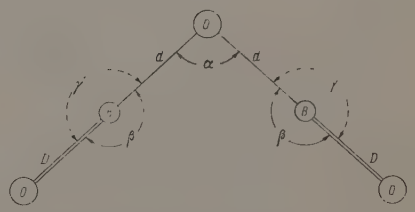

The potential energy matrix for the angular model of the molecule of the type X_2Y_3 can be represented in the form

$$2V = \begin{bmatrix} F_1 & 0 & & 0 & & & & & \\ 0 & F_2 & F_{23}\sqrt{2} & 0 & & & & & \\ 0 & F_{32}\sqrt{2} & F_3 & 0 & & & & & \\ 0 & 0 & 0 & F_4 & & & & & \\ & & & & F_5 & 0 & 0 & & \\ & & & & 0 & F_6 & 0 & & \\ & & & & 0 & 0 & F_7 & & \\ & & & & & & & F_8 & \\ & & & & & & & & F_9 \end{bmatrix},$$

where the force constants for B_2O_3 have the following values: $F_1 = F_5 = K_D = 13.4 \times 10^5$ dynes/cm, $F_2 = F_6 = K_d = 5.3 \times 10^5$ dynes/cm, $F_3 = K_\alpha = 1 \times 10^{-11}$ dyne-cm, $F_4 = F_7 = K_\beta = 1 \times 10^{-11}$ dyne-cm, $F_8 = F_9 = K_\gamma = 1 \times 10^{-11}$ dyne-cm, $F_{32} = K_{d\alpha} = 1 \times 10^{-3}$ dyne.

The force constant K_D was taken equal to that for the BO radical and was then increased by 0.1×10^5 dyne/cm, so that the data from the calculation of the antisymmetric vibrations (their bands are generally more intense than those of the totally symmetric ones) should agree with the experimental frequencies 2095 and 2035 cm^{-1} [3] for the two isotopic molecules $B_2^{10}O_3$ and $B_2^{11}O_3$. The force constant K_d was set equal to that for boric acid.[12] As a result of the fact that the vibrational spectra of boron compounds have been little studied, the remaining force constants were estimated on the basis of the data for other molecules: K_α from the force constants of the F_2O molecule,[13] K_β and K_γ from the data for ethylene and propylene,[14] in which there are a double and a single bond in sequence. The interaction constant $K_{d\alpha}$ was estimated from the data for F_2O.[13]

The kinetic energy matrix for the angular model of a molecule of the type X_2Y_3 can be represented in the form

$$2T = \begin{vmatrix} G_{11} & G_{12} & 0 & 0 & & & & & \\ G_{21} & G_{22} & G_{23}\sqrt{2} & G_{24} & & & & & \\ 0 & G_{32}\sqrt{2} & G_{33} & G_{34}\sqrt{2} & & & & & \\ 0 & G_{42} & G_{43}\sqrt{2} & G_{44} & & & & & \\ & & & & G_{55} & G_{56} & 0 & & \\ & & & & G_{65} & G_{66} & G_{67} & & \\ & & & & 0 & G_{76} & G_{77} & & \\ & & & & & & & G_{88} & \\ & & & & & & & & G_{99} \end{vmatrix}.$$

where, taking

$$\frac{1}{m(B)} = \mu_x, \quad \frac{1}{m(O)} = \mu_y, \quad \frac{1}{r(B{=}O)} = Q, \quad \frac{1}{r(B{-}O)} = q,$$

$$G_{11} = G_{55} = \mu_x + \mu_y,$$
$$G_{12} = G_{56} = -\mu_x,$$
$$G_{22} = \mu_x + \mu_y(1 + \cos\alpha),$$
$$G_{23} = -\mu_y q \cdot \sin\alpha,$$
$$G_{24} = \mu_y q \cdot \sin\alpha,$$
$$G_{33} = 2q^2[\mu_y(1 - \cos\alpha) + \mu_x],$$
$$G_{34} = -\mu_x q(q + Q) - 2\mu_y q^2 \sin^2\frac{\alpha}{2},$$
$$G_{44} = \mu_x(q + Q)^2 + \mu_y[q^2(1 - \cos\alpha) + Q^2],$$
$$G_{66} = \mu_x + \mu_y(1 - \cos\alpha),$$
$$G_{67} = -\mu_y q \cdot \sin\alpha,$$
$$G_{77} = \mu_x(q + Q)^2 + \mu_y[q^2(1 + \cos\alpha) + Q^2],$$
$$G_{88} = \mu_x(q + Q)^2 + \mu_y(2q^2 + Q^2),$$
$$G_{99} = \mu_x(q + Q)^2 + \mu_y Q^2.$$

In the determination of the kinetic energy coefficients, the following geometrical parameters were used[1]: D = 1.20 A, d = 1.36 A, $\alpha = 95°$, $\beta = \gamma = 180°$. The masses of the atoms B^{10} and B^{11} equalled 10.016118 and 11.012796.

The potential and kinetic energy submatrices were substituted into the secular equation by means of which the vibrational frequencies relating to the symmetry types A_1, B_1, A_2, and B_2 were evaluated. The results obtained for the $B_2^{10}O_3$ and $B_2^{11}O_3$ molecules are presented in the Table.

A change in the force constant K_D to 16.0×10^5 dynes/cm (the remaining constants were not changed) gives the following frequency values (cm^{-1}) for the antisymmetric vibrations: $\nu_5 = 2183$, $\nu_6 = 946$, $\nu_7 = 659$. In the same way, a change in K_d to 7.42×10^5 dynes/cm gives $\nu_5 = 2110$, $\nu_6 = 1044$, $\nu_7 = 669$, and a change in K to 2×10^{-11} dyne-cm gives $\nu_5 = 2029$, $\nu_6 = 1073$, $\nu_7 =$

Band Frequencies (cm^{-1}) in the Vibrational Spectra of the $B_2^{10}O_3$, $B^{10}B^{11}O_3$, $B_2^{11}O_3$, $B_2^{10}S_3$, and $B_2^{11}S_3$ Molecules

Vibration	Symmetry	$B_2^{10}O_3$	$B^{10}B^{11}O_3$	$B_2^{11}O_3$	$B_2^{10}S_3$	$B_2^{11}S_3$
ν_1	A_1	2084	2022	2015	1359	1306
ν_2		844	829	815	425	409
ν_3		755	754	749	399	396
ν_4		161	161	160	66	64
ν_5	B_1	2097	2091	2029	1364	1311
ν_6		938	936	933	463	461
ν_7		682	668	658	347	333
ν_8	A_2	778	768	753	374	360
ν_9	B_2	700	685	673	351	336

CALCULATION OF THE VIBRATIONAL SPECTRUM OF THE $B^{10}B^{11}O_3$ MOLECULE

As a result of the fact that boric anhydride of the natural isotopic composition consists basically of $B_2^{11}O$ molecules (64%) and $B^{10}B^{11}O_3$ molecules (32%), the calculation of the vibrational spectrum of $B^{10}B^{11}O_3$ is of considerable interest. When the boron atoms in B_2O_3 have different masses, the symmetry of the molecule is lowered to C_s. In this case, seven of the nine normal vibrations relate to planar vibrations of type A′ and t to nonplanar vibrations of type A″; i.e., on going over from C_{2v} to C_s symmetry, one has the correlation A_1 and $B_1 \rightarrow A'$, A_2 and $B_2 \rightarrow A''$.

All the vibrations are allowed in both the infrared and Raman spectra.

The potential energy matrix for the molecule of t type XZY_3 may be represented in the form

$$2V = \begin{vmatrix} F_1 & 0 & 0 & 0 & 0 & 0 & 0 & & \\ 0 & F_2 & F_{23} & 0 & 0 & 0 & 0 & & \\ 0 & F_{32} & F_3 & 0 & 0 & F_{36} & 0 & & \\ 0 & 0 & 0 & F_4 & 0 & 0 & 0 & & \\ 0 & 0 & 0 & 0 & F_5 & 0 & 0 & & \\ 0 & 0 & F_{63} & 0 & 0 & F_6 & 0 & & \\ 0 & 0 & 0 & 0 & 0 & 0 & F_7 & & \\ & & & & & & & F_8 & 0 \\ & & & & & & & 0 & F_9 \end{vmatrix}$$

where the force constants are the same as for $B_2^{10}O_3$ and $B_2^{11}O_3$. The kinetic energy matrix has the form

$$2T = \begin{vmatrix} G_{11} & G_{12} & 0 & 0 & 0 & 0 & 0 & & \\ G_{21} & G_{22} & G_{23} & 0 & 0 & G_{26} & G_{27} & & \\ 0 & G_{32} & G_{33} & G_{34} & 0 & G_{36} & G_{37} & & \\ 0 & 0 & G_{43} & G_{44} & 0 & G_{46} & G_{47} & & \\ 0 & 0 & 0 & 0 & G_{55} & G_{56} & 0 & & \\ 0 & G_{62} & G_{63} & G_{64} & G_{65} & G_{66} & 0 & & \\ 0 & G_{72} & G_{73} & G_{74} & 0 & 0 & G_{77} & & \\ & & & & & & & G_{88} & G_{89} \\ & & & & & & & G_{98} & G_{99} \end{vmatrix}$$

where, taking

$$\frac{1}{m(B^{10})} = \mu_{x_1} \text{ and } \frac{1}{m(B^{11})} = \mu_{x_2},$$

$$G_{11} = G_{22} = \mu_{x_1} + \mu_y,$$
$$G_{12} = -\mu_{x_1},$$
$$G_{23} = G_{36} = -\mu_y q \cdot \sin\alpha,$$
$$G_{26} = \mu_y \cos\alpha,$$
$$G_{27} = G_{46} = \mu_y q \cdot \sin\alpha,$$
$$G_{33} = q^2 [2\mu_y (1 - \cos\alpha) + (\mu_{x_1} + \mu_{x_2})],$$
$$G_{34} = -\mu_{x_1} q (q + Q) - \mu_y q^2 2 \cdot \sin^2 \frac{\alpha}{2},$$
$$G_{37} = -\mu_{x_2} q (q + Q) - \mu_y q^2 2 \sin^2 \frac{\alpha}{2},$$
$$G_{44} = G_{88} = \mu_{x_1} (q + Q)^2 + \mu_y (q^2 + Q^2),$$
$$G_{47} = -\mu_y q^2 \cos\alpha,$$
$$G_{55} = G_{66} = \mu_{x_3} + \mu_y,$$
$$G_{56} = -\mu_{x_3},$$
$$G_{77} = G_{99} = \mu_{x_2} (q + Q)^2 + \mu_y (q^2 + Q^2),$$
$$G_{89} = \mu_y q^2.$$

In the calculation of the kinetic energy coefficients, same parameters were used as for the $B_2^{10}O_3$ and O_3 molecules.

The results of the calculation are presented in the le.

LCULATION OF THE VIBRATIONAL SPECTRUM OF THE $B_2^{10}S_3$ AND $B_2^{11}S_3$ MOLECULES

Since the B_2S_3 molecule has just the same configura- as B_2O_3, the entire course of the calculation of the rational spectrum is exactly the same. The following es of the force constants were adopted for B_2S_3: 6.6×10^5 dynes/cm, $K_d = 2.6 \times 10^5$ dynes/cm, $K_\alpha = K_\gamma = 0.5 \times 10^{-11}$ dyne-cm, $K_{d\alpha} = 0.4 \times 10^{-3}$ dyne. force constant K_D, as in the case of B_2O_3, was sen from considerations of the best agreement be- on the results of the calculation and the experimental quencies 1361 and 1314 cm^{-1} [11] for the two isotopic ecules $B_2^{10}S_3$ and $B_2^{11}S_3$. The force constants K_d, K_α, K_γ, and $K_{d\alpha}$ were estimated from the corresponding stants of the B_2O_3 molecule, on the supposition that ratio of the K_D values for B_2O_3 and B_2S_3 would hold ghly for the remaining constants also.

The geometrical configuration of B_2S_3 is the follow- D = 1.65 A, d = 1.81 A, $\alpha = 96°$, $\beta = \gamma = 180°$.

The mass of the S^{32} atom was taken equal to 31.98085. results of the calculation are presented in the Table.

CUSSION OF RESULTS

The calculation carried out for the vibrational spec- n of the B_2O_3 molecule, and the variation of the force stants, clearly show that the 1302 cm^{-1} band observed ef. 3 cannot be assigned to a B—O stretching vibration the bent model of B_2O_3 in the gas phase. If there are arate B_2O_3 molecules in boric anhydride vapors, still ic anhydride in the liquid and solid phases is a sort of polymeric network, in which BO_3 groups are joined to one another through oxygen.[15,16] Therefore, there is no basis for considering, as these authors[3] have done, that the frequency in the 1300 cm^{-1} region which is characteristic for the antisymmetric stretching vibrations of the BO_3 groups in borate esters,[17] boric acid, and boric anhydride[16] is preserved in the O—B=O groups of the B_2O_3 molecule in the gas phase. As for the 742 cm^{-1} band, although with some variation in the force constants it can be obtained by calculation, still it also should be assigned to the spectrum of liquid B_2O_3, in which, like the 1302 cm^{-1} band, it is quite intense.[8]

Thus, for a more exact determination of the force constants and a refinement of the vibrational frequencies, a further more careful spectroscopic investigation is necessary, especially in the 900 cm^{-1} region, in which the presence of a band caused by the antisymmetric vibrations of the B—O bond is expected.

Comparison of the infrared emission spectrum of the vapors over boron sulfide[11] with the computed vibrational spectrum likewise shows that, as in the case of B_2O_3, the 993 cm^{-1} band is to be assigned to the spectrum of liquid B_2S_3.

REFERENCES

1. P. A. Akishin and V. P. Spiridonov, Doklady Akad. Nauk SSSR **131**, 557 (1960).
2. D. White, P. N. Walsh, and D. E. Mann, J. Chem. Phys. **28**, 508 (1958).
3. D. White, D. E. Mann, P. N. Walsh, and A. Sommer, J. Chem. Phys. **32**, 481 (1960).
4. V. N. Huff, S. Gordon, and V. E. Morrell, Natl. Advisory Comm. for Aeronaut., Rept. 1037 (1951).
5. D. A. Dowes and R. F. Porter, J. Am. Chem. Soc. **78**, 5165 (1956).
6. P. A. Akishin and V. P. Spiridonov, Doklady Akad. Nauk SSSR **129**, 1317 (1959).
7. A. A. Mal'tsev, V. N. Matveev, and V. M. Tatevskii, Doklady Akad. Nauk SSSR **137**, 123 (1961).
8. E. P. Markin and N. N. Sobolev, Izvest. Akad. Nauk SSSR, Ser. Fiz. **23**, 62 (1959).
9. A. A. Mal'tsev and V. M. Tatevskii, Opt. i Spektr. **10**, 564 (1961), Optics and Spectroscopy **10**, 295 (1961).
10. F. T. Greene and J. L. Margrave, J. Am. Chem. Soc. **81**, 5555 (1959).
11. A. Sommer, P. N. Walsh, and D. White, J. Chem. Phys. **33**, 296 (1960).
12. C. W. F. T. Pistorius, J. Chem. Phys. **31**, 1454 (1959).
13. K. Venkateswarlu and P. Thirugnanasamband, Z. physik. Chem. (East Germany) **212**, 138 (1959).
14. E. B. Wilson and A. J. Wells, J. Chem. Phys. **9**, 319 (1941).
15. A. H. Silver and P. J. Bray, J. Chem. Phys. **29**, 984 (1958).
16. J. L. Parsons and M. E. Milberg, J. Am. Ceram. Soc. **43**, 326 (1960).
17. R. L. Werner and K. G. O'Brien, Austral. J. Chem. **8**, 355 (1955).

VIBRATIONAL SPECTRA OF VINYL ALKYL SULFIDES—THEORETICAL ANALYSIS

E. M. Popov and G. I. Kagan (pp. 730-734)

Received 4 January 1961

The frequencies, forms, and atomic displacements have been computed for the symmetric vibrations of three of the possible conformations of the CH_2=CHSCH$_3$ molecule, and the sensitivity of the frequencies to changes in the force constants has been determined. The characteristic vibrations of the vinyl group are examined. The Raman spectra of certain unsubstituted, and also of α- and β-alkyl-substituted, vinyl alkyl sulfides are presented.

The chemistry of unsaturated sulfur-containing compounds has recently undergone extensive development, especially the chemistry of the vinyl sulfides. However, only fragmentary information on the vibrational spectra of vinyl sulfides has been published in the literature, and even that is exclusively of a qualitative nature. The study of the vibrational spectra of this class of compounds is of great interest both from the point of view of revealing the characteristic vibration frequencies of the molecules and of using them for structural and analytical purposes, and from the point of view of clarifying the nature of the interaction of the sulfur atom with the double bond. A theoretical examination of the vibrations of the simplest vinyl alkyl sulfide molecules may be of substantial help in this investigation.

The present work, which is devoted to the calculation of the normal vibrations of the vinyl sulfide CH_2=CHSCH$_3$, was undertaken with the purpose of revealing the characteristic vibration frequencies of this molecule and of finding the regularities which are common to the spectra of the vinyl alkyl sulfides.

In the literature, we have found only the one work of Price and Gillis,[1] in which the frequencies of the infrared spectrum of vinyl methyl sulfide in the 650-1700 cm^{-1} region are presented. Since the literature data proved insufficient for the verification of certain conclusions which followed from the calculations, we have obtained the Raman spectra of a number of unsubstituted, and also of α- and β-alkyl-substituted, vinyl alkyl sulfides.*

*The compounds were kindly furnished by N. K. Kul'bovskaya.

MATERIALS STUDIED, SYMBOLS, VALUES OF THE PARAMETERS, AND EXPERIMENTAL PART

We chose for calculation three of the possible rotational isomers of the CH_2=CHSCH$_3$ molecule, differing in the position of the methyl group; the models of these and the symbols adopted for the coordinates are represented in the Figure. The choice of several models is connected with the fact that the actual position of the methyl group is unknown. Examination of the vibrational spectra of the limiting models of the vinyl methyl sulfide molecule make it possible to elucidate the dependence of the normal vibration frequencies on the angle of rotation of the methyl group and to draw conclusions which will be valid for any realizable conformation.

In models I and II, which have C_s symmetry, the S—$C_{(7)}$ and $C_{(7)}$—$H_{(8)}$ bonds are located in the plane of the vinyl group; in model III, they are in a plane perpendicular to it. In accordance with the grometry, there must

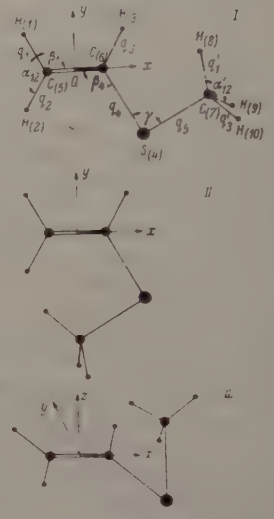

be 16 symmetric vibrations in models I and II, and 19 model III.

The generalized angular coordinates are connect by the supplementary relations:

$$\beta_1 + \beta_2 + \alpha_{12} = 0,\ \beta_3 + \beta_4 + \alpha_{34} = 0,$$
$$\beta'_1 + \beta'_2 + \beta'_3 + \alpha'_{12} + \alpha'_{13} + \alpha'_{23} = 0.$$

The elements of the T^{-1} matrix were evaluated a cording to formulas taken from the tables of ref. 2 fo the following values of the bond lengths (A): $L_{C=C}$ = 1 $L_{C-H(1,2,3)}$ = 1.07; $L_{C-H(8,9,10)}$ = 1.09; and $L_{C(6)-S,\ S-C(}$ 1.82. Angles β_i and α_{ij} were taken equal to 120°, an γ to 91°, and angles β'_i and α'_{ij} were taken to be tetra hedral. The length of the C—H bond in methane (1.09 was taken as the unit of bond length. The spectrosco mass of the hydrogen atom, m_H = 1.088, was taken as unit of mass.

The same force constants, the values of which ar presented in Table 1, were adopted for all three rota tional isomers. The force constants corresponding t CH_2=CH— group were taken from the results of a ca lation of the vibrations of the ethylene molecule,[3] and those corresponding to the SCH_3 group were taken fr the results of a calculation of the vibrations of the m captan molecule.[4] The partial derivatives of the freq cies with respect to the force parameters were evalu according to Mayants's method.[5] The calculation of t frequencies, zero-order amplitudes, and atomic disp ments was carried out on an electronic computer of t "Arrow" type according to programs developed by A M. Bogomolov.

Table 1. Force Constants (10^6 cm^{-2})

K_{σ_1}	K_{σ_2}	$K_{\sigma'_1}$	K_{σ_3}	$K_{\sigma_{ij}}$	K_τ	$K_{\tau'_1}$	$K_{\tau_{ij}}$	$h_{Q\alpha_1}$	$h_{Q\alpha_2}$	$h'_{1\beta_1}$	$h_{Q\alpha_3}$	$h'_{2\beta_1}$	$a_{\eta_{ij}}$	$am'_{1\gamma_1}$	$am'_{2\gamma_1}$	$a'_{\beta_1\gamma_1}$	$a_{\eta_4(5)\tau}$
5.3	5.0	8.1	0.80	0.58	1.05	0.91	0.71	0.1	0.03	0.05	0.03	0.03	0.43	0.55	0.35	0.35	0.50

: The coefficients $l_{ij} = -0.035$, $n_{ij} = -0.025$, $m_{ij} = 0.12$; the coefficients b_{ij} were taken equal to zero.

The Raman spectra of the unsubstituted and substituted vinyl alkyl sulfides listed below were obtained with exciting line 4358 A, using an ISP-67 three-prism trograph which possessed a linear dispersion of 22 m in the 4860 A region. The frequencies are given n^{-1}; the band intensities on a ten-point scale are ated in parentheses (b—broad line).

H_2=CH—S—C_2H_5*: 3095(7), 3048(1), 3006(8), 2929(9), 2873(5), 1587(10), 1458(3), 1430(2), 1382(10), 1280(10), 1067(4), 1056(2), 1024(1), 980(1b), 874(1b), 724(3b), 680(4), 666(4), 653(4), 601(0), 466(3b), 420(3), 397(3), 334(5b), 275(0), 193(1b).

H_2=CH—SC_3H_7*: 3097(7), 3050(3), 3010(7), 2970(5), 2925(7b), 2867(5b), 1586(10), 1484(3), 1444(2), 1431(2), 1372(5), 1333(1), 1291(2), 1271(10), 1236(3), 1214(1), 1084(3), 1023(4), 888(1), 831(1), 787(1), 737(1), 715(3), 641(2), 462(2), 432(1), 394(2), 353(1), 331(2), 281(1), 228(1), 172(2).

H_2=C(CH_3)S—C_2H_5: 3100(4), 3028(5), 2996(4), 2975(5), 2951(4), 2926(10), 2876(6b), 1609(10), 1453(3), 1430(3), 1404(6), 1376(2), 1340(1), 1295(2), 1263(1), 1214(2), 1107(0), 1056(3), 996(3), 926(4), 889(0), 843(1), 701(2), 694(1), 669(2), 645(1), 625(4), 325(2).

H_2=C(CH_3)SC_3H_7: 3099(4), 3027(5), 2995(2), 2971(6), 2338(5), 2917(10), 2875(6b), 1606(10), 1448(4), 1435(3), 1402(5), 1372(2), 1332(2), 1292(4), 1238(1), 1216(2), 1088(1), 1029(3), 992(3), 923(4), 879(0), 836(1), 651(2), 624(2).

H_2=C(CH_3)SC_4H_9: 3100(4), 3026(6), 2994(4), 2968(2), 2941(5), 2916(10), 2878(6b), 2863(6b), 1607(10), 1444(4), 1432(3), 1402(6), 1372(1), 1339(1), 1298(1), 1269(1), 1220(0), 1100(3), 1053(3), 994(4), 924(4), 894(2), 871(2), 807(1), 750(0), 649(0), 629(2), 354(1), 284(2).

$CH_3)_3$CCH=CHSC_2H_5: 3048(3), 2964(10b), 2930(9), 2803(7), 2873(6), 2858(6), 1668(2), 1642(2), 1603(10), 1458(3), 1443(4), 1423(2), 1386(1), 1302(6), 1267(3), 1242(2), 1197(2b), 1183(2b), 1051(3), 1022(2), 918(5), 883(5), 818(1), 784(1), 753(6), 684(3), 660(5), 496(2), 444(2), 348(2), 332(3).

$CH_3)_3$CCH=CHSC_4H_9: 3048(3), 2965(10b), 2931(6), 2904(9), 3048(3), 2965(10b), 2931(6), 2904(9), 2876(6), 861(6), 1665(2), 1643(2), 1601(10), 1461(3), 1441(4), 1419(2), 1388(1), 1361(1), 1302(5), 1266(2), 1245(2), 1198(2), 1185(2), 1096(2), 1050(2), 1026(1), 918(5), 890(2), 868(2), 833(5), 754(6), 653(3).

ectra obtained by T. N. Shkurina on an ISP-51 spectraph; the frequencies of the stretching vibrations of C=C bond are presented in the text.

CUSSION OF RESULTS

It follows from an analysis of the results obtained he calculation that all the symmetric vibrations of three models of the vinyl methyl sulfide molecule be divided—to a certain extent arbitrarily—into the alled C—H stretching and deformation vibrations of the vinyl and methyl groups, the stretching vibrations of the C=C group, the stretching vibrations of the =C—S and S—C groups, and the skeletal vibrations.

The C—H stretching and deformation vibrations. The computed values of the zero-order amplitudes in the C—H stretching and deformation vibrations ($\nu_1 - \nu_5$ and $\nu_7 - \nu_{10}$) are identical for all three models. These values are presented in Table 2. In the vibrations ν_1, ν_2, and ν_3, it is principally the =C—H bond lengths which change, while in the vibrations ν_8 and ν_{10} it is principally the angles in the CH_2=CH— group. Since these vibrations are localized within the limits of the vinyl group, the conclusions drawn from the calculations for the CH_2=CHSCH_3 molecule must also be valid for the unsubstituted vinyl alkyl sulfides. Actually, the spectra of the vinyl alkyl sulfides (see above, Nos. 1 and 2) confirm the specificity of the vibrations ν_1 (~3100 cm^{-1}), ν_2 (~3050 cm^{-1}), ν_3 (~3010 cm^{-1}), ν_8 (~1430 cm^{-1}), and ν_{10} (~1285 cm^{-1}). As was to be expected, the frequencies ν_2 and ν_{10} are considerably changed in the spectra of the α-substituted vinyl sulfides (Nos. 3-5), while ν_1 (~3100 cm^{-1}), ν_3 (~3025 cm^{-1}), and ν_8 (~1430 cm^{-1}) remain practically constant. At the same time, these latter frequencies undergo large changes in the spectra of the β-substituted vinyl sulfides. The frequency ν_2 (~3050 cm^{-1}), however, which is characteristic for the vibration of the unique =C—H bond, changes little. Thus the frequencies of the =C—H stretching and deformation vibrations of the vinyl group may be recommended for the identification of both unsubstituted and α- and β-substituted vinyl alkyl sulfides.

The calculated frequencies of the symmetric C—H stretching and deformation vibrations of the CH_3 group (ν_4, ν_5, and ν_9) have the values usually observed when a methyl group is present in a molecule (Table 2).

The C=C stretching vibration. The results of the calculation of the frequencies and zero-order amplitudes of the vibration ν_6 for the three models of vinyl methyl sulfide are presented in Table 2. It follows from the data presented that the so-called C=C stretching vibration is quite a complex vibration, in which, along with the predominant change in the C=C bond, the angles β_1, β_2, α_{12}, β_3, and α_{34} and the =C—S bond, which are all contiguous to the C=C, also take part. The angles and bonds of the SCH_3 group do not participate in this vibration. The changes in the force and kinematic parameters which take place on replacement of the methyl group by other radicals should not affect the ν_6 vibration, since this is fully characteristic in frequency and form for the CH_2=CHS— group. This is actually observed in the spectra of the vinyl alkyl sulfides CH_2=CHSR (for R = CH_3, C_2H_5, C_3H_7, C_4H_9, and C(CH_3)$_3$, ν_6 = 1588,[1] 1587, 1586, 1586, and 1586 cm^{-1} respectively).

The calculation for the three models of vinyl methyl sulfide gives values for the ν_6 frequencies which are very close together: 1627 (I), 1620 (II), and 1621 (III) cm^{-1}. Allowance for possible errors in the choice of the force constant values cannot substantially change the quantity $\Delta\nu_6$, since, as a calculation of the partial derivatives of this frequency with respect to all the force parameters has shown, the sensitivities of the ν_6 frequency in the different models are very similar. The lower values of the ν_6 frequencies in the observed spectra of the vinyl alkyl sulfides, as compared with the computed values, are probably brought about by a decrease in the magnitude of K_Q (in the calculation, K_Q = 14.2). A reduction in the force constant of the C=C bond in vinyl alkyl sulfide molecules may be brought about by interaction of the π-electrons of the double bond with the unshared

Table 2. Zero-Order Amplitudes of the Vibrations of CH_2=CHSCH$_3$

Vibr. no.	$\nu_{obs.}$ (cm^{-1})	$\nu_{calc.}$ (cm^{-1})	Q	q_1	q_2	q_3	q_4	q_5	β_1	β_2	α_{12}	β_3	β_4	α_{34}	γ	q'_1	q'_2	q'_3	β'_1	β'_2	β'_3	α'_{12}	α'_{23}
ν_1	—	3102	0.001	−0.052	0.050	−0.024	0.001	0	0.003	−0.003	0	−0.004	0.002	0.002	−0.001	0	0	0	0	0	0	0	0
ν_2	—	3052	0.004	0.012	−0.024	−0.070	0.002	0	−0.005	0.004	0.001	0.003	−0.007	0.004	−0.003	0	0	0	0	0	0	0	0
ν_3	—	3013	0.005	−0.054	−0.051	0.009	0	0	−0.003	−0.004	0.007	0	0	0	0	−0.004	−0.082	0.046	0.032	0.006	−0.004	−0.003	0	0.00
ν_4	—	2982	0	0	0	0	0	0	0	0	0	0	0	0	0	−0.004	0.045	0.058	0.043	0.003	0	0.001	−0.002	−0.00
ν_5	—	2905	0	0	0	0	0	−0.003	0	0	0	0	0	0	0	0	0	0	0	0	0	0	0	0
ν_6	1588	1627 (I)	0.038	0.002	0.003	0.003	−0.012	0	−0.034	−0.044	0.078	−0.029	−0.005	0.034	−0.008	0	0	0	0	0	0	−0.001	−0.002
		1620 (II)	0.038	0.002	0.002	0.003	−0.012	0	−0.035	−0.045	0.080	−0.028	−0.006	0.034	0.009	0	0	0	−0.001	0	0	0	0
		1621 (III)	0.038	0.002	0.002	0.003	−0.012	0	−0.035	−0.046	0.081	−0.028	−0.005	0.033	0	0	0	0	0.001	−0.001	0.001	0.002	0.00
ν_7	(?)	1428	0.001	0	0	0	−0.001	−0.012	0.001	0.005	−0.011	−0.003	0	0.003	0.001	0.003	0.002	−0.003	0.000	0.000	−0.004	−0.103	0.12
ν_8	1435	1410	0.014	0.001	0.002	0.002	−0.010	0.001	0.070	0.053	−0.123	−0.028	−0.002	0.030	−0.006	0	0	0	0	0	0	0	0
ν_9	1390	1387	0	0	0	0	0	0.013	0	0	0	0	0	0	0	−0.002	−0.003	−0.002	−0.057	−0.074	−0.057	0.074	0.07
ν_{10}	1280	1275	0.008	0.003	−0.002	−0.003	0.008	0	−0.040	0.050	−0.010	0.101	−0.024	−0.077	0	0	0	0	0.001	0	0	0	−0.00
ν_{11}	1040	1028	0	0.006	−0.006	0.001	0.011	0	−0.078	0.081	−0.003	−0.042	−0.023	0.065	−0.002	0	0	0	−0.010	0.010	−0.001	0	0.00
ν_{12}	852	965	0	0	0	0	0	0	−0.004	0.004	0	−0.003	0	0.003	0	−0.004	0	0.004	0.078	0.091	−0.079	0.038	−0.03
ν_{13}	742	719 (I)	0	0	0	0	0.005	−0.049	−0.002	0.002	0	−0.003	0.007	−0.004	0.007	0	−0.001	0	0.001	0.005	0.004	−0.005	−0.00
		718 (II)	0	0	0	0	0.001	−0.050	0.004	−0.004	0	0.005	−0.009	0.004	0.007	0	−0.001	0	0.002	0.003	0.004	−0.003	−0.00
		716 (III)	0	0	0	0	0.003	−0.049	0.002	−0.001	−0.001	0.001	−0.001	0	0.006	0	0	0	0.004	0.001	0.004	−0.003	−0.00
ν_{14}	675	674 (I)	0.005	−0.002	0.002	−0.001	0.044	0.005	0.025	−0.021	−0.004	0.016	−0.020	0.004	−0.018	0	0	0	−0.008	0.003	0.003	−0.001	−0.00
		684 (II)	0.004	−0.001	0.002	−0.001	0.043	0.001	0.027	−0.024	−0.003	0.017	−0.021	0.004	−0.018	0	0	0	−0.009	0.003	0.003	−0.001	−0.00
		677 (III)	0.005	0	0.001	−0.001	0.044	0	0.025	−0.022	−0.003	0.015	−0.019	0.005	−0.005	0	0	0	0.003	−0.006	0.003	−0.001	−0.00
ν_{15}	—	351 (I)	0.002	0.002	−0.001	0.003	0.001	0.001	−0.016	0.016	0	−0.027	0.057	−0.030	0.025	0	0	0	0.003	−0.001	0.001	0	0
		363 (II)	0.002	0.002	−0.002	0.003	0.006	0	−0.015	0.015	0	−0.024	0.053	−0.030	−0.005	0	0	0	−0.005	0.003	0.001	0	0
		331 (III)	0.001	0.002	−0.002	0.004	0.003	0.001	−0.016	0.015	0.001	−0.028	0.061	−0.035	−0.015	0	0	0	0	−0.002	0.001	0	0
ν_{16}	—	180 (I)	0.001	0	0	−0.001	−0.002	−0.005	0.004	−0.003	−0.001	0.006	−0.022	0.016	0.046	0	0	0	0.006	−0.001	−0.001	−0.001	0
		162 (II)	0	−0.001	0.001	−0.002	0.003	0.004	0.005	−0.004	−0.001	0.010	−0.025	0.015	−0.041	0	0	0	−0.005	0.001	−0.001	0.001	0
		282 (III)	0	0	0	0.001	−0.004	−0.005	−0.003	0.003	0	−0.008	0.014	−0.006	0.059	0	0	0	−0.001	0.007	−0.001	0	0

Note: The zero-order amplitudes of the linear coordinates are given in Angstroms, those of the angular coordinates in radians.

electron pairs of the sulfur atom. This is consistent with the data on the intensities of the C=C lines in the Raman spectra and with the position of the absorption band in the ultraviolet spectra of the vinyl alkyl sulfides.

The C−S stretching vibrations and the skeletal vibrations. The values of the computed zero-order amplitudes and atomic displacements in the vibrations ν_{13} and ν_{14} (Table 2) permit one to assign ν_{13} and ν_{14} to the −S−C and =C−S stretching vibrations. As can be seen from Table 2, the spatial position of the methyl group has little influence on the frequencies and forms of these vibrations. The vibrations ν_{13} and ν_{14} are almost entirely localized in the methyl and vinyl groups, respectively, of vinyl methyl sulfide. Although the independence of these vibrations is evidently preserved in the molecules of other unsubstituted and also α- and β-substituted vinyl alkyl sulfides, still, by virtue of the incomplete specificity of these vibrations with respect to form for the C−S bonds, one cannot expect strict specificity with respect to frequency. Therefore, in the spectra of CH_2=CHSR, the frequency ν_{14} will retain its value as R changes, while the frequency ν_{13} may change. In the spectra of R′CH=CHSR and CH_2=CR′SR, the frequencies ν_{13} and ν_{14} will evidently not be constant as R and R′ change. The insufficient experimental material and a certain arbitrariness in the choice of the force constants of the S−C bonds and the angles contiguous to them do not allow one to make a reliable assignment of the observed frequencies to the vibrations ν_{13} and ν_{14}.

The vibrations ν_{11}, ν_{12}, ν_{15}, and ν_{16} are associated with deformations of the angles of both the vinyl and methyl groups, and therefore they may be assigned to the skeletal vibrations of the whole molecule. The vibrations ν_{11} and ν_{12}, in both of which it is principally the angles α and β which change, are very close together for the three models. Accordingly, the values presented in Table 2 for the frequencies and zero-order amplitudes are valid for conformations I, II, and III.

The authors are very grateful to P. P. Shorygin and L. A. Gribov for detailed discussion of the work and for valuable counsel.

REFERENCES

1. C. C. Price and R. G. Gillis, J. Am. Chem. Soc. 75, 4750 (1953).
2. M. A. El'yashevich, Zhur. Fiz. Khim. 15, 847 (1941).
3. L. M. Sverdlov and N. L. Pakhomova, Zhur. Eksptl. Teoret. Fiz. 26, 64 (1954); Doklady Akad. Nauk SSSR 91, 51 (1953).
4. S. I. Ryskina, Zhur. Fiz. Khim. 22, 420 (1948).
5. L. S. Mayants, Opt. i Spektr. 5, 379 (1958).

TERPRETATION OF THE VIBRATIONAL SPECTRA OF NAPHTHALENE AND SOME OF ITS DEUTERIUM SUBSTITUTION PRODUCTS

G. V. Peregudov (pp. 735-741)

Received 7 January 1961

A frequency assignment according to symmetry classes has been carried out on the Raman and infrared absorption spectra of naphthalene, α- and β-tetradeuterionaphthalene, and octadeuterionaphthalene. The observance of the product rule and sum rule for all symmetry classes has been verified. Data on the infrared absorption spectra in the region from 700 to 3100 cm^{-1} are presented for the above-listed molecules.

The present investigation relates to a sequence of ks devoted to a study of the vibrational spectra of erium substitution products of the aromatic series. previously published communication,[1] the Raman tra of naphthalene ($C_{10}H_8$), α- and β-tetradeuteri- phthalene (α-$C_{10}H_4D_4$, β-$C_{10}H_4D_4$), and octadeuterio- thalene ($C_{10}D_8$) were presented.

In the present work, the infrared absorption spectra ese molecules in the region from 700 to 3100 cm^{-1} e been investigated by means of an IKS-14 double- m spectrophotometer with NaCl and LiF prisms. hthalene, α-tetradeuterionaphthalene, and octadeu- onaphthalene were studied in the melt; β-tetradeu- onapthalene was investigated in CCl_4 solution, in view he fact that we had only a very small quantity of this paration at our disposal. For the same reason, a thin was used. This circumstance resulted in a smaller ber of lines being recorded in this spectrum than in the spectra of the other substances. Unquestionably, some of the weak lines were not detected. The spectra of the molecules which we have investigated are presented in the Figure. The frequency values of the absorption bands are given in Table 1, as well as a qualitative estimate of the intensity (the accuracy of the frequency measurement was ~3-5 cm^{-1}). The spectra which we have obtained for naphthalene, α-tetradeuterionaphthalene, and octadeuterionaphthalene agree well with the literature data.[2,3] The spectrum of β-$C_{10}H_4D_4$ was obtained for the first time.

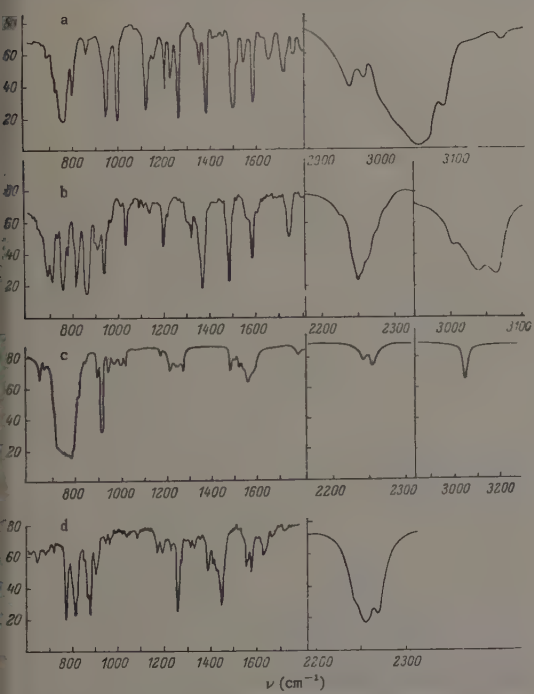

Infrared absorption spectra of naphthalene (a), α-tetradeuterionaphthalene (b), β-tetradeuterionaphthalene (c), and octadeuterionaphthalene (d). a, b, d—melt (thickness d = 0.05 mm); c—solution in CCl_4 (d = 0.01).

Table 1

ν (cm^{-1})			
$C_{10}H_8$	α-$C_{10}H_4D_4$	β-$C_{10}H_4D_4$	$C_{10}D_8$
Melt	Melt	Solution in CCl_4	Melt
674 w	660 w	670 m	650 vw
704 w	696 s	696 vw	684 vw
736 s	714 s	814 w	723 vw
772 vs	736 m	846 w	776 s
812 s	764 vs	900 m	805 m
832 w	784 s	921 s	816 m
864 w	818 s	948 m	870 m
942 w	866 vs	974 m	881 s
962 vs	902 m	998 m	908 m
980 vw	912 m	1020 m	974 vw
1012 vs	944 s	1173 w	965 vw
1088 vw	958 m	1220 m	1040 vw
1118 vs	975 m	1256 m	1180 w
1150 m	1018 vw	1278 m	1202 w
1172 w	1038 m	1486 m	1234 w
1218 m	1074 vw	1524 m	1268 s
1248 m	1094 w	1552 m	1284 m
1280 vs	1118 w	1564 m	1320 w
1312 vw	1140 w	1582 m	1344 w
1352 w	1204 m	1758 w	1364 vw
1372 m	1264 w	2263 s	1398 m
1396 s	1276 vw	2278 s	1422 m
1430 vw	1308 vw	3046 vs	1440 m
1440 vw	1318 m		1466 w
1470 vw	1372 vs		1562 m
1512 s	1426 vw		1586 m
1528 w	1458 vw		1636 m
1564 m	1490 vs		1668 w
1598 s	1518 vw		2248 m
1630 vw	1564 m		2266 s
1670 m	1590 s		2284 s
1704 w	1610 vw		
1730 m	1724 w		
1764 m	1750 s		
2960 m	2223 w		
2977 m	2254 vs		
3000 s	2260 s		
3020 s	2269 m		
3050 vs	2284 m		
3060 vs	2894 w		
3090 s	2960 w		
3170 w	3000 m		
	3042 s		
	3054 s		
	3062 s		

Note: Symbols for band intensities: vs – very strong, s – strong, m – medium, w – weak, vw – very weak.

There are in the literature a large number of works in which the problem of the interpretation of the vibrational spectra of naphthalene and its deuterium substitution products is discussed. A frequency assignment according to symmetry classes has been carried out in refs. 2-7 and 14; calculations of the frequencies of the naphthalene and octadeuterionaphthalene spectra have been performed in refs. 8-11. However, up to the present the problem of interpreting the spectra of naphthalene and its deuterium substitution products cannot be connot be considered as finally solved. The point is that the interpretations of the observed spectra proposed by different authors differ substantially from one another. What is more, even the same author gives different interpretations of the spectra at different times. The authors of the calculations, as a rule, have used a small number of force constants or have limited themselves to calculations of the frequencies of the "skeleton" of the naphthalene molecule only. It is therefore of interest to examine this problem again.

Using new data, both experimental and theoretical, we have carried out a frequency assignment according to symmetry classes for naphthalene, α- and β-tetradeuterionaphthalene, and octadeuterionaphthalene. In the assignment of frequencies according to symmetry classes, we have based our work on the results which we obtained in calculations of the spectra of diphenyl and its deuterium substitution products,[12] and also on those emerging from calculations for alkyl-substituted benzenes.[13] The calculations of the spectra of these compounds show that the frequencies of vibrations in which, for example, it is predominantly the CC bonds (the Q-coordinate), the CCC ring angles (the γ-coordinate), the CCH angles (the β-coordinate), or the CH bonds (the q-coordinate) which change, have quite specific values which change little on going from one aromatic compound to another. As an illustration of this claim, we present in Table 2 for a number of compounds the frequencies of vibrations in which it is predominantly the above-listed angles and bonds which change. The frequencies corresponding to the CH stretching vibrations in the 3050 cm^{-1} region are not shown in the table, since they change little on going from one substance to another.

The data of Table 2 show that there are quite narrow ranges of frequency variation, these ranges overlapping slightly for different internal coordinate. In the Raman and infrared absorption spectra of naphthalene, one observes a large number of frequencies whose values are very close to the frequency values listed in Table 2. We have made use of this circumstance in the frequency assignment according to symmetry classes fo naphthalene.

In the frequency assignment according to symme classes for $C_{10}D_8$, the majority of authors start from assumed analogy in the frequency changes on going fr $C_{10}H_8$ to $C_{10}D_8$ and from C_6H_6 to C_6D_6. However, these sumptions are not always fulfilled in practice. The ca culations which we have carried out for the deuterium substitution products of biphenyl[12] enable us to establ how the frequencies presented in Table 2 change on r placement of H by D. This simplifies to a considerab degree the frequency assignment in the spectra of C_{10} and α- and β-$C_{10}H_4D_4$.

The naphthalene molecule belongs to the symmet group $D_{2h} = V_{2h}$; i.e., it possesses three mutually per pendicular second-order axes, C_2, three mutually per pendicular planes of symmetry, σ, and a center of inversion, i. The distribution of the 48 possible vibrati of the molecule according to symmetry classes is sh in Table 3.

Table 2

Benzene	Toluene	o-xylene	m-xylene	p-xylene	Mesitylene	Durene	Biphenyl
			ν (cm^{-1})				
Combinations of the internal coordinates Q (CC bonds)							
992 (A_{1g})	786	733	725	829	995	735	742
1037 (E_{1u})	1031	1058	1094	1030	1035	1025	1032
	1076	1114	1167	1103	1104	1082	1092
1310 (B_{2u})	1331	1290	1318	1313	1298	1271	1320
1595 (E_{2g})	1586	1583	1592	1581	—	1560	1592
	1605	1609	1613	1618	1605	1620	1611
Combinations of the internal coordinates γ (CCC angles)							
606 (E_{2g})	521	506	514	458	508	437	—
	623	582	535	645	570	469	611
1010 (B_{1u})	1004	830	998	1001	—	997	1003
Combinations of the internal coordinates β (CCH angles)							
1178 (E_{2g})	1156	1159	—	—	—	—	1156
	1180	1178	1154	1183	1160	—	1185
1326 (A_{2g})	1278	1290	1262	1313	1298	1262	1326
1485 (E_{1u})	1437	1448	1426	1441	1425	1449	1452
	1504	1500	1490	—	—	1504	1504

Table 3

Symmetry class	Selection rules		Number of vibrations	Number of ring vibrations	Number of CH vibrations	Form of the vibration
A_{1g}	p	Ram.	9	5	4	Planar
A_{1u}	–	–	4	2	2	Nonplan
B_{1g}	dp	Ram.	8	4	4	Planar
B_{1u}	M_Z	IR	4	2	2	Nonplan
B_{2g}	dp	Ram.	3	1	2	Nonplan
B_{2u}	M_Y	IR	8	4	4	Planar
B_{3g}	dp	Ram.	4	2	2	Nonplan
B_{3u}	M_X	IR	8	4	4	Planar

Note: Symbols: p – polarized; dp – depolarized; M_Z, M_Y, M_X – electric momen along the Z, Y, X axes respectively; Ram. – active in the Raman spectrum; IR – in the infrared absorption spectrum.

The molecules of α-$C_{10}H_4D_4$, β-$C_{10}H_4D_4$, and C_{10} belong to the same symmetry group D_{2h}. Therefore, the conclusions concerning symmetry classes, select rules, etc., contained in Table 3 are applicable to the molecules also.

The frequency assignment according to symmetr classes which we propose for naphthalene and its deu terium substitution products is presented in Table 4. frequency assignment for each class is discussed sep arately below.

Symmetry class A_{1g}. It follows from an examina of the symmetry coordinates that in this case there a three active vibrations in which the CC ring bonds ch two vibrations in which the CCC angles change, two v brations in which the CCH angles change, and two CH stretching vibrations.

Our assignment of the $C_{10}H_8$ frequencies to A_{1g} incides with the data of other authors except for the cm^{-1} frequency. The majority of authors assign the cm^{-1} frequency to A_{1g}. The 1167 and 1147 cm^{-1} freq cies in the $C_{10}H_8$ molecule characterize CH bending v brations (changes in the CCH angles).

Calculations show that a symmetric vibration ha as a rule, a higher frequency than an unsymmetric on Therefore, we assign the 1167 cm^{-1} frequency to A_{1g}. For $C_{10}H_8$, our assignment agrees basically with the of ref. 13. In the spectrum of α-$C_{10}H_4D_4$, we have as signed to A_{1g} the 1405 cm^{-1} frequency, which charac terizes CH bending vibrations. The authors of ref. 3 ascribe the 908 cm^{-1} frequency to A_{1g}. However, suc

Table 4

	ν (cm^{-1})						
	α-$C_{10}H_4D_4$	β-$C_{10}H_4D_4$	$C_{10}D_8$	$C_{10}H_8$	α-$C_{10}H_4D_4$	β-$C_{10}H_4D_4$	$C_{10}D_8$
	Class A_{1g}			Class B_{1g}			
0	502	503	495	387	$(378)^*$	386	370
0	709	738	693	1087	1086^6	853	833
5	861	1030	864	1142	950	1080	957
7	1086	853	833	1238	$1125)$	1230	1080
7	1391	1380	1380	1437	1374	1398	1290
9	1405	1413	1290	1574	1560	1565	1550
4	1560	1565	1550	3006	2284	2263	2263
6	2284	2277	2275	3059	3054	3048	2302
9	3045	3048	2243				
	Class B_{2u}			Class B_{3u}			
1	338 **	(340)	328 **	618	(600)	(600)	593 **
8	1094	948	816	962	942	921	881
8	958	1020	965	1012	866	998	776
8	1118	1173	1040	1150	1038	900	870
6	1372	(1390)	1268	1512	1490	1487	1398
8	1564	1564	1562	1598	1590	1582	1586
0	2254	2263	2266	3000	2210	2278	2248
0	3062	3046	2284	3090	3042	3046	2284
	Class B_{2g}			Class B_{3g}			
7	(337)	353	339	483	(400)	415	408
9	704	710	540	778	673	710	765
1	716	872	710	876	871	(800)	760
				978	906	(908)	791
	Class B_{1u}			Class A_{1u}			
8	(~165)	(~165)	160	400	—	—	—
3	408 **	(~450)	408 **	704	660	696	—
7	714	670	618 **	864	—	—	723
2	818	814	738 **	980	912	—	758

*Calculated values.
**Observed in refs. 2 and 3.

equency value seems too low to correspond to CH nding vibrations (see Table 2).

Symmetry class B_{1g}. In this symmetry class there e two active CC stretching vibrations, two CC bending brations, two CH bending vibrations, and two CH stretch- vibrations. Our proposal for the assignment of fre- encies to this symmetry class differs from the data of her authors. The majority of authors consider the 5-611 cm^{-1} frequency of the $C_{10}H_8$ molecule and 569- 1 cm^{-1} of the $C_{10}D_8$ molecule as the lowest frequency class B_{1g}. These frequencies characterize CC ring nding vibrations. It seems to us that these frequencies ust lie below 400 cm^{-1}, as is the case for the molecules biphenyl and of the alkylsubstituted benzenes. There- re, we have assigned to B_{1g} the 361 cm^{-1} frequency of e $C_{10}H_8$ molecule and the corresponding frequencies in e spectra of the other deuterium substitution products naphthalene. We match the 1238 cm^{-1} frequency with e other CC bending vibration of $C_{10}H_8$, considering that high value is caused by strong interaction of the CCC gles and CC bonds on account of the fused rings. Three $_0D_8$ frequencies assigned to B_{1g} were used by us earlier the assignment to A_{1g} (the 833, 1290, and 1550 cm^{-1} equencies). In place of the 1574 cm^{-1} frequency of $_0H_8$ and 1550 cm^{-1} of $C_{10}D_8$, it is possible that the weak nds at 1624 cm^{-1} in the $C_{10}H_8$ spectrum and 1573 cm^{-1} the $C_{10}D_8$ spectrum, which have been observed by a mber of authors,[2,5,6] should be assigned to B_{1g}. How- er, as experiment shows, frequencies lying in this gion in the spectra of aromatic compounds usually ap- ar with adequate intensity. Therefore, we consider it ore justifiable to use the 1574 and 1550 cm^{-1} frequen- es in the interpretation, and also the 1560 cm^{-1} fre- ency of α-$C_{10}H_4D_4$ and 1565 cm^{-1} of β-$C_{10}H_4D_4$. In ref. the 1451 and 1610 cm^{-1} frequencies were assigned to e CC stretching vibrations of α-$C_{10}H_4D_4$. The 1451 cm^{-1} equency has too high a value to characterize a CC retching vibration (see Table 2). We assign the 1086 n^{-1} frequency to this vibration, and we match the 950 and 1374 cm^{-1} frequencies with the CH bending vibrations.

Symmetry classes B_{2g}, B_{3g}, B_{1u}, and A_{1u}. The calculation of the nonplanar vibrations carried out in ref. 11 enables us to assign frequencies to these symmetry classes. It should, however, be noted that our matching of the observed $C_{10}H_8$ and $C_{10}D_8$ frequencies with the calculated ones differs in a number of cases from the matching of ref. 11. Thus we match the observed 357 cm^{-1} frequency, and not the 389 cm^{-1} frequency,[11] with the calculated $C_{10}H_8$ frequency value of 365 cm^{-1}, etc.

Symmetry class B_{2u}. In the class B_{2u} there are two active CC stretching vibrations, two CC bending vibrations, two CH bending vibrations, and two CH stretching vibrations. One's attention is drawn to the fact that the same bonds and angles change both in vibrations of class B_{1g} and in vibrations of class B_{2u}. The result is that the frequencies of these vibrations are close to one another.

The assignment of frequencies to this symmetry class which we have proposed differs from the assignments of other authors.[2,3,6] The 752 cm^{-1} frequency was assigned to a CC bending vibration of $C_{10}H_8$ in ref. 2, and the 618 cm^{-1} frequency in ref. 7. We assign to it the 1218 cm^{-1} frequency, considering that the elevation of the frequency takes place on account of interaction of the CCC angles and CC bonds. To the CC stretching vibrations, we assign the 1086 and 1564 cm^{-1} frequencies of $C_{10}H_8$ and the corresponding frequencies of α- and β-$C_{10}H_4D_4$ and $C_{10}D_8$. In refs. 2 and 7, the 2947 and 3014 cm^{-1} frequencies are assigned to the CH stretching vibrations of $C_{10}H_8$. However, as the data show,[15] it is necessary to assign the frequencies 3050 and 3060 cm^{-1} to B_{2u}.

Symmetry class B_{3u}. Two CC stretching vibrations, two CC bending vibrations, two CH bending vibrations, and two CH stretching vibrations belong to class B_{3u}. In these vibrations, the same angles and bonds change as in the vibrations of symmetry A_{1g}. Therefore, the frequencies of these vibrations are close to the A_{1g} frequencies. The frequencies assigned by us to B_{3u} differ substantially from the frequencies proposed in refs. 2, 3, and 6. We have assigned the 618 and 1012 cm^{-1} frequencies to the CC bending vibrations of $C_{10}H_8$, 962 and 1598 cm^{-1} to the CC stretching vibrations, and 1150 and 1512 cm^{-1} to the CH bending vibrations. The corresponding frequencies have been assigned in the spectra of α- and β-$C_{10}H_4D_4$ and $C_{10}D_8$. In the assignment of the CH stretching vibrations of $C_{10}H_8$, we were guided by the data of ref. 15.

The fulfillment of the "product rule," and also of the "sum rule," has been verified for all symmetry classes. In our case, the sum rule has the form:

$$\sum_i \nu_i^2(C_{10}H_8) + \sum_i \nu_i^2(C_{10}D_8)$$

$$= \sum_i \nu_i^2(\alpha - C_{10}H_4D_4) + \sum_i \nu_i^2(\beta - C_{10}H_4D_4).$$

The results of a check of the "product rule" and "sum rule" are presented in Table 5. The frequency ratio values calculated with the help of the data of Table 4 are presented in columns "c," and the frequency ratio values computed theoretically with the help of data on the structure of the molecule[16] are in the columns "t."

It is easy to see that, for all the symmetry classes, both the product rule and the sum rule are well fulfilled. This circumstance is an indirect corroboration of the validity of the frequency assignment presented in Table 4. Not all the frequencies observed in the Raman and infrared spectra are interpreted by us as fundamentals. A

Table 5

Symmetry class	$\Pi\nu_4(C_{10}H_8)$ ↓ $\Pi\nu_4(\alpha\text{-}C_{10}H_7D_1)$		$\Pi\nu_4(C_{10}H_8)$ ↓ $\Pi\nu_4(\beta\text{-}C_{10}H_7D_1)$		$\Pi\nu_4(C_{10}H_8)$ ↓ $\Pi\nu_4(C_{10}D_8)$		$\sum_i^2(C_{10}H_8 + C_{10}D_8)$ $(10^6\,cm^{-2})$	$\sum_i^2(\alpha\text{-}C_{10}H_7D_1 + \beta\text{-}C_{10}H_7D_1)$ $(10^6\,cm^{-2})$
	c	t	c	t	c	t		
A_{1g}	1.94	2.00	2.00	2.00	4.02	4.00	44.5	45.5
B_{1g}	1.87	1.95	1.87	1.91	3.70	3.73	44.5	44.4
B_{2g}	1.40	1.40	1.33	1.34	1.88	1.88	2.43	2.51
B_{3g}	1.44	1.44	1.52	1.52	1.86	1.83	4.52	4.33
B_{1u}	1.54	1.39	1.50	1.39	1.82	1.94	2.86	2.71
B_{2u}	1.95	1.97	1.97	1.97	3.84	3.87	44.3	44.5
B_{3u}	1.92	1.97	1.97	1.97	3.87	3.88	44.3	44.4

number of frequencies in these spectra are combinations and can easily be accounted for with the help of the fundamental frequencies which we have derived.

The author offers his thanks to P. A. Bazhulin for his interest in the work and for discussion.

REFERENCES

1. A. I. Shatenshtein, G. V. Peregudov, E. A. Izrailevich, and V. R. Kalinachenko, Zhur. Fiz. Khim. **33**, 146 (1958).
2. E. R. Lippincott and E. J. O'Reilly, J. Chem. Phys. **23**, 238 (1955).
3. S. S. Mitra and H. J. Bernstein, Can. J. Chem. **37**, 553 (1959).
4. T. M. K. Nedenigadi, Proc. Indian Acad. Sci. **A15**, 376 (1942).
5. H. Luther, Z. Elektrochem. **52**, 210 (1948).
6. H. Luther and B. Hampel, Z. physik Chem. **A202**, 390 (1954).
7. A. L. McClellan and G. Pimentel, J. Chem. Phys. **23**, 245 (1955).
8. C. Maneback, J. Chem. Phys. **46**, 49 (1949).
9. J. Brandmuller and E. Schmid, Z. Phys. **144**, 428 (1956).
10. E. Schmid, Z. Elektrochem. **62**, 1005 (1958).
11. D. B. Seully and D. H. Whiffen, J. Mol. Spectrosco **1**, 257 (1957).
12. G. V. Peregudov, Opt. i Spektr. **9**, 295 (1960), Opti and Spectroscopy **9**, 155 (1960).
13. M. A. Kovner, Doctoral dissertation, Minsk, 1957.
14. H. Luther, G. Brandes, et al., Z. Elektrochem. **59**, 1012 (1955).
15. W. Braun and R. Mecke, Z. Elektrochem. **62**, 441 (1958).
16. G. Herzberg, "Molecular Spectra and Molecular Structures. II. Infrared and Raman Spectra of Poly atomic Molecules," p. 250. 2nd ed., Van Nostrand Princeton, New Jersey, 1945. Foreign Literature Press, Moscow, 1949.

OPTICAL PROPERTIES OF CRYSTALS WITH IMPURITIES. I
Absorption and Dispersion Characteristics of Anthracene Impurity in a 9,10-Dihydroanthracene Crystal

M. S. Brodin and Ya. O. Dovgii (pp. 742-749)

Received 2 January 1961

Absorption and dispersion curves of an anthracene impurity in a 9,10-dihydroanthracene crystal were measured. It can be concluded from an analysis of absorption curves, polarization relations, and their dependence on concentration that the anthracene molecules are unequally distributed in the lattice of the solvent. Experimental data on dispersion were compared with Kramers-Kronig formulas. A slight discrepancy was found, which increased with increase in impurity concentration.

I. INTRODUCTION

Facts concerning the severe violation of Kramers-Kronig dispersion relationships were established in earlier papers[1] which dealt with an investigation of the optical properties of some molecular crystals in the region of their natural absorption. It was shown that the extent of the violation increases with lowered temperature and that this extent is largest for exciton bands corresponding to a purely electronic transition. These facts indicate that the optical properties of crystals in the region of their exciton absorption, particularly at low temperatures, cannot be fully described by a theory which does does not take into account the effects of the crystalline field and of spatial dispersion. The nature of absorption and the part played by the interaction of particles (molecules) in the crystal can thus be judged on the criterion of agreement or disagreement of experimental results with Kramers-Kronig formulas. To confirm this criterion we found it expedient to verify the dispersion relationships in the case of absorption by a deliberately added impur with the absorbing molecules being located in the cryst line medium but widely separated one from the other. study of the dependence of the optical properties of the crystal solution on impurity concentration must point, its part, to those concentrations at which the interactio between impurity molecules is not apparent in such pr erties.

In connection with this, the object of the present w was an investigation of the optical properties of crystal containing impurities and of the dependence of these pr erties on the concentration of the impurity. The impur containing crystal anthracene-9,10-dihydroanthracene was selected as the object of this inquiry. Let us recal that the largest discrepancy between experimental resu and Kramers-Kronig formulas was observed precisely the case of the self-absorption of an anthracene crysta An oscillatory dependence of the absorption intensity i

thracene crystals on their thickness was moreover es-
blished, which pointed to a marked effect of spatial
spersion.[2]

There are, as far as we know, no quantitative data in
e literature concerning polarized absorption in molecu-
r crystals with impurities. The available references[3,4]
e basically devoted to the study of serial regularities
spectra without measurements of band intensities. It
uld be possible meanwhile to draw on the basis of such
ta some conclusions on the distribution of impurity
olecules in a foreign lattice and on the influences to
ich they are subjected from external effects.

. EXPERIMENTAL METHOD

9,10-dihydroanthracene[5] was selected as a solvent
ecause it is optically transparent in the region of the
st electron-vibrational transition in anthracene and be-
use a solid solution is formed in it at small impurity
ncentrations.

The samples were grown by the sublimation method.
ey were single crystal plane parallel plates of various
icknesses, suitable for quantitative optical investiga-
ons. The developed plane in them was plane a,b. In or-
r to obtain various impurity concentrations, a prede-
rmined amount of anthracene was added to the material
th the lowest concentration. Uniform mixing was ac-
mplished by fusion and boiling in ampoules filled with
trogen. The carefully crushed slug was used for subli-
ation. The impurity concentration in the crystal was
ecked by comparing the absorption spectra of its liquid
lutions with standard spectra. It should be pointed out
at the accuracy of a concentration value determined in
is way is not very high and we tried to exclude it there-
re, as much as possible, as a parameter for calcula-
ons.

Two methods were used to fasten the crystals—the
-called contactless fastening (the crystal plates were
aced in a paper envelope between two quartz plates) and
e method of setting the crystals in optical contact on
artz plates.

Absorption spectra were photographed on a spectro-
aph having high dispersion (4 A/mm). The spectral
ightness distribution of the source, the spectral sensi-
vity of the plates, and also, quite considerably, light re-
ection from crystal faces were taken into account in the
lculation of absorption coefficients. Two parallel
icols, placed on both sides of the crystals, were used
a polarizer. Dispersion curves were measured by an
terferometric method. The method of bands of equal
romatic order was used to determine the thickness of
e crystals.

I. CHARACTERISTICS OF OPTICAL ABSORPTION

Absorption curves were measured in the region of
e first electronic transition of anthracene on a series
samples containing the impurity in concentrations
nging from 0.2 to 5%. The measurements were made
several temperatures (290, 145, 77 and 20° K), but the
ain attention was focused on investigations at T = 20° K.

Before proceeding with the description of the obtained
ectra, let us note that the initial absorption bands are
splaced about 0.1 cm^{-1}/deg in the long wavelength direc-
on when the temperature is lowered.

In Fig. 1 (a, b, c) are shown absorption curves $\kappa(\nu)$,*

*The coefficients κ may be calculated from the formula $\kappa = \lambda \log (J_0/J)/4\pi d \times 0.43$, where $\log (J_0/J)$ is the optical density and d is the thickness of the crystal. The concentration is not introduced into the calculation, so that κ characterizes the intensity of absorption of the given specimen only.

pertaining to samples which have concentrations of 0.6, 1.0, and 1.8% by weight. (The light is polarized along the a and b axes of the 9,10-dihydroanthracene lattice, T = 20° K.)

After comparing these curves with the absorption curves of a pure anthracene crystal at the same temperature,[6] it can be stated that (1) the spectrum consists, as in the case of a pure crystal, of a series of bands, the most intense of which are the pure electronic transition

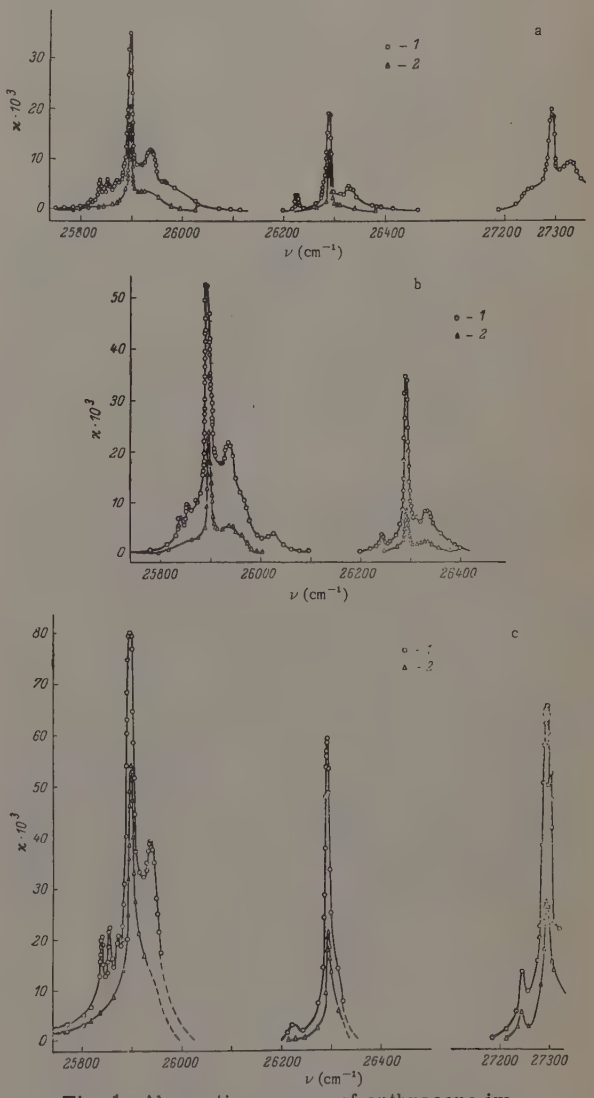

Fig. 1. Absorption curves of anthracene impurity in a crystal of 9,10-dihydroanthracene at T = 20° K. Polarization of the light: 1-‖b; 2-‖a. Anthracene concentration (in %): a-0.6; b-1; c-1.8.

band and the electron-vibrational bands with a vibration frequency of 1400 cm^{-1} (the bands are considerably narrowed. their structure is enriched); (2) the spectrum of impurity absorption is displaced by approximately 500 cm^{-1} to the short-wavelength side as compared with the spectrum of a pure anthracene crystal; (3) the absorption is dichroic, the bands being more intense when light is polarized along the b-axis, than for a-polarization; (4) in the vicinity of the fundamental band in the spectrum ν_m = 25898 cm^{-1} there is a group of closely located bands with frequencies of the maxima (at T = 20° K) equal to 25,840, 25,855, and 25,872 cm^{-1}. Similar bands are also observed in the spectra of pure anthracene crystals,[7] but in these they are located further away from the fundamental maximum and appear at considerably larger effective thicknesses. There is a separate band near 25,937 cm^{-1} on the short wavelength side of the 25,898 cm^{-1} maximum.

It can be concluded, by taking the narrowness of the bands and the quite clearly pronounced dichroism of impurity absorption into account, that the anthracene molecules are oriented approximately alike in the 9,10-dihydroanthracene lattice and are uniformly distributed in the macroscopic sense. The latter conclusion is substantiated by the quite clear interference picture obtained with a Jamin interferometer on crystals of sufficiently large area.*

*If the impurity were localized in the crystal in separate centers, this would have changed the path difference along the crystal area and led to a washing out of the interference picture, which we did not observe.

The analysis of absorption curves pertaining to samples with different impurity concentration indicates that the relative intensity of the corresponding absorption bands (ν_m = 26,855, 25,898, and 25,937 cm^{-1})* is different.

*We consider here and below the group of bands near 25,840, 25,855, and 25,872 cm^{-1} as a band at 25,855 cm^{-1}.

The intensity also depends on the state of the sample (free or contact fastened). This can be seen in Table 1, where the ratios of the ordinates of the maxima ν_m = 25,698, 25,855, 25,898 and 25,937 cm^{-1} are listed for a number of specimens. It follows from the table that the intensity ratios of the indicated maxima decrease systematically with an increase in concentration. Two samples constitute an exception, the deviation of results pertaining to them from the indicated rule being small. In the spectra of crystals fastened by contact means, and being therefore in a strained condition at low temperature, the intensities of the maxima at 25,898 and 25,937 cm^{-1} are equalized, while the relative intensity of the group of bands at 25,855 cm^{-1} is raised. At the same time

Table 1

C (%)	$\frac{\varkappa_{m25898}}{\varkappa_{m25855}}$	$\frac{\varkappa_{m25698}}{\varkappa_{m25937}}$	State
0.2	11.5	7	Free
0.4	8	6	"
0.6	6	3	"
1	2.36	2.6	"
1.8	3.6	2.05	"
2.1	3.8	2.00	"
3.6	1.85	1.33	"
4.9	3	2.2	"
1	1.33	1	In contact
1.2	1.33	1	" "
1.8	2.5	2.54	" "

the bands at 25,898 and 25,937 cm^{-1}, are washed out. Putting aside temporarily the question of the origin of the band at 25,937 cm^{-1}, it can be concluded from the data in Table 1 that the group of bands at 25,855 cm^{-1} and the band at 25,898 cm^{-1} are related to anthracene molecules differently situated in the 9,10-dihydroanthracene lattice. The same conclusions can also be made on the basis of luminescence spectra in which bands were discovered, coincident by resonance with the bands at 25,855 cm^{-1} and with the band at 25,898 cm^{-1} in the absorption spectrum. It appears that, at small concentrations, it is from the energy viewpoint more advantageous for impurity molecules to occupy sites determining the band at 25,89 cm^{-1}, the absolute majority of molecules being in these sites, judging from the intensity of the band. With an increase in concentration the number of molecules which are located at sites determining the 25,855-cm^{-1} group bands increases.

Absorption curves obtained for two directions of light polarization (∥ a and ∥ b) indicate that the polarization ratio, i.e., the value $P_m = \kappa_b/\kappa_a$ is considerably larger at the maxima of the 25,855- and 25,937-cm^{-1} bands than at the 25,898-cm^{-1} band. This indicates a dissimilar orientation of anthracene molecules in the corresponding states. Inasmuch as the relative intensity of the bands at 25,855 cm^{-1} and 25,937 cm^{-1} increases with an increase in impurity concentration, this must lead to a variability of the integral polarization ratio calculated for the whole group of bands. In order to elucidate this question, values of $S_b/S_a = P_s$ relating to the groups of bands at 25,898 and 26,292 cm^{-1} are listed in Table 2 for a number of samples. It follows from Table 2 that the P_s values do indeed vary with the concentration. A systematic regular connection between P_s and C cannot be established, but P_s is in general smaller for small concentrations, and, vice versa, larger for large concentrations. As can be seen in the Table, the value of P_s also depends on the state of the sample (free or contact fastening) and on temperature. The absorption dichroism is larger in the region of an electronic-vibrational band than in the region of a pure electronic band.

The question arises concerning the location of anthracene impurity molecules in the 9,10-dihydroanthracene lattice. There are, as far as we know, no x-ray structural data on this subject available in the literature.

Table 2

C (%)	$\frac{S_b}{S_a}$ (ν_m = 25898 cm)	$\frac{S_b}{S_a}$ (ν_m = 26292 cm)	T (°K)	State
0.6	2.97	4.42	20	Free
1	3.74	5.1	20	"
1.8	2.15	2.85	20	"
2.1	5.45	9.35	20	"
3.6	5.45	—	20	"
1	2.8	4.03	20	In contact
1.2	4.3	4.93	20	" "
1	[illegible]	—	77	Free
1.5	3.85	—	77	"
2.1	2.36	—	77	"

Data exist pertaining to other solid organic solutions.[8] They point to a possibility of realizing substitutional solutions and placing impurity molecules at block boundaries. In our case an attempt to express some opinions can only be based on spectral and optical data. As far as the group of bands about 25,855 cm^{-1} is concerned, they can be attributed to molecules occupying defect sites in the solvent lattice, as is admitted in ref 4 (in particular sites at block boundaries). Besides the abovementioned resonance coincidence of absorption and luminescence

nds, the fact of the presence of similar bands in the ectrum of a pure anthracene crystal[7] can serve as an gument for such a conclusion. The bands have also in s case their luminescence resonance lines and are ked to the presence of lattice defects. Their somewhat fferent spacing from the fundamental maximum in the ectrum of the pure crystal is evidently caused by the ference in the nature of the medium.

It is difficult to express a definite opinion concerning e states which determine the band at 25,898 cm^{-1}. The ssibility is not excluded that the anthracene molecules rresponding to it are located at the nodes of dihydro-thracene cells, forming a substitutional solution. As a tter of fact this band is narrow and the absorption in region is dichroic. The possibility of an interblock cation of the corresponding molecules does not, how-er, meet with any serious objections from the point of w of existing data.

Following ref. 4, in which the absorption and lumi-scence spectra of anthracene in 9,10-dihydroanthracene carefully analysed and compared, the band at 25,937 $^{-1}$ can be attributed to a combination of an intermolec-r transition with lattice vibrations of the solvent. The pendence of its relative intensity on the concentration the impurity is, however, not quite understandable in nnection with such a treatment.

VERIFICATION OF KRAMERS-KRONIG DISPERSION EQUATIONS

Dispersion curves were obtained for the majority of mples for which absorption curves had been measured. e results of the dispersion investigation indicate that refraction coefficients in the region of impurity ab-rption, calculated per unit of concentration, are, like absorption coefficients, unstable. For the verification the dispersion equations it is therefore necessary to data on absorption and dispersion obtained on the me specimens. This is also advantageous because there nc need to introduce data on concentration into the cal-ations, possibly reducing the accuracy of the latter.

Dispersion curves obtained from samples with con-itrations of 0.6, 1.0, and 1.8% are shown in Fig. 2 b, c) as an illustration. In every single case the value characterizes the refraction of the given specimen only. e curves are shown for light linearly polarized along b-axis of the solvent lattice, T = 20° K, and contact e fastening of the crystals.

The Kramers-Kronig formula expressing refraction efficients in terms of absorption coefficients

$$n_\omega^2 = 1 + \varkappa_\omega^2 - \frac{4}{\pi}\int_0^\infty \frac{\omega' n(\omega')\cdot\varkappa(\omega')}{(\omega')^2-\omega^2}\,d\omega',$$

s subjected to verification using experimental material ained on "freely" attached samples at 20° K. The nds become widened at higher temperatures and the culation becomes less convenient. Peculiarities con-ted with the effect of a crystal field[2] can, moreover, expected precisely at low temperatures. The verifica-n was conducted in the region of the purely electronic nsition band at 25,898 cm^{-1} and in the region of the ctron-vibrational transition band at ν_m = 27,292 cm^{-1}. e spread of the dispersion curves Δn^2 within the se-ted absorption band was chosen as a measure of the ference between experimental results and calculation.

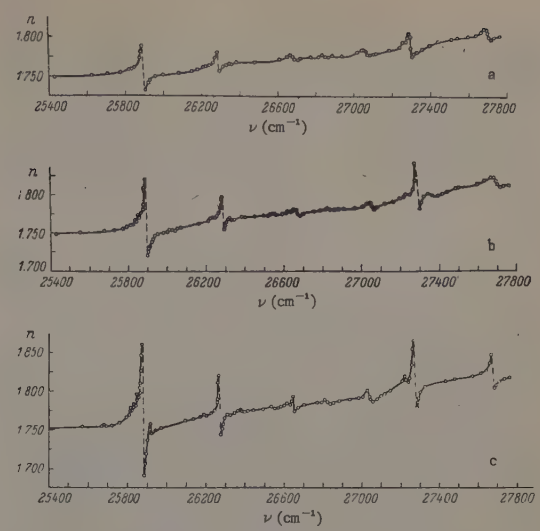

Fig. 2. Dispersion curves of impurity-containing crystals anthracene-9,10-dihydroanthracene at T = 20° K (‖b). For the anthracene concentrations see Fig. 1.

tive thicknesses were used in all cases and the measured optical densities and path differences were not very different in samples of different concentrations. These deviations have therefore a physical cause related to the fact that at concentrations of 1% and more the interaction between impurity molecules begins to bear on their optical properties. It can be seen in the table that concentration effects are felt only in the purely electronic band, the values of K being practically equal to 1 for all specimens in the region of the electronic-vibrational maximum.

Δn^2 values obtained from experiment and by calculation for a number of samples containing different concentrations of impurity are shown in Table 3. Values of the ratios $K = \Delta n^2_{exp.}/\Delta n^2_{theor.}$ which give an opportunity to ascertain the discrepancy between $\Delta n^2_{exp.}$ and $\Delta n^2_{theor.}$ are likewise listed in the table. The data of the table pertain to light with polarization along the b-axis. Comparing Δn^2 values for the first band, it is easy to see that on the whole if there are some discrepancies among them, such discrepancies are small and do not transgress very much beyond the limits of experimental and calculational errors. It is however noticeable that these small deviations systematically increase with increase in impurity concentration. It could be supposed that the deviations increase at higher concentration because the accuracy of measurement is reduced. This supposition must however be dropped since specimens of approximately equal effec-

If a uniform distribution of anthracene molecules at the nodes of the 9,10-dihydroanthracene lattice is assumed, the distances between impurity molecules should

Table 3.

C (%)	ν_m = 25898 cm^{-1}			ν_m = 27292 cm^{-1}		
	$\Delta n^2_{theor.}$	$\Delta n^2_{exp.}$	K	$\Delta n^2_{theor.}$	$\Delta n^2_{exp.}$	K
0.2	0.065	0.07	1.07	2	—	—
0.4	0.12	0.09	0.75	—	—	—
0.6	0.16	0.21	1.3	0.09	0.1	≈1
1	0.24	0.35	1.45	—	—	—
1.8	0.45	0.60	1.33	0.26	0.27	≈1
4.9	0.69	0.99	1.44	0.41	0.40	≈1

be equal in a 5% solution to approximately 20 A, that is, not very large. It must however be kept in mind that in an interblock distribution of impurities, the possibility of which was pointed out above, the distances between impurity molecules may be substantially smaller, in connection with which their interaction effect may be quite real.

The authors thank A. F. Prikhot'ko for his interest in the present work.

REFERENCES

1. M. S. Brodin, A. F. Prikhot'ko and M. S. Soskin, Opt. i Spektr. 6, 28 (1959), Optics and Spectroscopy 6, 14 (1959).
M. S. Brodin and A. F. Lubchenko, Opt. i Spektr. 7, 83 (1959), Optics and Spectroscopy, 7, 48 (1959).
2. M. S. Brodin and S. I. Pekar, Zhur. Eksptl. i Teoret. Fiz. 38, 74 (1960), Soviet Phys.-JETP 11, 55 (1960); ibid. 38, 1910 (1960), Soviet Phys.-JETP 11, 1373 (1960).
3. D. S. McClure, J. Chem. Phys. 22, 1668 (1954); ibid 24, 1 (1956); Y. W. Sidman, Phys. Rev. 102, 96 (195 Y. W. Sidman, J. Chem. Phys. 25, 115 (1956); Y. W. Sidman and D. S. McClure, J. Chem. Phys. 24, 757 (1956); P. Pesteil, Ann. Phys. 10, 128 (1955); E. V. Shpol'skii, Uspekhi Fiz. Nauk 71, 215 (1960). Soviet Phys.-Uspekhi 3, 372 (1960).
4. V. N. Vatulev, Ukrain. Fiz. Zhur. 5, 40 (1960); V. N Vatulev, Opt. i Spektr. 8, 727 (1960), Optics and Spe troscopy 8, 383 (1960).
5. J. Iball, J. Chem. Soc. 1938, 1074.
6. M. S. Brodin and A. F. Prikhot'ko, Opt. i Spektr. 2, 448 (1957); M. S. Brodin and S. V. Marisova, Opt. i Spektr. 10, 473 (1961), Optics and Spectroscopy 10, 242 (1961).
7. I. V. Obreimov and A. F. Prikhot'ko, Soviet Phys. 48 (1936); D. P. Craig and P. C. Hobbins, J. Chem. Soc. 1955, 2309; A. F. Prikhot'ko and I. Ya. Fugol', Opt. i Spektr. 4, 335 (1958).
8. A. I. Kitaigorodskii and R. M. Myasnikova, Kristallografiya 5, 247 (1960).

PHASE RELATIONS FOR THE p- AND s-COMPONENTS OF A REFLECTED LIGHT WAVE DETERMINED BY THE FRESNEL EQUATIONS

N. Ya. Gorban' and I. A. Shaikevich (pp. 750-753)

Received 5 March 1960

The problem of signs in the Fresnel equations and the phase shifts of the p- and s-components of the reflected wave is considered. It is shown that the Fresnel equations give correct information about the phase shifts of the p- and s-components of the reflected electric vector if, and only if, the phase is calculated with the observer looking at the oncoming ray. Direct measurements of the dependence of the phase difference $\Delta = \delta_p - \delta_s$ of the reflected wave on the angle of incidence φ were made for dielectrics (glass) and several metals by the polarization method, and also the sign of the phase difference Δ was determined. It is concluded that $\delta_p > 0$, $\delta_s > 0$, and that the phase of a wave reflected from a metal leads that of the incident wave.

DO THE SIGNS IN THE FRESNEL EQUATIONS ALWAYS GIVE CORRECT INFORMATION ABOUT THE PHASE SHIFT OF THE REFLECTED WAVE RELATIVE TO THE INCIDENT WAVE?

In the literature[1-12] there is no single universal opinion on the question of signs in the Fresnel equations for the p- and s-components of the electric vector of the reflected wave. The existence of several ways of writing these components leads to contradictory conclusions concerning the phase relations in the reflected wave. This situation at least seems paradoxical, considering that all the above-mentioned ways of writing the Fresnel equations are obtained starting from the same boundary conditions for **E** and **H** and in the same fixed coordinate system connected with the interface between media.

In order to remove the contradictions caused by the existence of several forms of Fresnel equations, it is necessary: (1) to clarify the meaning of the signs and the reasons for the different ways of writing the Fresnel equations, and (2) to determine the conditions under which the signs in the Fresnel equations can give correct information about the phase relations for the reflected electric wave. In solving the first problem, we naturally turn to those facts which depend neither on the boundary conditions nor on the choice of coordinate system, but which allow the unequivocal determination of the relative orientation of the p- and s-components of the electric vector in the reflected and incident waves. Among these experimental facts belong the well-known experiments of Wiener (1890) and Drude and Nernst (1892) for normal incidence and Lloyd's experiment with a mirror at grazing incidence. In complete accordance with the results of these experiments, the relative orientations of the p- and s-components of the reflected and incident electric vectors must be as shown in Fig. 1.

A comparison of the orientations of components which various authors have taken as resulting from the

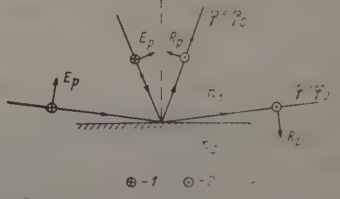

Fig. 1. Relative orientation of p- and s-components of electric vector in incident and reflected waves for reflection of light from interface of two dielectrics with $n_2 > n_1$.
1—s-vector directed into plane of diagram;
2—s-vector directed out from plane of diagram;
φ_0—Brewster's angle.

esnel equations with the orientations of these same nponents as given in Fig. 1 leads to a simple interpre- on of the signs in the Fresnel equations, namely: a s sign shows that the relative direction of vectors in incident and reflected waves is taken in agreement h Fig. 1, and a minus sign indicates noncorrespon- ace of these directions. This conclusion is completely nfirmed by the initial conditions and form of equations refs. 1, 3, 7, and 9. Thus, any signs in the Fresnel uations actually lead to the very same relative orien- ion of components in the incident and reflected waves presented in Fig 1, and it would seem that no mis- derstanding should arise. This is in fact the case until signs in the Fresnel equations are not associated with ase relations in the reflected wave and with the phase ft of the reflected wave relative to the incident wave. misinterpretations appear at this point.

In all calculations in the optics of metals, thin-film atings, etc., it is usually assumed that the phase of the flected wave relative to the incident wave does not ange if there is a plus sign in the Fresnel equations d changes by 180° if there is a minus sign.* Analysis

*This assumption is valid, strictly speaking, only for di- ctrics, since in the case of metals, even for a plus n and $\varphi \sim 0$, a certain phase shift $\delta < 90°$ arises as a sult of the complex index of refraction.

all possible ways of writing the Fresnel equations leads the conclusion that the signs will correctly character- the phase change of the reflected wave relative to the ident wave for all angles of incidence φ only if, in the ivation of these equations, the initial orientations of appropriate vector components in the incident and flected waves are not chosen arbitrarily, but in such a y that these components are in phase. Only under this ndition will the plus sign in the Fresnel equations indi- e no phase change on reflection for a given component d the minus sign, a phase change of 180°.

Usually the phases of the reflected, refracted, and ident waves are calculated in a coordinate system fixed the interface between media. Also, it is considered that vectors $\mathbf{E}_p$ and $\mathbf{R}_p$, as well as $\mathbf{E}_s$ and $\mathbf{R}_s$, in Fig. 1 ve opposite phase for $\varphi < \varphi_0$ since they are oppositely ected in this system. In order to insure phase agree- nt of the p- and s-components of the incident and re- cted waves in the derivation of the Fresnel equations, relative orientations of the electric components when φ_0 are taken as was done in ref. 7, and the Fresnel uations for the components of the reflected wave are tained in the form

$$R_p = -E_p \cdot \frac{\tan(\varphi - \psi)}{\tan(\varphi + \psi)}, \quad R_s = -E_s \cdot \frac{\sin(\varphi - \psi)}{\sin(\varphi + \psi)}, \qquad (1)$$

ere ψ is the angle of refraction.

Now, the minus sign in Eqs. (1) implies two circum- nces: (1) in order that the p- and s-components of the flected wave coincide with the directions which follow m experimental data, i.e., have relative orientations in Fig. 1 for $\varphi < \varphi_0$, it is necessary that the directions $\mathbf{R}_p$ and $\mathbf{R}_s$ be reversed from the way they were chosen ref. 7 for fixed directions of $\mathbf{E}_p$ and $\mathbf{E}_s$; (2) the phases both p- and s-components are changed by 180° as a sult of reflection.

However, because of the fact that $\tan(\varphi + \psi) < 0$ for gles of incidence $\varphi > \varphi_0$, a plus sign appears in Eq. (1) the p-component. From the point of view of the phase lations this must mean that for $\varphi > \varphi_0$ the vectors $\mathbf{R}_p$ and $\mathbf{E}_p$ are in phase. But from Fig. 1 it follows that $\mathbf{R}_p$ and $\mathbf{E}_p$ have opposite phase because they are directed oppositely to one another. Thus, when calculating phases, if we characterize a light wave by the p- and s-components and use a system attached to the interface, we arrive at a contradiction with experiment. This contradiction was explained by Kravets who correctly noted in ref. 10 that, in a system fixed to the interface, p- and s-components must not be used, and that it is necessary instead to change to projections on the three coordinate axes or to take into account the angles made by the vectors with the positive directions of the axes.

In the description of phenomena at the interface, if the idea of p- and s-components is to be preserved in a form such that no contradiction arises in the phase relations either for $\varphi < \varphi_0$, or for $\varphi > \varphi_0$, evaluation of the phase must be carried out in a coordinate system rigidly connected, not with the interface, but with the ray. This is equivalent to the requirement that phases in the incident and in the reflected (or refracted) waves be always calculated by an observer toward (or away from) whom the ray is propagated. In calculating phase in a system rigidly connected with the ray, phase agreement of the p- and s-components of the electric vectors of the incident and reflected waves for $\varphi > \varphi_0$ is achieved by the orientation given in ref. 3, where, in spite of the opposite directions of the vectors $\mathbf{E}_p$ and $\mathbf{R}_p$, they are in phase for an observer looking at the oncoming ray in both the incident and reflected waves. In this case, the Fresnel equations, in agreement with refs. 1-6, have the form

$$R_p = E_p \frac{\tan(\varphi - \psi)}{\tan(\varphi + \psi)}, \quad R_s = -E_s \frac{\sin(\varphi - \psi)}{\sin(\varphi + \psi)}. \qquad (2)$$

Contrary to statements by the authors of refs. 11 and 12, in a calculation of the phase of light waves in a system connected with the ray, the signs in Eq. (2) are in complete agreement with experimental results for normal and grazing incidence and give correct information about the phase relations for the reflected wave.

EXPERIMENTAL TEST OF PHASE RELATIONS IN THE REFLECTED LIGHT WAVE AND DIRECT DETERMINATION OF THE SIGN OF $\Delta = \delta_p - \delta_s$

A direct test of the phase relations in the reflected wave and a determination of the sign of Δ can be carried out by the polarization method using a Babinet compensator.

1. For experimental measurements of the phase difference Δ between p- and s-components of waves reflected from air-dielectric and air-metal interfaces, the axes of the Babinet compensator wedges were aligned with the p- and s-components of the reflected electric vector, and the magnitude of shift of the central dark fringe was ascertained for different angles of incidence φ. The measured results for the dependence of Δ on φ for a dielectric (glass with $n_D = 1.54$) are given by the solid curve a in Fig. 2A, and the results for the same dependence for a metal (aluminum for $\lambda = 579$ mμ) by the solid curve a in Fig. 2B. These experimental results agree completely with conclusions about the phase relations which follow from the Fresnel equations in the form of Eq. (2). If the phase relations were determined from the Fresnel equations in the form of Eq. (1), the corresponding dependence $\Delta = \Delta(\varphi)$ would be given by the broken curves b in Figs. 2A and B.

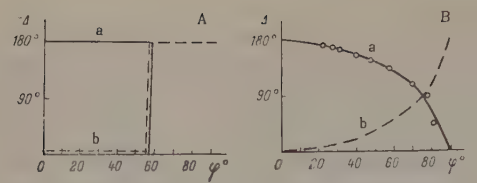

Fig. 2. Dependence of $\Delta = \delta_p - \delta_s$ on angle of incidence φ for glass (A) and aluminum (B).

2. For direct determination of the sign of the phase difference $\Delta = \delta_p - \delta_s$ between the p- and s-components of the reflected wave, the optic axes of the quartz compensator wedges were aligned with the p- and s-planes in such a way that the phase difference Δ' introduced by the compensator for the p- and s-components of the wave passing through it was determined by the relationship

$$\Delta' = \frac{360°}{\lambda} \cdot (n_e - n_0)(d_1 - d_2), \qquad (3)$$

where n_e and n_0 are the refractive indices of quartz for the extraordinary and ordinary rays, and d_1 and d_2 are the thicknesses of the first and second compensator wedges. By ascertaining the direction of shift of the central dark fringe when light which has been reflected from the metal with a phase shift Δ is passed through the compensator, and making use of the compensation condition $\Delta + \Delta' = 0$, it is possible to determine the sign of the phase difference Δ. Investigations carried out for various metals (Cu, Ni, Al, steel) showed that Δ is negative. Here δ_p and δ_s themselves must be positive because, according to Eq. (2), $|\delta_p| < |\delta_s|$. Consequently, the wave reflected from a solid metal leads the incident wave with regard to phase.

In conclusion, we consider it our pleasant duty to express our thanks to A. A. Shishlovskii for valuable advice and interest in this work.

REFERENCES

1. M. Born, "Optik." Springer, Berlin, 1933. United Scientific and Technical Press, Moscow, 1937.
2. P. Drude, "Optics." United Scientific and Technic Press, Moscow, Leningrad, 1935.
3. G. S. Landsberg, "Optics." State Press for Techn cal and Theoretical Literature, Moscow, 1952.
4. R. W. Wood, "Researches in Physical Optics," C lumbia Univ. Press, New York, 1913. United Scie tific and Technical Press, Moscow, Leningrad, 19
5. S. E. Frish and A. V. Timoreva, "Course in Gene Physics," Vol. 3. State Press for Technical and oretical Literature, Moscow, Leningrad, 1951.
6. "Fundamental Formulas of Physics."* Foreign L erature Press, Moscow, 1957. 2nd rev. ed., Dove New York, 1959.
7. G. V. Rozenberg, "Optics of Thin-Layered Coatin State Press for Physical and Mathematical Litera ture, Moscow, 1958.
8. J. A. Stratton, "Electromagnetic Theory." McGra Hill, New York, 1941. State Press for Technical a Theoretical Literature, Moscow, Leningrad, 1948
9. A. Sommerfeld, "Lectures in Theoretical Physics Vol. 4. Optics." Foreign Literature Press, 1953. Academic Press, New York, 1954.
10. T. P. Kravets, "Trudy Po Fizike," (sic.), p. 167. Academy of Sciences Press, Moscow, Leningrad, 1959.
11 I. N. Shklyarevskii and V. K. Miloslavskii, Opt. i Spektr. 3, 361 (1957).
12. J. R. Beattie and G. K. T. Conn, Phil. Mag. 46, 22 (1955).

* Translation Editor's note: This is possibly the book edited by D. H. Menzel, presently being published by Dover, New York.

HAVE YOU SENT IN YOUR SUBSCRIPTION FOR 1962? – SEE ORDER CARD IN THIS ISSUE.

Filler Material – Not in Russian original.

A STUDY OF SCATTERING OF LIGHT IN OBJECTS SUBJECT TO FADING

A. P. Ivanov (pp. 754-758)

Received 9 January 1961

The laws of the scattering of light in objects which are subject to fading were studied by a finite differences method. The case in which the absorption constant varies exponentially with time was studied in detail.

Changes in the reflecting power of light-scattering ects while they are fading is an entirely unstudied field he theory of scattering of light. This is explained by great difficulties in calculation which are encountered n absorption in a substance becomes a function of the nsity of light. However, prediction of changes with e in the reflection factor of textiles, coverings, eens, and walls of various structures that are sub- ed to intense light irradiation is a very urgent prob- .

The purpose of this article is to present a method for ulating the reflection and transmission factors of a t-scattering layer as functions of the optical constants, intensity of the light, and time. The analytic solution of problem is a practically insuperable task, even for tain special cases. A numerical finite differences hod which is now beginning to be applied to the inves- tion of complex problems in the theory of transfer of iation[1-4] is considerably more convenient. A simple cedure based on a finite differences method has been gested[4] for determining the reflection factor R and transmission factor T for media with variable optical ameters.

This method can be applied readily to a case in which yer is fading under the action of incident light.

Let a horizontal plane-parallel layer of thickness x_0 illuminated from above by a diffuse monochromatic m of light which produces the illuminance E_0 on the face. Such an object will fade with time under the ac- of the light. Since the intensity of the radiation is erent at different depths of the medium, the absorp- power of the layer varies with changes in depth. If values of R and T as functions of the thickness of layer are known, it is not difficult to determine the t field at any point in the medium.

Let us conceptually separate the layer to be studied he horizontal plane at depth x into two parts. The t layer of thickness x is characterized by the reflec- factor R_1 and the transmission factor T_1. The sec- layer of thickness $x_0 - x$ is characterized by the val- R_2 and T_2. It is easy to show that, as a result of re- ted reflection of light between these layers, the total inous flux per unit surface area will be*

$$E = \frac{(1 + R_2) T_1}{1 - R_1 R_2} . \qquad (1)$$

he true illuminance is equal to the product EE_0 (the ntity E is dimensionless).

Let the change in the absorption constant under the ion of the light be determined by the differential equa- n

$$dk = df(k_0, E\tau) \qquad (2)$$

Here k_0 is the value of the absorption constant at the initial time, while $\tau = E_0 ct$ is called the reduced time,*

*In a large number of photochemical reactions fading is not determined by the three parameters mentioned here, but by their product.

where c is the fading constant and t is the time. In this case one may suggest the following method for calculating R and T:

1. At the time $\tau_1 = 0$, when the properties of the medium are the same at any point, the intensity E is determined by (1) as a function of x by means of well known expressions for the reflection and transmission factors (see, for example, ref. 5).

2. We now let an increment $\Delta\tau_1$ occur. During this time interval the absorption constant k changes under the action of the intensity E in accordance with formula (2). At the same time, the increment $\Delta\tau_1$ is selected in such a manner that E may be considered constant over this interval. Thus, the absorption constant is equal to $k_2 = k_1 + \Delta k_1$ by the time $\tau_2 = \tau_1 + \Delta\tau_1$.

3. Thus, at the time τ_2 the absorption constant and, consequently, the ratio k_2/s (s is the scattering constant which is considered as always constant), which is the only factor on which the scattering of light is dependent, is a known function of the thickness of the layer. We shall make use of the method suggested in ref. 4 to find R_1, R_2, and T_1, and then also E for different optical thicknesses $y = sx$.

4. We now let an increment $\Delta\tau_2$ occur and calculate, as in Point 2, the change in the value of the absorption constant at different depths. This cycle of calculations is continued until the entire layer has faded.

The size of the step for y and τ is determined by the following procedure. The interval of time or thickness is divided into a finite number of elementary intervals, then a trial calculation is carried out for R and T. This is followed by a similar calculation, but with finer intervals. Those values of Δy and $\Delta\tau$ which when changed produce practically no change in the reflection and transmission factors are taken as working values.

To illustrate the possibilities of the method selected here, let us consider the case of fading of a light-scattering object in which the absorption constant of an element of volume varies according to the law

$$k = k_0 e^{-E\tau}, \qquad (3)$$

where k_0 is the absorption constant of the layer when $\tau = 0$.

Figure 1 gives an idea of the light field and the values of the optical parameters within a semi-infinite medium

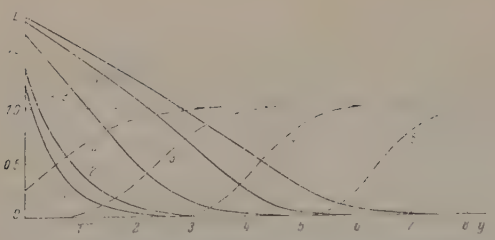

Fig. 1. Dependence of E and k/s on the depth y for different values of τ and $y_0 = \infty$. The Solid curves—E = f(y); dashed curves—k/s = f(y). The values of τ are: Curve 1—0; curve 2—1.05; curve 3—5.5; curve 4—18; curve 5—30.

for different depths and for different times. The values of E (solid curves) and k/s (dashed curves) are plotted against y. The figures shown near the curves correspond to different values of τ. At the initial time (curves 1) when k/s is a constant, the change in total illuminance with depth is described by the formula*

$$E = (1 + R)\, e^{-Ly}, \qquad (4)$$

*See, for example, ref. 6.

where R is the reflection factor of an infinitely thick layer and

$$L = \sqrt{\left(\frac{k}{s}\right)^2 + 2\frac{k}{s}}.$$

Since the absorption in the surface layers decreases sharply (curves 2-5), the illuminance in the medium increases strongly with time (particularly in depth). It is necessary to call attention to the fact that E varies linearly within thicknesses in which k/s is zero.

The case of radiation emerging from a layer is of special interest. Calculations show that both the reflection and transmission factors increase most rapidly in the initial period of time for all k/s in the process of fading. This process slows down gradually with time.

In order to show how the different factors affect the reflecting and transmitting powers of light-scattering screens, curves of $R(\tau)$ and $T(\tau)$ for different optical thicknesses of the layer y_0 and different values of k/s are presented in Fig. 2. Let us examine curves 1-3 which show changes in T with time for different thicknesses y_0 and for k/s = 1. It can be seen from the figure that layers which originally had a small transmission factor, or which transmitted absolutely no light, become quite translucent with time due to fading. When $\tau = \infty$, T tends to its limit value (dashed lines) which corresponds to a completely faded layer.

Curves 4, 5, 6, and 8 show the relation $R = f(\tau)$ for layer thicknesses of 0.75, 1.5, 3, and ∞ with an initial

Values of Reflection Factors for Different Values of k/s and τ

τ \ $\frac{k}{s}$	0	0.003	0.01	0.03	0.1	0.3	1	3	10
0	1.000	0.921	0.869	0.784	0.642	0.465	0.268	0.125	0.043
0.5	1.000	0.940	0.894	0.830	0.712	0.540	0.350	0.192	0.062
1.0	1.000	0.955	0.924	0.870	0.764	0.602	0.402	0.230	0.083
2.0	1.000	0.962	0.947	0.912	0.830	0.690	0.510	0.331	0.120
4.0	1.000	0.970	0.953	0.930	0.882	0.790	0.647	0.457	0.185
10	1.000	0.975	0.965	0.950	0.922	0.860	0.766	0.622	0.355
20	1.000	0.975	0.967	0.958	0.937	0.895	0.822	0.711	0.485
40	1.000	0.975	0.967	0.960	0.945	0.922	0.865	0.772	0.585
100	1.000	0.975	0.967	0.960	0.951	0.935	0.893	0.817	0.672
1000	1.000	0.985	0.977	0.972	0.967	0.955	0.925	0.872	0.775

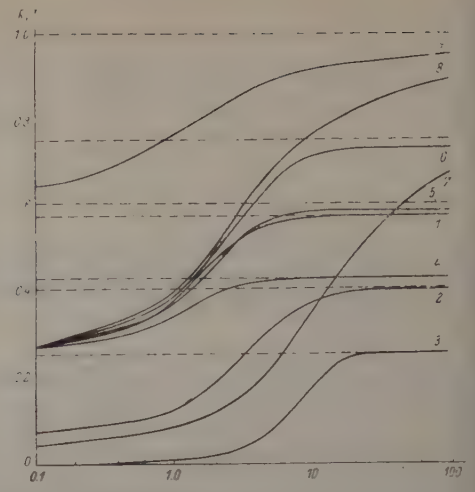

Fig. 2. Dependence of R and T on τ for different values of k/s and y_0. Curves 1, 2, 3 are $T = f(\tau)$ for k/s = 1 and thicknesses y_0 of 0.75, 1.5, and 3, respectively; curves 4, 5, 6 are $R = f(\tau)$ for the above values of the parameters; curves 7, 8, 9 are $R = f(\tau)$ for $y_0 = \infty$ and values of k/s equal to 10, 1, and 0.1, respectively.

value of k/s = 1. An outstanding feature is the fact th when $\tau = 0$ the reflection factors of layers of differen thicknesses coincide. This is explained by the fact th when k/s = 1, the layers under consideration are pra cally infinitely thick. As they fade, the light in thick o jects begins to be reflected from greater depths, whic leads to a considerable increase in R with large valu of y_0. At the same time, in spite of significant light i tensities which exist in thick layers, the latter fade m slowly than thin layers. The maximum divergence in flection factors is seen for $\tau = \infty$.

The effect of the ratio k/s on changes in reflecti power is illustrated in the example of an infinitely thi layer (curves 7, 8, and 9). Due to the considerable di ference in values of k/s, the reflection factors at the ginning of the fading process differ greatly from each other but tend toward unity in the limit. Since the cas $y_0 = \infty$ is of special practical interest, we here introd for the case of exponential fading of an element of vol a table which can be used to determine the reflection tor over wide ranges of values of k/s and τ.

The method examined in this article can be exten without difficulty to the case of nonmonochromatic ill nation of a medium.

In conclusion, the author wishes to express his g tude to S. I. Kobylevskaya for a large amount of comp tational work.

REFERENCES

1. O. V. Lokutsievskii, Uspekhi Mat. Nauk 11, 224 (19
2. G. I. Marchuk, "Collection: Physical and Heat Eng neering Reactors," 22. Atomizdat, Moscow, 1958.
3. N. I. Buleev, Atomnaya Energ. 6, 338 (1953).
4. A. P. Ivanov and E. B. Khodos, Opt. i Spekt. 8, 556 (1960), Optics and Spectroscopy 8, 293 (1960).
5. M. M. Gurevich, Trudy Gosudarst. Opt. Inst. 6, No 1 (1931).
6. A. A. Gershun, Trudy Gosudarst. Opt. Inst. 11, No 43 (1936).

THEORY OF THE SELECTIVITY OF OPTICAL ABSORPTION ANALYZERS FOR THE COMPOSITION OF GASEOUS OR LIQUID MIXTURES. II

A. O. Sall' (pp. 759-764)

Received 29 September 1960

The causes which limit the selectivity of nondispersive absorption analyzers are examined. Methods for increasing the selectivity are described.

The expression obtained in the first part of the present work[1] for the selectivity coefficient of a nondispersive analyzer [relation (2.7)] is valid only when a whole series of conditions are fulfilled. Let us examine these conditions.

I. ELIMINATION OF THE EFFECT OF ADMIXTURES OF RADIATION-ABSORBING INTERFERING COMPONENTS LOCATED IN THE OPTICO-ACOUSTICAL DETECTOR

If the content of radiation-absorbing unsought components in the mixture which fills an optico-acoustical detector exceeds a certain limiting value, which is subject to approximate calculation,[2] then, to avoid a marked impairment of the selectivity of the gas analyzer, filter cells filled with the same interfering components as are present in the detector cell are set up in the path of the light beams. As calculations have shown, when the volume concentration of interfering components in the detector is of the order of 10^{-3}%, the necessary length of the filter cell does not usually exceed 10 mm. The same value has been adopted for commercial optico-acoustical gas analyzers intended for the separate determination of CO, CO_2 and CH_4.[3]

In an optico-acoustical gas analyzer intended for the simultaneous determination of three components in a mixture,[4] the optico-acoustical detector is filled with a mixture of these components. Let us calculate the necessary length of the filter cell for the case where the absorption spectra of the desired components do not overlap. Such a calculation reduces, in the last analysis, to the successive carrying out of very simple individual calculations, each of which is performed for the case when one component is being determined and likewise only one component interferes with the conduct of the analysis. Let us assume that the absorption coefficients of the desired and the interfering components are expressed in series form (for symbols, see ref. 1):

$$\varkappa(\nu) = \sum_p \frac{\varkappa_p (\Delta\nu)^2}{(\Delta\nu)^2 + (\nu - \nu_p)^2}, \qquad (1.1)$$

$$\varkappa_M(\nu) = \sum_n \frac{\varkappa_n (\Delta\nu)_M^2}{(\Delta\nu)_M^2 + (\nu - \nu_n)^2}. \qquad (1.2)$$

From the necessary value of v_m, one can obtain

$$\left(\frac{v_M}{u}\right) \approx 0.6 \left(\frac{w_M}{u}\right)^{3/5} \left(1 - \sqrt{\frac{u}{w+u}}\right)^{-2/5} \left(\frac{u_M}{u}\right)^{2/5} \left[\frac{(\Delta\nu)_M \sum_n \sqrt{\varkappa_n}}{(\Delta\nu) \sum_p \sqrt{\varkappa_p}}\right]^{2/5} \left(\frac{\Delta c}{c}\right)_M^{-2/5}, \qquad (1.3)$$

where $(\Delta c/c)_M$ is the admissible value of the relative error caused by a change in the content of interfering component in the mixture being analyzed; w_m and w are the products of the length of the light path in the absorbing cylinder by the concentration of the interfering component in the mixture which fills the radiation detector and by the concentration of the desired component, respectively.

Calculation according to this formula (for u = 100%-mm) leads to values for the length of the filter cell from a few tens to two or three hundred millimeters. Actually, the necessary length turns out to be less, in consequence of the fact that at such a length of the filter cell, overlapping of the neighboring absorption lines in the band of the interfering component sets in.

The effect of admixtures of interfering components in a selective gas radiation source or in Luft modulating cells can also be entirely eliminated by using filter cells filled with the interfering components. The content of the desired component in such filter cells must be minimal.[2]

II. EFFECT OF THE THICKNESS OF THE PASSIVE LAYER ON THE MAGNITUDE OF THE SELECTIVITY COEFFICIENT

The heat evolved in the "passive" layer near the window of the absorbing cell in an optico-acoustical detector is given off to the window and does not participate in the excitation of acoustical vibrations.[5] Let us denote by η the ratio of the thickness of the passive layer to the length of the light path in the absorbing cylinder. Substituting the expression for the spectral sensitivity $s = e^{-\kappa w\eta} - e^{-\kappa w}$ into the relation (2.1), under the condition $\kappa w \ll 1$, we obtain

$$\frac{\Delta c_M}{\Delta c} = \frac{\int_0^\infty I e^{-\varkappa_M \theta_M \varkappa} (e^{-\varkappa w\eta} - e^{-\varkappa w})\, d\nu}{\int_0^\infty I e^{-\varkappa_M \theta_M \varkappa_M} (e^{-\varkappa w\eta} - e^{-\varkappa w})\, d\nu}$$

$$\approx \frac{\int_0^\infty e^{-\varkappa_M \theta_M \varkappa} [\varkappa w - 0.5(1+\eta)(\varkappa w)^2]\, d\nu}{\int_0^\infty e^{-\varkappa_M \theta_M \varkappa_m} [\varkappa w - 0.5(1+\eta)(\varkappa w)^2]\, d\nu}$$

$$\approx \left(\frac{\Delta c_M}{\Delta c}\right)_{\eta=0} \left[1 - 0.5\eta \frac{\int e^{-\varkappa_M \theta_M \varkappa} \varkappa^3 d\nu}{\int e^{-\varkappa_M \theta_M \varkappa} \varkappa^2 d\nu} w\right]$$

$$\approx \left(\frac{\Delta c_M}{\Delta c}\right)_{\eta=0} [1 - B\eta w \varkappa_{\max.}], \qquad (2.1)$$

where $(\Delta c_M/\Delta c)_{\eta=0}$ is the selectivity coefficient which would exist in the ideal case of no passive layer; B is a

numerical coefficient depending on the fine structure of the absorption band of the desired component.

If the modulation frequency is so high that the depth of the absorbing cell in an optico-acoustical detector significantly exceeds the depth of penetration of the temperature oscillations, then the thickness of the passive layer at the window of the absorbing cell will be approximately equal to half the depth of penetration of the temperature oscillations.[2] As the modulation frequency is reduced, the thickness of the passive layer grows, and the value of η increases. In the limiting case of a modulation frequency so low that the depth of the absorbing cell does not exceed the depth of penetration of the temperature oscillations, the thickness of the passive layer becomes comparable to the depth of the cell. As a result of the solution of the generalized heat transfer equation[5] for the case of a sufficiently low modulation frequency, an expression has been obtained determining the spectral sensitivity of a detector in which the absorbing cylinder has a reflecting rear surface; a formula has also been deduced for the selectivity coefficient of a gas analyzer. In order for the formula thus obtained to coincide with the expression (2.1), it is necessary to set $\eta \approx 2$ in the latter. As approximate calculations have shown, the numerical value of the coefficient B for diatomic and linear polyatomic molecules lies between the limits of 0.17 and 0.22. Let the product $w\kappa_{max.}$ have a value of the order of 1. The selectivity coefficient of an optico-acoustical gas analyzer will then differ from the maximum possible value (which would exist at $\eta = 0$) by not more than a factor of two.

If $w\kappa_{max.} \gg 1$, then it is necessary to use other expressions to determine the relative decrease in the selectivity coefficient caused by the presence of the passive layer. For example, if the absorption of radiation by the desired and the interfering components follows a square-root law, then the dependence of the selectivity coefficient on η for the case $u \ll w$ takes the form

$$\frac{\Delta c_M}{\Delta c} \approx \left(\frac{\Delta c_M}{\Delta c}\right)_{\eta=0} \cdot \left[1+\left(\frac{w\eta}{u}\right)^2\right]^{-0.5}. \qquad (2.2)$$

Formulas (2.1) and (2.2) can also be extended to the case when an increase in the selectivity of the absorptiometer is realized with the help of supplementary modulating cells containing the desired component, set up in the path of both light beams. The thickness of the gas layer in such a modulating cell may be decreased to some limit determined by the construction of the cell. This is equivalent to having, in the paths of the two beams which are being compared, supplementary cells filled with the desired component which diminish the selectivity of the analyzer. In this case η equals the ratio of the minimum thickness of the modulating layer of the desired component to the maximum thickness of this layer.

It follows from examination of formulas (2.1) and (2.2) that, by diminishing η, one can practically reduce to zero the effect of the passive layer in optico-acoustical detectors, or the effect of the minimum thickness of the modulating layer in absorptiometers with selective modulation of the beams. We shall make use of this fact hereafter.

The presence of admixtures of the desired component in the filter cell filled with the interfering component, like the passive layer of gas near the window of the absorbing cylinder of an optico-acoustical detector, increases the error resulting from the presence of the interfering components. This increase in the error may be estimated approximately quantitatively, using formulas (2.1) and (2.2), if one sets $\eta = L_f c_f w^{-1}$, where L_f is t length of the filter cell and c_f is the concentration in admixture of the desired component in the filter cell.

III. CHANGE IN THE ABSORPTION SPECTRUM OF THE DESIRED COMPONENT WITH A CHANGE IN THE COMPOSITION OF THE MIXTURE BEING ANALYZED

We have examined above that term in the error o absorptiometer which is governed by a change in the c tent of unsought radiation-absorbing components in th mixture being analyzed. However, with a change in th concentration of those unsought components in the mix ture which do not absorb radiation in the spectral regi used for analysis, the readings of an absorption analyz may still change. This is explained by the fact that, w a change in composition of the mixture being analyzed the absorption spectrum of the desired component changes.[2,6] For example, the infrared absorption spec of gases change with a change in the half-width of the sorption lines. An increase in the half-width leads to decrease in the absorption coefficient at the center an an increase in its value in the wings of the line. The readings of an infrared absorption gas analyzer will thereby be changed. The greatest change in the readin will be observed in the case when the product of the le of the absorbing cell and the concentration of the desi component in the mixture being analyzed is so large th the absorption of radiation takes place principally in t wings of the lines.

In the first approximation, we shall consider that intensity of the absorption lines (the integral $\int \kappa d\nu$) is practically independent of the composition of the gas m ture being analyzed. The magnitude of the relative cha in the absorptiometer readings in this case will be nu- merically equal to the relative change in the half-widt of the absorption line of the desired component. With considerable reduction in the length of the cell, the co tion $\kappa_{max.} u \ll 1$ may be attained. If at the same time t product $\kappa_{max.} w \ll 1$, then the signal from the gas will proportional to the quantity $\int \kappa^2 d\nu$. The magnitude of relative change in the readings in this case is approxi mately equal to half the relative change in the half-wi of the line, taken with the opposite algebraic sign. Th by changing u and w, the algebraic sign of the error be reversed. Consequently, the numerical values of u w can be chosen such that for at least two points of th absorptiometer scale (one of which is the scale origin the error caused by the replacement of one accompany component by another in the mixture being analyzed w equal zero. In other words, the decrease in the absor tion of radiation in the central parts of the absorption as its width increases is then compensated by an incr in the absorption in the wings. For the remaining poi of the scale, the relative error, although different fro zero, is still at least several times smaller than the tive change in the line width. This also holds true in t real case of an absorption band consisting of a large n ber of lines of different intensity.

To diminish the error brought about by a change the absorption coefficient of the desired component wi change in the composition of a liquid mixture being an lyzed (as also in the analysis of a mixture of gases), can also make use of the method of dilution of the mix or the method of selective compensation, which, in se

ie compensating mixture, uses a known addition of lesired component to the mixture being analyzed.[2,6] n the method of known additions is used, the error ed by a change in the absorption spectrum of the de- d component may be reduced to a value considerably than the other terms in the absorptiometer error.[2,6]

MAXIMUM LIMITING VALUE OF THE SELECTIVITY COEFFICIENT FOR NON-DISPERSIVE ABSORPTIOMETERS

Let us now estimate the order of magnitude of the ting possible value of the selectivity coefficient for co-acoustical gas analyzers. It is evident that this tained when the absorption spectra of the desired and fering components have practically no overlap. For spectral sensitivity of an optico-acoustical detector, g account of nonselective absorption of radiation by valls and windows of the absorbing cell[2] and neglect- he passive layer at the window of the absorbing [2,5] we obtain approximately: $s(\nu) \approx (1 - e^{-\varkappa w}) + s_H$, e s_H is that spectral sensitivity of the detector which ntrolled by the nonselective absorption of radiation e walls and windows of the absorbing cell. Substitut- he expression just presented into formula (2.1) of the part of the present work,[1] we have

$$\left(\frac{\Delta c_M}{\Delta c}\right)_{sel.} \approx \frac{\int_0^\infty I e^{-\varkappa_M p_M \varkappa} \left[1 - e^{-\varkappa w} + s_H\right] d\nu}{\int_0^\infty I e^{-\varkappa_M p_M \varkappa_M} \left[1 - e^{-\varkappa w} + s_H\right] d\nu}$$

$$\approx \frac{\int_0^\infty I e^{-\varkappa_M r_M \varkappa} \left[1 - e^{-\varkappa w} + s_H\right] d\nu}{s_H \int_0^\infty I e^{-\varkappa_M p_M \varkappa_M} d\nu}$$

$$\geqslant \frac{\int_0^\infty e^{-\varkappa_M p_M \varkappa} d\nu}{s_H \int_0^\infty I e^{-\varkappa_M p_M \varkappa_M} d\nu} \approx \frac{1}{s_H} \left(\frac{\Delta c_M}{\Delta c}\right)_{nonsel.}, \qquad (4.1)$$

re $(\Delta c_M/\Delta c)_{nonsel.}$ is the selectivity coefficient which ld exist if a nonselective radiation detector were used. numerical value of the modulus $|s_H|$ can be reduced quantity of the order of 10^{-5}-10^{-6}.[2] Therefore, even $\Delta c_M/\Delta c)_{nonsel.} \approx 1$, a value of the order of 10^5-10^6 can btained for the selectivity coefficient when a selective co-acoustical detector is used. If the absorption of ation by the desired and interfering components fol- a square-root law and the intensities of absorption approximately the same for the desired and interfer- components, then considering $u \ll w$, we have for the ctivity coefficient

$$\frac{\Delta c_M}{\Delta c} \approx \frac{0.5 u_M}{s_H} \left(\frac{1}{\sqrt{u}} - \frac{1}{\sqrt{w+u}}\right) \left(\sqrt{v_M + u_M} - \sqrt{v_M}\right)^{-1}$$

$$\geqslant \frac{0.5}{s_H} \sqrt{\frac{u_M}{u}}. \qquad (4.2)$$

Comparing the formula just presented (with $u_M = u$) formula (4.1), we find that the selectivity coefficient e case where the square-root law is fulfilled has the e order of magnitude as in the case of radiation ab- tion according to a linear law. Thus when an optico- stical gas analyzer is used for the analysis of gases with nonoverlapping absorption bands, the selectivity coefficient may reach values of the order of 10^5-10^6. For most practical problems, it is sufficient to have a considerably lower value of the selectivity coefficient. For example, suppose the gas analyzer has a scale from 0 to 1% (by volume) and the concentration of the interfering component in the mixture being analyzed can reach 100%. Let the calibration error of the gas analyzer have a value of the order of ±0.02% (by volume). In order for the error caused by a change in the content of interfering components in the mixture being analyzed not to exceed the calibration error, the selectivity coefficient must be of the order of $100\%/0.02\% = 5 \times 10^3$. This condition is fulfilled in the commercial optico-acoustical gas analyzers intended for the separate analysis of carbon monoxide, carbon dioxide, and methane.[3]

Almost the same values of the selectivity coefficient can be obtained for an infrared absorptiometer with a selective gas radiation source. This is explained by the fact that the modulated radiation from the window and walls of the radiation source vessel, in those portions of the spectrum in which absorption of light by the desired component of the mixture being analyzed takes place, is lower in intensity by several orders of magnitude than the radiation of the gas in the region of its bands. Let us carry out a comparative estimate of the spectral intensity of the radiation from the gas and from the vessel walls. We shall consider the case where the amplitude of the variation in the average volume temperature $\bar{\vartheta}$ of the radiating gas is significantly less than the absolute temperature T. The amplitude of the temperature variation of the radiating gas in a thin layer at the window of the source vessel is less than $\bar{\vartheta}$, as a result of thermal interaction with the vessel window. The thickness of such a layer is comparable with the depth of penetration of the temperature oscillations.[5] A part of the radiation emitted by the gas in the central part of the vessel is absorbed in this layer. This leads to a reduction in the spectral radiation intensity in those portions of the spectrum corresponding to the centers of the relatively strong bands. To avoid such a reduction in the spectral radiation intensity, the depth of the "radiating" vessel must be considerably more than the depth of penetration of the temperature oscillations. In this case, solving the heat transfer equation[2] for the amplitude of the temperature variation of the vessel walls, we obtain

$$\vartheta_{wall} \approx \sqrt{\frac{\lambda c_p}{\lambda' c'}}\, \bar{\vartheta},$$

where λ and c_p are respectively the thermal conductivity and heat capacity of a unit volume of the gas, and λ' and c' are the analogous quantities for a unit volume of the material of the vessel walls. The spectral intensity of the modulated radiation beam produced by emission from the gas in the central portions of the bands is proportional to the quantity $\bar{\vartheta}$; the spectral intensity produced by emission from the walls is proportional to $\alpha_{wall} \vartheta_{wall}$, where α_{wall} is the absorption coefficient for the radiation from the vessel walls. The ratio of the spectral intensities equals

$$\frac{\alpha_{wall}\, \vartheta_{wall}}{\bar{\vartheta}} = \alpha_{wall} \sqrt{\frac{\lambda c_p'}{\lambda' c'}}.$$

The value of this ratio, which is numerically equal to $\varphi_2(\nu)$,[2] is less than 10^{-5} in favorable cases.[2] It can be shown that the ratio of the intensity of modulated emission from the window to that of emission from the gas, in

a narrow spectral interval corresponding to the most intense part of the spectrum of the emitting gas, is approximately equal to $|\varphi_3(\nu)|;^2$ i.e., it is often less than 10^{-6}.[2]

We have considered the case where $\overline{\vartheta} \ll T$. If however $\overline{\vartheta}$ is comparable with T, then the nonselective emission from the window and walls of the vessel is still negligibly small in comparison with the emission from the gas.

The expressions (4.1) and (4.2) can also be used for the case where selective absorption analysis is realized by means of a periodic variation in the concentration of the desired component in the path of both beams (for example, by the use, in both beams, of supplementary modulating cells with movable reflecting surfaces). As experiments have shown, even in the absence of a radiation-absorbing component in the modulating cell, periodic changes in the beam of radiation falling on the detector arise as the reflecting plate oscillates. In the calculation of the selectivity coefficient, the relative change in the beam falling on the detector which is brought about by oscillations of the reflecting surface of the modulating cell, while the desired component is absent from the latter, is included in s_H. If the amplitude of the periodic change in the layer thickness of the modulating mixture as the reflecting surface of the modulating cell oscillates does not exceed one millimeter, then values of $s_H < 10^{-2}$ are relatively easily attained. Selective modulation of the two beams being compared can also be realized by the use of the so-called "transmitting" modulating cells. Such a cell has two windows, and the radiation beam passes in succession through these windows. The change in the layer thickness of the modulating gas is accomplished by a change in the distance between the cell windows. The value of s_H is thereby diminished by mor than an order of magnitude in comparison with an ab tiometer with reflecting modulating cells.

The investigation just presented shows that the e terms caused (1) by a change in the absorption spect of the desired component with a change in the compos of the mixture being analyzed, (2) by the presence of desirable impurities in the mixtures filling the absor and filter cells of an optico-acoustical gas analyzer, (3) by the presence of a passive layer in an optico-ac tical radiation detector, etc., may in the general case made sufficiently small. Therefore, if the spectra ar practically nonoverlapping, the selectivity coefficient usually be made sufficiently high. On this basis, we s examine in detail, in a continuation of the present wo only those error terms which are brought about by th overlap of the absorption spectra of the components.

REFERENCES

1. A. O. Sall', Opt. i Spektr. **11**, 672 (1961), Optics an Spectroscopy **11**, 361 (1961).
2. A. O. Sall', Zhur. Tekh. Fiz. **29**, 330 (1959); Soviet Phys.-Tech. Phys. **4**, 295 (1959).
3. V. A. Pavlenko, "Collection: Heat Power and Che ical Engineering Instruments and Regulators," p. State Scientific-Technical Press for Machine Con- struction Literature, Moscow-Leningrad, 1959.
4. K. F. Luft, Angew. Chem. **B59**, 2 (1947).
5. A. O. Sall', Zhur. Tekh. Fiz. **26**, 157 (1956); Soviet Phys.-Tech. Phys. **1**, 152 (1956).
6. A. O. Sall', Opt. i Spektr. **5**, 316 (1958).

ERRATA IN VOL. XI

Page	Line	Printed	Correction
87	8 from the bottom, R.H. column	(28:31:50)	(14:31:50)
198	14 from the bottom, L.H. column	(11, 12)	(11)
369	Fig. 3	The given wavelength Fe 2512.363 refers to the second line on the right, and Cr 2512.40 to the extreme right line.	

LETTER TO THE EDITOR

In our article "The Study of the Emissive Power Certain High-Melting Compounds in the Infrared Regi published in the journal Optics and Spectroscopy, **11**, 219 (1961), due to an oversight no mention was made E. T. Lysak's participation and help in the part of the study pertaining to the investigation of the radiative properties.

We ask the editor to please correct our mistake publishing our letter in one of the future issues of the journal.

G. V. Samso

CALCULATION OF CATHODE LENS ABERRATIONS

P. P. Kas'yankov (pp. 765-767)

Received 9 January 1961

1. The well-known expressions for first order chro-
ic aberrations and third order geometric aberrations
athode lenses contain algebraic fractions.[1] For low
gy electrons the denominators of these fractions ap-
ach zero but the numerators do not. In cathode lenses
mage is formed by low energy electrons. Conse-
tly near the cathode these fractions become very
e and the formulas containing them are unsuitable
calculating cathode lens aberrations. For the same
on the paraxial equation of a trajectory near the cath-
has a singular point and series for calculating auxil-
rays converge poorly.

The well-known formulas are derived assuming that
es between the symmetry axis and the tangents to the
tron trajectory are small enough so that the series
nsion of the sine of such an angle need only be taken
o the term of third order. For some of the electrons
h contribute to formation of the image of the cathode
angle may reach 90° in the vicinity of the cathode. It
mpossible to use the familiar formulas for such large
ture beams.

The plane of the best arrangement does not usually
cide with a Gaussian plane. The formulas found in the
ature for calculating aberrations in an arbitrary
e of an arrangement[2] are also unsuitable for cathode
aberration calculations because again fractions with
ll denominators are present.

In this paper we present aberration formulas which do
contain fractions with small denominators. These ex-
ssions are suitable for calculating aberrations of large
ture beams and they give the aberration in an arbi-
y plane of an arrangement. The proposed formulas
be used to calculate aberrations of arbitrary axially
metric systems, including mirror systems.

2. First, let us consider the equation of motion of an
tron with mass m and charge e in the electromag-
c system of units which has the form

$$m\ddot{\mathbf{r}} = -e\,\mathrm{grad}\,\varphi - [\mathbf{r},\ \mathrm{grad}\,\psi]. \tag{1}$$

The scalar potentials φ and ψ of the electrostatic
magnetostatic fields and the radius vector r are ex-
ssed in terms of the coordinates x, y, z of a fixed rec-
ular cartesian coordinate system in which the z-axis
cides with the symmetry axis of the system. A dot in-
tes differentiation with respect to time and a prime
indicate differentiation with respect to z. The values
and the magnetic field intensity along the z-axis are
oted by Φ and H, respectively. Using the familiar se-
for φ and ψ and expanding only to first order, assu-
g x and y small, we obtain from (1) the paraxial equa-
s of motion

$$\left.\begin{aligned} L(x,\ y,\ z) &\equiv \ddot{x} + 2\alpha\left(\frac{1}{2}x\Phi'' + \dot{y}H - \frac{1}{2}\dot{z}yH'\right) = 0,\\ M(x,\ y,\ z) &\equiv \ddot{y} + 2\alpha\left(\frac{1}{2}y\Phi'' - \dot{x}H - \frac{1}{2}\dot{z}xH'\right) = 0,\\ N(x,\ y,\ z) &\equiv \ddot{z} - 2\alpha\Phi' = 0 \end{aligned}\right\} \tag{2}$$

and, considering terms as small as the third order, the equations

$$\left.\begin{aligned} L(x_3,\ y_3,\ z_3) &= f_1,\\ M(x_3,\ y_3,\ z_3) &= f_2,\\ N(x_3,\ y_3,\ z_3) &= f_3, \end{aligned}\right\} \tag{3}$$

where

$$\alpha = \frac{e}{2m}, \tag{4}$$

$$\left.\begin{aligned} f_1 &= 2\alpha\left(x_3^2 + y_3^2\right)\left[\frac{1}{16}x_3\Phi^{\mathrm{IV}} + \frac{1}{4}\dot{y}_3H'' + \frac{1}{16}\dot{z}_3y_3H'''\right],\\ f_2 &= 2\alpha\left(x_3^2 + y_3^2\right)\left[\frac{1}{16}y_3\Phi^{\mathrm{IV}} - \frac{1}{4}\dot{x}_3H'' - \frac{1}{16}\dot{z}_3x_3H'''\right],\\ f_3 &= 2\alpha\left[-\frac{1}{4}\left(x_3^2 + y_3^2\right)\Phi''' + \frac{1}{2}\left(\dot{x}_3y_3 - x_3\dot{y}_3\right)H'\right]. \end{aligned}\right\} \tag{5}$$

The calculations are performed by making use of the auxiliary variables p and q, related to x and y by the following equations

$$\left.\begin{aligned} x &= p\cos\theta - q\sin\theta,\\ y &= p\sin\theta + q\cos\theta, \end{aligned}\right\} \tag{6}$$

$$\dot{\theta} = \alpha H. \tag{7}$$

3. The chromatic aberrations Δx_1 and Δy_1 corresponding to the magnitude of the difference $\varepsilon = \dot{z}_{10} - \dot{z}_0$, are determined by (6) in terms of the auxiliary quantities Δp_1 and Δq_1, which are given by the expressions

$$\left.\begin{aligned} \Delta p_1 &= (s_1\dot{x}_0 + s_2\dot{y}_0 + s_3x_0)\,\varepsilon,\\ \Delta q_1 &= (-s_2\dot{x}_0 + s_1\dot{y}_0 + s_4x_0)\,\varepsilon, \end{aligned}\right\} \tag{8}$$

where

$$\left.\begin{aligned} s_1 &= \sigma_1 + r_1'\omega_1 + \frac{r_1}{\dot{z}_0},\\ s_2 &= -r_1\omega,\\ s_3 &= \sigma_2 + r_2'\omega_1 + \dot{\theta}_0 r_1\omega,\\ s_4 &= r_2\omega - \dot{\theta}_0(\sigma_1 + r_1'\omega_1) - \dot{\theta}_0\frac{r_1}{\dot{z}_0}, \end{aligned}\right\} \tag{9}$$

$$\left.\begin{aligned} \sigma_1 &= r_2\int_{t_0}^{t} h_1T'r_1^2dt - r_1\int_{t_0}^{t} h_1T'r_1r_2dt,\\ \sigma_2 &= r_2\int_{t_0}^{t} h_1T'r_1r_2dt - r_1\int_{t_0}^{t} h_1T'r_2^2dt, \end{aligned}\right\} \tag{10}$$

$$\omega_1 = -\frac{h_1(t)}{\dot{z}(t)}, \quad \omega = \alpha H\omega_1 + \alpha\int_{t_0}^{t} H'h_1dt, \tag{11}$$

$$T = T(z) = \alpha\Phi'' + \alpha^2H^2. \tag{12}$$

Here r_1 and r_2 are solutions of the equation

$$r'' + Tr = 0, \tag{13}$$

satisfying the initial conditions

$$\left\|\begin{matrix} r_2 & r_1\\ r_2' & r_1' \end{matrix}\right\|_{t=t_0} = \left\|\begin{matrix} 1 & 0\\ 0 & 1 \end{matrix}\right\|; \tag{14}$$

h_1 is the solution of the equation

$$h - 2\alpha\Phi'' h = 0, \tag{15}$$

satisfying the conditions

$$h_1(t_0) = 0, \quad \dot{h}(t_0) = 1; \tag{16}$$

x_0, $\dot{x}_0$, y_0, and θ_0 are respectively the initial values of x, $\dot{y}$, $\dot{x}$, and $\dot{\theta}$. To calculate Δp_1 and Δq_1 in the plane $z = z_u$ it is necessary to replace t everywhere with its value from the equation

$$z(t) = z_u, \tag{17}$$

where $z(t)$ is the solution of the third of Eqs. (2) subject to the initial conditions z_0 and $\dot{z}_0$.

4. The third order aberrations Δx_3 and Δy_3 are determined from Eqs. (6) by means of the auxiliary quantities Δp_3 and Δq_3:

$$\Delta p_3 = dp_3 + \Delta p_1, \quad \Delta q_3 = dq_3 + \Delta q_1, \tag{18}$$

where

$$\left.\begin{aligned} dp_3 &= (\dot{x}_0^2 + \dot{y}_0^2)(k_{11}\dot{x}_0 + k_{12}\dot{y}_0) + x_0[(\dot{x}_0^2 + \dot{y}_0^2)k_{13} + \dot{y}_0^2 k_{21} \\ &+ k_{22}\dot{x}_0\dot{y}_0] + x_0^2[(k_{23} + k_{31})\dot{x}_0 + k_{32}\dot{y}_0] + k_{33}x_0^3, \\ dq_3 &= (\dot{x}_0^2 + \dot{y}_0^2)(-k_{12}\dot{x}_0 + k_{11}\dot{y}_0) + x_0[-(\dot{x}_0^2 + \dot{y}_0^2)k_{14} \\ &- k_{22}\dot{y}_0^2 + k_{21}\dot{x}_0\dot{y}_0] + x_0^2[-(k_{24} + k_{32})\dot{x}_0 + k_{31}\dot{y}_0] - k_{34}x_0^3. \end{aligned}\right\} \tag{19}$$

The coefficients of aberration k_{ij} for a particular class of electrostatic systems are given by the expressions

$$\left.\begin{aligned} k_{11} &= s_{11} + d_1, \quad k_{13} = s_{13} + d_5, \\ k_{21} &= s_{21} + d_2, \quad k_{23} = s_{23} + d_6, \quad k_{i2} = k_{i4} = 0, \\ k_{31} &= s_{31} + d_3, \quad k_{33} = s_{33} + d_7, \end{aligned}\right\} \tag{20}$$

$$s_{ik} = r_1 \int_{t_0}^{t} \sigma_{ik} r_2 dt - r_2 \int_{t_0}^{t} \sigma_{ik} r_1 dt,$$

$$\left.\begin{aligned} \sigma_{11} &= (a_1 r_1 - c_1 T')\, r_1, \quad \sigma_{13} = a_3 r_1^2 - c_1 T' r_2, \\ \sigma_{21} &= (2a_1 r_2 - c_2 T')\, r_1, \quad \sigma_{23} = (2a_3 r_1 - c_2 T')\, r_2, \\ \sigma_{31} &= a_1 r_2^2 - c_3 T' r_1, \quad \sigma_{33} = (a_3 r_2 - c_3 T')\, r_2, \end{aligned}\right\}$$

$$a_1 = \frac{1}{8}\alpha\Phi^{IV} r_1, \quad a_3 = \frac{1}{8}\alpha\Phi^{IV} r_2,$$

$$C_1 = -\frac{1}{2}\alpha\Phi''' r_1^2, \quad C_2 = -\alpha\Phi''' r_1 r_2, \quad C_3 = -\frac{1}{2}\alpha\Phi''' r_2^2,$$

$$C_i = h_1 \int_{t_0}^{t} h_2 \bar{C}_i dt - h_2 \int_{t_0}^{t} h_1 \bar{C}_i dt,$$

$$d_i = -\frac{r_1}{i} C_i, \quad d_{i+4} = -\frac{r_2}{i} C_i \quad (i = 1, 2, 3),$$

where h_1 and h_2 are solutions of Eq. (15), which satisfy the initial conditions (14). The quantities Δp_1 and Δq_1 may be calculated from formulas (8) if ϵ is replaced by

$$\epsilon = z_0 - \sqrt{\dot{z}_0^2 + (\dot{x}_0^2 + \dot{y}_0^2)}$$

(for electrostatic systems it is necessary to take H equal to zero in these formulas). In the usual case of third order aberrations the slopes of the trajectories x_0' and y_0' are small, so that from (27) we have the approximation

$$\epsilon = -\frac{1}{2\dot{z}_0}(\dot{x}_0^2 + \dot{y}_0^2) = -\frac{1}{2}\dot{z}_0(x_0'^2 + y_0'^2).$$

REFERENCES

1. V. Glazer, "Fundamentals of Electron Optics." State Press for Technical and Theoretical Literature, Moscow, 1957.
2. O. I. Seman, Uchenye Zapiski Rostovsk. Univ. 68, (1958).

SHORT COMMUNICATIONS

DETERMINING THE REFRACTIVE INDICES OF CRYSTALS USING A JAMIN INTERFEROMETER

M. S. Soskin (pp. 768-769)

Received 8 March 1961

Measurement of the refractive indices of crystals
n a Jamin interferometer, as described in ref. 1, re-
res determination of the order of the interference
ges in the spectral interference pattern. When there
ntense absorption in the spectral region of interest,
interference fringes suffer a discontinuity. As a re-
of this, determination of their order becomes diffi-
and the refractive indices obtained are not reliable.
this reason it would be desirable to have a method of
asurement which does not require a determination of
order of the interference fringes. Such a method is
cribed below.

The refractive index $\mu(\lambda)$ for a wavelength λ is
en by the formula

$$\mu(\lambda) = 1 + \frac{\Delta y}{h} \cdot \frac{\lambda}{d}. \qquad (1)$$

re d is the thickness of the crystal, Δy is the dis-
cement of the interference fringes when the specimen
nserted into one of the interfering beams, and h is
fringe spacing measured in the same units as Δy. It
ows from Eq. (1) that a displacement of the interfer-
e pattern of one fringe ($\Delta y = h$) changes the value of
refractive index $\mu(\lambda)$ by λ/d. Hence, when the location
he zero order fringe is determined with an error of
s or minus a whole number of fringes, $\mu(\lambda)$ will be de-
mined to within an accuracy of a multiple of λ/d:

$$\mu(\lambda) = 1 + \frac{\Delta y^*}{h} \cdot \frac{\lambda}{d} \pm k\frac{\lambda}{d}. \qquad (2)$$

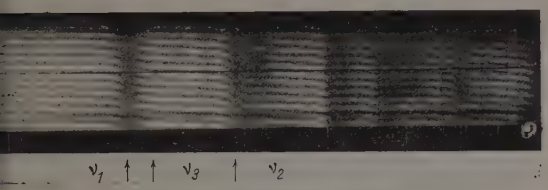

A spectrointerferogram of a single crystal of naphthalene at 20° K in light polarized along the monoclinic axis of the crystal. There are absorption bands at $\nu_1 = 31623$ cm^{-1} and $\nu_2 = 31960$ cm^{-1}, the point at which the refractive index of the crystal was measured is $\nu_3 = 31704.6$ cm^{-1}, on the short wavelength side of the absorption band ν_1.

where Δy^* is the displacement of the interference fringe assumed to be the zero-order fringe, and k is a whole number. We obtain a whole series of possible values for the refractive index, of which only one is correct. On investigating the dispersion of light in crystals of different thicknesses d_i, one obtains a set of progressions with differences λ/d_i. For a sufficient number of specimens, only one value of $\mu_{true}(\lambda)$ will be common to all series within the error of measurement. This is the correct value of the refractive index for a given wavelength λ. At the same time the true displacement of the interference pattern Δy_{true} is found and hence also the location of the zero order fringe.

We shall illustrate the above by determining the refractive index of a crystal of naphthalene at 20° K beyond the absorption band at $\nu = 31623$ cm^{-1}; viz., at $\nu = 31704.6$ cm^{-1} ($\lambda = 3153.2$ A) (see figure). The results of measurements of $\mu(\lambda)$ for crystals of six different thicknesses and the resulting value of the refractive index $\mu_{true}(\lambda)$ are shown in the Table.

$d_{cryst.}$ (μ)	$\lambda/d_{cryst.}$	Possible values of $\mu(\lambda)$			
0.675	0.47	1.30	1.77	2.24	2.71
0.82	0.38	1.46	1.84	2.22	2.60
0.90	0.35	1.60	1.95	2.30	2.65
0.96	0.33	1.595	1.925	2.255	2.585
1.28	0.245	1.785	2.03	2.275	2.52
2.27	0.14	1.96	2.10	2.24	2.38

$$\mu_{true}(\lambda) = 2.25 \pm 0.02.$$

It will be seen that $\mu_{true}(\lambda)$ was determined with a mean relative error of less than 1%, as is usual for measurements of crystals having very small thicknesses.[2] The above method can be applied in all cases in which formula (1) is valid; that is, when the influence of the spatial dispersion of the dielectric permeability is small.

REFERENCES

1. I. V. Obreimov and A. F. Prikhot'ko, Jubilee Publication to Commemorate the 70th Birthday of Academician A. F. Joffe. Academy of Science Press, Moscow-Leningrad, 1950.
2. M. S. Brodin, A. F. Prikhot'ko, and M. S. Soskin, Opt. i Spektr. **6**, 28 (1959), Optics and Spectroscopy **6**, 14 (1959).

DETERMINATION OF THE ELECTRON CONCENTRATION IN THE CONDUCTIVITY ZONE AT THE LIMIT OF TRANSITION OF THIN ALUMINUM FILMS IN THE VACUUM ULTRAVIOLET REGION

M. D. Borisov, I. I Demidenko, and V. G. Padalka (pp. 769-771)

Received 27 April 1961

INTRODUCTION

The optical properties of metals have been investigated mainly in the infrared, visible, and ultraviolet regions since a number of experimental and theoretical difficulties arise in investigations in the vacuum ultraviolet region.

Wood[1,2] has investigated the properties of alkali metals in the ultraviolet and vacuum ultraviolet regions. He showed that although alkali metal films are opaque in the visible, they are transparent in the ultraviolet region. The transmission cutoff shifts to shorter wavelengths with decrease in the atomic number of the metal: Cs—4400 A, Rb—3600 A, K—3150 A, Na—2100 A, Li—2050 A. At wavelengths shorter than the corresponding transmission cutoff, the alkali metals acquire the properties of a transparent medium. In particular, light reflected at Brewster's angle is linearly polarized, and it is possible to calculate the refractive index μ from the angle at which complete polarization occurs.

The optical properties of metals other than alkalis have been investigated very inadequately in the vacuum ultraviolet region. The reflectivity of many metals was investigated in ref. 3, while in ref. 4 the reflectivity, transmissivity, and photoelectric properties of many metals were studied in the 2000-400 A region.

In the present investigation, we measured the transmission cutoff of thin aluminum films in the vacuum ultraviolet region and used this figure to calculate the electron concentration in the conduction band.

THE RADIATION SOURCE

A high-voltage discharge in a quartz capillary placed between aluminum electrodes was used as the source of continuous radiation in the vacuum ultraviolet region.

The Figure shows a schematic diagram of the source. The discharge takes place between electrodes 1 and 8, which are enclosed in molybdenum glass tube 2. Electrode 1, 30 mm long, has an internal bore 4 mm in diameter, through which the emitted radiation passes on its way to the entrance slit of the vacuum diffraction spectrograph. Electrode 8 is enclosed in a quartz tube; a quartz capillary 3, 30 mm long and 2.5 mm in diameter is sealed to one end of the quartz tube. The other end of the quartz tube is insulated with rubber collar 6, insuring that the discharge passes only through the capillary 3. Tube 2 is connected through a Kovar seal to the adjusting mechanism. The mobile element is a tombac sylphon 5; the adjustment of the capillary along the axis of the discharge tube is achieved by means of three screws 4.

The radiation source was placed in front of the entrance slit of a DFS-6 vacuum spectrograph. The spectrograph chamber and the radiation source were evacuated independently of each other. The vacuum in the spectrograph chamber was ~ 1×10^{-4} mm Hg. The pressure in the radiation source (~ 1×10^{-2} mm Hg) was regulated a needle valve. Substitution of hydrogen or nitrogen fo air did not affect the nature or intensity of the emitted spectrum. The capillary was placed at a distance of 70 mm from the spectrograph entrance slit to ensure equate intensity.

The discharge through the quartz capillary was re alized by means of a 3.1 μf condenser charged to ~ 10 An enclosed air gap was used as the commutator. The current was measured with a Rogovski collar whose si nal was integrated and fed through a cathode repeater into an OK-17M oscillograph. The current in the first maximum was ~ 100 ka; the corresponding density of current through the capillary was ~ 20 ka/mm^2.

This source emitted a fairly intense continuum be tween 2000 and 200 A. The spectrograms also exhibite some 30 lines ascribed to aluminum, silicon, carbon, oxygen. Some of these lines were self-reversed. The capillary was able to sustain several thousand dischar without damage.

EXPERIMENTAL RESULTS

We investigated the vacuum ultraviolet transmiss of thin aluminum films prepared by vacuum evaporati The glass surface was first baked out in vacuum at ~350° C for two hours. After cooling to room tempera a thin layer of sodium chloride was deposited by evapo ration. Then the glass was heated to ~ 150° C for an h to ensure an adequate homogeneity of the salt film. Af the glass plate had cooled to room temperature, alumi num of better than 99.99% purity was evaporated onto plates from a tungsten evaporator in a vacuum of ~1×10^{-5} mm Hg.

The thicknesses of the aluminum films were dete mined interferometrically using lines of equal chroma order[5] and turned out to be ~1000 A. The plates were pletely opaque to visible light.

The plates were then placed in water in order to move the aluminum films. After 5-10 min., the sodiu chloride layer dissolved away and the aluminum films were separated from the glass plates. They were lifte from the water by means of special frames and dried; this completed the preparation.

The 10 × 20 mm frames holding the stretched alu num films were attached to the diaphragm of the DFS- spectrograph, between the diffraction grating and the The spectrograph slit-width was always 0.03 mm.

The spectra were photographed on type DN film h ing a sensitivity of 350 GOST units. The films were s sitized to vacuum ultraviolet by a short immersion in a saturated solution of sodium salicylate in ethyl alco and subsequent drying for 20-30 min.

The transmission spectra of the thin aluminum fi obtained in the 200-2000 A region indicate that the film opaque to wavelengths longer than ~ 800 A; at shorter

elengths, transmission was observed, in agreement h ref. 4. The optical density of the aluminum films is siderable and no interference was observed in the ctrograms.

It is possible to calculate the concentration of elecns in the conduction band of aluminum from the transsion cutoff.

The dielectric permeability

$$\varepsilon = 1 - \frac{\Omega^2}{\omega^2}, \qquad (1)$$

ere

$$\Omega = \left(\frac{4\pi Ne^2}{m^*}\right)^{1/2}$$

he plasma frequency, N is the electron concentration he conduction band, e and m* are the charge and effive mass of the electron, and ω is the cyclic frency of light.

According to ref. 6, when $\omega > \Omega$ the electron plasma he metal is capable of supporting an electromagnetic ve, and optical transmission takes place. If $\omega < \Omega$, n the metal is opaque. Thus the electron concentration n the conduction band is related to the transmission off λ_0:

$$N = \frac{\pi c^2 m^*}{e^2 \lambda_0^2}. \qquad (2)$$

Assuming that $m^* = m = 9.1 \times 10^{-28}$ gm and $\lambda_0 = 800$ A have $N = 1.74 \times 10^{23}$ cm^{-3}.

The concentration of atoms in the aluminum lattice is $N_a = 6.0 \times 10^{22}$ cm^{-3}. If we assign three electrons in the conduction band to each atom then the electron concentration would be $N = 1.80 \times 10^{23}$ cm^{-3} and the transmission cutoff $\lambda_0 = 785$ A, in agreement with our results.

It must be noted that the free electron concentration values obtained from optical measurements in the infrared region and specific conductivity measurements do not agree with our result. According to the measurements of Motulevich et al.[7] the electron concentration is $N = 7.4 \times 10^{22}$ cm^{-3}—less than half of our value.

REFERENCES

1. R. W. Wood, Phys. Rev. **44**, 353 (1933).
2. R. W. Wood and C. Lukens, Phys. Rev. **54**, 332 (1938).
3. G. Sabine, Phys. Rev. **55**, 1064 (1939).
4. W. S. Walker, O. P. Rustig, and G. L. Weissler, J. Opt. Am. **49**, 471 (1959).
5. I. N. Shklyarevskii, Opt. i Spektr. **5**, 617 (1958).
6. D. Bohm and D. Pines, Phys. Rev. **82**, 625 (1951); **92**, 609 (1953).
7. A. I. Golovashkin, G. P. Motulevich, and A. A. Shubin, Zhur. Eksptl. i Teoret. Fiz. **38**, 51 (1960); Soviet Phys.—JETP **11**, 38 (1960).

ON THE RELATIVE VIBRATIONAL TRANSITION PROBABILITIES IN THE $^2\Delta - {}^2\Delta$ BAND SYSTEM OF THE VO MOLECULE

F. S. Ortenberg (pp. 772-774)

Received 12 May 1961

The question of the band intensities in the well-wn yellow-green band system of the VO molecule has en discussed in several works[1-4] in recent years. In 1, the intensity distribution over the emission bands s studied in a furnace with photoelectric recording of spectrum. The relative band intensities were deterned by a choice of calculated contours which was apopriate to the observed band contours. In refs. 2 and 3, relative vibrational probabilities were determined in irect-current carbon arc. The intensity of the band d on a photographic plate was used as an indication of total band intensity. In connection with an investigan of the effect of the mass asymmetry of the atoms ming a diatomic molecule on the vibrational transition obabilities, as obtained in Hutchisson's harmonic apximation, calculations of the Franck-Condon factors $q_{v''}$ were carried out in these same articles[2,3] with the p of the old ($r_{e1} = 2.033$ A, $r_{e2} = 1.890$ A)[5] and new $_1 = 1.67$ A, $r_{e2} = 1.59$ A)[6] molecular constants respecely. On comparison of all these results, a significant ference is observed between the experimental and oretical probability values, and also between values ained by different methods.

In the present work, an attempt is made to clarify causes of the discrepancy, the Franck-Condon factors $_{v''}$ are recalculated in a better approximation, the dependence of the electronic transition moment R_e on the internuclear distance r is determined, and the relative vibrational probabilities $p_{v'v''}$ are found. The connection between these quantities and the band intensity $J_{v'v''}$ is given by the relations

$$J_{v'v''} = k \frac{N_{v'} p_{v'v''}}{\lambda_{v'v''}^4}, \qquad (1)$$

$$p_{v'v''} = R_e^2(\bar{r}_{v'v''}) \cdot q_{v'v''}. \qquad (2)$$

Here $\lambda_{v'v''}$ is the wavelength of the band, $\bar{r}_{v'v''}$ is the average internuclear distance for the given band, $N_{v'}$ is the population of the vibrational level v' of the upper electronic state, and k is a constant depending on the units and the geometry of the system. To obtain the Franck-Condon factors $q_{v'v''}$, we used, as potentials of the upper and lower electronic states, the best representation of the potentials for low quantum numbers: the Morse potential function. The calculation was carried out according to formulas (11) and (12) of ref. 7 on the "Arrow" high-speed electronic computer.* The subsequent treatment

*The details of the calculation of the quantities $q_{v'v''}$ for certain band systems of the molecules VO, TiO, ZrO, YO, and MgO, as carried out on the "Arrow," are being prepared for publication.

was analogous to that set forth in ref. 8. The values of $r_{v'v''}$ were determined by a graphical method. The change in the quantities $(p_{v'v''}/q_{v'v''})^{1/2}$ as a function of $\bar{r}_{v'v''}$ reflects the character of the variations of the electronic moment R_e with r. The analytical form of the function $R_e(r)$ was found by least-squares treatment of these results. The experimental values of the vibrational probabilities $p_{v'v''}$ used in the computations were borrowed from refs. 1 and 2. However, the results obtained on the basis of the data of ref. 2 led to such a pronounced scatter of the points that a determination of the function $R_e(r)$ was not possible. The vibrational probabilities measured by Phillips,[1] on the other hand, enable one to obtain (see Figure) the dependence of the electronic transition moment on the internuclear distance in the form

$$R_e(r) = 1 - 0.18\ r \qquad (3)$$

within the limits $1.53\ A < r < 1.68\ A$ for the variation of r. The superiority of the experimental results of ref. 1 over ref. 2 apparently indicates that carrying out such quantitative measurements in a furnace with photoelectric recording and with the intensities being determined on the basis of band profiles is preferable to making the analogous photographic measurements in an arc on the basis of peak band intensities.

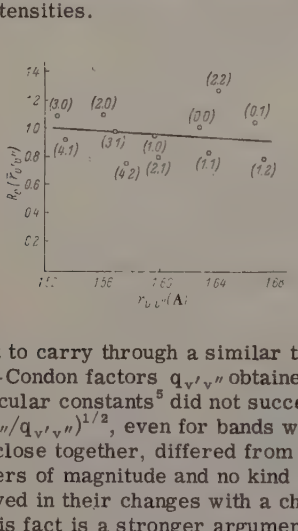

An attempt to carry through a similar treatment using the Franck-Condon factors $q_{v'v''}$ obtained on the basis of the old molecular constants[5] did not succeed, since the quantities $(p_{v'v''}/q_{v'v''})^{1/2}$, even for bands with $\bar{r}_{v'v''}$ values which are close together, differed from one another by several orders of magnitude and no kind of regularity could be observed in their changes with a change in r. We note that this fact is a stronger argument in favor of the correctness of the new rotational analysis[6] than the nonrigorous and ill-defined criterion adopted in refs. 2 and 3 for the correctness of one or another analysis on the basis of the number of close correspondences of the experimental probabilities with those computed by the use of one set or another of molecular constants.

In the calculations of band intensities according to Eq. (1), the intensity distribution at infinite temperature, $J_{\infty v'v''}$, when all the $N_{v'}$'s are equivalent, is of interest; this is characterized by the quantities $p_{v'v''}/\lambda^4_{v'v''}$, or $q_{v'v''}/\lambda^4_{v'v''}$ if the function $R_e(r)$ is not taken into account. These quantities, as well as the other characteristics of the band intensities, $q_{v'v''}$ and $p_{v'v''}$, are presented in the table on a scale in which the values corresponding to the (0,0) band are taken equal to 1.000 for convenience in comparison. The Franck-Condon factors $q_{v'v''}$ computed with the help of the harmonic-oscillator potential function and the Morse potential function are collected in the table. As can be seen from these results the harmonic approximation, even at low quantum numbers, can serve only for qualitative estimates of the Franck-Condon factors. In the next two colums are presented the experimental relative vibrational probabilities and the vibrational probabilities "smoothed" according to Eq. (2) for those bands whose $\bar{r}_{v'v''}$ values lie within the limits where the dependence (3) of the electronic transition moment on the internuclear distance is found. It is important that these more precise probabilities are free from the error in the experimental probabilities which arises on account of the different accuracy in the measurement of the intensities of weak and of strong bands. Comparison of the last two columns of the table shows that, even with such a weak dependence $R_e(r)$ as has been obtained by us for the $^2\Delta \rightarrow {}^2\Delta$ system of the V molecule, it is desirable to carry out the computation of the intensities taking account of this dependence.

v', v''	$\lambda_{v'v''}$ (A)	$\bar{r}_{v'v''}$ (A)	$q_{v'v''}$ Hutchisson's method[4]	$q_{v'v''}$ Using the Morse potential	$p_{v'v''}$ Experiment[1]	$p_{v'v''}$ "Smoothed"	$J_{\infty v'v''}$ Without allowing for $R_e(r)$	$J_{\infty v'v''}$ Allo for R
0,0	5736.7	1.630	1.00*	1.000*	1.000	1.000	1.000	1.
0,1	6087.1	1.669	1.00	1.103	1.205	1.081	0.870	0.
1,0	5469.2	1.597	1.17	1.091	1.048	1.110	1.321	1.
1,1	5786.3	1.636	0.01	0.015	0.01	0.015	0.015	0.
1,2	6139.6	1.674	0.35	0.408	0.249	0.399	0.311	0.
2,0	5228.3	1.564	0.59	0.621	0.724	0.642	0.900	0.
2,1	5547.8	1.602	0.59	0.391	0.256	0.397	0.457	0.
2,2	5887.7	1.642	0.32	0.380	0.605	0.378	0.354	0.
3,0	5010.6	1.530	—	0.243	0.287	0.256	0.418	0.
3,1	5275.7	1.570	0.85	0.706	0.674	0.728	0.987	1.
4,1	5056.8	1.537	—	0.507	0.452	0.532	0.840	0.
4,2	5324.2	1.577	—	0.369	0.215	0.379	0.498	0.

*The values of q_{00} computed by Hutchisson's method and by using the Morse potential amount to 0.34 and 0.329 respectively.

The author thanks P. G. Strelkov for his interest in the work, and V. B. Glasko for his help in the calculations on the computer.

REFERENCES

1. J. G. Phillips, Mem. Roy. Soc. Liège **14**, III, 452 (1954). (Russian translation in the collection "Nuclear Processes in Stars," p. 348, Foreign Literature Press, Moscow, 1957.
2. N. R. Tawde and P. V. Chandratreya, Indian J. Phys. **29**, 388 (1955).
3. N. R. Tawde and N. S. Murthy, Indian J. Phys. **31**, 3 (1957).
4. R. W. Nicholls, Ann. Geophys. **14**, 208 (1958).
5. P. C. Mahanti, Proc. Phys. Soc. **47**, 433 (1935).
6. A. Lagerquist and E. Selin, Naturwissenschaften **42**, 65 (1955).
7. P. A. Fraser and W. R. Jarmain, Proc. Phys. Soc. **A66**, 1145 (1953).
8. F. S. Ortenberg, Opt. i Spektr. **9**, 147 (1960), Optics and Spectroscopy **9**, 80 (1960).

A CALCULATIONAL FORMULA FOR THE INTENSITIES OF THE RAMAN SPECTRA OF POLYATOMIC MOLECULES

L. M. Sverdlov (pp. 774-775)

Received 30 May 1961

The semiclassical theory of Raman spectral intensi-s in the zeroth and first approximations of the valence-ical scheme was first proposed by Vol'kenshtein and rked out by him together with El'yashevich.[1] In the rk of Ferigle and Weber[2] a method is given for calcu-ing the tensor components of the polarizability deriva-es with respect to the normal coordinates $\partial a_{uv}/\partial Q_l$ in ch the condition that the linear and angular momenta st be equal to zero is automatically included:

$$\frac{\partial a_{uv}}{\partial Q_l} = \sum_{nk} \left[\frac{\partial \alpha_{n2}}{\partial q_n} + \cos(n1u)\cos(n1v)\left(\frac{\partial \alpha_{n1}}{\partial q_n} - \frac{\partial \alpha_{n2}}{\partial q_n} \right) \right] \frac{\partial q_n}{\partial q_k^{(x)}} L_{lk}$$

$$\sum_{nt} (\alpha_{n1} - \alpha_{n2})\, \sigma_n \left[\cos n1v)\, e_u + \cos(n1u)\, e_v - 2\cos(n1u)\cos(n1v)\, e_{n1} \right]$$

$$\times (\varepsilon_i S_i^t - \varepsilon_j S_j^t)(L^{-1})_t^l. \qquad (1)$$

An inadequacy of the formula for $\partial a_{uv}/\partial Q_l$ derived them consists of the fact that it is applicable only to lecules with bonds possessing axial symmetry. More-er this formula is deduced in the zeroth approximation the valence-optical scheme, i.e., the dependence of the nsor components of the bond polarizabilities on changes the length of adjacent bonds and on changes in the mag-udes of the bond angles is not considered.

A formula is given below for $\partial a_{uv}/\partial Q_l$ free from the dicated inadequacies:

$$\frac{\partial a_{uv}}{\partial Q_l} = \left(\frac{\partial a_{uv}}{\partial Q_l} \right)_I + \left(\frac{\partial a_{uv}}{\partial Q_l} \right)_{II} + \left(\frac{\partial a_{uv}}{\partial Q_l} \right)_{III}, \qquad (2)$$

$$\left(\frac{\partial a_{uv}}{\partial Q_l} \right)_I = \sum_{nrk} \left[\frac{\partial \alpha_{n2}}{\partial q_r}\, \delta_{uv} + \left(\frac{\partial \alpha_{n1}}{\partial q_r} - \frac{\partial \alpha_{n2}}{\partial q_r} \right) \cos(n1u)\cos(n1v) \right.$$

$$\left. + \left(\frac{\partial \alpha_{n3}}{\partial q_r} - \frac{\partial \alpha_{n2}}{\partial q_r} \right) \cos(n3u)\cos(n3v) \right] \frac{\partial q_r}{\partial q_k^{(x)}} L_{lk}, \qquad (2a)$$

$$\left(\frac{\partial a_{uv}}{\partial Q_l} \right)_{II} = \sum_{nsk} \left[\frac{\partial \alpha_{n2}}{\partial \gamma_s}\, \delta_{uv} + \left(\frac{\partial \alpha_{n1}}{\partial \gamma_s} - \frac{\partial \alpha_{n2}}{\partial \gamma_s} \right) \cos(n1u)\cos(n1v) \right.$$

$$\left. + \left(\frac{\partial \alpha_{n3}}{\partial \gamma_s} - \frac{\partial \alpha_{n2}}{\partial \gamma_s} \right) \cos(n3u)\cos(n3v) \right] \frac{\partial \gamma_s}{\partial \gamma_k^{(x)}} L_{lk}. \qquad (2b)$$

$$\left. \frac{\partial a_{uv}}{\partial Q_l} \right)_{III} = \sum_{nt} \left\{ (\alpha_{n1} - \alpha_{n2}) \left[\cos(n1v)\cos(n2u) + \cos(n1u)\cos(n2v) \right] e_{n2} \right.$$

$$\left. + (\alpha_{n1} - \alpha_{n3}) \left[\cos(n1v)\cos(n3u) + \cos(n1u)\cos(n3v) \right] e_{n3} \right\}$$

$$\times \sigma_n (\varepsilon_i S_i^t - \varepsilon_j S_j^t)(L^{-1})_t^l$$

$$\sum_{nt} \left\{ (\alpha_{n1} - \alpha_{n2}) \left[(\cos n1v)\, e_u + \cos(n1u)\, e_v - 2\cos(n1u)\cos(n1v)\, e_{n1} \right] \right.$$

$$\left. + (\alpha_{n2} - \alpha_{n3}) \left[\cos(n1v)\cos(n3u) + \cos(n1u)\cos(n3v) \right] e_{n3} \right\}$$

$$\sigma_n (\varepsilon_i S_i^t - \varepsilon_j S_j^t)(L^{-1})_t^l. \qquad (2c)$$

Here u,v = ξ, η, ζ; $\mathbf{e}_u$, $\mathbf{e}_v$ are unit vectors along these axes; α_{nm} are the tensor components of the polarizability of the nth bond, m = 1, 2, 3 are respectively the three principal directions of the bond polarizability; $\mathbf{e}_{nm}$ are unit vectors along these directions; cos (n m v) is the direction cosine of the mth direction of the nth bond with respect to the axis v; k, t are members of the independent symmetry coordinates; L_{lk} are normalizing coefficients of the form of the lth normal vibration; $\mathbf{S}_i^t$, $\mathbf{S}_j^t$ are vectors relating the tth symmetry coordinate with displacements of the atoms i, j where $e_n = e_{ji}$; $\sigma_n = 1/r_n$ where r_n is the equilibrium length of the nth bond; $\epsilon_i = 1/m_i$ where m_i is the mass of the ith atom.

Considering the orthonormal properties of the direction cosines it is easy to see that the trace of the third term in formula (2)

$$\sum_n \left(\frac{\partial a_{nm}}{\partial Q_l} \right)_{III}$$

equals zero.

In the case where

$$\frac{\partial a_{nm}}{\partial q_r} = \frac{\partial a_{nm}}{\partial \gamma_s} = 0$$

and $\alpha_{n2} = \alpha_{n3}$, formula (2) transforms into formula (1) of Ferigle and Weber.[2]

REFERENCES

1. M. V. Vol'kenshtein, Doklady Akad. Nauk SSSR 30, 784 (1941); M. V. Vol'kenshtein, Zhur. Eksptl. i Teoret. Fiz. 11, 642 (1941); M. A. El'yashevich and M. V. Vol'kenshtein, J. Phys. U.S.S.R. 9, 101 (1944); M. V. Vol'kenshtein and M. A. El'yashevich, Zhur. Eksptl. i Teoret. Fiz. 15, 124 (1945); M. V. Vol'kenshtein, M. A. El'yashevich, and B. I. Stepanov, "Molecular Vibrations," Vol. 2, State Press for Technical and Theoretical Literature, Moscow-Leningrad, 1949.
2. S. M. Ferigle and A. Weber, Can. J. Phys. 32, 799 (1954).

EFFECTIVE CROSS SECTIONS FOR EXCITATION OF CERTAIN SPECTRAL LINES OF SODIUM

L. M. Volkova (pp. 775-777)

Received 14 June 1961

1. In the papers of Yakhontova and Kliot-Dashinski,[1] St. John, Bronco, and Fowler,[2] and Phelps[3] it has been shown that, at pressures ranging from 10^{-4} to 10^{-1} mm of Hg, the intensity of the 5016 A line is enhanced by transfer of resonance radiation from the helium line 537 A to the 5016 A line. This enhancement leads to increased values of the effective cross sections for excitation of the 5016 A line when they are determined within the above pressure range. Thieme,[4] for instance, obtained a maximum cross section, $q_{max} = 82 \times 10^{-20}$ cm^2 at the pressure 1.7×10^{-2} mm of Hg, while Yakhontova,[5] taking the transfer of resonance radiation into consideration, obtained $q_{max} = 3.5 \times 10^{-20}$ cm^2.

Haft[6] determined values of the effective cross sections for excitation of the spectral lines of the sharp and diffuse series of sodium, using the helium line 5016 A as standard of comparison, and assuming for this line Thieme's value of q_{max}. Haft could only obtain correct results for the effective cross sections for excitation of the sodium lines if the size of the tubes and the helium pressures in them were the same in his and Thieme's experiments.

Haft, however, does not mention what pressures were used in his measurements; it thus remains doubtful whether the results of his measurements of the sodium line cross sections are valid. Since Haft's data were used repeatedly,[7] their verification appeared to be of some interest.

In this paper, effective cross sections for excitation of 10 sodium lines have been measured by comparison of the intensities of the sodium lines with the intensities of the corresponding sections of the continuous spectrum of a calibrated tungsten lamp; the latter intensities are compared with the intensities of helium lines which are not subject to the above-mentioned influence of the transfer of radiative energy.

2. For the measurements, tubes similar to those used in Haft's[6] work were employed. Metallic sodium was first purified by six times repeated distillation in a high vacuum, and then placed in an appendix at the bottom of the tube. During the experiment, the tube was continuously pumped out through a capillary located in the upper section of the tube. The tube was placed in an oven with two independent windings. The lower winding was used to maintain the pressure in the tube, the upper to maintain a 20° higher temperature so as to prevent precipitation of sodium on the glass and on the electrodes. The pressure of the sodium vapor in the appendix was determined according to the formula:[8]

$$p_1 = 10.71 - \frac{5480}{T_1}$$

where T_1 is the temperature of the appendix in °K, and p_1 is the pressure in μ of Hg. The value of the pressure in the collision domain is corrected by taking into consideration the change in temperature between the appendix and the tube; for this purpose, the formula $p_2 = p_1\sqrt{T_2/T_1}$ is used, where T_2 is the temperature of the collision domain.

The measurements were performed at temperature $T_1 \sim 455°$K and $T_2 \sim 475°$K; to determine these temperatu a mercury thermometer with 0.1°C gradations was use The pressure of the sodium vapor at these working tem peratures was $p_2 \simeq 5 \times 10^{-5}$ mm of Hg. The electron gun permitted the obtaining of an electron beam of almost h mogeneous energy (of 0.8 ev energy spread) and unchan ing shape; the energy of the electrons could be varied b tween 4 and 100 ev with an electron current at the receiver of 200 μa.

The radiation from the tube was projected by a con verging lens onto the slit of a spectrograph ISP-51. As source of the continuous spectrum an elongated, flat tun sten lamp of the type SI-8-200 was used, which was cali brated at the All Union Scientific Research Institute of Standards, Measures, and Measuring Apparatus. The temperature of the tungsten lamp, 2073° K, was maintai constant by an accumulator battery of large capacity. T spread in the intensities of the four lamps used in our e periments amounted to 11%. The light from the tungste lamp was attenuated by a neutral filter so as to produce a blackening lying within the linear section of the chara teristic curve of the film. Equal exposures were used i our work with the tube and with the tungsten lamp. A graded attenuator was calibrated for the whole measure range of wavelengths with the aid of a mercury light filter. The readings of all the electric measuring devices both in the power supply of the tube and in the power su ply of the tungsten lamp were verified in a laboratory fo the testing of apparatus. The spectra were photographe on films of the type RT-1 and RF-3. The exposure time was four hours.

The work with sodium presented some difficulties: the reaction of sodium with glass led to a darkening of t glass, and lowered the intensity of the light from the tub This led to an apparent reduction of the calculated effec tive cross sections of the sodium lines from measurem to measurement. The decreasing transparency compell us to use for the measurement of the effective cross se tions for excitation of sodium lines a method based on comparison with the intensities of helium lines.

3. The change in the intensity of the light from the tube resulting from the darkening of the glass was taken into consideration in the following way: we photographe on each film the spectrum of helium excited by an electron beam in the same tube at room temperature and 4×10^{-3} mm of Hg pressure, both before and after our work with sodium. Since the attenuation of light after each heating of the oven is different for different wavelengths (e.g., for 4388 A it amounts to 11%, and for 4713 to 19%), we have used as a standard of comparison heli lines of wavelengths near those of the sodium lines unde investigation. In the evaluation of the effective cross se tions for the sodium lines we have used the values for the effective cross sections of the helium lines deter-

ned by Yakhontova,[5] * and have also taken into consid-

e determined the values of the effective cross sections some helium lines by comparing their intensities with intensities of the radiation from the corresponding ctions of the continuous spectrum of the tungsten lamp 8-200. The results of our measurement agreed with khontova's results[5] within the limits of experimental curacy.

ation the changes in the sensitivity of the film and the spersion of the spectrograph. The results of the measements are given in the Table. In the first column the velengths of the measured sodium lines are listed; in e second column—the transitions giving rise to the

Na	Na transitions	He	q_{max}Na $\times 10^{16}$ cm^2	Na(Haft[6]) $\times 10^{16}$ cm^2
5684.21	$3^2P_{1/2} - 4^2D_{3/2}$	5875	40	1960
5689.78	$3^2P_{3/2} - 4^2D_{3/2}$	5875	82	
4666.11	$3^2P_{1/2} - 6^2D_{3/2}$	4713	12.9	121.7
4669.86	$3^2P_{3/2} - 6^2D_{3/2}$	4713	21.4	
4495.44	$3^2P_{1/2} - 7^2D_{3/2}$	4472	8.6	76.6
4498.91	$3^2P_{3/2} - 7^2D_{3/2}$	4472	14.3	
4391.20	$3^2P_{1/2} - 8^2D_{3/2}$	4388	3.6	28.1
4394.52	$3^2P_{3/2} - 8^2D_{3/2}$	4388	9.7	
4322.57	$3^2P_{1/2} - 9^2D_{3/2}$	4388	2.7	—
4325.78	$3^2P_{3/2} - 9^2D_{3/2}$	4388	4.6	—

emission of these sodium lines; in the third—the wavelengths of the helium lines whose effective cross sections are used in the calculation of the effective cross sections of the sodium lines; if the fourth—the values of the effective cross sections for excitation of sodium lines at the maximum of the excitation function; in the fifth—the results of Haft[6] for the unresolved sodium doublets.

The data in the table confirm our supposition that the results of Haft[6] are too high because of the incorrect choice of a standard helium line.

REFERENCES

1. V. E. Yakhontova and M. I. Kliot-Dashinskii, Opt. i Spektr. 7, 446 (1959), Optics and Spectroscopy 7, 290 (1959).
2. R. M. St. John, C. J. Bronco, and R. G. Fowler, J. Opt. Soc. Am. 50, 28 (1960).
3. A. V. Phelps, Phys. Rev. 110, 1362 (1958).
4. O. Thieme, Z. Physik 78, 412 (1932).
5. V. E. Yakhontova, Vestnik Leningrad Gosudarst. Univ. 10, No. 2, 27 (1959).
6. O. Haft, Z. Physik 82, 73 (1933).
7. V. M. Zakharova and Yu. M. Kagan, Vestnik Leningrad Gosudarst. Univ. No. 2, 125 (1955).
8. "Smithsonian Physical Tables," 1954.

SPECTROSCOPIC OBSERVATION OF THE ROTATION OF A POSITIVE COLUMN OF A DISCHARGE IN A MAGNETIC FIELD

V. M. Zakharova, Yu. M. Kagan, and V. I. Perel' (pp. 777-779)

Received 21 June 1961

It was demonstrated in refs. 1 to 3 that there is a lant'' of ion lines in a high-current, low-pressure arc aced in a magnetic field, due to the rotation of ions ound the arc axis. The "slant line effect" was also observed in atomic hydrogen. The authors attributed the served azimuthal movement of ions to the action of the agnetic field on the radial flow of ions.

The rotational magneto-mechanical effect in a low-essure plasma was also observed in ref. 4. However, quantitative results were obtained in that work.

It was found in the present work, by means of a spectographic method used previously in the work on determination of directional movements of ions in plasma,[5] at there is a rotation of the neutral gas in the positive scharge column in a magnetic field.

A discharge in argon was investigated in a tube of 5 cm diameter, 180 cm long, at argon pressures of om 0.5 to 2.5 mm Hg, a discharge current of 1.6 amp, magnetic fields of 250, 600, and 1000 oe. The middle rt of the positive column was enclosed within two coils th a total length of 60 cm and with a gap of 1.5 cm for tical observations. The method of observation consisted projecting the image of the tube edge upon a specially nstructed slit of the spectrograph which was crossed th a 30 cm thick Fabry-Perot etalon and permitted obning of two adjoining images of a given line taken with agnetic fields of opposite directions.

The obtained pictures showed a shift of the interference rings for the lines of argon atoms. The shift depended on the direction of the magnetic field. In order to prove that the shift of the rings was due to a rotation of the neutral gas in the magnetic field, the following control pictures were taken.

1. The change of the direction of the field did not cause a shift of the interference rings when the central part of the tube was photographed.

2. The shift had the opposite sign upon projecting the right and the left edges of the tube onto the spectrograph slit.

3. The shift changed sign (see figure) with a change of the direction of the magnetic field with respect to either half of the slit.

4. The shift did not change sign upon a change of the direction of the current through the tube, for a constant direction of the magnetic field.

The lines of ionized argon did not appear under our discharge conditions, and it was not possible to make observations simultaneously of atoms and ions.

The determination of the velocities of rotation of the atoms on the basis of the measured shifts of the lines at 4300 and 4044 A gave the following results.

1. The direction of rotation of the atoms coincides with that which positive ions should have under these conditions.

2. The velocity of rotation depends nonmonotonically on the field strength, having a maximum at 600 oe. The rotation velocity at the maximum for a pressure of 1 mm Hg is equal to 1.5×10^4 cm/sec. At 250 and 1000 oe the rotation velocity was $0.3\text{-}0.4 \times 10^4$ cm/sec.

3. At a pressure of p = 0.5 mm Hg no rotation could be observed. At p = 2.5 mm Hg the velocity of rotation is smaller than at 1 mm, and reaches a maximum of 1×10^4 cm/sec.

In addition to the shift, a broadening of the lines was observed with an increase of the magnetic field, the broadening being related to the Zeeman effect.

Probe measurements were also conducted by means of two cylindrical probes placed on the discharge axis.[6] The concentration and temperature of the electron gas remained the same with changes of the magnetic field and were equal, $n_e = 2 \times 10^{13}$ cm^{-3}, whereas the magnitude of the longitudinal field dropped somewhat with increase of the magnetic field, from 0.9 volt/cm without the field to 0.5 volt/cm in a field of 1000 oe.

Explanation of the observed rotation is difficult. The simplest assumption would be the following: charged particles moving toward the wall are deflected by the magnetic field, and the resulting rotation of the charged particles is transferred to the neutral gas by collisions. However, since the fluxes of both the electrons and ions toward the wall are the same, the amounts of momentum which they receive from the magnetic field in the azimuthal direction per unit volume and per unit time are equal in magnitude [$(eH/c)nv_r$, where nv_r is the flux density of the charged particles toward the wall] and are opposite in sign. In a stationary state both the ions and the electrons must completely transfer this momentum to the gas atoms. As a result, there is no change of momentum in the gas in the azimuthal direction due to charged particles. It could be assumed that such compensation will not be complete for the following reasons.

1. The free path of an electron λ_- is larger than that of an ion λ_+ by approximately an order of magnitude; therefore, in the layer of thickness $\sim\lambda_-$ adjoining the wall the atoms will receive the momentum from the ions, whereas the electrons will transfer their momentum to the wall.

2. A phenomenon considered by Simon[7] may take place, namely, electrons may leave the volume along the lines of force of the field.

3. Some lack of compensation may be explained by considering the inertia forces, as well as by taking into consideration the formation of electrons and ions in the volume.

Our estimates show that the lack of compensation due to the reasons mentioned should be small under our conditions. But even if there were a complete lack of compensation, it would produce an effect smaller than the observed one. Indeed, the equation of motion of a neutral gas can be written thus: $\eta \Delta v_\varphi = F$, where F is the force acting on a unit volume of gas, and $\eta = (1/3)NMv\lambda$ (η is the viscosity coefficient of the gas, N is the atomic concentration, M is the mass of an atom, v is the thermal velocity of the atom, and λ is the length of the gas-kinetic free path). If one assumes that only ions transfer momentum to the gas, then $F = (eH/c)nv_r$. In that case

$$v_\varphi \sim 3 \frac{eH}{Mc} \frac{n}{N} \frac{v_r}{v} \frac{R^2}{\lambda}$$

Substituting the values which correspond to the conditions of our experiments, we obtain $v_\varphi \sim 10^3 v_r/v$ for $H = 5 \times 10^2$ oe. It is difficult to imagine that v_r could be larger than v by an order of magnitude. The rotation of a plasma filament can be connected with the instability of the filament in the magnetic field.[8] However, the magnetic fields used by us are smaller than the critical values necessary for the appearance of these instabilities. Moreover, the measured dependence of the longitudinal gradient of the electric field on the magnetic field does not exhibit the anomalies which are characteristic in the occurence of instability.[9]

REFERENCES

1. J. R. McNally and M. R. Skidmore, J. Opt. Soc. Am. 47, 863 (1957).
2. J. R. McNally, J. Opt. Soc. Am. 49, 328 (1959).
3. J. M. Wilcox, Revs. Modern Phys. 31, 1045 (1959).
4. V. L. Granovskii and E. I. Urakasov, Zhur. Eksptl. i Teoret. Fiz. 38, 1354 (1960); Soviet Physics JETP 11, 974 (1960).
5. S. E. Frish and Yu. M. Kagan, Zhur. Eksptl. i Teoret. Fiz. 17, 577 (1947).
6. S. D. Vagner, Yu. M. Kagan, and V. I. Perel', Vestnik Leningrad. Univ. No. 22, 75 (1956).
7. A. Simon, Proc. 2nd Conf. Peaceful Uses Atomic Energy 32, 343 (1958).
8. B. Kadomzev and A. Nedospasov, J. Nuclear Energy C 1, 230 (1960).
9. T. Hoh and B. Lehnert, Phys. Fluids 3, No. 4 (1960).

A TELECENTRIC OPTICAL SYSTEM FOR ILLUMINATION OF THE ENTRANCE SLIT OF A SPECTRAL INSTRUMENT

V. R. Muratov (pp. 779-780)

Received 21 June 1961

A disadvantage of existing optical systems for illuating spectral instruments is that the amount of light passing into the entrance slit of the instrument nges if the luminous region of the light source moves. s introduces errors in spectrophotometric measure-ts and requires the experimenter to take certain sures to fix the location of the luminous volume. In y cases, especially in studying the radiation of a spark harge, stabilizing the position of the luminous region xceedingly difficult.

In the present paper we suggest a variation of the il-ination system for a spectral instrument, which en-es that the radiation flux entering the instrument re-ns constant for an arbitrary position of the light rce inside a certain volume of space.

The illumination system suggested (see the Figure) sists of a condenser O_1, at the focus of which is placed instrument entrance slits of height 2h. Thus the con-ser O_1 and the collimator objective O_3 form a tele-pic system. To avoid losses of light in the instrument, in order to fill its collimator objective completely, a ector lens O_2 is placed before the entrance slit, imag-the condenser O_1 on to the objective O_3. The light flux ching the instrument is proportional to the axial lumi-s intensity of the source and to the solid angle sub-led by the instrument entrance slit at the rear princi-point of the condenser O_1. (In the Figure the maximum e angle corresponding to this solid angle is designated 2α.) With a suitable choice of the ratio between the ht of the entrance slit 2h and the size 2H of the dis-sing element D, the entrance slit of the spectral instru-t will be the field stop of the whole optical system. this case it can be shown[1] that if the condenser O_1 an identical transmission coefficient over its whole

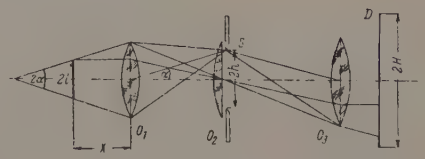

extent and if its field aberrations are sufficiently well corrected, the light flux entering the instrument will be constant for arbitrary displacement of the light source within the limits of a certain volume of space.[2] The boundary of this volume is a conical surface with apex angle 2α, based on the aperture of the condenser O_1. Since, in the overwhelming majority of cases, the height of the instrument entrance slit exceeds its width, the maximum distance X at which the light flux from the source 2l remains constant is determined by the height of the slit.

The proposed optical system can be used in measuring the spectral density of the emission from a light source when the luminous region of the source changes in position, and also in recording the radiation of extended light sources.

Finally, the author wishes to thank M. P. Vaniukov for proposing the problem, and D. S. Volosov and I. V. Peisakhson for a valuable discussion of the essentials of the problem.

REFERENCES

1. A. A. Gershun, Doklady Akad. Nauk SSSR 51, 8, 595 (1946).
2. B. V. Byvshev and Yu. M. Kutev, Svetotekhnika 6, 14 (1958).

INCANDESCENT LAMP WITH A RADIOMETRIC MODULATOR

M. L. Veingerov, A. A. Sivkov, and Byan' Nan Khua (pp. 780-781)

Received 26 January 1961

Earlier, we reported research which demonstrated the theoretical possibility of using a Crookes radiometer as a radiation chopper.[1] In the present paper we describe an incandescent lamp in which part of the radiation flux is interrupted by vanes placed inside the envelope of the lamp and rotated by radiometric forces. Figure 1 shows the design of the lamp. The heater is a straight, cylindrical spiral of tungsten wire. Above, and close to the heater, are the vanes, twelve in number, attached to a hub so as to form a 45° angle between the planes of the vanes and the axis of the hub. The vanes are made of aluminum foil 0.05 mm thick to which is cemented mica of thickness 0.03 mm. The axle of the vane-wheel is made of tempered steel and is terminated at each end in a cone with a point radius of about 10μ. The axle is secured by two ruby thrust bearings of spherical shape held in a metal bracket. The heater is placed parallel to the radius of the vane-wheel so that each vane, as it passes over the heater, completely interrupts the upward radiation flux in a fairly large solid angle. The lamp is filled with nitrogen at a pressure of several hundredths mm Hg.

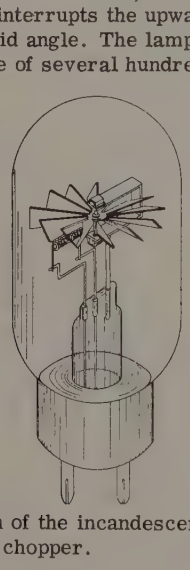

Fig. 1. Design of the incandescent lamp with a radiometric chopper.

Both sides of the vanes are coated with soot in our apparatus, while in the Crookes radiometer the vanes are coated with soot on one side only, the other sides being

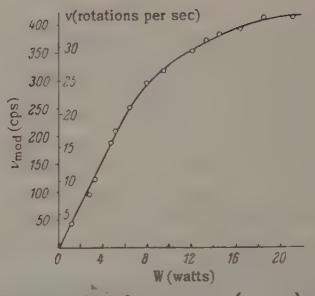

Fig. 2. Modulation frequency (ν_{mod}) and vane-wheel rotation speed (v) plotted against the lamp power.

silvered. The reason for this difference is that in the Crookes radiometer the radiation flux, propagating perpendicularly to the axis of rotation, illuminates simultaneously diametrically opposite vanes, and if these were heated identically the radiometric moments would balance out. In our case the vanes are turned through a 45° angle and are illuminated by flux propagating parallel to the axis of rotation, in consequence of which illumination of all the vanes simultaneously gives the maximum effect. This permits us to cover both sides of the vanes with soot, in order to increase the temperature gradient and thus the radiometric effect.

Figure 2 shows the way in which the rotation speed of the vanes varies with heater power when the lamp is used. The corresponding modulation frequencies were determined by observing Lissajous figures obtained with a photocell, a cathode ray oscilloscope, and an audio frequency generator. The curve shows saturation owing to drag on the vane rotation at the bearings and in the gas. Thus, when working at high rotation rates the latter depend little on the voltage applied to the lamp. The saturation effect can be obtained at lower speeds by increasing the gas pressure in the envelope.

REFERENCES

1. M. L. Veingerov, A. A. Sivkov, and A. P. Petrov, Opt. i Spektr. 6, 713 (1959), Optics and Spectroscopy 6, [illegible] (1959).

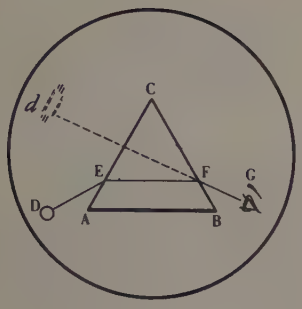

optics and spectroscopy

volume xi

OPTICAL SOCIETY OF AMERICA

USSR ACADEMY OF SCIENCES

AUTHOR LIST

VOLUME XI: JULY-DECEMBER

(Numbers in parentheses refer to pages in Russian original)

Adamov, V. S.,(419) 226
Agranovich, V. M., (369) 199, (498) 269
Agyrbichanu, I., (289) 155
Aleksanyan, V., (434) 236
Andrianov, A. S. (422) 228
Arvan, Kh. L., (74) 38
Ashchechlov, A., (295) 159

Babenko, N. S., (112) 58
Baikov, V. I., (41) 21
Bancie-Grillot, M., (84) 43
Barchukov, A. I., (129) 67
Belashov, Yu. G., (523) 282
Belashova, L. V., (523) 282
Belous, V. M., (431) 234
Belikova, G. S., (623) 335
Belyaev, L. M., (623) 335
Beridze, D. K., (282) 150
Bersuker, I. B., (319) 172
Bobovich, Ya. S., (131) 69, (161) 85, (342) 184
Bochkova, O. P., (697) 376
Boitsov, V. G., (691) 372
Bonch-Bruevich, A. M., (87) 45, (216) 114, (623) 335
Borisov, M. D., (769) 416
Borod'ko, Yu. G., (482) 261
Borgest, V. A., (558) 303
Brodskii, V. Ya., (266) 140
Brodin, M. S., (742) 400
Bubnov, N. N., (78) 40
Bulanin, M. O., (551) 298
Bundel, A. A., (656) 352
Bursian, E. V., (131) 69

Chaika, M. P., (695) 375
Charnaya, F. A., (549) 296
Chernevskaya, E. G., (513) 277
Chetkin, M. V., (274) 145
Chizhikova, Z. A., (271) 143

Dashchenko, A. I., (679) 365
Demidenko, I., (769) 416
Denisov, G. S., (428) 232
Dianov-Klokov, V., (439) 239
Dokunikhin, N. S., (134) 71
Dovgii, Ya. O., (742) 400
Drozd, L., (648) 348
Dubinin, V. G., (518) 279
Dunaisky, L., (547) 295

Eringis, K. K., (297) 161
Ermolaev, V. L., (492) 266

Faizullov, F. S., (571) 310
Feofilov, P., (439) 239
Fok, M. V., (93) 48, (98) 50
Fok, N. V., (78) 40
Fridberg, P. Sh.,(297) 161
Fridkin, V. M., (105) 54
Frish, S. E., (697) 376

Gabrichidze, Z. A., (359) 193
Galanin, M. D., (271) 143
Gerasimov, F. M., (259) 136
Georgobiani, A. N., (93) 48, (426) 231
Giurgea, M., (424) 229
Gol'dfarb, B. M., (445) 243
Gorban, A. N., (273) 144
Gorban, N. Ya., (750) 404
Gotlib, Yu. Ya., (691) 372
Gribkov, V. I., (629) 338
Gribov, L. A., (146) 77
Grillot, E., (84) 43
Grinev, V. S., (486) 263
Gross, E. F., (84) 43
Guretskaya, Z. I., (656) 352
Gurevich, E. L., (67) 34
Gusak, G. M., (555) 301
Gutman, A. M., (277) 147

Il'ina, E. V., (445) 243
Iogansen, L. V., (542) 292
Ivanov, A. P., (754) 407
Ivanova, T. V., (598) 322
Izmailov, N. A., (67) 34

Kagan, Yu. M., (308) 166, (777) 421
Kagen, G. I., (730) 394
Kantardzhyan, L. T., (419) 226
Kard, P. G., (237) 125
Kariss, Ya. E., (87) 45
Kasyankov, P. P., (765) 413
Kats, M. L., (422) 228
Khalimonova, I. N., (185) 97, (332) 179
Khalupovskii, M. E., (617) 332
Khan-Magometova, I. D., (629) 338
Khomazyuk, V. G., (417) 224
Khrustalev, O. A., (441) 241
Kilin, S. F., (390) 209
Kirei, G. G., (55) 28, (196) 103
Kiyanskaya, L. A., (613) 330
Kondilenko, I. I., (169) 89, (262) 137
Koloshnikov, V. G., (556) 302
Konobeev, Yu. V., (369) 199, (498) 269, (504) 272
Koptev, G. S., (724) 391
Koritskii, Ya. P., (308) 166
Korol'kov, V. S., (137) 73
Koronkevich, V. P., (112) 58
Korotkov, P. A., (169) 89
Kotlyar, I. P., (175) 92
Kovalev, B. P., (623) 335
Kovyrzina, K. A., (390) 209
Kozlov, Yu. I., (606) 327
Krinchik, G. S., (274) 145
Kristesku, G. D., (424) 229
Krushinskii, L. L., (24) 12, (151) 80
Kukurezyanu, I., (289) 155
Kukushkin, L. S., (385) 206

Lavrov, A. V., (128) 66
Lazarev, A. I., (439) 239
Lazarev, A. N., (584) 316
Lazeeva, G. S., (636) 341
Lenkova, G. A., (112) 58
Leontovskii, M. P., (471) 256
Levchuk, M. S., (118) 61
Levikov, S. I., (689) 371
Levshin, L. V., (278) 148
Levshin, V. L., (362) 195, (648) 348
Lisitsa, M. P., (55) 28, (185) 97, (196) 103, (332) 179
Litvinova, P. S., (264) 139
Lokhmatov, A. I., (112) 58
Lonskaya, I. S., (278) 148
Lushchik, Ch. B., (560) 304

Makhanek, A. G., (12) 6
Mal'tsev, A. A., (724) 391
Mandel'shtam, S. L., (556) 302
Marasanov, Yu. P., (556) 302
Marchak, I. S., (118) 61
Mazing, M. A., (556) 302
Melankholin, N. M., (286) 153
Meleshina, A. M., (706) 381
Miloslavskii, V. K., (403) 216, (536) 289
Milevskaya, I. S., (349) 188
Minakova, S. V., (353) 190
Molchanov, V. A., (87) 45
Mukhitdinova, I. A., (312) 169
Muratov, V. P., (779) 423
Muratov, V. R., (312) 169

Nagornaya, L. L., (385) 206
Nan-khua, Byan, (780) 423
Nazimova, N. A., (273) 144
Nikitin, E. E., (452) 246
Nikitin, V. A., (293) 158, (294) 158
Noskova, M. N., (656) 352
Novikova, G. E., (353) 190
Nurmukuhametov, P. N., (134) 71, (606) 327

Odintsov, V. I., (553) 299
Onichek, I. L., (555) 301
Orlova, N. D., (551) 298
Ortenberg, F. S , (772) 417
Osiko, V. V., (642) 345
Ostrovskii, Yu. I., (3) 1, (565) 30
Ovander, L. N., (129) 68

alka, V. G., (527) 285, (769) 416
kratov, N. A., (681) 366
sakhson, I. V., (125) 65
kin, N. P., (3) 1, (565) 307
'kovskii, V. V., (410) 219
egudov, G. V., (735) 397
el, V. I., (777) 421
rov, A. A., (588) 318, (594) 320
rov, Yu. N., (129) 67
ulevskii, G. V., (434) 236
ai, K., (51) 26
esku, I., (289) 155
ov, E. M., (730) 394
ova, E. A., (203) 107
ova, E. G., (134) 71
shivalko, A. P., (248) 131, (555) 301
kof'ev, V. K., (291) 156
votorov, B. N., (123) 63
enichnov, E. A., (16) 8
hkov, V. A., (606) 327

otkina, L. P., (264) 139
nazanov, P. E., (264) 139
yuk, A. I., (536) 289
birin, B. S., (84) 43
kin, V. F., (268) 141
sudova, G. N., (259) 136
, O. I., (486) 263
umovskaya, L. P., (697) 376
asheva, T. N., (284) 152
sikhin, V. S., (415) 223
man, I. M., (390) 209
s, L. G., (133) 72

, A. O., (667) 358, (672) 361, (759) 409
nsonov, G. V., (410) 219
hianandan, K., (46) 24
chenko, O. Ya., (223) 118

Selivenenko, A. S., (694) 374
Shainkevich, I. A., (750) 404
Shakhparonov, M. I., (282) 150
Shelimov, B. N., (78) 40
Sherudilo, A. I., (266) 140
Shifrin, K. S., (268) 141
Shigorin, D. N., (606) 327
Shishatskaya, L. P., (689) 371
Shklyarevskii, I. N., (403) 216, (527) 285, (661) 355
Shorygin, P. P., (24) 12, (151) 80
Shugurov, V. K., (297) 161
Shvarts, K. K., (560) 304
Sidorov, A. N., (175) 92, (325) 175
Sil'd, O. I., (141) 75
Sivkov, A. A., (780) 423
Smirnov, L. V., (457) 249
Snegirev, B. N., (577) 313
Sobolev, N. N., (571) 310
Sokolov, N. D., (16) 8
Sokolov, V. A., (273) 144
Sokolovskaya, A. I., (478) 259
Soskin, M. S., (768) 415
Sotskii, B. A., (229) 121
Standnichuk, M. D., (588) 318
Stanevich, A. E., (61) 31
Stekhanov, A. I., (203) 107, (359) 193
Strizhevskii, V. L., (169) 89, (262) 137
Suprunenko, A. I., (457) 249
Sverdlov, L. M., (774) 419
Sveshnikov, B. Ya., (598) 322, (613) 330
Svidzinsky, K. K., (713) 385
Svishchev, G. M., (486) 263
Syrkin, Ya. K., (482) 261

Tarasov, K. I., (683) 368
Tatevskii, V. M., (724) 391
Tenisheva, T. F., (439) 239, (584) 316
Terenin, A. N., (325) 175
Trapeznikova, O. N., (353) 190
Tsikora, I. L., (415) 223
Tsyashchenko, Yu. P., (192) 101
Turkin, Yu. I., (695) 375

Vainshtein, L. A., (301) 163
Vakulenko, O. V., (196) 103
Valiev, K. A., (465) 253
Vanyukov, M. P., (312) 169
Varshavskii, Yu. A., (686) 369
Vasicek, A., (242) 128
Vasiliev, V. I., (118) 61
Vasilevskii, K. P., (41) 21, (207) 109
Vasiliu, V., (289) 155
Veingerov, M. L., (780) 423
Venkatesvarlu, K., (46) 24, (51) 26
Vlasenko, N. A., (403) 216
Voevodskii, V. V., (78) 40
Vol'kenshtein, M. V., (349) 188
Volkova, L. M., (775) 420
Vul'fson, K. S., (549) 296

Yakovleva, T. V., (588) 318, (594) 320
Yaroslavskii, N. G., (61) 31
Yarovaya, R. G., (661) 355

Zaidel, A. N., (636) 341
Zaitseva, N. E., (74) 38
Zakharova, V. M., (777) 421
Zapesochnyi, I. P., (679) 365
Zastavenko, L. G., (441) 241
Zelikin, Ya. M., (397) 212
Zhevandrov, N. D., (629) 338
Zhukovskii, A. P., (397) 212
Zubov, V. A., (275) 146

CONTENTS

VOLUME XI: JULY-DECEMBER

(Numbers in parenthesis refer to pages in Russian original)

No. 1—July

Yu. I. Ostrovskii and N. P. Penkin, The Measurement of the Absolute Values of Oscillator Strengths in Atomic Spectra. I. Sodium—(3) 1

A. G. Makhanek, The Effect of Vibration on Hyperfine Structure Constants—(12) 6

E. A. Pshenichnov and N. D. Sokolov, Quantum Effects in a Double Potential Well and Spectroscopy of the Hydrogen Bond—(16) 8

L. L. Krushinskii and P. P. Shorygin, The Theory of Line Intensities in the Spectrum of Scattered Light. I. The Quantum Model (Condon Approximation)—(24) 12

L. M. Sverdlov, Calculation of the Electro-Optical Parameters and Integrated Infrared Band Intensities of the Acetylene and Hydrocyanic Acid Molecules and Their Deuterium Substitution Products—(35) 18

K. P. Vasilevskii and V. I. Baikov, The Infrared Spectrum of Lithium Vapor—(41) 21

K. Venkatesvarlu and K. Sathianandan, Molecular Vibrations of Sulfur Compounds: SF_5Cl—(46) 24

K. Venkatesvarlu and K. Pillai, Molecular Vibrations of Sulfur Compounds: SF_4—(51) 26

G. G. Kirei and M. P. Lisitsa, Infrared Absorption Spectrum and Symmetry of the Hexaethyldisiloxane Molecule—(55) 28

A. E. Stanevich and N. G. Yaroslavskii, Transmission of Organic Solvents in the Far Infrared Region of the Spectrum—(61) 31

N. A. Izmailov and E. L. Gurevich, Study of the Equilibria in Nonaqueous Solutions of Electrolytes by Means of Absorption Spectra. III. Picric Acid and Sodium Picrate in Dioxane-Water and Benzene-Alcohol Mixtures—(67) 34

Kh. L. Arvan and N. E. Zaitseva, Spectral Investigation of the Aggregation of Dyes in Solvents of Low Polarity—(74) 38

N. N. Bubnov, V. V. Voevodskii, N. V. Fock, and B. N. Shelimov, Study of Electronic Phototransfer Reactions in the Solid Phase by EPR—(78) 40

E. F. Gross, M. Bancie-Grillot, E. Grillot, and B. S. Rasbirin, Effect of Mechanical Treatment on the Absorption Spectrum of Cadmium Sulphide Crystals at Low Temperature—(84) 43

A. M. Bonch-Bruevich, Ya. E. Kariss, and V. A. Molchanov, Microscopic Studies of Electroluminescence in ZnS-Cu,Al Single Crystals—(87) 45

A. N. Georgobiani and M. V. Fock, The Phase of Electroluminescence Light Pulses as a Function of Excitation Voltage Parameters—(93) 48

M. V. Fok, The Relation Between the Blue and Green Bands in the Electroluminescence of ZnS:Cu Phosphors—(98) 50

V. M. Fridkin, On the Luminescence of Charged Polycrystalline ZnS Layers Under the Action of DC Electric Fields—(105) 54

V. P. Koronkevich, G. A. Lenkova, N. S. Babenko, and A. I. Lokhmatov, Photoelectric Method of Recording an Achromatic Interference Fringe—(112) 58

V. I. Vasiliev, M. S. Levchuk, and I. S. Marchak, Duration of the Flash of Tubular Flash Lamps—(118) 61

B. N. Provotorov, On Nuclear Magnetic Resonance in Solids—(123) 63

I. V. Peisakhson, Effect of Spectrographic Camera Ob tive Distortion on Spectral Line Curvature—(125)

A. V. Lavrov, ZnS:Ag Phosphor With Boron as a Coac vator—(128) 66

A. I. Barchukov and Yu. N. Petrov, Dipole Moment of CH_3GeH_3 Molecule—(129) 67

L. N. Ovander, The Temperature Dependence of Infra Absorption Lines—(129) 68

Ya. S. Bobovich and E. V. Bursian, The Raman Spectr of Barium Titanate—(131) 69

Letters to the Editor—(133) 72

No. 2—August

V. S. Korol'kov, Calculation of $\overline{r^{-3}}(n, l)$ From the Fine Structure of Spectra—(137) 73

O. I. Sil'd, Recurrence Formulas in the Calculations o Moments of Distributions of Transition Probabilit —(141) 75

L. A. Gribov, Theory of Infrared Absorption Band Inte ties of Complex Molecules Containing Several Ide cal Groups—(146) 77

L. L. Krushinskii and P. P. Shorygin, On the Theory o Line Intensities in Raman Spectra. II. The Quantu Model (Taking Account of Anharmonicity and Devi tion from the Condon Approximation)—(151) 80

Ya. S. Bobovich, The Intensity of Raman Bands and the Character of the Chemical Bond—(161) 85

I. I. Kondilenko, P. A. Korotkov, and V. L. Strizhevski An Investigation of the Raman Indicatrix—(169) 89

A. N. Sidorov and I. P. Kotlyar, Infrared Spectra of Phthalocyanines. I. The Effect of Crystalline Stru ture and of the Central Metallic Atom on the Phth cyanine Molecule in the Solid State—(175) 92

M. P. Lisitsa and I. N. Khalimonova, Frequencies and tensities of the Absorption Bands of Monosubstitu Benzenes in the Region of the Stretching Vibratio $C-H_{arom.}$ Bonds—(185) 97

Yu. P. Tsyashchenko, Shape of the Vibrational Absorp Band Contours of Liquid Chloroform and Bromo- form—(192) 101

O. V. Vakulenko, G. G. Kirei, and M. P. Lisitsa, The fect of Temperature on the Infrared Spectra of Or gano-Silicon Compounds. I. Crystalline Hexaethyl siloxane—(196) 103

A. I. Stekhanov and E. A. Popova, Evidence for Hydro Bonding in the Infrared Spectra of Crystalline Lit Hydroxides—(203) 107

K. P. Vasilevskii, The Effect of Foreign Gases on the sorption of Infrared Radiation by Water Vapor—(109

A. M. Bonch-Bruevich, Certain Regularities in the El troluminescence of ZnS:Cu:Al Phosphors with Hig Copper Content—(216) 114

O. Ya. Savchenko, The Action of an Alternating Magne Field on the Propagation of Circularly Polarized diation in Matter—(223) 118

B. A. Sotskii, A Molecular Theory of Refraction of Li in Crystals—(229) 121

. Kard, Optical Principle of Reversibility and Its Application in the Theory of Thin-Layer Coatings—(237) 125
ašíček, Theory of Light Reflection From a Thin Absorbing Film Deposited on a Metal—(242) 128
. Prishivalko, Accuracy of Determining Optical Constants of Absorbing Substances by Reflection in an Arrangement Using a Polarizer and Analyzer—(248) 131
. Rassudova and F. M. Gerasimov, Precision Diffraction Gratings for Metrologic Purposes—(259) 136
Kondilenko and V. L. Strizhevskii, The Frequency Dependence of Raman Line Intensities—(262) 137
. Litvinova, L. P. Rabotkina, and P. E. Ramazanov, Investigation of the Initial Stages in the Onset of Electroluminescence of a ZnS:Cu:Al Phosphor—(264) 139
. Sherudilo and V. Ya. Brodskii, Microphotometric Determination of the Quantity of Absorbing Material in Inhomogeneous Objects—(266) 140
. Shifrin and V. F. Raskin, Spectral Transmission and the Inverse Problem of Scattering Theory—(268) 141
O. Galanin and Z. A. Chizhikova, Duration of the Photo- and Radioluminescence of Anthracene and Naphthalene Crystals—(271) 143
. Sokolov, A. N. Gorban, and N. A. Nazimova, The "Selectivity" of the Thermal Emission of CaO and MgO—(273) 144
. Krinchik and M. V. Chetkin, An Infrared Electronic Transition in the Er^{3+} Ion—(274) 145
. Zubov, On the Differentiation of Spectra—(275) 146
M. Gutman, Vector Coupling in X-Ray Spectra—(277) 147
V. Levshin and I. S. Lonskaya, Dependence of the Association of Rhodamines on the Structure of Their Molecules and the Nature of the Solvent—(278) 148
K. Beridze and M. I. Shakhparonov, The Krishnan Effect—(282) 150
N. Rekasheva, The Free Electron Model Applied to the Thiophene Molecule—(284) 152
M. Melankholin, New Data on the Absorption Spectra of Thiazine Dye Crystals—(286) 153
gyrbichanu, I. Kukurezyanu, V. Vasiliu, and I. Popesku, The Effect of Nitrogen on Excited Mercury Atoms—(289) 155

OK REVIEWS

K. Prokof'ev, Emission Analysis of Atomic Materials. By A. N. Zaidel', N. I. Kaliteevskii, L. V. Lipis, and M. P. Chaika—(291) 156
A. Nitkin, Infrared Methods, Principles, and Applications. By G. K. T. Conn and D. G. Avery—(293) 158
A. Nitkin, Infrared Radiation. By H. L. Hackforth—(294) 158
Ashchechlov, Optical Image Assessment Using Frequency Response Techniques; Tables of Optical Frequency Response for the Cases of Spherical Aberration and Coma—(295) 159

3—September

K. Eringis, P. Sh. Fridberg, and V. K. Shugurov, The Extended Fok Method in a Multiconfiguration Approximation for the Helium Atom—(297) 161
A. Vainshtein, The Excitation of Atoms and Ions by Electron Impact. I. Calculation Ignoring Exchange—(301) 163
Yu. M. Kagan and Ya. P. Koritskii, A Direct Method of Measuring the Mean Lifetime of Excited Ionic Levels—(308) 166
M. P. Vanyukov, V. R. Muratov, and I. A. Mukhitdinova, Time Resolved Emission Spectra of a Spark Discharge in Inert Gases in the Region 5000-10,000 A—(312) 169
I. B. Bersuker, Restricted Motions in Transition Metal Complexes—(319) 172
A. N. Sidorov and A. N. Terenin, Infrared Spectra of Phthalocyanines. II. Interaction of Sublimed Layers of Phthalocyanines With Gaseous CH_3COOH, HCl, and HBr—(325) 175
M. P. Lisitsa and I. N. Khalimonova, Effect of Temperature on the Absorption of Monosubstituted Benzenes in the Region of the C–H Stretching Vibrations—(332) 179
Ya. S. Bobovich, Second-Order Raman Spectra in Some Liquids—(342) 184
I. S. Milevskaya and M. V. Vol'kenshtein, Determination of Macroradical Conformations by Their Electron Paramagnetic Resonance (EPR) Spectra—(349) 188
O. N. Trapeznikova, G. E. Novikova, and S. V. Minakova, Light Scattering in Crystalline Polymers. II. Investigation of the Temperature Dependence of the Index of Refraction of the Crystalline and Amorphous Phases of Polychloroprene and the Determination of the Degree of Crystallization—(353) 190
A. I. Stekhanov and Z. A. Gabrichidze, On the Influence of Crystal Structure on the Vibrational Spectrum of the Hydrogen Bond—(359) 193
V. L. Levshin, Notes on the Concept of "Yield," "Mean Lifetime," and "Decay Law" and Their Use in Luminescence—(362) 195
V. M. Agranovich and Yu. B. Konobeev, Reabsorption in Crystals of a Finite Thickness. II.—(369) 199
L. S. Kukushkin and L. L. Nagornaya, Some Concentration Effects in Plastic Scintillators—(385) 206
S. F. Kilin, K. A. Kovyrzina, and I. M. Rozman, Luminescence of p-Terphenyl in a Mixture of Toluene and Carbon Tetrachloride—(390) 209
Ya. M. Zelikin and A. P. Zhukovskii, The Yellow Luminescence of Zinc Oxide—(397) 212
N. A. Vlasenko, V. K. Miloslavskii, and I. N. Shklyarevskii, Interference of Luminescent Emission From an Evaporated Phosphor—(403) 216
G. V. Samsonov and V. V. Pen'kovskii, Study of the Emissive Power of Certain High-Melting Compounds in the Infrared Region—(410) 219
V. S. Rossikhin and I. L. Tsikora, On the Mechanism of the Weakening of the CN Bands (Violet Systems) in an Arc—(415) 223
V. G. Khomazyuk, Single Slit, Three-Beam Interferometry—(417) 224
V. S. Adamov and L. T. Kantardzhyan, Luminescence of Ionic Forms of Uranin in Liquid and Solid Solutions—(419) 226
A. S. Andrianov and M. L. Kats, Electro-X-Ray Luminescence of KBr Crystals—(422) 228
G. D. Cristescu and M. Giurgea, Results of Spectrochemical Analysis With a Combination Electric Discharge as a Light Source—(424) 229
A. N. Georgobiani, On the Electroluminescence Excitation Process in Zinc Sulfide—(426) 231
G. S. Denisov, Hydrogen Bonding of Ketones with Chloroform as Revealed in the Band of the Carbonyl Group Stretching Vibration—(428) 232

V. M. Belous, The Redistribution of Electrons Among the Localized Levels of Silver Halide Phosphors and the Stimulating Action of the Exciting Light—(431) 234

BOOK REVIEW

G. V. Pigulevskii and V. Aleksanyan. Die Terpene. Sammlung der Spektren und physikalischen Konstanten. Teil I. Sesquiterpene. By J. Pliva, M. Horak, V. Herout, and F. Šorm—(434) 236

The 15th Rozhdestvenskii Lecture—(436) 237

The 69th Birthday of Boris Yakovlevich Sveshnikov—(437) 238

S. E. Frish, Honored Worker in Science and Technology of the RSFSR—(438) 238

V. Dianov-Klokov, On the Article—The Absorption Spectrum of Liquid and Solid Oxygen Under Pressure (12,600-3000 A), by V. Dianov-Klokov—(439) 239

P. Feofilov, Erratum—(439) 239

A. I. Lazarev and T. F. Tenisheva, Errata—(439) 239

No. 4—October

L. G. Zastavenko and O. A. Khrustalev, Determination of the Lifetime of Optical Transitions by Using the Interference of Quantum Levels—(441) 241

B. M. Gol'dfarb and E. V. Il'ina, Determination of the Mean Time Spent by the Atoms, and of the Diffusion Coefficient in the Plasma of the Arc Discharge—(445) 243

E. E. Nikitin, Nonadiabatic Transitions Near the Turning Point in Atomic Collisions—(452) 246

L. V. Smirnov and A. I. Suprunenko, The Electronic Spectra of Simple Benzene Derivatives as a Function of pH. II. The Absorption Spectra of Nitrobenzene and Nitrophenol—(457) 249

K. A. Valiev, On the Theory of Line Widths in Vibrational and Raman Spectra of Molecules in Dipole Liquids—(465) 253

M. P. Leontovskii, Calculation of the Frequencies and Intensities of the Infrared Spectrum of Propenyl Bromide—(471) 256

A. I. Sokolovskaya, Raman Line Intensities in the Liquid and Gas Phase—(478) 259

Yu. G. Borod'ko and Ya. K. Syrkin, Resonance Splitting of the Carbonyl Band in the Infrared Spectrum of Sydnones—(482) 261

V. S. Grinev, O. I. Rau, and G. M. Svishchev, On the Automatic Treatment of Absorption Spectra of Additive Multicomponent Mixtures—(486) 263

V. L. Ermolaev, The Luminescence of Simple Derivatives of Benzene. I. The Aromatic Amines—(492) 266

V. M. Agranovich and Yu. V. Konobeev, The Influence of the Reabsorption of Light on the Spectral Dependence of Photoconductivity in Molecular Crystals—(498) 269

Yu. V. Konobeev, Reabsorption in Crystals of Finite Thickness. III—(504) 272

E. G. Chernevskaya, The Transparency of CaF_2, SrF_2, and BaF_2 Crystals and the Effect of Hard Radiation on Them—(513) 277

V. G. Dubinin, An Investigation of the Effect of a Flux on Activator Concentration in a Phosphor by the Paramagnetic Absorption Method—(518) 279

Yu. G. Belashov and L. V. Belashova, Study of Electrical Conductivity and Optical Transmission of Thin Layers of Certain Intermetallic Compounds of Antimony—(523) 282

V. G. Padalka and I. N. Shklyarevskii, Determination o the Microcharacteristics of Silver and Gold from t Infrared Optical Constants and the Conductivity at and 295°K—(527) 285

V. K. Miloslavskii and A. I. Ranyuk, Optical Constants Cadmium Oxide in the Infrared—(536) 289

L. V. Iogansen, On the Role of Dimensional Limitations of Total Reflection Resonance Filters—(542) 292

L. Dunaisky, Invariance of Maxwell's Equations and the Principles of Reversibility for a Plane Harmonic Wave—(547) 295

K. S. Vul'fson and F. A. Charnaya, Measurement of the Diameter of the High-Pressure Pulse Discharge Channel in Various Spectral Regions—(549) 296

M. O. Bulanin and N. D. Orlova, On the Infrared Absorption Spectra of Hydrogen in Solutions—(551) 298

V. I. Odintsov, The Use of Reflected Light in Work with a Fabry-Perot Etalon—(553) 299

A. P. Prishivalko, G. M. Gusak, and I. L. Onichek, Tables of Fresnel's Coefficients for Absorbing Media (555) 301

V. G. Koloshnikov, M. A. Mazing, S. L. Mandel'shtam, and Yu. P. Marasanov, Use of a Fabry-Perot Etalo for Studying Spectral Line Widths in Pulsed Discharges—(556) 302

V. A. Borgest, Determination of Deuterium in Water at Concentrations Close to the Natural Abundance on the Basis of Infrared Absorption Spectra—(558) 30

EVENTS

Ch. B. Lushchik and K. K. Shvarts, The Second Confere on the Physics of Alkali Halide Crystals—(560) 304

OBITUARY

N. N. Kachalov—(563) 306

Nos. 5 and 6—November-December

Yu. I. Ostrovskii and N. P. Penkin, Measurement of the Absolute Values of Oscillator Strengths in Atomic Spectra. II. Resonance Lines of Atoms in Group II-(565) 307

F. S. Faizullov and N. N. Sobolev, Determination of the Effective Cross Section for Collisions of Excited B rium Ions with Argon Atoms—(571) 310

B. N. Snegirev, Vibrational Spectra of Aromatic Compounds. XI. Calculation of Intensities in the Infrare Spectrum of Toluene—(577) 313

A. N. Lazarev and T. F. Tenisheva, Vibrational Spectra of Silicates. III. Infrared Spectra of the Pyroxenoid and Other Chain Metasilicates—(584) 316

T. V. Yakovleva, A. A. Petrov, and M. D. Standnichuk, Vibrational Spectra and Structure of Ene-Yne Silic Hydrocarbons—(588) 318

T. V. Yakovleva and A. A. Petrov, Depolarization of Ra man Lines of Multiple Bonds of Vinylacetylenic Hy drocarbons as Related to their Structures—(594) 32

T. V. Ivanova and B. Ya. Sveshnikov, The Luminescenc of Alcoholic Solutions of Benzene at −196° C—(598) 322

R. N. Nurmukhametov, D. N. Shigorin, Yu. I. Kozlov, a V. A. Puchkov, The Effect of Hydrogen Bonds on th Luminescence of Oxy- and Amino- Azo Compounds (606) 327

L. A. Kiyanskaya and B. Ya. Sveshnikov, On Quenching Fluorescence in Solutions at Liquid Air Temperatu by Iodides—(613) 330

E. Khalupovskii, Phosphorescence of Organic Molecules with Two Metastable Levels—(617) 332
M. Bonch-Bruevich, B. P. Kovalev, L. M. Belyaev, and G. S. Belikova, A Study of the Kinetics of the Sensitized Emission of Radiation Due to Certain Additions in Naphthalene Crystals—(623) 335
D. Zhevandrov, V. I. Gribkov, and I. D. Khan-Magometova, Influence of Excited Light Birefringence on the Luminescence Polarization in Molecular Crystals—(629) 338
N. Zaidel' and G. S. Lazeeva, Photoluminescence of Solutions and Crystals of Gadolinium Salts—(636) 341
V. Osiko, Intracrystalline Reactions in Crystalline Phosphors and the Structure of Luminescence Centers—(642) 345
Drozd and V. L. Levshin, Location of Energy Levels in ZnS-CdS Phosphors—(648) 348
A. Bundel', Z. I. Guretskaya, and M. N. Noskova, Separating the Selenium Band in the Spectra of Sulfide-Selenide Phosphors—(656) 352
N. Shklyarevskii and R. G. Yarovaya, Optical Properties of Beryllium in the Infrared Spectral Region—(661) 355
O. Sall, The Sensitivity Threshold for Optical Absorption Analysis of the Composition of Liquid or Gaseous Mixtures—(667) 358
O. Sall, Theory of the Selectivity of Optical Absorption Analyzers for the Composition of Gaseous or Liquid Mixtures. I—(672) 361
P. Zapesochnyi and A. I. Dashchenko, An Oscillographic Method of Studying Optical Excitation Functions—(679) 365
A. Pankratov, Nonselective Optico-Acoustic Radiation Detectors with Electrodynamic Microphone—(681) 366
I. Tarasov, A Crossed-Dispersion Spectrograph Built on a New Optical Design—(683) 368
. S. Varshavskii, Relation Between the Frequencies of N–H Symmetric and Antisymmetric Vibrations in the Molecules of Primary Amines—(686) 369
I. Levikov and L. P. Shishatskaya, Comparison of Spectral Intensities of the Hydrogen and Deuterium Radiation—(689) 371
G. Boitsov and Yu. Ya. Gotlib, Calculation of the C=O Stretching Vibration Frequency for Cis- and Gauche Isomers of Molecules of the Type $ClCH_2-C\overset{O}{\underset{R}{<}}$—(691) 372
S. Selivanenko, Exciton Relaxation Times in Molecular Crystals—(694) 374
. I. Turkin and M. P. Chaiko, Anomalous Ratio of the HFS Component Intensities of Indium Lines—(695) 375
he Journal of Quantitative Spectroscopy and Radiative Transfer—(696) 375

. 6—December

P. Bochkova, L. P. Razumovskaya, and S. E. Frish, Spectroscopic Investigation of a High Frequency Discharge in Neon—(697) 376
A. M. Meleshina, The Use of the Metal Molecular Model in the Calculation of the Influence of Molecular Vibrations on Forbidden Transitions—(706) 381
K. K. Svidzinskii, Calculation of the Hyperfine Structure of Molecular Rotational Spectra—(713) 385
V. M. Tatevskii, G. S. Koptev, and A. A. Mal'tsev, Vibrational Spectra of the B_2O_3 and B_2S_3 Molecules—(724) 391
E. M. Popov and G. I. Kagan, Vibrational Spectra of Vinyl Alkyl Sulfides—Theoretical Analysis—(730) 394
G. V. Peregudov, Interpretation of the Vibrational Spectra of Naphthalene and Some of Its Deuterium Substitution Products—(735) 397
M. S. Brodin and Ya. O. Dovgii, Optical Properties of Crystals with Impurities. I. Absorption and Dispersion Characteristics of Anthracene Impurity in a 9,10-Dihydroanthracene Crystal—(742) 400
N. Ya. Gorban' and I. A. Shaikevich, Phase Relations for the p- and s-Components of a Reflected Light Wave Determined by the Fresnel Equations—(750) 404
A. P. Ivanov, A Study of Scattering of Light in Objects Subject to Fading—(754) 407
A. O. Sall', Theory of the Selectivity of Optical Absorption Analyzers for the Composition of Gaseous or Liquid Mixtures. II—(759) 409
P. P. Kas'yankov, Calculation of Cathode Lens Aberrations—(765) 413
M. S. Soskin, Determining the Refractive Indices of Crystals Using a Jamin Interferometer—(768) 415
M. D. Borisov, I. I. Demidenko, and V. G. Padalka, Determination of the Electron Concentration in the Conduction Band of Thin Aluminum Films from Their Transmission Cutoff in the Vacuum Ultraviolet Region—(769) 416
F. S. Ortenberg, On the Relative Vibrational Transition Probabilities in the $^2\Delta \rightarrow {}^2\Delta$ Band System of the VO Molecule—(772) 417
L. M. Sverdlov, A Calculational Formula for Raman Spectral Intensities of Polyatomic Molecules—(774) 419
L. M. Volkova, Effective Cross Sections for Excitation of Certain Spectral Lines of Sodium—(775) 420
V. M. Zakharova, Yu. M. Kagan, and V. I. Perel', Spectroscopic Observation of Rotation of the Positive Column of a Discharge in a Magnetic Field—(777) 421
V. R. Muratov, A Telecentric Optical System for Illuminating the Entrance Slit of a Spectral Instrument—(779) 423
M. L. Veingerov, A. A. Sivkov, and Byan' Nan Khua, An Incandescent Lamp with a Radiometric Chopper—(780) 423

Errata in Volume VI—(789) 412
Letter to the Editor—(789) 412
Author List to Volume XI—(782) 426
Contents List to Volume XI—(790) 428
Announcement—(803) 432
Book Review—(804) 432

ANNOUNCEMENT

The International Conference on Spectroscopy

The International Conference on Spectroscopy and the Tenth International Colloquium on Spectroscopy will be held 18-22 June, 1962 at the University of Maryland, College Park (Washington, U.S.A.). The conference is being organized by the Society for Applied Spectroscopy in collaboration with the International Consultative Council. A number of review reports dealing with current problems in spectroscopy, as well as original papers related to the same problems, will be presented at this conference.

Authors wishing to present a 20 minute report to be included in the program of the conference should submit in advance the title, author's name, and summary (250-300 words) before December 31, 1961. All material and further specific inquiries pertaining to the conference should be directed to Mr. Bourdon F. Scribner, Chairman, International Conference on Spectroscopy in 1962, National Bureau of Standards, Washington 25, D.C., U.S.A.

BOOK REVIEW

STEREOSCOPY by N. A. Valyus, a new publication of the Academy of Sciences of the U.S.S.R.

The monograph by N. A. Valyus deals in detail with questions of stereoscopic vision and the conditions responsible for spatial representation. It describes and classifies optical principles of the construction of spatial representations. A considerable portion of it deals with different technical means for the creation of stereoscopic representations and the application of stereoscopic methods for observation and measurement in science, technology, and the arts.

The author touches upon questions dealing with modern technical problems related to the creation of stereoscopic television and cinematographic representations, stereoscopic projection on wide and curved screens, the creation of spatial integral representations, the creation of stereoscopic scenery, and photosculpture. In the chapter on metrics of stereoscopic space, the concept of quantitative evaluation of stereoscopic representations is introduced for the first time.

The book contains a great number of original stereoscopic illustrations showing visual examples of the application of the stereoscopic method in such fields as electron microscopy, aerial photography, radiolocation, astronomy, biology, medicine, x-ray spectroscopy, and architecture. However, it is especially directed to optical physicists, physiologists, and scientific and engineering personnel in the movie and film industries.

Its clear and intelligible style of presentation makes it useful to a wide circle of readers—both those concerned with solving technical and scientific problems dealing with stereoscopic instruments and stereoscopic methods of observation and measurement and those who are interested in familiarizing themselves with questions of stereoscopy.

The book consists of 30 pages, including the stereoscopic illustrations; anaglyphic glasses are also enclosed. The price is 2 rubles 50 kopecs.

To procure the book by mail, orders should be sent to:

Moskva, Tsentr, B. Cherkasskii per., 2/10,

Kontora "Akademkniga," otdel "Kniga-pochtoi,"

or to the nearest bookstore of the "Akademkniga."

Addresses of the Akademkniga Bookstores: Moskva, ulitza Gor'kogo, 6 (Magazin No. 1); Moskva, 1-i Akademicheskii proezd, 55/5 (Magazin No. 2); Leningrad, Liteinyi prospect, 57; Sverdlwsk, ulitza Belinskogo, 71-v; Alma-Atn, ulitza Furmanova, 129; Tashkent, ulitza Karla Marksa, 29; Baku, ulitza Dzhaparidze, 13; Kiev, ulitza Lenina, 42; Khar'kov, Goryainovskii pereulok, 4/6.

"AKADEMKNIGA"

Sixth Year of Publication

The journal is published monthly, 2 volumes per year (6 issues in each volume).

Address of the Publisher of the Journal of "Optika i Spektroskopiya" (Optics and Spectroscopy):

Leningrad, V-164, Mendeleevskaya liniya, d.1,
Telefon A-3-79-72

Accepted for publication on November 13, 1961. M-71572. Paper 70×108/16. Paper page $3\frac{3}{8}$. Printer's page $6\frac{3}{4}$ = 9.24 approximate typed pages. Uch.-izd. 1. 11.35. Number of copies is 2785. Order No. 312.*

First Publishing House, Publication of the Academy of Sciences of the USSR,
Leningrad, V-34, 9 liniya, d.12

* This is quoted for English edition readers' information—Translation Editor.

Subscription Openings

for the Journals of the Academy of Sciences of the USSR for 1962

Name of Journal	Annual number of issues	Subscription rate in rubles	
		Annual	Semi-annual
General Journals of the Academy			
Vestnik Akademii Nauk SSSR (Bulletin of the Academy of Sciences of the USSR)	12	9.60	4.80
Doklady Akademii Nauk SSSR (without jackets) (Proceedings of the Academy of Sciences of the USSR)	36	51.84	25.92
Doklady Akademii Nauk SSSR (with 6 imprinted calico jackets) (Proceedings of the Academy of Sciences of the USSR)	36	54.24	27.12
Priroda (Nature)	12	8.40	4.20
Physics—Mathematical Sciences			
Akusticheskii Zhurnal (Journal of Acoustics)	4	4.80	2.40
Astronomicheskii Zhurnal (Journal of Astronomy)	6	9.90	4.95
Geomagnetizmi Aeronomiya (Geomagnetism and Aeronomy)	6	9.00	4.50
Zhurnal Vychislitel'nei Matematiki i Matimaticheskii Fiziki (Journal of Computer Mathematics and Mathematical Physics)	6	9.00	4.50
Zhurnal Technicheskoi Fiziki (Journal of Technical Physics)	12	12.60	6.30
Zhurnal Eksperimental'noi i Teoreticheskoi Fiziki (Journal of Experimental and Theoretical Physics)	12	28.80	14.40
Izvestiya Akademii Nauk SSSR, Seriya Geofizicheskaya (Bulletin of the Academy of Sciences of the USSR, Geophysical Series)	12	18.00	9.00

Subscription Openings (continued)

Name of Journal	Annual number of issues	Subscription rate in rubles	
		Annual	Semi-annual
Izvestia Akademii Nauk SSSR, Seriya Matematiki (Bulletin of the Academy of Sciences of the USSR, Mathematical Series)	6	9.00	4.50
Izvestia Akademii Nauk SSSR, Seriya Fiziki (Bulletin of the Academy of Sciences of the USSR, Physical Series)	12	14.40	7.20
Kristallografiya (Crystallography)	6	9.00	4.50
Matematicheskii Sbornik (Revue of Mathematics)	12	14.40	7.20
Optika i Spektroskopiya (Optics and Spectroscopy)	12	16.20	8.10
Pribory i Tekhnika Eksperimenta (Instruments and Experimental Technique)	6	9.78	4.89
Teoriya Veroyntnostei i ee Primeneniya (Theory of Probability and its Application)	4	4.52	2.26
Fizika Tverdogo Tela (Solid State Physics)	12	30.00	15.00

Subscriptions are accepted at all centers of "Soyuzpechati," post offices, bureau and departments of communication, authorized representatives at factories and plants, at scientific and research institutes, educational institutions and organizations, and also by the departments and stores of "Akademkniga," and the office of "Akademkniga" located at: Moskva, Tsentr, B. Cherkasskii per., 2/10.

Calculation of the C=O Stretching Vibration Frequency for Cis- and Gauche Isomers of Molecules of the Type $ClCH_2-C\overset{O}{\underset{R}{}}$ . . . . . V. G. Boitsov and Yu. Ya. Gotlib 372 (691)
Exciton Relaxation Times in Molecular Crystals . . . . . A. S. Selivanenko 374 (694)
Anomalous Ratio of the HFS Component Intensities of Indium Lines . . Yu. I. Turkin and M. P. Chaiko 375 (695)
The Journal of Quantitative Spectroscopy and Radiative Transfer 375 (696)

CONTENTS (Issue 6)

Spectroscopic Investigation of a High Frequency Discharge in Neon . . . . . O. P. Bochkova, L. P. Razumovskaya, and S. E. Frish 376 (697)
The Use of the Metal Molecular Model in the Calculation of the Influence of Molecular Vibrations on Forbidden Transitions . . . . . A. M. Meleshina 381 (706)
Calculation of the Hyperfine Structure of Molecular Rotational Spectra . . . . . K. K. Svidzinskii 385 (713)
Vibrational Spectra of the B_2O_3 and B_2S_3 Molecules . . . . . V. M. Tatevskii, G. S. Koptev, and A. A. Mal'tsev 391 (724)
Vibrational Spectra of Vinyl Alkyl Sulfides—Theoretical Analysis . . . E. M. Popov and G. I. Kagan 394 (730)
Interpretation of the Vibrational Spectra of Naphthalene and Some of Its Deuterium Substitution Products . . . . . G. V. Peregudov 397 (735)
Optical Properties of Crystals with Impurities. I. Absorption and Dispersion Characteristics of Anthracene Impurity in a 9,10-Dihydroanthracene Crystal . . . . M. S. Brodin and Ya. O. Dovgii 400 (742)
Phase Relations for the p- and s-Components of a Reflected Light Wave Determined by the Fresnel Equations . . . . . N. Ya. Gorban' and I. A. Shaikevich 404 (750)
A Study of Scattering of Light in Objects Subject to Fading . . . . . A. P. Ivanov 407 (754)
Theory of the Selectivity of Optical Absorption Analyzers for the Composition of Gaseous or Liquid Mixtures. II . . . . . A. O. Sall' 409 (759)
Calculation of Cathode Lens Aberrations . . . . . P. P. Kas'yankov 413 (765)

SHORT COMMUNICATIONS

Determining the Refractive Indices of Crystals Using a Jamin Interferometer . . . . . M. S. Soskin 415 (768)
Determination of the Electron Concentration in the Conduction Band of Thin Aluminum Films from Their Transmission Cutoff in the Vacuum Ultraviolet Region . . . . . M. D. Borisov, I. I. Demidenko, and V. G. Padalka 416 (769)
On the Relative Vibrational Transition Probabilities in the $^2\Delta - {}^2\Delta$ Band System of the VO Molecule . . . . . F. S. Ortenberg 417 (772)
A Calculational Formula for Raman Spectral Intensities of Polyatomic Molecules. . . L. M. Sverdlov 419 (774)
Effective Cross Sections for Excitation of Certain Spectral Lines of Sodium . . . . . L. M. Volkova 420 (775)
Spectroscopic Observation of Rotation of the Positive Column of a Discharge in a Magnetic Field . . . . . V. M. Zakharova, Yu. M. Kagan, and V. I. Perel' 421 (777)
A Telecentric Optical System for Illuminating the Entrance Slit of a Spectral Instrument . . . . . V. R. Muratov 423 (779)
An Incandescent Lamp with a Radiometric Chopper . . . . . M. L. Veingerov, A. A. Sivkov, and Byan' Nan Khua 423 (780)

Errata in Volume VI 412 (789)
Letter to the Editor 412 (789)
Author List, Vol. XI 426 (782)
Contents List, Vol. XI 428 (790)
Announcement 432 (803)
Book Review 432 (804)

NOTICE TO READERS

The November and December issues are published under one cover, because the November Russian Original was late in the mails.

UNIVERSITY OF ILLINOIS
LIBRARY
UNDERGRADUATE DIV.
NAVY PIER GRAND AVE.
CHICAGO 11, ILL.

VOL. XI, NOS. 5 AND 6 DECEMBER 1961

(Nu

These Russian page numbers are also quoted at the head of each paper.)

CONTENTS (Issue 5)

Measurement of the Absolute Values of Oscillator Strengths in Atomic Spectra. II. Resonance Lines of Atoms of Group II . . . . . Yu. I. Ostrovskii and N. P. Penkin 307 (565)
Determination of the Effective Cross Section for Collisions of Excited Barium Ions with Argon Atoms . . . . . F. S. Faizullov and N. N. Sobolev 310 (571)
Vibrational Spectra of Aromatic Compounds. XI. Calculation of Intensities in the Infrared Spectrum of Toluene . . . . . B. N. Snegirev 313 (577)
Vibrational Spectra of Silicates. III. Infrared Spectra of the Pyroxenoids and Other Chain Metasilicates . . . . . A. N. Lazarev and T. F. Tenisheva 316 (584)
Vibrational Spectra and Structure of Ene-Yne Silico-Hydrocarbons . . . . . T. V. Yakovleva, A. A. Petrov, and M. D. Standnichuk 318 (588)
Depolarization of Raman Lines of Multiple Bonds of Vinylacetylenic Hydrocarbons as Related to their Structures . . . . . T. V. Yakovleva and A. A. Petrov 320 (594)
The Luminescence of Alcoholic Solutions of Benzene at −196° C . . . . . T. V. Ivanova and B. Ya. Sveshnikov 322 (598)
The Effect of Hydrogen Bonds on the Luminescence of Oxy- and Amino- Azo Compounds . . . . . R. N. Nurmukhametov, D. N. Shigorin, Yu. I. Kozlov, and V. A. Puchkov 327 (606)
On Quenching of Fluorescence in Solutions at Liquid Air Temperatures by Iodides . . . . . L. A. Kiyanskaya and B. Ya. Sveshnikov 330 (613)
Phosphorescence of Organic Molecules with Two Metastable Levels. . . . . M. E. Khalupovskii 332 (617)
A Study of the Kinetics of the Sensitized Emission of Radiation Due to Certain Additions in Naphthalene Crystals . . . . . A. M. Bonch-Bruevich, B. P. Kovalev, L. M. Belyaev, and G. S. Belikova 335 (623)
Influence of Excited Light Birefringence on the Luminescence Polarization in Molecular Crystals . . . . . N. D. Zhevandrov, V. I. Gribkov, and I. D. Khan-Magometova 338 (629)
Photoluminescence of Solutions and Crystals of Gadolinium Salts. . A. N. Zaidel' and G. S. Lazeeva 341 (636)
Intracrystalline Reactions in Crystalline Phosphors and the Structure of Luminescence Centers . . . . . V. V. Osiko 345 (642)
Location of Energy Levels in ZnS-CdS Phosphors . . . . . L. Drozd and V. L. Levshin 348 (648)
Separating the Selenium Band in the Spectra of Sulfide-Selenide Phosphors . . . . . A. A. Bundel', Z. I. Guretskaya, and M. N. Noskova 352 (656)
Optical Properties of Beryllium in the Infrared Spectral Region . . . . . I. N. Shklyarevskii and R. G. Yarovaya 355 (661)
The Sensitivity Threshold for Optical Absorption Analysis of the Composition of Liquid or Gaseous Mixtures. . . . . A. O. Sall 358 (667)
Theory of the Selectivity of Optical Absorption Analyzers for the Composition of Gaseous or Liquid Mixtures . . . . . A. O. Sall 361 (672)

SHORT COMMUNICATIONS

An Oscillographic Method of Studying Optical Excitation Functions. . . . . I. P. Zapesochnyi and A. I. Dashchenko 365 (679)
Nonselective Optico-Acoustic Radiation Detectors with Electrodynamic Microphone . . . . . N. A. Pankratov 366 (681)
A Crossed-Dispersion Spectrograph Built on a New Optical Design . . . . . K. I. Tarasov 368 (683)
Relation Between the Frequencies of N—H Symmetric and Antisymmetric Vibrations in the Molecules of Primary Amines . . . . . Yu. S. Varshavskii 369 (686)
Comparison of Spectral Intensities of the Hydrogen and Deuterium Radiation . . . . . S. I. Levikov and L. P. Shishatskaya 371 (689)

(Contents continued on inside back cover)